THESIS FOR THE DEGREE OF DOCTOR OF PHILOSOPHY

Correlations in Low-Dimensional Quantum Many-Particle Systems

Erik Eriksson

UNIVERSITY OF GOTHENBURG

Department of Physics
University of Gothenburg
May 30, 2013

Vetenskaplig avhandling för avläggande av filosofie doktorsexamen
i fysik vid Göteborgs universitet. Avhandlingen presenteras vid ett seminarium
fredagen den 31 maj 2013, kl 13.15 i sal Euler, Skeppsgränd 3, Göteborg.
Avhandlingen försvaras på engelska.

Opponent:	Prof. Karyn Le Hur, Centre de Physique Théorique, École Polytechnique, Frankrike
Betygsnämnd:	Doc. Eddy Ardonne, Fysikum, Stockholms universitet
	Prof. Edwin Langmann, Institutionen för teoretisk fysik, KTH
	Prof. Nancy Sandler, Department of Physics and Astronomy, Ohio University, USA
Examinator:	Prof. Stellan Östlund
Handledare:	Prof. Henrik Johannesson

Institutionen för fysik
Göteborgs universitet

GÖTEBORGS UNIVERSITET

This version: May 30, 2013
Published version available at http://hdl.handle.net/2077/32678

Correlations in Low-Dimensional Quantum Many-Particle Systems

Erik Eriksson

Department of Physics
University of Gothenburg

Abstract

This thesis concerns correlation effects in quantum many-particle systems in one and two dimensions. Such systems show many exotic non-Fermi liquid phenomena, which can be treated analytically using non-perturbative field-theory methods.

Quantum phase transitions between topologically ordered phases of matter, which do not break any symmetries, are studied. It is shown that although there is no local order parameter, a local measure from quantum information theory called reduced fidelity can detect such transitions.

Entanglement in quantum impurity systems is also studied. The general expression for scaling corrections in entanglement entropy from boundary perturbations is derived within conformal field theory, showing that the asymptotic decay of Kondo screening clouds follow the same power-law as the impurity specific heat.

Furthermore, the effects from spin-orbit interactions on Kondo physics in helical Luttinger liquids are studied. Such helical liquids occur on the edges of two-dimensional topological insulators. It is shown that Rashba and Dresselhaus interactions can potentially destroy Kondo singlet formation in such a system, and that the coupling to an electric field gives a mechanism to control transport properties.

The most recent work focuses on correlations in interacting one-dimensional Bose gases. The asymptotic expression for correlation functions in a generalized Gibbs ensemble, where all the local conservation laws appear, is obtained from Bethe Ansatz and conformal field theory.

In addition to the research papers with the above results, the thesis also contains an introductory text reviewing background material.

Acknowledgments

It is a great pleasure to thank my thesis supervisor Prof. Henrik Johannesson for invaluable support and encouragement while guiding me towards the completion of this thesis. Without the enthusiasm and positive attitude I always met when asking for advice, my years as a PhD student would certainly not have been as stimulating and enjoyable.

I also wish to thank Dr. Anders Ström for the many rewarding discussions during the time we shared office as fellow PhD students, and for the collaboration resulting in Paper IV.

Furthermore, it is with pleasure I thank Prof. Vladimir Korepin for a very nice collaboration. The hospitality of the C.N. Yang Institute for Theoretical Physics in Stony Brook, USA when I was visiting is gratefully acknowledged. The support from Prof. Alexander Stolin in making this work possible is very much appreciated.

Also the collaboration with Girish Sharma on Paper IV is acknowledged. Many thanks go to Matteo Bazzanella and Hugo Strand for the stimulating discussions while sharing office. I wish to thank my examiner Prof. Stellan Östlund, my assistant supervisor Dr. Mats Granath, as well as Dr. Johan Nilsson and Prof. Bernhard Mehlig with students for contributing to the great atmosphere in the group.

Last but not least, I wish to thank family and friends for support and inspiration.

List of papers

This thesis consists of an introductory text and the following papers:

Paper I:
Erik Eriksson and Henrik Johannesson, *Reduced fidelity in topological quantum phase transitions*, Phys. Rev. A **79**, 060301(R) (2009).

Paper II:
Erik Eriksson and Henrik Johannesson, *Corrections to scaling in entanglement entropy from boundary perturbations*, J. Stat. Mech. (2011) P02008.

Paper III:
Erik Eriksson and Henrik Johannesson, *Impurity entanglement entropy in Kondo systems from conformal field theory*, Phys. Rev. B **84**, 041107(R) (2011).

Paper IV:
Erik Eriksson, Anders Ström, Girish Sharma, and Henrik Johannesson, *Electrical control of the Kondo effect in a helical edge liquid*, Phys. Rev. B **86**, 161103(R) (2012).

Paper V:
Erik Eriksson, *Spin-orbit interactions in a helical Luttinger liquid with a Kondo impurity*, Phys. Rev. B (in press).

Paper VI:
Erik Eriksson and Vladimir Korepin, *Finite-size effects from higher conservation laws for the one-dimensional Bose gas*, J. Phys. A: Math. Theor. **46**, 235002 (2013).

Papers not included in this thesis

Erik Eriksson and Henrik Johannesson, *Multicriticality and entanglement in the one-dimensional quantum compass model*, Phys. Rev. B **79**, 224424 (2009).

Henrik Johannesson, David F. Mross, Erik Eriksson, *Two-Impurity Kondo Model: Spin-Orbit Interactions and Entanglement*, Mod. Phys. Lett. B **25**, 1083 (2011).

Licentiate thesis[1]

Erik Eriksson, *A Quantum Information Perspective on Two Condensed Matter Problems*, University of Gothenburg, 2011.

[1]The Licentiate thesis is a part of the PhD thesis, covering Papers I-III. It contains most parts of Chapters 3 and 4 as well as Sections 5.1 and 7.1 and Appendix A.

Contents

Outline

This thesis on correlation effects in low-dimensional quantum many-particle systems is organized as follows. Chapters 1-6 give a review over existing literature on the physical systems and methods that are treated in the thesis. In Chapter 1 we discuss the paradigms that have dominated condensed matter physics for much of the 20th century, and the new developments in correlated systems that go beyond those paradigms. Chapter 2 introduces first the bosonization technique to treat interacting fermions in one dimension, and then conformal field theory which provides a unifying framework for gapless one-dimensional systems. Chapter 3 treats the Kondo effect in various systems, in particular the boundary conformal field theory approach is reviewed. In Chapter 4 we discuss an intrinsic phenomena in correlated quantum systems, namely entanglement, and review the universal results that can be obtained for gapless one-dimensional systems using conformal field theory. In Chapter 5 we review topological phases of matter, discussing topological order and topological quantum phase transitions as well as two-dimensional topological insulators and their edge states. Finally in Chapter 6 we introduce the Bethe Ansatz solution for the interacting one-dimensional Bose gas and discuss the generalized Gibbs ensemble.

In Chapter 7 we give a brief introduction to Papers I-VI, and summarize the main results in them. The introductory text ends with a summary and discussion in Chapter 8. Appendix A contains a general derivation of the conformal field theory results for the von Neumann entropy presented in Papers II-III. Finally the thesis contains Papers I-VI which are published, or submitted, research papers containing the new results of this thesis.

1

Introduction

Our attempts to understand Nature must inevitably take into account that the whole is often not just a simple sum of its parts [1]. An overly reductionistic view on physics as merely a development towards an understanding of smaller and smaller constituents eventually leading to a "Final Theory" in terms of the most elementary parts [2], would not shed much light on those rich and fascinating collective phenomena that we know by experience will emerge when putting many such constituents together [3, 4]. It is usually not possible in practice to reconstruct the laws governing collective behavior from the underlying laws for the elementary parts. Understanding the mechanisms that govern human society for example, can hardly be accomplished through elementary particle physics. Similar arguments are valid also within theoretical physics itself. Namely, although we now believe that we have a good understanding of the quantum mechanics that govern individual particles [5–7], the complexity of *quantum many-particle systems* [8, 9] continue to confront us with many intriguing challenges [10].

The relevant degrees of freedom for the description of a physical system are not the same at different energy scales. If one is interested in the dynamical properties of a system at room temperature one usually do not need to take subatomic processes into account, and at even lower temperatures there should be even fewer details needed to formulate an effective theory at that energy scale. For a many-particle system in some condensed phase, i.e. a condensed matter system, an effective low-energy theory will often be in terms of collective degrees of freedom varying over large distances. In such situations the effective low-energy theory should be a field theory [11, 12], where only such details as underlying symmetries need to be accounted for. The notion of symmetry

indeed pervades modern physics, and in particular the physics of condensed matter. With symmetries comes conservation laws, generically associated with low-energy excitations. The framework relating physical theories at different energy scales is known as the renormalization group. It explains the mechanism behind the observed universality of physical phenomena, where low-energy properties of large classes of systems are remarkably similar as long as they share the same underlying symmetries. These symmetries thus allows for the classification of different phases of matter, and with the renormalization group follows an understanding of phase transitions in terms of scale invariance [13].

It is indeed natural that physical theories in general are just effective theories for the energy range of their confirmed validity, and that they in principle always could be just a limiting case of some "Final Theory" [14]. We should not be surprised therefore to find exotic new phenomena regardless if one goes towards higher or lower energies.

1.1 Quantum many-particle systems

It is an easy task to write down a many-particle Hamiltonian, such as

$$\hat{H} = \sum_i \frac{\hat{\mathbf{p}}_i}{2m_e} + \sum_i \hat{V}_{\text{ei}}(\mathbf{r}_i) + \sum_{i<j} \hat{V}_{\text{ee}}(\mathbf{r}_i - \mathbf{r}_j) \tag{1.1}$$

for electrons moving in a static Coulomb potential V_{ei} from lattice ions[1] and the Coulomb potential V_{ee} from the other electrons, with m_e the electron mass and $\hat{\mathbf{p}}_i$ the momentum operator. However solving the problem exactly, i.e. finding the solutions $|\Psi\rangle$ to the Schrödinger equation [16]

$$i\hbar \frac{\partial}{\partial t} |\Psi\rangle = \hat{H} |\Psi\rangle \tag{1.2}$$

presents a formidable challenge already for just a few particles. Just as in classical mechanics, no general analytical solution for three or more interacting particles can be found. Various approximation schemes however often work very well. An example of the quantum three-particle problem is the He atom, which can be treated quite accurately using perturbation theory. In order to treat problems perturbatively one must however choose a proper reference state to perturb around.

[1] Already by assuming this lattice potential to be static has a first separation of energy scales been done. This so called Born-Oppenheimer approximation [15] can be justified by the large difference in mass between the ions and electrons.

Correlated systems

Condensed matter systems consists of a macroscopic number of particles, typically on the order of $\sim 10^{23}$ per cm^3 for bulk systems. Finding a good ground state that allows for a perturbative treatment is not a trivial thing. Remarkably however, for many systems it turns out that although the electrons interact with strong Coulomb repulsion, they can qualitatively be treated as almost non-interacting. These systems show weak *correlations*, meaning that they effectively can be described in terms of single-particle states. For such solid-state systems it is a good first approximation to consider non-interacting electrons in a periodic potential, for which the wave functions $\psi_{n\mathbf{k}}(\mathbf{r}) = e^{i\mathbf{k}\cdot\mathbf{r}}u_{n\mathbf{k}}(\mathbf{r})$ are given in terms of the Bloch wave functions $u_{n\mathbf{k}}(\mathbf{r})$ which have the periodicity of the lattice [17]. The resulting band theory in terms of some effective single-particle states, where interactions can be treated within a mean-field framework, works remarkably well in most cases and forms the basis for our understanding of electronic structure [18]. However, for some systems such methods fail because of electronic correlations, and these are then referred to as *strongly correlated systems*. For these systems it might not be possible to find some effective single-particle description. In other cases this may still be possible, but with new effective particles that are qualitatively very different from the original electrons.

1.2 Beyond Landau's paradigms

One may wonder why electrons interacting through the long-ranged Coulomb potential should possibly allow an effective description as free particles . The explanation to this is provided by Landau's Fermi liquid theory [19] for interacting fermions, which shows that excitations at the Fermi surface are stable and behave as effectively free quasiparticles, "dressed" particles with the same quantum numbers as the non-interacting fermions.

An important case where correlations play a role is at continuous phase transitions. Here increasing fluctuations at all length scales cause a divergence in the spatial extent of correlations in the system. A phenomenological model by Landau [20], relying solely on the concept of broken symmetry, has laid the foundations on which most of our understanding of critical phenomena, as well as collective excitations, is built.

Together these two theories, *Landau's Fermi-liquid theory* and the *Landau theory of continuous phase transitions*, have formed a paradigm dominating much of 20th century condensed matter physics [21].

1.2.1 Fermi liquids and non-Fermi liquids

For a non-interacting Fermi system at zero temperature all states up to the Fermi energy will be filled. This implies a distribution function taking the form of a step function

$$n(p) = \theta(p - p_F) = \begin{cases} 1 & \text{when} \quad p < p_F \\ 0 & \text{when} \quad p > p_F \end{cases} \tag{1.3}$$

as a function of momentum p, defining the Fermi momentum p_F. The basic idea behind the concept of the Fermi liquid is that of "adiabatic continuity". When turning on the interactions, the states will be adiabatically connected to those in the free system, provided no phase transition occurs. Hence the interacting system will also have a Fermi surface, and the excitations will carry the same quantum numbers as the original electrons but with renormalized, "dressed", values of their energy and dynamical properties such as mass [22]. The fundamental excitations are thus no longer electrons but so called quasiparticles, which still are electron-like. In particular, there is still a discontinuity in the distribution function at the Fermi level, given by the quasiparticle weight Z. The weight of the delta-function peak in the spectral function for free electrons is $Z = 1$, becoming $Z < 1$ for the quasiparticle when interactions are turned on. The reason why such quasiparticles are stable excitations is purely kinematic: A quasiparticle with momentum $\mathbf{p}_1$ close to $\mathbf{p}_F$ can decay into another state with momentum $\mathbf{p}_2$ by simultaneously creating a quasiparticle-quasihole pair. Conservation of energy however severely restricts the available states for this scattering event to be possible. In three dimensions it leads to a scattering rate $\sim |\mathbf{p}_1 - \mathbf{p}_F|^2$, which vanishes sufficiently close to the Fermi surface hence showing the stability of the quasiparticle. This also shows that the resistivity should go as $\sim T^2$ at low temperatures. Similarly, since the quasiparticles qualitatively behave as the original free electrons, one recovers the free electron expressions for specific heat, $C_v \sim T$, and magnetic susceptibility, $\chi \sim const.$, as the temperature $T \to 0$. Note that the phase space argument, which can be confirmed rigorously with a renormalization group analysis [23], does not assume the original particles to be weakly interacting. Hence it provides an explanation for how strongly interacting electrons can result in weakly interacting quasiparticles.

Non-Fermi liquids are simply those metals for which Fermi liquid theory fails [24]. Situations where Landau's paradigm breaks down include

- Superconductivity. The Fermi liquid is unstable to arbitrarily small attractive interaction between electrons, leading to the formation of Cooper pairs [25, 26].

- In one dimension. Here the quasiparticle decay rate $\sim T$, which is comparable to its excitation energy. Hence they are unstable and the Fermi liquid will never form. The corresponding universal theory in one dimension is instead the Luttinger liquid [27, 28].

- Near a quantum critical point [29]. When there is a continuous phase transition at zero temperature there are fluctuations at all length scales, dramatically enhancing the scattering rate destabilizing the quasiparticles.

- Kondo systems with multiple electron channels or impurities. A Kondo resonance at the Fermi level due to electrons scattering off magnetic impurities can in many cases lead to a breakdown of the Fermi-liquid picture [30, 31].

As we have seen, reduced dimensionality can play an important role in invalidating the Fermi-liquid paradigm. This may also be the case for the still poorly understood high-temperature cuprate superconductors where the 2d CuO_2 planes are expected to be responsible for most of the exotic properties, including the non-Fermi liquid normal state [32].

Indeed, understanding non-Fermi liquids has become one of the central challenges in modern condensed matter physics, pushing the development of new ideas and concepts as well as mathematical methods and experimental techniques.

1.2.2 Symmetry breaking and local order parameters

The second paradigm of condensed matter physics is Landau's theory of phase transitions [20, 33]. The approach is to identify a symmetry that is spontaneously broken in one of the phases. This is unambiguous since a symmetry always is either present or not present. For example, when a liquid crystalizes the translational symmetry is broken. The broken symmetry gives a local order parameter from which one can construct an effective field theory, allowing for the calculation of critical exponents from symmetry considerations alone. The paradigm for the classification of condensed matter thus goes from identifying a symmetry that is broken in an ordered phase, thereby obtaining a local order parameter. Then the collective excitations are obtained as fluctuations in this local order parameter. In particular, for spontaneously broken continuous symmetries the these will be the massless Nambu-Goldstone bosons [34–36]. As an example, in a ferromagnetic phase the time-reversal symmetry is spontaneously broken, and the order parameter is therefore the local

magnetization. The massless excitations are here the spin waves, also known as the magnons.

However, some systems defy this kind of analysis, with the fractional quantum Hall effect [37] as the primary example. Here the different phases all have the same symmetry (i.e. they all look the same locally) but they have different topological quantum numbers characterizing such global quantities as ground state degeneracy and quasiparticle statistics. This leads to the concept of *topological order* [38], when these new quantum numbers are of topological origin. An understanding of topologically ordered phases and the phase transitions between them thus need to go beyond the Landau paradigm. Attempts to do so have frequently relied on ideas and concepts from quantum information, such as entanglement and fidelity [39].

1.3 Why low-dimensional systems are special

Quantum many-body physics can change dramatically when the number of spatial dimensions is reduced. In this thesis we will concentrate on the following effects

- As we have seen, in one dimension the Fermi liquid paradigm breaks down. This is somehow expected since the electrons now cannot move independently, without constantly colliding. Stable low-energy elementary excitations will instead be particle-hole pairs, which are bosons and can propagate coherently, cf. Fig 1.1. The universal low-energy theory in one dimension, replacing the Fermi liquid, is the *Luttinger liquid* [40–42] where the relevant degrees of freedom are collective bosonic waves. The technique of mapping fermions to bosons is known as *bosonization*, and it turns out that the interacting fermion problem can be mapped to a free boson problem. The electrons are now no longer the fundamental particles, instead they are split up into their charge and spin components, which can propagate with different velocities [27, 28].

- Gapless systems with sufficiently short-ranged interactions have an emerging conformal symmetry at low energies, and for one-dimensional quantum systems this makes it possible to use very powerful predictions from *conformal field theory* [43].

- Some interacting quantum many-particle systems in one dimension can be solved exactly, by their so called *integrability*. The technique to obtain solutions is known as Bethe Ansatz [44]. It provides

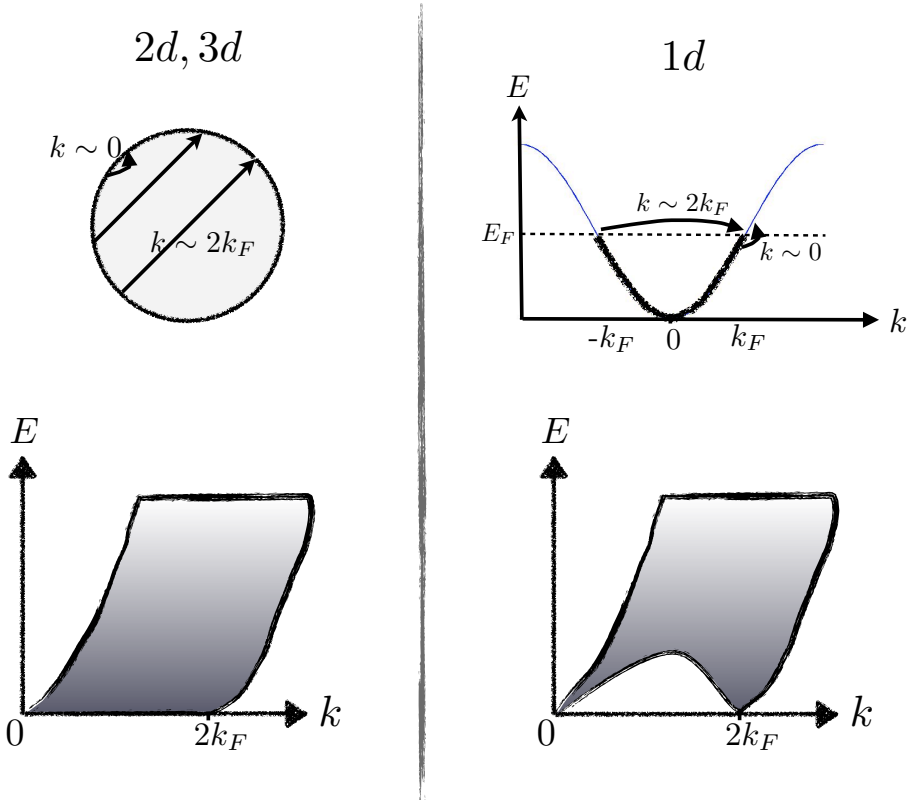

Figure 1.1: The qualitative differences between the spectra of particle-hole excitations in different dimensions. In $d > 1$ it is possible to create low-energy excitations for all momenta $0 \leq k \leq 2k_F$, whereas in one dimension low-energy excitations are restricted to momenta $k \sim 0$ and $k \sim 2k_F$. The linear dispersion $E \sim v_F k$ at $k \sim 0$ means the bosonic particle-hole excitations can propagate coherently and form density fluctuations [27].

important exact solutions that can be used as input in effective theories. In higher dimensions integrability is much less powerful, and only applies to systems that can be reduced to free particles.

- In two spatial dimensions the statistics of quasiparticles is not restricted to being either fermionic or bosonic as it is in higher dimensions. Instead the wavefunction can acquire any phase as particles are exchanged [45], which has given them the name "anyons". In fact, particle exchange does not even need to commute, and quasiparticles with that property are called non-Abelian anyons. The existence of anyons is associated with a ground-state degeneracy that is dependent on the topology of the system, and they are therefore

a manifestation of *topological order*. This is a new type of order that is not associated with local symmetry-breaking [38]. Hence *topological quantum phase transitions* cannot be treated within the Landau paradigm.

1.4 Quantum criticality and the renormalization group

Quantum phase transitions

Phase transitions that take place at zero temperature are called *quantum phase transitions* [29, 46]. Hence they do not involve thermal fluctuations but instead quantum fluctuations within the ground state. The mechanism can be understood by considering the analogy between d-dimensional quantum systems and $d+1$ dimensional classical systems: In the imaginary-time formalism, the inverse temperature is the size of the quantum system in the imaginary-time direction, hence calculating the thermodynamics of a quantum system can be mapped into calculating the thermodynamics of a classical system in one spatial dimension higher. In the thermodynamic limit this becomes particularly clear at zero temperature, as then also the size in the imaginary-time direction goes to infinity. A phase transition in a classical system can then be mapped to some phase transition in a quantum system at zero temperature, with some driving parameter in the Hamiltonian. Analyzing the finite-temperature region around the quantum critical point, sketched in Fig. 1.2 is on the other hand highly non-trivial.

In typical examples this driving parameter of the quantum phase transition corresponds to doping, magnetic field, etc. To make this more clear, and at the same time introduce some other interesting concepts, let us consider the example of the quantum Ising chain.

Quantum phase transition in the quantum Ising chain

We will now outline the technical details of the exact solution of the one-dimensional quantum Ising model, also known as the transverse Ising model. This will allow us to discuss some of the concepts introduced above in a rather simple way. The spin chain is described by the Hamiltonian

$$H = -J \sum_i \left[\sigma_i^z \sigma_{i+1}^z + h\, \sigma_i^x \right] \tag{1.4}$$

with $J > 0$. We will here work in the thermodynamic limit where the number of sites $N \to \infty$, neglecting boundary conditions. The spin

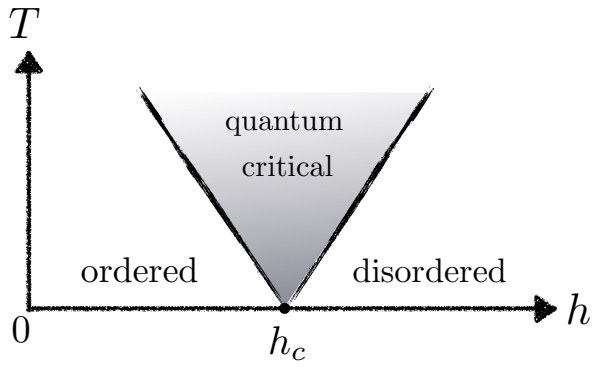

Figure 1.2: Typical phase diagram around a quantum critical point, here for the quantum Ising chain. At zero temperature, the ordered phase with $h < h_c$ and the disordered phase $h > h_c$ are separated by the quantum critical point at h_c, where the system is gapless. In the low-temperature phase diagram there is a quantum critical region which extends above the quantum critical point, where non-Fermi liquid behavior can arise [29].

operators, given by the Pauli matrices, satisfy the relations

$$\{\,\sigma_i^\alpha, \sigma_i^\beta\,\} = 2\delta_{\alpha,\beta}\,, \tag{1.5}$$

$$[\,\sigma_i^\alpha, \sigma_j^\beta\,] = 0 \qquad i \neq j\,. \tag{1.6}$$

To see how a quantum phase transition can arise, consider the ground state in the two simple limits $h \to 0$ and $h \to \infty$:

$$|\Psi_0\rangle = \prod_i |\uparrow\rangle_i \quad \text{or} \quad \prod_i |\downarrow\rangle_i \qquad \text{when } h \to 0, \tag{1.7}$$

$$|\Psi_0\rangle = \prod_i |\rightarrow\rangle_i \qquad \text{when } h \to \infty \tag{1.8}$$

where $|\uparrow\rangle_i, |\downarrow\rangle_i$ are the σ_i^z eigenstate with positive/negative eigenvalue at site i, and $|\rightarrow\rangle_i$ the σ_i^x eigenstate with positive eigenvalue at site i. When $h \to 0$ the ground state is two-fold degenerate, whereas there is only one ground state when $h \to \infty$. Since the degeneracy is an integer, it will not change continuously and there must therefore be a phase transition in between. With zero magnetic field there is a spontaneous breaking of the $\mathbb{Z}_2$ symmetry of the ground state, and this is the ordered phase. For high magnetic fields there is no spontaneous symmetry breaking, and that phase is called disordered. The order parameter is therefore the local magnetization $\langle 0|\sigma_i^z|\Psi_0\rangle$.

Let us now outline the solution of the model, as obtained in Refs. [47–49]. From Eq. (1.5) we see that the spins have fermionic character at

the same site but bosonic between different sites, which complicates the analysis. By the *Jordan-Wigner transformation*

$$\sigma_i^x = 1 - 2c_i^\dagger c_i \,, \tag{1.9}$$

$$\sigma_i^y = i\,(c_i - c_i^\dagger) \prod_{j<i} (1 - 2c_j^\dagger c_j) \,, \tag{1.10}$$

$$\sigma_i^z = -(c_i + c_i^\dagger) \prod_{j<i} (1 - 2c_j^\dagger c_j) \,, \tag{1.11}$$

it is possible to map the spin problem to a spinless fermion problem, where the fermion operators satisfy

$$\{c_i, c_j^\dagger\} = \delta_{i,j} \,, \qquad \{c_i, c_j\} = 0 \,, \qquad \{c_i^\dagger, c_j^\dagger\} = 0 \tag{1.12}$$

This is a first example showing that in one dimension there is no clear connection between spin and statistics. The Jordan-Wigner transformation brings the Hamiltonian on the form

$$H \;=\; J \sum_i \Big[2h c_i^\dagger c_i - c_i^\dagger c_{i+1} - c_{i+1} c_i - c_{i+1}^\dagger c_i - c_i^\dagger c_{i+1}^\dagger \Big] \tag{1.13}$$

in terms of the spinless fermions, which are seen to have a pairing mechanism as in superconductivity [26]. Now, performing a Fourier transformation

$$c_j = \frac{1}{\sqrt{N}} \sum_k c_k e^{ikj} \,, \tag{1.14}$$

and then the *Bogoliubov transformation*

$$c_k = u_k \gamma_k - i v_{-k} \gamma_{-k}^\dagger \,, \tag{1.15}$$

where the γ quasiparticle operators are fermionic

$$\{\gamma_k^\dagger, \gamma_{k'}\} = \delta_{k,k'}, \qquad \{\gamma_k, \gamma_{k'}\} = 0 \qquad \{\gamma_k^\dagger, \gamma_{k'}^\dagger\} = 0 \,, \tag{1.16}$$

the Hamiltonian (1.4) is diagonalized:

$$H = \sum_k \epsilon_k \, (\gamma_k^\dagger \gamma_k - \frac{1}{2}) \,, \tag{1.17}$$

The eigenvalues ϵ_k are given by

$$\epsilon_k = 2J\sqrt{1 + h^2 - 2h\cos k} \,. \tag{1.18}$$

and the ground state can be written as

$$|\Psi_0\rangle = \prod_{k>0} (u_k + i v_k c_k^\dagger c_{-k}^\dagger)\, |0\rangle. \tag{1.19}$$

The parameters u and v are determined through the Bogoliubov-de Gennes equations

$$\epsilon_k u_k = 2J(h - \cos k)\, u_k + 2J \sin k\, v_k\,, \tag{1.20}$$
$$\epsilon_k v_k = 2J \sin k\, u_k - 2J(h - \cos k)\, v_k\,. \tag{1.21}$$

Now, from Eq. (1.18) it is clear that when $h = 1$ there will be gapless quasiparticles with $k = 0$. Hence the quantum critical point is at $h_c = 1$. The energy gap ΔE vanishes as $\Delta E \sim |h - 1|$, and hence follows the power-law $\Delta E \sim |h - h_c|^{z\nu}$ with the *critical exponent* $z\nu = 1$. It is connected to another quantity, the *correlation length* ξ, through $\Delta \sim \xi^{-z}$, where z is called the "dynamic critical exponent" since it determines the relative scaling between space and time. The correlation length $\xi \sim |h - h_c|^{-\nu}$, with critical exponent ν, sets the length scale for the exponential decay of correlation functions $\langle \sigma_i \sigma_{i+r} \rangle \sim \exp[-r/\xi]$. The diverging correlation length as $h \to h_c$ implies that the exponential decay is replaced by a power-law decay at the critical point. Another power-law is that for the order parameter, which here vanishes as $\langle \sigma_i^z \rangle \sim |h - h_c|^{1/8}$ as h approaches h_c from below. The exact solution therefore shows the appearance of power-law scalings in physical quantities near the quantum critical point, just as for classical critical phenomena [13]. In fact, the quantum phase transition is in the same universality class as that in the 2d classical Ising model [50], showing a nice example of the analogy between quantum d-dimensional and classical $d+1$-dimensional systems. In the language of the renormalization group, this means that the classical two-dimensional and the quantum one-dimensional Ising models are governed by the same fixed-point theory at their phase transitions, which is that of a free Majorana fermion. Let us see explicitly how this comes about in the quantum case.

The spinless fermion operator in Eq. (1.13) can be decomposed into a pair of Majorana operators as [51]

$$c_j = \frac{e^{-i\pi/4}}{2}\,(a_j + i b_j)\,, \tag{1.22}$$

where the Majorana particles obey

$$\{a_i, a_j\} = \{b_i, b_j\} = 2\delta_{ij}, \qquad \{a_i, b_j\} = 0. \tag{1.23}$$

Hence a Majorana fermion is its own antiparticle [52]. With this mapping, the quantum Ising chain at the critical point $h = 1$ becomes

$$H = -i\frac{J}{2}\sum_j \left[\, a_j a_{j+1} - b_j b_{j+1} + a_j b_{j+1} - b_j a_{j+1} - 2 a_j b_j \right]. \tag{1.24}$$

Now, since we are interested in the low-energy properties at the critical point we can take the continuum limit, by letting the positions x be continuous, with $x = ja$ and a is the lattice constant, and defining the continuum field

$$\chi_1(x) = \frac{1}{a}\, a_j\,, \quad \chi_2(x) = \frac{1}{a}\, b_j\,. \tag{1.25}$$

This leads to the low-energy Hamiltonian

$$H \sim iv \int \mathrm{d}x\, \left[\chi_1(x)\partial_x\chi_1(x) - \chi_2(x)\partial_x\chi_2(x)\right] \tag{1.26}$$

which describes the two free counterpropagating components of the Majorana field $\chi = (\chi_1, \chi_2)^T$. This model features a *conformal symmetry*, i.e. if the coordinates are expressed in complex form $ix \pm \tau$ where τ is the imaginary time, then the model (1.26) is invariant under all conformal coordinate transformations in the complex plane [43]. More on this in Section 2.2.

It is also interesting to note that in the spinless fermion representation (1.11), $\langle\sigma_i^z\rangle$ is a highly *non-local order parameter*. Since the Hamltonian (1.13) only conserve the parity of the number of fermions (i.e. the number being odd/even), the two-fold *ground-state degeneracy* is connected to the existence of an even or odd number of the fermions. In the ordered phase there is an energy gap, so if the fermions were to have open boundary conditions there must be some *gapless edge states* responsible for the degeneracy, and these will be in terms of the Majorana fermions. Hence if one were to consider the fermions as the physical objects, i.e. in the case of a quantum wire of spinless fermions with superconducting pairing [53], the model would feature a *topological phase of matter*.

The renormalization group

The idea behind the renormalization group [54, 55] is to systematically study what happens when removing information about the fine structure of the system, i.e. when "zooming out", hence obtaining a new effective theory at a smaller energy scale. By doing this in an infinitesimal step, differential equations can be obtained for the change in the coupling constants of the theory as the energy scale is reduced. Let us now outline this procedure for a general field theory [12].

A field theory is generally defined through its action $S(\phi)$, with the partition function as a path integral

$$Z = \int \mathcal{D}[\phi]\, e^{-S(\phi)}, \tag{1.27}$$

in terms of a set of fields ϕ, i.e. some smooth mappings $z \mapsto \phi(z)$ where z denotes the coordinates $(\mathbf{x}, \tau)$ in $D = d + 1$ dimensional space-time. Since a field theory generically is an effective theory valid only within some energy scale, there is generally some cutoffs involved. In condensed matter the continuum theories are naturally restricted to distances larger than the lattice spacing a. The inverse lattice spacing then sets a high-energy cutoff $\Lambda \sim 1/a$.

Let us now for simplicity assume there is only one field in the theory, defined for energies below the cutoff Λ. By Fourier expanding this field

$$\phi(z) = \frac{1}{(2\pi)^D} \int_{|q|<\Lambda} \mathrm{d}^D q \; \phi_k \, e^{iq\cdot z} \tag{1.28}$$

it follows that it can be decomposed into a low-energy component $\phi_<$ and a high-energy component $\phi_>$,

$$\begin{aligned} \phi(z) &= \phi_<(z) + \phi_>(z) = \\ &= \frac{1}{(2\pi)^D} \int_{|q|<\Lambda/b} \mathrm{d}^D q \; \phi_k \, e^{iq\cdot z} + \frac{1}{(2\pi)^D} \int_{\Lambda/b<|q|<\Lambda} \mathrm{d}^D q \; \phi_k \, e^{iq\cdot z}, \end{aligned} \tag{1.29}$$

where b is a scale factor and $q = (\mathbf{k}, \omega)$. Now we wish to see the effect of successively integrating out the high-energy modes, increasing $b > 1$. This will give us the same Z but expressed in terms of only the low-energy modes, i.e.

$$Z = \int \mathcal{D}[\phi_>] \int \mathcal{D}[\phi_<] \, e^{-S(\phi_< + \phi_>)} = \int \mathcal{D}[\phi_<] \, e^{-S_{\text{eff}}(\phi_<)}, \tag{1.30}$$

with a new effective action $S_{\text{eff}}(\phi_<)$ for the low-energy modes. However, on this form the length/time scale has been altered by the scale factor b, giving $|q| < \Lambda/b$ and $|x| > ba$ Hence one needs to *rescale* the expression to get the correct units, which is done by

$$z \to z' = z/b\,, \qquad q \to q' = b\,q\,, \tag{1.31}$$

such that the rescaled variables have the correct units, $|q'| < \Lambda$ and $|x'| > a$. These two steps are the *renormalization-group transformation*,

(1) Integrate out high-energy modes above cutoff Λ/b,
(2) Rescaling $z \to z/b$, $q \to bq$. (1.32)

Considering the action to be defined by a (perhaps infinite) set of coupling constants, successive renormalization-group (RG) transformations will generate a flow of these coupling constants as the cutoff Λ successively decreases. Such a flow will have fixed-points, which will define the different phases and phase transitions of the system.

Now, a fixed-point action S^* is by definition an action for which

$$S^*_{\text{eff}}(\phi_<) = S^*(\phi), \tag{1.33}$$

i.e. S^* is invariant under the renormalization-group transformation. Hence the system has *scale invariance*, i.e. it "looks the same" on all length (and time) scales. This means that the correlation length has to be either zero or infinite. Zero correlation length, and hence infinite energy gap, means that there are no fluctuations and thus it describes a *stable* phase of matter. Infinite correlation length, hence zero energy gap, means that the system is *critical* with fluctuations on all scales. This is the case at a *phase transition*, which is an unstable phase where there exists at least one infinitesimal perturbation that will drive the system away from the fixed point.

Let us now consider the *perturbative renormalization group* around a fixed point. The fixed-point Hamiltonian density H^* will then be perturbed with all the local operators in the theory, $H = H^* + \sum_j g_j \phi_j$, so that the action becomes

$$S(\phi) = S^*(\phi) + \int \mathrm{d}^D z \sum_j g_j \phi_j(z) \tag{1.34}$$

with coupling constants g_j. Under a scale transformation $z \to z' = z/b$, the fields transforms as

$$\phi_j(z) \to \tilde{\phi}_j(z/b) = b^{\Delta_j} \phi_j(z), \tag{1.35}$$

which defines the *scaling dimension* Δ_j of the field ϕ_j. Hence under the RG transformation

$$S(\phi) \;\to\; S^*(\phi) + \int \mathrm{d}^D z \sum_j b^{\Delta_j - D} g_j \phi_j(z) \tag{1.36}$$

to first order in the coupling constants g_j. This means that

$$g_j \;\to\; g'_j = b^{\Delta_j - D} g_j. \tag{1.37}$$

Writing the rescaling parameter $b > 1$ as $b = e^{-\delta\ell}$, in terms of a "renormalization length" ℓ, this can be written as $g'_j - g_j = -(D - \Delta_j)\delta\ell$. As differential equations they become the first-order *renormalization-group equations*

$$\frac{\partial g_j}{\partial \ell} = (D - \Delta_j)\, g_j + \ldots \tag{1.38}$$

which determine the flow of the coupling constants as the energy scale is reduced.

We now see that the scaling dimensions Δ_j determines whether a coupling constant increases or decreases as the energy scale is reduced. Fields can therefore be classified as

- *Relevant*: If $\Delta_j < D$, the coupling g_j grows under the renormalization group and the field ϕ_j becomes "more important" at lower energy scales.
- *Irrelevant*: Conversely, if $\Delta_j > D$ then the coupling g_j decreases and the field ϕ_j becomes "less important" at lower energies.
- *Marginal*: If $\Delta_j = D$, the coupling g_j does not change to first order. To determine whether it grows or not one must go to higher orders in the perturbation expansion. If it grows due to higher-order contributions, then ϕ_j is *marginally relevant*, and if it decreases then ϕ_j is *marginally irrelevant*. Otherwise it is exactly marginal.

2

Bosonization and conformal field theory

In this chapter we give a short introduction to bosonization and conformal field theory[1]. This provides us with a unifying framework for the low-energy physics in gapless one-dimensional quantum systems.

Individual motion of electron-like quasiparticles is no longer possible when they are confined to one dimension. Instead one should expect a collective behavior. It turns out that this can be described in terms of density fluctuations. The technique known as bosonization allows a mapping from fermions to bosons, which express these collective degrees of freedom. It is a remarkable result that the low-energy limit of interacting fermions in one-dimension can be mapped exactly onto a free (i.e. non-interacting) boson field theory, with the Luttinger liquid replacing the Fermi liquid as the universal theory in one dimension [40–42, 58, 59]. Together with the concept of the renormalization group [23] this paradigm gives effective solutions for a multitude of different kinds of interacting models.

Emergent conformal invariance at low energies makes complete solutions possible in terms of conformal field theories [60]. In higher dimensions this is no longer true; not only is the general possibility of extending the bosonization procedure to higher dimensions unclear [61–63], in addition conformal invariance then no longer provides infinitely many local symmetries which makes conformal field theory much less powerful.

[1] See Refs. [27, 28, 43, 56, 57] for more complete accounts.

2.1 Interacting fermions in one dimension: The Luttinger liquid

2.1.1 Non-interacting Dirac fermions

Consider first non-interacting spinless fermions with some dispersion $\varepsilon(k)$, given by the hamiltonian

$$H_0 = \sum_k \varepsilon(k) c_k^\dagger c_k, \tag{2.1}$$

in terms of the fermion annihilation operator c_k at wavevector k, with

$$\{c_k^\dagger, c_{k'}^\dagger\} = \{c_k, c_{k'}\} = 0, \tag{2.2}$$

$$\{c_k^\dagger, c_{k'}\} = \delta_{k,k'}. \tag{2.3}$$

For fermions on a lattice, $\varepsilon(k)$ typically describes the cosine-dispersion of nearest-neighbor hopping, depicted in Fig. 2.1. Now, at sufficiently low energies all the physics takes place at the Fermi points, and we can make an approximation by linearizing the dispersion so that $E(k) \approx E_F + v_F(\pm k - k_F)$. While this linearization is only valid for momenta within some momentum cufoff Λ from the Fermi points $k = \pm k_F$, the Tomonaga-Luttinger model is obtained by extending the linearization to all momenta, shown in Fig. 2.2, thereby introducing an independent fermion for each of the two different branches,

$$H_0 = \sum_{r=\pm} \sum_k v_F(rk - k_F) c_{k,r}^\dagger c_{k,r}. \tag{2.4}$$

In the continuum limit, we can introduce the fermion field

$$\Psi(x) = \frac{1}{2\pi} \int \mathrm{d}k \, c_k \, e^{ikx}. \tag{2.5}$$

for the fermions in Eq. (2.1). The mode expansion of the field $\Psi(x)$ can be written as

$$\Psi(x) = \frac{1}{2\pi} \int \mathrm{d}k \left[c_{k_F+k} \, e^{i(k_F+k)x} + c_{-k_F+k} \, e^{i(-k_F+k)x} \right]. \tag{2.6}$$

Hence we can write $\Psi(x) = \Psi_R(x) + \Psi_L(x)$, with $\Psi_R(x) \equiv \psi_R(x) \, e^{ik_F x}$ and $\Psi_L(x) \equiv \psi_L(x) \, e^{-ik_F x}$ such that

$$\Psi(x) \;\; = \;\; \psi_R(x) \, e^{ik_F x} + \psi_L(x) \, e^{-ik_F x}, \tag{2.7}$$

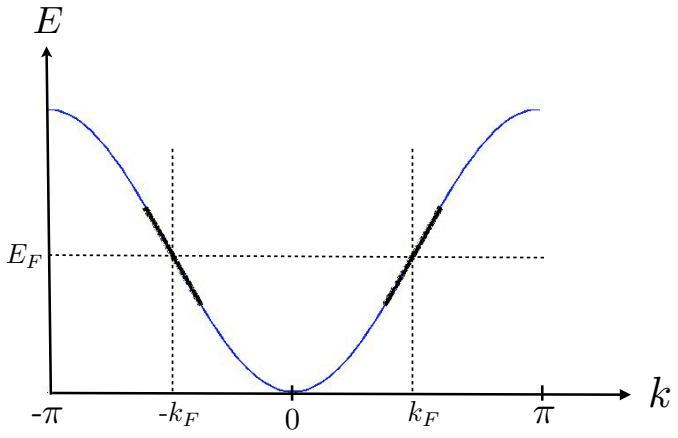

Figure 2.1: Dispersion relation for an electron nearest-neighbor hopping model in one dimension without interactions. In the ground state all the available electron states with energy below the Fermi energy E_F are filled. For sufficiently low energies the excitations can be described within a linearized approximation of the dispersion at the Fermi points $k = \pm k_F$.

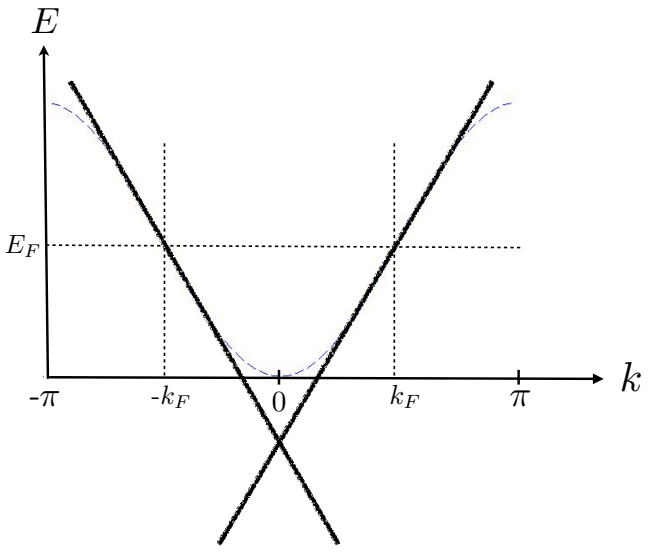

Figure 2.2: By extending the linearized dispersion at the Fermi points $k = \pm k_F$ in Fig. 2.1 to all momenta k, one obtains the one-dimensional Dirac Hamiltonian (2.14), for which the ground state is the filled Dirac sea below E_F. The divergences occurring in the theory due to this infinite Dirac sea are treated by normal-ordering the operators.

where

$$\psi_R(x) = \frac{1}{2\pi}\int \mathrm{d}k\, c_{k_F+k}\, e^{ikx}, \tag{2.8}$$

$$\psi_L(x) = \frac{1}{2\pi}\int \mathrm{d}k\, c_{-k_F+k}\, e^{ikx}, \tag{2.9}$$

with

$$\{\psi_R^\dagger(x),\psi_R^\dagger(y)\} = \{\psi_L(x),\psi_L(y)\} = 0, \tag{2.10}$$

$$\{\psi_R^\dagger(x),\psi_R^\dagger(y)\} = \{\psi_R(x),\psi_R(y)\} = 0, \tag{2.11}$$

$$\{\psi_R^\dagger(x),\psi_R(y)\} = \{\psi_L^\dagger(x),\psi_L(y)\} = \delta(x-y). \tag{2.12}$$

The fields $\psi_{R/L}$ are usually referred to as the slowly varying fields around the right/left Fermi points, since originally the theory is restricted to around the Fermi points,

$$\Psi(x) \approx \frac{1}{\sqrt{L}}\Big[\underbrace{\sum_{-\Lambda<k-k_F<\Lambda} c_k\, e^{ikx}}_{\psi_R(x)\,e^{ik_Fx}} + \underbrace{\sum_{-\Lambda<k+k_F<\Lambda} c_k\, e^{ikx}}_{\psi_L(x)\,e^{-ik_Fx}}\Big]. \tag{2.13}$$

In terms of these fields, the Hamiltonian (2.4) becomes

$$H_0 = -iv_F\int \mathrm{d}x\,\Big[\psi_R^\dagger\partial_x\psi_R - \psi_L^\dagger\partial_x\psi_L\Big] \tag{2.14}$$

which is the one-dimensional massless Dirac Hamiltonian [64]. The time-dependence of the fields follow from $e^{iH_0t}\psi_R(k)e^{-iH_0t} = \psi_R(k)e^{-iv_Ft}$ and $e^{iH_0t}\psi_L(k)e^{-iH_0t} = \psi_L(k)e^{+iv_Fkt}$, such that

$$\psi_R(x,t) = \frac{1}{2\pi}\int \mathrm{d}k\,\psi_R(k)\, e^{ik(x-v_Ft)}, \tag{2.15}$$

$$\psi_L(x,t) = \frac{1}{2\pi}\int \mathrm{d}k\,\psi_L(k)\, e^{ik(x+v_Ft)}, \tag{2.16}$$

hence ψ_R is a *right-moving*, and ψ_L a *left-moving* field, and we have that $\Psi(x,t) = \psi_R(x-v_Ft)e^{ik_Fx} + \psi_L(x+v_Ft)e^{-ik_Fx}$.

2.1.2 The Luttinger model

Consider now the interacting problem for electrons with spin. Then the field is given in terms of the two-component Dirac spinor $\Psi(x) = [\Psi_\uparrow(x),\Psi_\downarrow(x)]^T$, with each component $\Psi_\sigma(x) = \psi_{R\sigma}(x)\,e^{ik_Fx} + \psi_{L\sigma}(x)\,e^{-ik_Fx}$. The Coulomb repulsion between the electrons is given by

$$H_{int} = \int \mathrm{d}x\int \mathrm{d}y\; V(x-y)\,\rho_c(x)\,\rho_c(y), \tag{2.17}$$

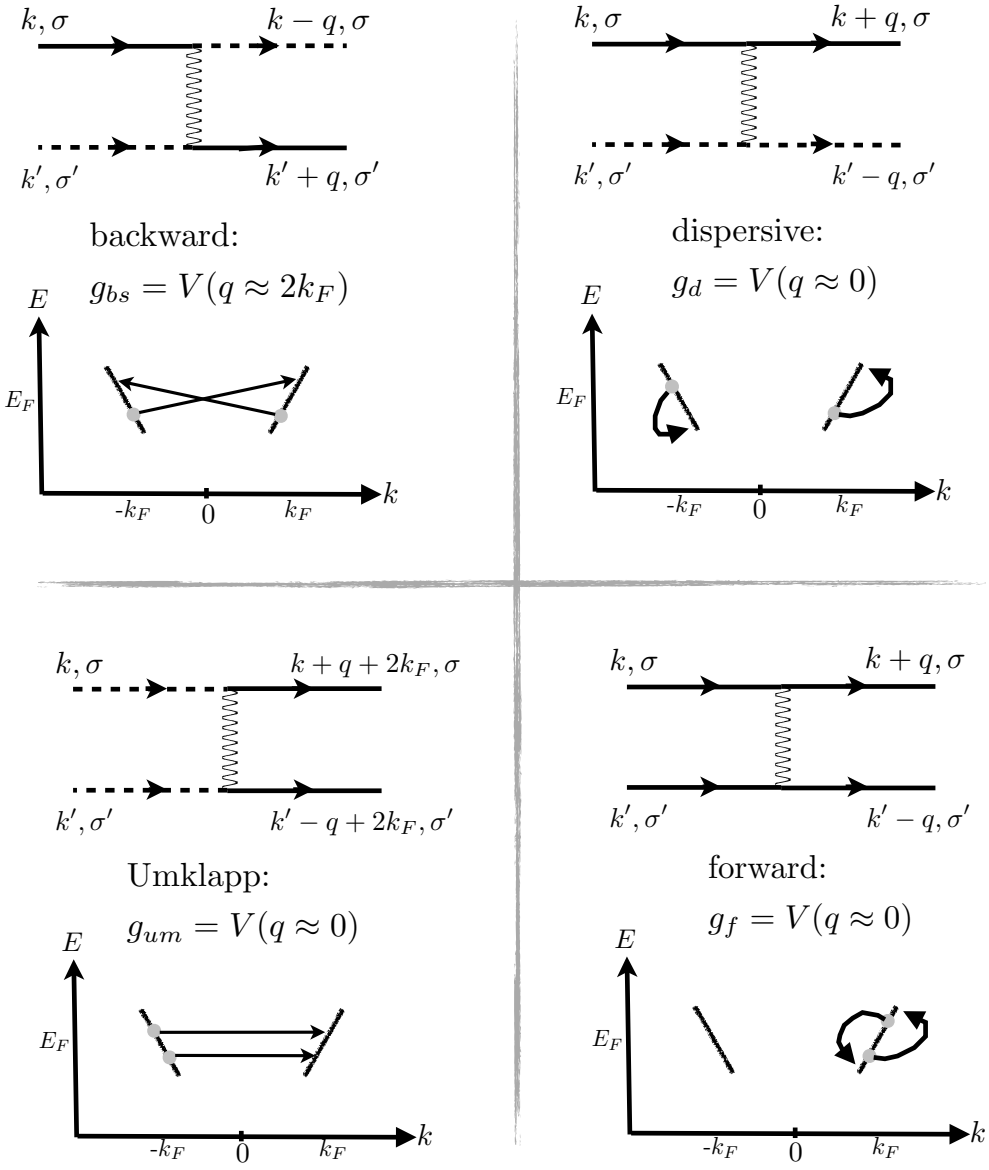

Figure 2.3: The four types of low-energy scattering processes for right-moving (full lines) and left-moving (dashed lines) electrons in one dimension. Sometimes they are also referred to as $g_1 = g_{bs}$, $g_2 = g_d$, $g_3 = g_{um}$ and $g_4 = g_f$. Each scattering type is associated with two values of the g parameter, $g_\perp$ and $g_{||}$ depending on whether the spins σ and σ' are equal or opposite, respectively [27].

where $\rho_c(x) = \Psi^\dagger(x)\Psi(x) = \Psi^\dagger_\uparrow(x)\Psi_\uparrow(x) + \Psi^\dagger_\downarrow(x)\Psi_\downarrow(x)$ is the electron charge density and $V(x-y)$ the Coulomb potential. In momentum space this becomes

$$H_{int} = \frac{1}{2L}\sum_{\sigma,\sigma'}\sum_{k,k',q} V(q)\, c^\dagger_{k+q,\sigma} c^\dagger_{k'-q,\sigma'} c_{k',\sigma'} c_{k,\sigma}, \tag{2.18}$$

where σ is the spin index. At low energies, the scattering processes around the Fermi points can be categorized into *backward*, *forward*, *dispersive* and *Umklapp* scattering, according to Fig. 2.3. The corresponding terms added to the Hamiltonian are

$$H_{bs} = g_{bs}\int \mathrm{d}x \sum_{\sigma=\uparrow,\downarrow} \psi^\dagger_{R,\sigma}(x)\psi_{L,\sigma}(x)\psi^\dagger_{L,-\sigma}(x)\psi_{R,-\sigma}(x), \tag{2.19}$$

$$\begin{aligned} H_d = \int \mathrm{d}x \sum_{\sigma=\uparrow,\downarrow} \Big[& g_{d\|}\, \psi^\dagger_{R,\sigma}(x)\psi_{R,\sigma}(x)\psi^\dagger_{L,\sigma}(x)\psi_{L,\sigma}(x) \\ & + g_{d\perp}\, \psi^\dagger_{R,\sigma}(x)\psi_{R,\sigma}(x)\psi^\dagger_{L,-\sigma}(x)\psi_{L,-\sigma}(x)\Big], \end{aligned} \tag{2.20}$$

$$H_{um} = g_{um}\frac{1}{2}\int \mathrm{d}x \sum_{\sigma=\uparrow,\downarrow} e^{-i4k_F x}\, \psi^\dagger_{R,\sigma}(x)\psi^\dagger_{R,-\sigma}(x)\psi_{L,\sigma}\psi_{L,-\sigma}(x) + \text{H.c.} \tag{2.21}$$

$$\begin{aligned} H_f = \frac{1}{2}\int \mathrm{d}x \sum_{\sigma=\uparrow,\downarrow}\sum_{r=R,L} \Big[& g_{f\|}\, \psi^\dagger_{r,\sigma}(x)\psi_{r,\sigma}(x)\psi^\dagger_{r,\sigma}(x+a)\psi_{r,\sigma}(x+a) \\ & + g_{f\perp}\, \psi^\dagger_{r,\sigma}(x)\psi_{r,\sigma}(x)\psi^\dagger_{r,-\sigma}(x)\psi_{r,-\sigma}(x)\Big]. \end{aligned} \tag{2.22}$$

Here the $g_{f\|}$ term in Eq. (2.22) has been *point splitted* by the short-distance cutoff a. The Umklapp process H_{um} arise due to the fact that the wave vectors are only defined up to a reciprocal lattice vector Q (i.e. a multiple of 2π, in units of the inverse lattice spacing). Hence in a scattering process one may have $k_1 + k_2 = k_3 + k_4 + Q$, but if all momenta are to be at the Fermi surface, i.e. the two Fermi points, one must have $4k_F = Q$. From this it follows that Umklapp scattering only occurs at half filling, i.e. when $k_F = \pi/2$. Away from half filling, and for the moment neglecting the backscattering, one has the Tomonaga-Luttinger model [40, 41], given by

$$H_{TL} = H_0 + H_d + H_f, \tag{2.23}$$

which can be solved exactly with bosonization.

2.1.3 Bosonization

The reason that the Tomonaga-Luttinger model can be solved exactly is that both the non-interacting term H_0 and the dispersive and forward

interactions are quadratic in the density fluctuations of right- and left-movers. These charge densities

$$\rho_R(x) = :\psi_R^\dagger(x)\psi_R(x):, \tag{2.24}$$
$$\rho_L(x) = :\psi_L^\dagger(x)\psi_L(x): \tag{2.25}$$

are bosonic in character

$$\left[\rho_r^\dagger(k)\,,\,\rho_{r'}^\dagger(-k')\right] = -r\,\delta_{r,r'}\delta_{p,p'}p\frac{L}{2\pi}. \tag{2.26}$$

Note that the normal-ordering[2] in Eqs. (2.24) and (2.25) is crucially needed due to the infinitely filled Dirac sea. It is readily checked that Eqs. (2.20) and (2.22) can be rewritten in terms of the densities as

$$H_d = \int \mathrm{d}x \sum_{\sigma=\uparrow,\downarrow}\Big[\,g_{d||}\,\rho_{R,\sigma}(x)\rho_{L,\sigma}(x) + \,g_{d\perp}\,\rho_{R,\sigma}(x)\rho_{L,-\sigma}(x)\Big], \tag{2.27}$$

$$H_f = \frac{1}{2}\int \mathrm{d}x \sum_{\sigma=\uparrow,\downarrow}\sum_{r=R,L}\Big[\,g_{f||}\,\rho_{r,\sigma}(x)\rho_{r,\sigma}(x) + \,g_{f\perp}\,\rho_{r,\sigma}(x)\rho_{r,-\sigma}(x)\,\Big]. \tag{2.28}$$

That the Dirac Hamiltonian (2.14) is quadratic in the density fluctuations can heuristically be expected from the naive classical analogue: With a linear dispersion, shifting the right Fermi point an amount δq_F gives an energy

$$\delta E \sim \frac{1}{2\pi}\int_0^{\delta q_F} \mathrm{d}q\, v_F\, q = \frac{v_F}{4\pi}(\delta q_F)^2, \tag{2.29}$$

and with $\rho_R \approx \delta q_F/2\pi$ one gets $E \sim \pi v_F \rho_R^2$. Hence one expects $H_0 \sim \rho_R^2 + \rho_L^2$.

A more formal approach is to note that the $U(1)_R \otimes U(1)_L$ symmetry, $\psi_R \to e^{i\theta_R}\psi_R$ and $\psi_L \to e^{i\theta_L}\psi_L$, of the Dirac Hamiltonian (2.14) means that the right- and left-moving densities $\rho_{R/L}(x)$ are the conserved "currents" $J_{R/L}(x)$ associated with the $U(1)$ symmetry. Writing the Hamiltonian quadratic in the currents,

$$H_0 = \pi v_F \int \mathrm{d}x\,\big[\,:J_R^2(x): + :J_L^2(x):\,\big], \tag{2.30}$$

is known as the Sugawara construction. We will return to this in Section 3.2, when treating the Kondo effect.

[2]Normal-ordering consists of putting all annihilation operators to the right of the creation operators, which is the same as subtracting the vacuum expectation value, $:\mathcal{O}_1\mathcal{O}_2: = \mathcal{O}_1\mathcal{O}_2 - \langle 0|\mathcal{O}_1\mathcal{O}_2|0\rangle$.

Temporarily neglecting the spin of the electrons, the bosonic version of H_0 follows by defining boson creation and annihilation operators

$$b_p^\dagger = \left(\frac{2\pi}{L|p|}\right)^{1/2} \rho_R^\dagger(p), \tag{2.31}$$

$$b_{-p}^\dagger = \left(\frac{2\pi}{L|p|}\right)^{1/2} \rho_L^\dagger(-p), \tag{2.32}$$

$$b_p = \left(\frac{2\pi}{L|p|}\right)^{1/2} \rho_R^\dagger(-p), \tag{2.33}$$

$$b_{-p} = \left(\frac{2\pi}{L|p|}\right)^{1/2} \rho_L^\dagger(p), \tag{2.34}$$

with $p > 0$, where

$$[b_p, b_{p'}^\dagger] = 2\pi\delta_{p,p'}. \tag{2.35}$$

In terms of these operators the Hamiltonian is mapped to

$$H = \sum_{k\neq 0} v_F|k| b_k^\dagger b_k + \frac{\pi v_F}{L}\left[N_R^2 + N_L^2\right], \tag{2.36}$$

i.e. free bosons. Here the last term, corresponding to the zero mode, contains the normal-ordered fermion number operators $N_r = \sum_k : c_r^\dagger(k)c_r(k) :$ (i.e. with the infinite vacuum expectation value subtracted), where $r = R/L$. The b-operators now define the bosonic field φ and its conjugate Π by mode expansion,

$$\varphi(x) = \frac{1}{2\pi}\int \mathrm{d}k \left(\frac{1}{2|k|}\right)^{1/2}\left[b_k e^{ikx} + b_k^\dagger e^{-ikx}\right], \tag{2.37}$$

$$\Pi(x) = \frac{1}{2\pi}\int \mathrm{d}k \left(\frac{|k|}{2}\right)^{1/2}\left[-ib_k e^{ikx} + ib_k^\dagger e^{-ikx}\right], \tag{2.38}$$

with canonical commutation relations

$$[\varphi(x), \Pi(y)] = i\delta(x-y), \tag{2.39}$$

$$[\varphi(x), \varphi(y)] = 0, \qquad [\Pi(x), \Pi(y)] = 0. \tag{2.40}$$

The field Π, being conjugate to φ, can be written as $\Pi = v_F^{-1}\partial_t\varphi$. In terms of this free boson field, the Hamiltonian H_0 is given by

$$H_0 = \int \mathrm{d}x \,\frac{v_F}{2}\left[\left(\partial_t\varphi(x)/v_F\right)^2 + \left(\partial_x\varphi(x)\right)^2\right]. \tag{2.41}$$

The boson field φ can be separated into a right-moving part ϕ and a left-moving part $\bar{\phi}$,

$$\varphi(x,t) = \phi(x - vt) + \bar{\phi}(x + v_F t), \tag{2.42}$$

with ϕ and $\bar{\phi}$ being chiral fields as opposed to φ and Π. With the complex notation $z = -i(x - v_F t)$, $\bar{z} = i(x + v_F t)$, which will be used extensively in Sec. 2.2, we have $\varphi(x,t) = \phi(z) + \bar{\phi}(\bar{z})$.

It is now common practice to introduce the so called dual boson field $\vartheta(x,t)$, defined through $\partial_x \vartheta = -\Pi = -v_F^{-1}\partial_t \varphi$, and with commutation relation

$$[\varphi(x), \vartheta(y)] = -i\theta(x-y), \tag{2.43}$$

where θ is the step function. The chiral fields can now be expressed as,

$$\phi = \frac{1}{2}(\varphi + \vartheta), \qquad \bar{\phi} = \frac{1}{2}(\varphi - \vartheta). \tag{2.44}$$

From the definition of ϑ it is clear that the fields have very non-local relations.

Bosonization formulas

Let us now write down the *bosonization formulas for the electron fields*:

$$\psi_{R\sigma}(x) = \frac{1}{\sqrt{2\pi a}}\eta_\sigma e^{-i\sqrt{4\pi}\phi_\sigma(x)}, \quad \psi^\dagger_{R\sigma}(x) = \frac{1}{\sqrt{2\pi a}}\eta_\sigma e^{i\sqrt{4\pi}\phi_\sigma(x)}, \tag{2.45}$$

$$\psi_{L\sigma}(x) = \frac{1}{\sqrt{2\pi a}}\bar{\eta}_\sigma e^{i\sqrt{4\pi}\bar{\phi}_\sigma(x)}, \quad \psi^\dagger_{L\sigma}(x) = \frac{1}{\sqrt{2\pi a}}\bar{\eta}_\sigma e^{-i\sqrt{4\pi}\bar{\phi}_\sigma(x)}, \tag{2.46}$$

with spin indexes $\sigma = \uparrow, \downarrow$. Here the Hermitian so called Klein factors η_σ and $\bar{\eta}_\sigma$, obeying the Clifford algebra

$$\{\eta_\sigma, \eta_{\sigma'}\} = \{\bar{\eta}_\sigma, \bar{\eta}_{\sigma'}\} = 2\delta_{\sigma,\sigma'}, \qquad \{\eta_\sigma, \bar{\eta}_{\sigma'}\} = 0, \tag{2.47}$$

and hence being Majorana particles, are needed to ensure the correct anticommutation relations for the fermionic fields. The lattice constant a enters as a short-distance cutoff.[3] For spinless fermions, these formulas can be compactly written in terms of the non-chiral fields as

$$\psi_{R/L}(x) = \frac{1}{\sqrt{2\pi a}}\,\eta\, e^{-i\sqrt{\pi}[\vartheta(x) \pm \varphi(x)]}, \tag{2.48}$$

with Klein factor η. For spinful fermions, one can introduce the charge and spin fields

$$\varphi_c = \frac{1}{\sqrt{2}}\left(\varphi_\uparrow + \varphi_\downarrow\right), \qquad \varphi_s = \frac{1}{\sqrt{2}}\left(\varphi_\uparrow - \varphi_\downarrow\right) \tag{2.49}$$

$$\vartheta_c = \frac{1}{\sqrt{2}}\left(\vartheta_\uparrow + \vartheta_\downarrow\right), \qquad \vartheta_s = \frac{1}{\sqrt{2}}\left(\vartheta_\uparrow - \vartheta_\downarrow\right) \tag{2.50}$$

[3] We will see in Eq. (2.80) that this is equivalent to making the exponentiated expression normal-ordered.

in terms of which the bosonization formula compactly can be written as

$$\psi_{r\sigma}(x) = \frac{1}{\sqrt{2\pi a}}\,\eta_{r\sigma}\, e^{-i\sqrt{2\pi}[r\varphi_c(x)-\vartheta_c(x)+\sigma(r\varphi_s(x)-\vartheta_s(x)]} \tag{2.51}$$

with $r = \pm$ for R/L and $s = \pm$ for $\uparrow, \downarrow$. With the fields decomposed into spin and charge parts, it follows that the Hamiltonian separates into a spin and a charge sector,

$$H = H_s + H_c, \tag{2.52}$$

also in the presence of the interactions. From a detailed analysis it follows that the independent spin and charge degrees of freedom propagates with different velocities, and this remarkable fact is known as *spin-charge separation.*

Solving the Tomonaga-Luttinger model

For simplicity, we will now restrict ourselves to the spinless case, and show how to exactly solve the interacting Tomonaga-Luttinger model. The non-interacting Hamiltonian density is given by

$$\mathcal{H}_0(x) = \frac{v_F}{2}\left[(\partial_x\vartheta(x))^2 + (\partial_x\varphi(x))^2\right], \tag{2.53}$$

in terms of the non-chiral fields φ and ϑ. The field gradients can be expressed in terms of the densities as

$$\partial_x\varphi(x) = -\pi\left[\rho_R(x) + \rho_L(x)\right], \tag{2.54}$$

$$\partial_x\vartheta(x) = \pi\left[\rho_R(x) - \rho_L(x)\right], \tag{2.55}$$

such that $\partial_x\varphi(x)$ is the total density and $\partial_x\vartheta(x)$ the electrical current operator. Then the forward interaction (2.22) is now given by

$$\begin{aligned}\mathcal{H}_f(x) &= \frac{g_f}{2}\Big[\rho_R(x)\rho_R(x) + \rho_L(x)\rho_L(x)\Big] \\ &= \frac{g_f}{2(2\pi)^2}\Big[(\partial_x\varphi - \partial_x\vartheta)^2 + (\partial_x\varphi + \partial_x\vartheta)^2\Big] \\ &= \frac{g_f}{(2\pi)^2}\left[(\partial_x\vartheta(x))^2 + (\partial_x\varphi(x))^2\right].\end{aligned} \tag{2.56}$$

Comparing to Eq. (2.53) one sees that the forward interaction is exactly the same as the Hamiltonian density, thus only changing the Fermi velocity when they are added together. Similarly, the dispersive interaction (2.20) becomes

$$\mathcal{H}_d(x) = g_d\,\rho_R(x)\rho_L(x) = \frac{g_d}{(2\pi)^2}\left[(\partial_x\vartheta(x))^2 - (\partial_x\varphi(x))^2\right]. \tag{2.57}$$

Thus, while the forward interaction only renormalizes the Fermi velocity, the dispersive term changes the relative weight between the $\partial_x\vartheta$ and $\partial\varphi$ terms in the Hamiltonian. One can incorporate these two effects by introducing two parameters, the renormalized Fermi velocity v and the Luttinger parameter K, such that $H = H_0 + H_f + H_d$ can be written as

$$H = \frac{v}{2}\int \mathrm{d}x \, \left[K \left(\partial_x\vartheta(x)\right)^2 + \frac{1}{K}\left(\partial_x\varphi(x)\right)^2 \right], \tag{2.58}$$

with

$$v = \left[\left(v_F + \frac{g_f}{\pi} \right)^2 - \left(\frac{g_d}{\pi} \right)^2 \right]^{1/2}, \tag{2.59}$$

$$K = \left[\frac{\pi v_F + g_f - g_d}{\pi v_F + g_f + g_d} \right]^{1/2}. \tag{2.60}$$

A rescaling of the fields,

$$\varphi/\sqrt{K} \mapsto \varphi, \tag{2.61}$$

$$\vartheta\sqrt{K} \mapsto \vartheta, \tag{2.62}$$

brings the Hamiltonian back to canonical form

$$H = \frac{v}{2}\int \mathrm{d}x \, \left[\left(\partial_x\vartheta(x)\right)^2 + \left(\partial_x\varphi(x)\right)^2 \right], \tag{2.63}$$

while changing the exponents in the bosonization formula to

$$\psi_{R/L}(x) = \frac{1}{\sqrt{2\pi a}}\,\eta\, e^{-i\sqrt{\pi}\left[\vartheta(x)/\sqrt{K} \pm \sqrt{K}\varphi(x)\right]}, \tag{2.64}$$

2.1.4 Correlation functions

Correlation functions can now readily be obtained since the theory is quadratic in the bosonic fields. Expectation values are evaluated as

$$\langle \mathcal{O} \rangle = \frac{1}{Z}\int \mathcal{D}[\varphi] \int \mathcal{D}[\vartheta] \; \mathcal{O} \; e^{-S[\varphi,\vartheta]}, \tag{2.65}$$

where the imaginary-time action is given by

$$S[\varphi,\vartheta] = -\int_0^\beta \mathrm{d}\tau \int \mathrm{d}x \left[\frac{i}{\pi}\partial_x\vartheta\partial_\tau\varphi - \frac{v}{2}\left((\partial_x\vartheta)^2 + (\partial_x\varphi)^2\right) \right] \tag{2.66}$$

which is on quadratic form in Fourier space

$$\begin{aligned} S[\varphi,\vartheta] = & -\frac{1}{\beta L}\sum_q \sum_{\omega_n} \Big[-\frac{iq\omega_n}{\pi}\varphi(q,\omega_n)\vartheta(-q,-\omega_n) \\ & -\frac{v}{2}\left(q^2\vartheta(q,\omega_n)\vartheta(-q,-\omega_n) + q^2\varphi(q,\omega_n)\varphi(-q,-\omega_n) \right) \Big]. \end{aligned} \tag{2.67}$$

Using the relation $-v\partial_t\vartheta = \partial_x\varphi$, completing the square in the action, and using the standard rules for Gaussian integration, one obtains

$$\langle\varphi^*(q_1,\omega_{n1})\varphi(q_2,\omega_{n2})\rangle = \frac{\pi\delta_{q_1,q_2}\delta_{\omega_{n1},\omega_{n2}}L\beta}{\omega_{n1}^2/v + vk_1^2} \tag{2.68}$$

for the boson field, hence giving the correlation function

$$\begin{aligned}\langle\varphi(x,\tau)\varphi(0,0)\rangle &- \langle[\varphi(0,0)]^2\rangle \\ &= \frac{1}{2\pi\beta}\sum_{\omega_n}\int \mathrm{d}q\,\frac{2\pi}{\omega_n^2/v + vk^2}\left(\cos(qx+\omega_n\tau)-1\right).\end{aligned} \tag{2.69}$$

The asymptotic of the correlation function at zero temperature is obtained as

$$\langle\varphi(x,\tau)\varphi(0,0)\rangle - \langle[\varphi(0,0)]^2\rangle \;\sim\; -\frac{1}{4\pi}\ln\left[\frac{x^2+\tau^2}{a^2}\right] \tag{2.70}$$

when $x,\tau \gg a$. The correlator for the dual bosonic field ϑ follows in exactly the same way. The chiral fields have similar chiral correlators

$$\langle\phi(z)\phi(z')\rangle - \langle[\phi(z)]^2\rangle \quad\sim\quad -\frac{1}{4\pi}\ln\left[\frac{z-z'}{a}\right] \tag{2.71}$$

$$\langle\bar\phi(\bar z)\bar\phi(\bar z')\rangle - \langle[\bar\phi(\bar z)]^2\rangle \quad\sim\quad -\frac{1}{4\pi}\ln\left[\frac{\bar z-\bar z'}{a}\right] \tag{2.72}$$

The Dirac fermion correlation function follows from the same procedure. The imaginary-time action corresponding to the Dirac Hamiltonian (2.14) is given by

$$S[\psi^\dagger,\psi] = -\int_0^\beta \mathrm{d}\tau\int \mathrm{d}x\Big[\,\psi_R^\dagger(iv_F\partial_x-\partial_\tau)\psi_R + \psi_L^\dagger(-iv_F\partial_x-\partial_\tau)\psi_L\Big], \tag{2.73}$$

which allows the correlation functions to be evaluated in standard fashion[4],

$$\begin{aligned}\langle\psi_{R/L}^\dagger(x,\tau)\psi_{R/L}(0,0)\rangle &- \langle\psi_{R/L}^\dagger(0,0)\psi_{R/L}(0,0)\rangle \\ &= \frac{1}{L\beta}\sum_{q,\omega_n}\frac{1}{-i\omega_n \mp v_F q}e^{-iqx-i\omega_n\tau} \approx \frac{1}{2\pi}\left(\frac{1}{v_F\tau \mp ix}\right)\end{aligned} \tag{2.74}$$

where the last equality follows in the zero-temperature limit. In complex coordinates, $z = -i(x-v_Ft) = v_F\tau - ix$, we can write this as

$$\langle\psi_R(z)\psi_R^\dagger(z')\rangle \quad\sim\quad \frac{1}{2\pi}\,\frac{1}{z-z'} \tag{2.75}$$

$$\langle\psi_L(\bar z)\psi_L^\dagger(\bar z')\rangle \quad\sim\quad \frac{1}{2\pi}\,\frac{1}{\bar z-\bar z'}. \tag{2.76}$$

[4]See e.g. Ref. [11].

We are now in a position to calculate the correlation functions for the interacting electrons in the Tomonaga-Luttinger model (2.63). The bosonization formula (2.64) is an example of a normal-ordered exponential known as a *vertex operator*. The multiplication rule for vertex operators of the form $e^{i\alpha\phi(z)}$ follows from the Campbell-Baker-Hausdorff formula $e^A e^B = e^{A+B}e^{[A,B]/2}$ when $[A,B]$ is a constant. For a single bosonic operator b, and $A = \alpha b + \alpha' b^\dagger$, $B = \beta b + \beta' b^\dagger$,

$$: e^A :: e^B := e^{\alpha' b^\dagger} e^{\alpha b} e^{\beta' b^\dagger} e^{\beta b} = e^{\alpha' b^\dagger} e^{\beta' b^\dagger} e^{\alpha b} e^{\beta b} e^{\alpha\beta'} =: e^{A+B} : e^{\langle 0|AB|0\rangle}. \tag{2.77}$$

Since they are just combinations of independent harmonic oscillators, it follows that Eq. (2.77) also applies to the boson field ϕ and $\bar{\phi}$. Hence we arrive at the important formula

$$e^{i\alpha\phi(z)} e^{i\beta\phi(z')} = e^{i\alpha\phi(z)+i\beta\phi(z')} e^{-\alpha\beta\langle\phi(z)\phi(z')\rangle}, \tag{2.78}$$

where normal-ordering of the vertex operators is implied. From the expression (2.71) for the boson correlator, it follows that

$$e^{i\alpha\phi(z)} e^{i\beta\phi(z')} = e^{i\alpha\phi(z)+i\beta\phi(z')} (z-z')^{\alpha\beta/4\pi}. \tag{2.79}$$

It also follows that the normal-ordering is the same as normalizing the vacuum expectation value of the vertex operator,

$$\begin{aligned} : e^{i\alpha\phi(z)} : \;&=\; \frac{e^{i\alpha\phi(z)}}{\langle e^{i\alpha\phi(z)}\rangle} = \frac{e^{i\alpha\phi(z)}}{e^{\langle[i\alpha\phi(z)]^2\rangle/2}} = \frac{e^{i\alpha\phi(z)}}{e^{-2\alpha^2\langle\phi(a)\phi(0)\rangle}} \\ &= \frac{e^{i\alpha\phi(z)}}{e^{(\alpha^2/8\pi)\ln a}} = \frac{e^{i\alpha\phi(z)}}{a^{\alpha^2/8\pi}}. \end{aligned} \tag{2.80}$$

Since the bosonization formula (2.48) has $\alpha = \sqrt{4\pi}$ in the exponent, we see that the prefactor $a^{-1/2}$ is simply another way of writing that the operator is normal-ordered.

We can now obtain the electron correlation function in the Tomonaga-Luttinger model. First, note that in the non-interacting case (i.e. $g_f = g_d = 0 \Rightarrow K = 1$), the bosonization formula (2.48) gives

$$\begin{aligned} \langle\psi_R^\dagger(x,\tau)\psi_R(0,0)\rangle \;&=\; \frac{1}{2\pi a}\langle\, e^{i\sqrt{\pi}[\vartheta(x,\tau)+\varphi(x,\tau)]} e^{-i\sqrt{\pi}[\vartheta(0,0)+\varphi(0,0)]}\rangle \\ &= \frac{1}{2\pi a}\langle\, e^{i\sqrt{4\pi}\phi(x,\tau)} e^{-i\sqrt{4\pi}\phi(0,0)}\rangle = \frac{1}{2\pi a}\langle\, e^{i\sqrt{4\pi}[\phi(x,\tau)-\phi(0,0)]}\rangle \\ &= \frac{1}{2\pi a} e^{-2\pi\langle[\phi(x,\tau)-\phi(0,0)]^2\rangle} = \frac{1}{2\pi a} e^{4\pi[\langle\phi(x,\tau)\phi(0,0)\rangle - \langle[\phi(0,0)]^2\rangle]} \\ &= \frac{1}{2\pi a} e^{4\pi[\langle\phi(x,\tau)\phi(0,0)\rangle - \langle[\phi(0,0)]^2\rangle]} = \frac{1}{2\pi a} e^{-\ln[(v_F\tau - ix)/a]} \\ &= \frac{1}{2\pi}\,\frac{1}{v_F\tau - ix}, \end{aligned} \tag{2.81}$$

and similarly $\langle \psi_L^\dagger(x,\tau)\psi_L(0,0)\rangle = (2\pi)^{-1}(v_F\tau+ix)^{-1}$. Hence the bosonization formula (2.48) reproduces the correct correlation functions (2.74) for non-interacting electrons. For interacting spinless fermions, we instead get

$$\begin{aligned}
\langle \psi_R^\dagger(x,\tau)\psi_R(0,0)\rangle = \;& = \\
&= \frac{1}{2\pi a}\big\langle\, e^{i\sqrt{\pi}\left[\vartheta(x,\tau)/\sqrt{K}+\sqrt{K}\varphi(x,\tau)\right]} e^{-i\sqrt{\pi}\left[\vartheta(0,0)/\sqrt{K}+\sqrt{K}\varphi(0,0)\right]}\big\rangle \\
&= \frac{1}{2\pi a}\big\langle\, e^{i\sqrt{\pi}\left(\sqrt{K}+\frac{1}{\sqrt{K}}\right)\phi(x,\tau)} e^{i\sqrt{\pi}\left(\sqrt{K}-\frac{1}{\sqrt{K}}\right)\bar\phi(x,\tau)} \\
&\qquad\qquad \times e^{-i\sqrt{\pi}\left(\sqrt{K}+\frac{1}{\sqrt{K}}\right)\phi(0,0)} e^{-i\sqrt{\pi}\left(\sqrt{K}-\frac{1}{\sqrt{K}}\right)\bar\phi(0,0)}\big\rangle \\
&= \frac{1}{2\pi a}\big\langle\, e^{i\sqrt{\pi}\left(\sqrt{K}+\frac{1}{\sqrt{K}}\right)\phi(x,\tau)} e^{-i\sqrt{\pi}\left(\sqrt{K}+\frac{1}{\sqrt{K}}\right)\phi(0,0)}\big\rangle \\
&\qquad\qquad \times \big\langle e^{i\sqrt{\pi}\left(\sqrt{K}-\frac{1}{\sqrt{K}}\right)\bar\phi(x,\tau)} e^{-i\sqrt{\pi}\left(\sqrt{K}-\frac{1}{\sqrt{K}}\right)\bar\phi(0,0)}\big\rangle \\
&= \frac{1}{2\pi}\,\frac{1}{(v\tau-ix)^{(\sqrt{K}+1/\sqrt{K})^2/4}}\frac{1}{(v\tau+ix)^{(\sqrt{K}-1/\sqrt{K})^2/4}},
\end{aligned} \tag{2.82}$$

and similarly for the left-moving fermion,

$$\begin{aligned}
\langle \psi_L^\dagger(x,\tau)\psi_L(0,0)\rangle \;& = \\
&= \frac{1}{2\pi}\,\frac{1}{(v\tau+ix)^{(\sqrt{K}+1/\sqrt{K})^2/4}}\frac{1}{(v\tau-ix)^{(\sqrt{K}-1/\sqrt{K})^2/4}}.
\end{aligned} \tag{2.83}$$

We thus see that the interactions (in fact, only the dispersive) mix the right- and left-moving bosonic fields, such that a fermion which is right-moving in the unperturbed theory becomes a mixture of right- and left-moving fields. For the spinless fermion field we thus have

$$\begin{aligned}
\langle \Psi^\dagger(x,\tau)\Psi(0,0)\rangle = & \\
&= \frac{1}{2\pi}\,\frac{1}{(v\tau-ix)^{(\sqrt{K}+1/\sqrt{K})/2}}\frac{1}{(v\tau+ix)^{(\sqrt{K}-1/\sqrt{K})^2/4}} \\
&\quad + \frac{1}{2\pi}\,\frac{1}{(v\tau+ix)^{(\sqrt{K}+1/\sqrt{K})/2}}\frac{1}{(v\tau-ix)^{(\sqrt{K}-1/\sqrt{K})^2/4}}.
\end{aligned} \tag{2.84}$$

The density-density correlator is obtained from

$$\begin{aligned}
\rho(x) \;&=\; \psi_R^\dagger(x)\psi_R(x) + \psi_L^\dagger(x)\psi_L(x) \\
&\quad + \psi_R^\dagger(x)\psi_L(x)e^{-i2k_Fx} + \psi_L^\dagger(x)\psi_R(x)e^{i2k_Fx} \\
&= \frac{1}{2\pi}\left[\partial_x\varphi(x) + e^{i\sqrt{4\pi}\varphi(x)}e^{-i2k_Fx} + e^{-i\sqrt{4\pi}\varphi(x)}e^{i2k_Fx}\right]
\end{aligned} \tag{2.85}$$

which gives

$$\begin{aligned}\langle\rho(x,\tau)\rho(0,0)\rangle &= \frac{K}{4\pi^2}\left[\frac{1}{(v\tau+ix)^2}+\frac{1}{(v\tau-ix)^2}\right] \\ &\quad +\frac{2}{(2\pi a)^2}\cos(2k_Fx)\left(\frac{x}{a}\right)^{-2K} \end{aligned} \tag{2.86}$$

in the large-distance limit $x \gg a$.

In order to get the above correlation functions in real time one needs to perform the analytic continuation $\tau \to it$.

2.1.5 Backscattering interactions

Even though we now have solved the Tomonaga-Luttinger model, we must understand the effects of the electron backscattering terms (2.19) from the Coulomb interaction in order to get a full understanding of the spinful Luttinger liquid. On bosonized form we have

$$H_{bs} = g_{bs}\frac{1}{2\pi^2}\int \mathrm{d}x\, \cos\left[\sqrt{8\pi K}\varphi_s(x)\right], \tag{2.87}$$

where $\varphi_s = (\varphi_\uparrow - \varphi_\downarrow)/\sqrt{2}$. With the Hilbert space completely separated into a charge and a spin sector, known as the *spin-charge separation*, the backscattering takes place in the spin sector. The charge sector is thus completely described by a free boson Hamiltonian, whereas the spin sector is governed by a Hamiltonian $H_s = H_{s0} + H_{bs}$. This is known as the *sine-Gordon model*, and is solved, in the sense of obtaining the phase diagram and critical exponents, using the renormalization group[5].

As seen, the electron-electron backscattering interaction in Eq. (2.19) can only occur if the fermions have spin. However, in the presence of impurities there can also be single-particle backscattering generated at the impurity site. Such single-particle backscattering operators, $\psi_R^\dagger(x)\psi_L(x)$ and $\psi_L^\dagger(x)\psi_R(x)$, will also be described by vertex operators after bosonization. The equal-time, equal-position vertex operators $e^{\pm i\sqrt{4\pi}\varphi}$ and $\partial_x\vartheta$ have the same commutation relations as the spin matrices $\sigma^\pm$ and σ^z, which is what one expects from the identification $\psi_R^\dagger\psi_L = \sigma^+$, $\psi_L^\dagger\psi_R = \sigma^-$ and $\psi_R^\dagger\psi_R - \psi_L^\dagger\psi_L = \sigma^z$.

[5]For a pedagogical review, see Ref. [65].

2.2 Conformal field theory

One of the most striking features of the linearization procedure at low energies above, resulting in the relativistic Dirac fermions and the free bosonic field, is that it shows the appearance of conformal symmetry. This roughly corresponds to translational, rotational and scale invariance, and field theories with these symmetries are known as conformal field theories. They provide a unified framework for describing universal low-energy properties of gapless one-dimensional quantum and two-dimensional classical systems [60]. There are also other applications: For some topological quantum systems (which will be discussed in Chapter 5) there is a correspondence between the gapless one-dimensional edge and the gapped two-dimensional bulk that seems to allow the bulk wavefunctions to be described using a 2D conformal field theory [66]. For some other special systems there are "conformal quantum critical points" where a two-dimensional conformal theory represents the ground state wave function in two spatial dimensions [67]. Boundary conformal field theory provides a powerful way to understand non-Fermi liquid behavior in quantum impurity problems [68, 69], as we will see in Section 3.2.

2.2.1 Conformal invariance in two dimensions

In the imaginary-time formalism, a one-dimensional quantum system and a two-dimensional classical system are both effectively two-dimensional. When discussing conformal field theory in two dimensions, we do not need to make a distinction between the two.

Conformal transformations

Let us first define conformal transformations in arbitrary dimensions. Distances are given through

$$\mathrm{d}s^2 = g_{\mu\nu}\mathrm{d}x^\mu \mathrm{d}x^\nu, \tag{2.88}$$

with metric $g_{\mu\nu}$. Under a coordinate transformation $\mathbf{x} \to \mathbf{x}'$, the metric transforms covariantly,

$$g'_{\mu\nu}(\mathbf{x}') = \frac{\partial x^\alpha}{\partial x'^\mu}\frac{\partial x^\beta}{\partial x'^\nu} g_{\alpha\beta}(\mathbf{x}). \tag{2.89}$$

The coordinate transformation is a *conformal transformation* if it leaves the metric invariant up to a local scale factor, i.e. if

$$g'_{\mu\nu}(\mathbf{x}') = \Lambda(\mathbf{x}) g_{\mu\nu}(\mathbf{x}). \tag{2.90}$$

The name comes from the fact that these transformations preserve the angle between two vectors.

Under an infinitesimal transformation $x^\mu \to x^\mu + \varepsilon^\mu(\mathbf{x})$ the metric transforms as $g_{\mu\nu} \to g_{\mu\nu} - (\partial_\mu \varepsilon_\nu + \partial_\nu \varepsilon_\mu)$. For the transformation to be conformal, the expression in parenthesis must be proportional to the metric. This leads to the constraint

$$\partial_\mu \varepsilon_\nu + \partial_\nu \varepsilon_\mu = \frac{2}{d} \partial_\rho \varepsilon^\rho g_{\mu\nu} \tag{2.91}$$

in D dimensions. For $D > 2$ it can be shown that this constraint on the infinitesimal transformations only allows translations, dilations, rotations and what is known as "special conformal transformations". Upon "exponentiation" the finite versions of these transformations are

$$x'^\mu = x^\mu + a^\mu \qquad \text{translation,} \tag{2.92}$$

$$x'^\mu = \alpha x^\mu \qquad \text{dilatation,} \tag{2.93}$$

$$x'^\mu = M^\mu{}_\nu x^\nu \qquad \text{rotation,} \tag{2.94}$$

$$x'^\mu = \frac{x^\mu - b^\mu \mathbf{x}^2}{1 - 2\mathbf{b}\cdot\mathbf{x} + b^2\mathbf{x}^2} \qquad \text{"special conformal transformation".} \tag{2.95}$$

Hence the group of conformal transformations is finite-dimensional for $D > 2$.

For $D = 2$ dimensions however, Eqs. (2.91) become the Cauchy-Riemann equations, $\partial_1 \varepsilon_1 = \partial_2 \varepsilon_2$ and $\partial_1 \varepsilon_2 = \partial_2 \varepsilon_1$. This shows that the conformal transformations in two dimensions are the analytic functions, hence the conformal group is infinite-dimensional. Let us Introduce complex coordinates,

$$z = \tau - ix, \quad \bar{z} = \tau + ix. \tag{2.96}$$

Then, under a change of coordinates $z \to w(z)$, $\bar{z} \to \bar{w}(\bar{z})$, Eq. (2.89) for the transformation of the metric becomes

$$g \to (\partial w/\partial z)(\partial \bar{w}/\partial \bar{z}) g, \tag{2.97}$$

and the Cauchy-Riemann equations are

$$\frac{\partial w^2}{\partial z^1} = \frac{\partial w^1}{\partial z^2} \quad \text{and} \quad \frac{\partial w^1}{\partial z^1} = -\frac{\partial w^2}{\partial z^2} \tag{2.98}$$

for holomorphic functions $w(z)$ and

$$\frac{\partial w^2}{\partial z^1} = -\frac{\partial w^1}{\partial z^2} \quad \text{and} \quad \frac{\partial w^1}{\partial z^1} = \frac{\partial w^2}{\partial z^2} \tag{2.99}$$

for antiholomorphic functions $\bar{w}(\bar{z})$, with (z^1, z^2) the coordinates in the complex z plane and similarly for w.

Generators and global conformal transformations

Now, any infinitesimal transformation can be written as $w(z) = z + \varepsilon(z)$, $\bar{w}(\bar{z}) = \bar{z} + \bar{\varepsilon}(\bar{z})$. Assuming $\varepsilon(z)$ and $\bar{\varepsilon}(\bar{z})$ can be Laurent expanded around the origin, one arrives at the following infinite set of generators

$$\ell_n = -z^{n+1}\partial_z \ , \qquad \bar{\ell}_n = -\bar{z}^{n+1}\partial_{\bar{z}} \tag{2.100}$$

for the effect on a *classical* field. They have the commutation relations

$$\begin{array}{rcl} [\ell_n, \ell_m] & = & (n-m)\ell_{m+n} \\ \left[\bar{\ell}_n, \bar{\ell}_m\right] & = & (n-m)\bar{\ell}_{m+n},, \\ \left[\ell_n, \bar{\ell}_m\right] & = & 0, \end{array} \tag{2.101}$$

known as the loop, or Witt, algebra. It shows that the infinite-dimensional conformal algebra is decomposed into a direct sum of one generated by the set of ℓ_n and the other by the set of $\bar{\ell}_n$.

The algebra (2.101) has two finite-dimensional subalgebras generated by $\{\ell_{-1}, \ell_0, \ell_1\}$ and $\left\{\bar{\ell}_{-1}, \bar{\ell}_0, \bar{\ell}_1\right\}$ respectively. These generate translation, dilatation, rotation and special conformal transformations. Each set generates so called *projective conformal transformations*, also known as Möbius transformations,

$$w(z) = \frac{az+b}{cz+d} \ , \qquad ad - bc = 1, \tag{2.102}$$

with a, b, c and d complex numbers.

Two-dimensional conformal field theories

Now we are ready to state what conformal field theory is [60]: Given a set of local scaling fields $A_j(z, \bar{z})$, transforming as $A_j \to \lambda^{-d_j} A_j$ under scale transformations and forming a complete set in the sense that they can generate all states, a conformal field theory is described by the correlation functions of this set of scaling fields. In particular,

(a) There is a subset of the fields $A_j(z, \bar{z})$ consisting of *primary fields* $\phi_n(z, \bar{z})$, which transform under *any* conformal transformation as

$$\phi_n(z, \bar{z}) \to \left(\frac{\partial w}{\partial z}\right)^{\Delta_n} \left(\frac{\partial \bar{w}}{\partial \bar{z}}\right)^{\bar{\Delta}_n} \phi'_n(w(z), \bar{w}(\bar{z})), \tag{2.103}$$

when inside a correlator. Here Δ_n and $\bar{\Delta}_n$ are real non-negative numbers known as the dimension of the field $\phi_n(z, \bar{z})$, and $x_n = \Delta_n + \bar{\Delta}_n$ as the *scaling dimension* and $s_n = \Delta_n - \bar{\Delta}_n$ as the "*spin*".

(b) A complete set of the scaling fields A_j consists of "conformal families" or "towers" $[\phi_n]$. The tower $[\phi_n]$ contains the primary field ϕ_n and infinitely many *secondary*, or *descendant*, fields, with dimensions $\Delta_n^{(k)} = \Delta_n + k$, $\bar{\Delta}_n^{(\bar{k})} = \bar{\Delta}_n + \bar{k}$, where $k, \bar{k} = 0, 1, 2, ...$ Under conformal transformations, a secondary field A_j is transformed into a linear combination of other fields in the same tower. Hence, each conformal tower corresponds to some irreducible representation of the conformal group.

(c) Correlation functions of any secondary field can be obtained from the corresponding primary fields, therefore the correlation functions of the primary fields contain all the information about the conformal field theory.

(d) The fields which transform as in Eq. (2.103) under projective conformal transformations (2.102) are called *quasi-primary fields*. Hence every primary field is also quasi-primary, but a secondary field may or may not be quasi-primary.

(e) Any local field A_j can be written as a linear combination of quasi-primary fields and their derivatives to all orders.

(f) The assumed completeness of the set $\{A_j\}$ of local fields means that there is an operator algebra, the *operator product expansion*,

$$A_j(z)A_j(0) = \sum_k C_{ij}^k(z)A_k(0) \tag{2.104}$$

inside correlators, where $C_{ij}^k(z)$ are c-number functions which should be single-valued for locality.

(g) The vacuum is invariant under projective conformal transformations.

2.2.2 Correlation functions

The expectation values $\langle\phi(\mathbf{x})\rangle$ will generally vanish unless there is some spontaneous symmetry breaking. Therefore two-point functions are the same as correlation functions. The form (2.103) for the correlation functions of the quasi-primaries under projective conformal transformations determine their two-point functions up to a non-universal constant. Consider first a scale transformation $\mathbf{x} \to \lambda\mathbf{x}$, for which Eq. (1.35) gives

$$\langle\phi_1(\mathbf{x}_1)\phi_2(\mathbf{x}_2)\rangle = \lambda^{\Delta_1+\Delta_2}\langle\phi_1(\lambda\mathbf{x}_1)\phi_2(\lambda\mathbf{x}_2)\rangle, \tag{2.105}$$

and then invariance under translation and rotation which means that the two-point function can only depend on the distance $|\mathbf{x}_1 - \mathbf{x}_2|$. This constrains the form of the two-point function to

$$\langle \phi_1(\mathbf{x}_1)\phi_2(\mathbf{x}_2)\rangle = \frac{C_{12}}{|\mathbf{x}_1 - \mathbf{x}_2|^{\Delta_1+\Delta_2}}. \tag{2.106}$$

Furthermore, invariance under the special conformal transformations constrains it even further, such that two quasi-primary fields are only correlated if they have the same dimension

$$\langle \phi_1(\mathbf{x}_1)\phi_2(\mathbf{x}_2)\rangle = \begin{cases} C_{12}|\mathbf{x}_1 - \mathbf{x}_2|^{-2\Delta_1} & \Delta_1 = \Delta_2, \\ 0 & \Delta_1 \neq \Delta_2. \end{cases} \tag{2.107}$$

In complex coordinates

$$\langle \phi_1(z_1,\bar{z}_1)\phi_2(z_2,\bar{z}_2)\rangle = \frac{C_{12}}{(z_1 - z_2)^{2\Delta}(\bar{z}_1 - \bar{z}_2)^{2\bar{\Delta}}}, \tag{2.108}$$

when $\Delta_1 = \Delta_2 = \Delta$ and $\bar{\Delta}_1 = \bar{\Delta}_2 = \bar{\Delta}$. The coefficient C_{12} is in fact just a normalization parameter, one can always choose a basis such that $C_{ij} = \delta_{ij}$.

Similarly, the three-point function must have the form

$$\begin{aligned} &\langle \phi_1(z_1,\bar{z}_1)\phi_2(z_2,\bar{z}_2)\phi_3(z_3,\bar{z}_3)\rangle \\ &\qquad = \mathcal{C}_{123} z_{12}^{-(\Delta_1+\Delta_2-\Delta_3)} z_{23}^{-(\Delta_2+\Delta_3-\Delta_1)} z_{13}^{-(\Delta_1+\Delta_3-\Delta_2)} \\ &\qquad\quad \times \bar{z}_{12}^{-(\bar{\Delta}_1+\bar{\Delta}_2-\bar{\Delta}_3)} \bar{z}_{23}^{-(\bar{\Delta}_2+\bar{\Delta}_3-\bar{\Delta}_1)} \bar{z}_{13}^{-(\bar{\Delta}_1+\bar{\Delta}_3-\bar{\Delta}_2)}. \end{aligned} \tag{2.109}$$

If one normalizes the coefficient in the two-point function to $C_{ij} = \delta_{ij}$, then the coefficient $\mathcal{C}_{123}$ is universal, and equal to the constant part of the coefficient C_{ij}^k in the operator product expansion (2.104).

2.2.3 Stress-energy tensor and Virasoro algebra

The stress-energy tensor

The *stress-energy tensor* $T^{\mu\nu}$, also known as the energy-momentum tensor, is the conserved current associated with translational invariance as given by Noether's theorem. The effect on the Hamiltonian from a general infinitesimal local coordinate transformation $x^\mu \to x^\mu + \varepsilon^\mu(\mathbf{x})$ can therefore be written as

$$\delta H = -\frac{1}{2\pi}\int \mathrm{d}^2x\, T^{\mu\nu}\partial_\mu \varepsilon_\nu \tag{2.110}$$

which can be seen as the definition of $T^{\mu\nu}$. Hence the energy-momentum tensor encapsulates the departure from the fixed-point by non-conformal transformations. Invariance under rotations implies that $T^{\mu\nu} = T^{\nu\mu}$ is symmetric, and global scale invariance implies zero trace $T^{\mu}_{\ \mu} = 0$.

Now, the effect of this infinitesimal transformation on correlation functions $\langle\phi_1 ... \phi_n\rangle$ of primary fields can be obtained perturbatively from $H \to H + \delta H$, giving the so called conformal Ward identity

$$\begin{aligned}\delta\langle\phi_1(z_1,\bar{z}_1)...\phi_n(z_n,\bar{z}_n)\rangle = \\ = \ -\frac{1}{2\pi i}\oint_C \mathrm{d}z\,\varepsilon(z)\langle T(z)\phi_1(z_1,\bar{z}_1)...\phi_n(z_n,\bar{z}_n)\rangle \\ +\frac{1}{2\pi i}\oint_C \mathrm{d}\bar{z}\,\bar{\varepsilon}(\bar{z})\langle\bar{T}(\bar{z})\phi_1(z_1,\bar{z}_1)...\phi_n(z_n,\bar{z}_n)\rangle,\end{aligned} \tag{2.111}$$

with $T(z) = T_{11} - T_{22} - 2iT_{12}$, $\bar{T}(\bar{z}) = T_{11} - T_{22} - 2iT_{12}$ being the holomorphic and antiholomorphic components of the stress-energy tensor. On local form this can be written as

$$\begin{aligned}&\langle T(z)\phi_1(z_1,\bar{z}_1)...\phi_n(z_n,\bar{z}_n)\rangle = \\ &\quad = \sum_i \left(\frac{\Delta_i}{(z-z_i)^2} + \frac{1}{z-z_i}\partial_{z_I}\right)\langle\phi_1(z_1,\bar{z}_1)...\phi_n(z_n,\bar{z}_n)\rangle + \text{reg.},\end{aligned} \tag{2.112}$$

$$\begin{aligned}&\langle\bar{T}(\bar{z})\phi_1(z_1,\bar{z}_1)...\phi_n(z_n,\bar{z}_n)\rangle = \\ &\quad = \sum_i \left(\frac{\bar{\Delta}_i}{(\bar{z}-\bar{z}_i)^2} + \frac{1}{\bar{z}-\bar{z}_i}\partial_{\bar{z}_I}\right)\langle\phi_1(z_1,\bar{z}_1)...\phi_n(z_n,\bar{z}_n)\rangle + \text{reg.},\end{aligned} \tag{2.113}$$

where "reg." means the terms that are regular as the coordinates approach each other. Hence we have the operator product expansion

$$T(z)\phi(w,\bar{w}) \sim \frac{\Delta}{(z-w)^2}\phi(w,\bar{w}) + \frac{1}{z-w}\partial_w\phi(w,\bar{w}), \tag{2.114}$$

and similarly for the antiholomorphic part, where $\sim$ means considering the singular part. Since the holomorphic and antiholomorphic parts essentially decouple we can treat them separately in the following.

The central charge

Eqs. (2.112)-(2.113) show that the stress-energy tensor has scaling dimension equal to 2. Hence, since $\langle T(z)\rangle = 0$ by translational invariance, the correlation function is given by the two-point function

$$\langle T(z)T(w)\rangle = \frac{c/2}{(z-w)^4}, \tag{2.115}$$

where the coefficient defines the *central charge* c. It is a universal number which characterizes the different conformal field theories. In a sense, it somehow corresponds to the effective number of gapless degrees of freedom: A free boson or fermion has $c = 1$, whereas a theory with N such fields has $c = N$, and a free Majorana fermion (1.26) has $c = 1/2$. It also gives the proportionality constant for the finite-size scaling of the free energy and hence encodes the analogue of the Casimir effect. It enters into the operator product expansion of the stress-energy tensor with itself

$$T(z)T(w) \sim \frac{c/2}{(z-w)^4} + \frac{2}{(z-w)^2}T(z) + \frac{1}{z-w}\partial_z T(z). \qquad (2.116)$$

Comparing to Eq. (2.114) for a primary field, we see that the stress-energy tensor is not a primary. Instead, under conformal transformations it transforms as

$$T(z) \to \left(\frac{\partial w}{\partial z}\right)^2 T'(w) + \frac{c}{12}\{w, z\}, \qquad (2.117)$$

where the Schwarzian derivative is given by

$$\{w, z\} = \frac{\partial_z^3 w}{\partial_z w} - \frac{3}{2}\left(\frac{\partial_z^3 w}{\partial_z w}\right)^2. \qquad (2.118)$$

Hence the central charge somehow encodes how much the stress-energy tensor deviates from being a primary field of dimension 2 (which is what one expects classically, it therefore describes an anomaly).

The Virasoro algebra

In order to treat quantum systems, one must employ the operator formalism where a distinction is made between space and time. A suitable choice is to use what is known as radial quantization, where the radial direction is taken as the direction of time. Then equal-time commutators of operators can be expressed as contour integrals in the complex plane,

$$[A_1, A_2] = \oint_0 \mathrm{d}w \oint_w \mathrm{d}z\, a_1(z)a_2(w), \quad A_i = \oint \mathrm{d}z\, a_i(z). \qquad (2.119)$$

Now, the generator Q of conformal transformations, i.e. the charge Q which gives $\delta\phi(z) = -[Q, \phi(z)]$ for the transformation of an operator $\phi(z)$ under an infinitesimal coordinate transformation, is given in terms of the stress-energy tensor as

$$Q = \frac{1}{2\pi i}\oint \mathrm{d}z\, \varepsilon(z)T(z). \qquad (2.120)$$

If $T(z)$ is mode expanded,

$$T(z) = \sum_n z^{-n-2} L_n \,, \qquad L_n = \frac{1}{2\pi i} \oint \mathrm{d}z \, \varepsilon(z) T(z), \tag{2.121}$$

and similarly for $\varepsilon(z)$, then

$$Q = \sum_n \varepsilon_n L_n, \tag{2.122}$$

with n integers. Hence the mode operators L_n (and $\bar{L}_n$) of the stress-energy tensor are the generators of conformal transformations on the Hilbert space, being the quantum version of Eq. (2.100). They obey the *Virasoro algebra*

$$\begin{aligned} [L_n, L_m] &= (n-m) L_{m+n} + \frac{c}{12} n(n^2-1) \delta_{n+m,0}, \\ \left[\bar{L}_n, \bar{L}_m\right] &= (n-m) \bar{L}_{m+n} + \frac{c}{12} n(n^2-1) \delta_{n+m,0}, \\ \left[L_n, \bar{L}_m\right] &= 0. \end{aligned} \tag{2.123}$$

So we have two commuting infinite-dimensional algebras. For the subalgebras with $n = -1, 0, 1$, the terms proportional to the central charge c vanish and one recovers the loop algebra (2.101) for the projective conformal transformations.

The representation theory of the Virasoro algebra gives the structure of the Hilbert space. Given a vacuum $|0\rangle$ which is invariant under projective conformal transformations, and imposing vanishing vacuum expectation value of the stress-energy tensor, one has

$$L_n|0\rangle = 0, \quad \bar{L}_n|0\rangle = 0 \qquad \text{for } n \geq -1. \tag{2.124}$$

The Hermitian conjugate of the Virasoro generators are given by $L_n^\dagger = L_{-n}$. With states obtained by acting with the operators on the vacuum,

$$|\Delta, \bar{\Delta}\rangle \equiv \phi(0,0)|0\rangle, \tag{2.125}$$

one has

$$L_0|\Delta, \bar{\Delta}\rangle = \Delta|\Delta, \bar{\Delta}\rangle, \text{ and } L_n|\Delta, \bar{\Delta}\rangle = 0 \text{ for } n > 0 \tag{2.126}$$

and the state at any z is obtained through $\phi(z)|0\rangle = \exp[zL_{-1}]\,|0\rangle$. States with higher dimensions can now be obtained from the state $|\Delta, \bar{\Delta}\rangle$ by acting with the generators L_{-m} $(m > 0)$. By the Virasoro algebra,

$$L_0(L_{-k_1}...L_{-k_n})|\Delta, \bar{\Delta}\rangle = (\Delta + k_1 + ... + k_n)(L_{-k_1}...L_{-k_n})|\Delta, \bar{\Delta}\rangle. \tag{2.127}$$

These states are the descendants of the state $|\Delta, \bar{\Delta}\rangle$, hence defining the descendant fields in the conformal tower of the primary $\phi(0,0)$.

Conformal field theories with a finite number of primary operators, and hence of conformal tower, are called *minimal models*. The *Kac formula*, relating the value of the central charge c to the possible values of the dimensions Δ of the operators, then provides a complete classification of all *unitary* (i.e. without negative-norm states) minimal models with $c < 1$.

As a last remark, let us note that the quantum Hamltonian can be expressed in terms of Virasoro generators by

$$H = \frac{2\pi}{L}\left(L_0 + \bar{L}_0\right) \tag{2.128}$$

as the system size $L \to \infty$.

2.2.4 Finite-size effects

It is now an important question to ask what sort of effects it has on correlation functions to put the system in a finite geometry, by either imposing periodic boundary conditions in the spatial direction or being at finite temperature [70,71]. Since the results so far has been for the infinite complex plane, these results can actually be extended to finite geometries rather straight-forwardly by conformal transformations. Consider the transformation

$$w(z) = \frac{L}{2\pi}\ln z \quad \Leftrightarrow \quad z = e^{2\pi w/L} \tag{2.129}$$

from the infinite z-plane to the w-cylinder. Using the transformation properties (2.117) for the stress-energy tensor, one obtains a non-zero vacuum expectation value of the stress-energy tensor on the cylinder. This results in a finite-size correction for the ground-state energy given by

$$\delta E = -\frac{\pi c v}{6L}, \tag{2.130}$$

showing that the central charge c serves as the proportionality constant for the Casimir effect.

From Eq. (2.103) is follows that the effect of the conformal transformation (2.129) on the two-point correlation function (2.108) is

$$\begin{aligned}
&\langle\phi(w_1,\bar{w}_1)\phi(w_2,\bar{w}_2)\rangle = \\
&\quad = \left(\frac{\partial w}{\partial z}\right)^{-\Delta}_{w=w_1}\left(\frac{\partial w}{\partial z}\right)^{-\Delta}_{w=w_2}\left(\frac{\partial \bar{w}}{\partial \bar{z}}\right)^{-\bar{\Delta}}_{\bar{w}=\bar{w}_1}\left(\frac{\partial \bar{w}}{\partial \bar{z}}\right)^{-\bar{\Delta}}_{\bar{w}=\bar{w}_2}\langle\phi(z_1,\bar{z}_1)\phi(z_2,\bar{z}_2)\rangle \\
&\quad = \left(\frac{L}{\pi}\sinh\left[\frac{\pi}{L}(w_1-w_2)\right]\right)^{-2\Delta}\left(\frac{L}{\pi}\sinh\left[\frac{\pi}{L}(\bar{w}_1-\bar{w}_2)\right]\right)^{-2\bar{\Delta}}
\end{aligned} \tag{2.131}$$

Note that for $|w_1 - w_2| \ll L$ one recovers the usual correlation function (2.108) for the infinite plane. An important relation will follow by taking the other limit, $|w_1 - w_2| \gg L$:

$$\begin{aligned}\langle\phi(w_1,\bar{w}_1)\phi(w_2,\bar{w}_2)\rangle &= \\ &= \left(\frac{2\pi}{L}\right)^{\Delta+\bar{\Delta}} \exp\left[-\frac{2\pi}{L}\Delta(w_1-w_2) - \frac{2\pi}{L}\bar{\Delta}(\bar{w}_1-\bar{w}_2)\right] \\ &= \left(\frac{2\pi}{L}\right)^{\Delta+\bar{\Delta}} \exp\left[-\frac{2\pi}{L}(\Delta+\bar{\Delta})v(\tau_1-\tau_2) - i\frac{2\pi}{L}(\Delta-\bar{\Delta})(x_1-x_2)\right],\end{aligned} \tag{2.132}$$

where the complex coordinates are given by $w = v\tau - ix = -i(x - vt)$ and $\bar{w} = v\tau + ix = i(x + vt)$. This should be compared to the spectral decomposition of the correlation function obtained by inserting a resolution of the identity,

$$\begin{aligned}&\langle\phi(w_1,\bar{w}_1)\phi(w_2,\bar{w}_2)\rangle = \\ &= \sum_Q |\langle 0|\phi(0,0)|Q\rangle|^2 \exp\left[-(E_n - E_Q)(\tau_1-\tau_2) - i(P_Q - P_0)(x_1-x_2)\right],\end{aligned} \tag{2.133}$$

where $|Q\rangle$ is a complete set of states labelled by their quantum numbers Q, with energy eigenvalues E_Q and momentum eigenvalues P_Q. Hence we arrive at the important relations

$$E_Q - E_0 = \frac{2\pi v}{L}\left(\Delta + \bar{\Delta}\right), \tag{2.134}$$

$$P_Q - P_0 = \frac{2\pi}{L}\left(\Delta - \bar{\Delta}\right), \tag{2.135}$$

relating the dimensions of the operators in the conformal field theory to the finite-size corrections of the energy and momentum of the states. It is therefore possible to extract the dimensions, which determine the correlation functions, from finite-size corrections which are usually much easier to obtain. In particular, the correlation length ξ, determining the exponential decay $\langle\phi(x,\tau)\phi(0,0)\rangle \sim \exp[-x/\xi]$, follows as

$$\xi = \frac{L}{2\pi x}, \tag{2.136}$$

where $x = \Delta + \bar{\Delta}$ is the scaling dimension.

Replacing the finite length L in the conformal transformation (2.129) with the finite "length" β in the imaginary time direction, i.e. the inverse

temperature, one instead obtains the finite-temperature correlation functions. Hence

$$\langle\phi(w_1,\bar{w}_1)\phi(w_2,\bar{w}_2)\rangle = \\ = \left(\frac{\beta}{\pi}\sinh[\frac{\pi}{\beta}(w_1-w_2)]\right)^{-2\Delta}\left(\frac{\beta}{\pi}\sinh[\frac{\pi}{\beta}(\bar{w}_1-\bar{w}_2)]\right)^{-2\bar{\Delta}}, \quad (2.137)$$

at temperature $T = 1/\beta$, where the correlation function is given by $\langle\phi(w_1,\bar{w}_1)\phi(w_2,\bar{w}_2)\rangle = \mathrm{Tr}\,\rho\,\phi(w_1,\bar{w}_1)\phi(w_2,\bar{w}_2)$, with $\rho = \exp[-\beta H]/Z$ the density matrix.

2.2.5 Boundary conformal field theory

Another important case is systems with a boundary [72–74]. This is for example often the case in quantum impurity problems, where effectively the system can be described as one-dimensional with a boundary at the impurity position [68]. Let us therefore consider a conformal field theory with complex coordinates restricted to the upper half-plane ($\mathbb{C}^+$).

A model with a boundary now restricts the conformal transformations to those that map the boundary onto itself. This implies that the holomorphic and antiholomorphic sectors are no longer independent. It also implies that the boundary conditions must be homogeneous, for example as the "free" boundary condition where the field vanish at the boundary, $\phi|_\partial = 0$.

The lack of independence between the holomorphic and antiholomorphic sectors makes it possible to introduce a mirror image of the system on the lower half-plane, by the identification $\bar{z} = z^*$, where $z, \bar{z} \in \mathbb{C}^+$ and therefore $z^* \in \mathbb{C}^-$. Thus $T(z^*) = \bar{T}(z)$, $\bar{T}(z^*) = T(z)$, etc.. The conformal Ward identities then show that the correlation function $\langle\phi(z_1,\bar{z}_1)...\phi(z_n,\bar{z}_n\rangle_{\mathbb{C}^+}$, which is a function of $z_1,...,z_n,\bar{z}_1,...,\bar{z}_n$ in the upper half-plane, is the same as $\langle\phi(z_1)...\phi(z_n)\phi(z_1^*)\phi(z_n^*)\rangle_{\mathbb{C}}$. This is analogous to the *method of images* in electrostatics, since the correlation functions behave just as if the fields interact with their mirror images on the other side of the boundary. The theory with holomorphic and antiholomorphic dependence on the upper half-plane has therefore been mapped to a theory with only holomorphic dependence on the entire complex plane. In particular, the expectation value of a field in the half-plane no longer vanish, instead it has correlations with its mirror image,

$$\langle\phi(z,\bar{z})\rangle_{\mathbb{C}^+} = \langle\phi(z)\phi(z^*)\rangle_{\mathbb{C}} \sim y^{-\Delta} \quad (2.138)$$

where y is the distance from the boundary, see Fig. 2.4.

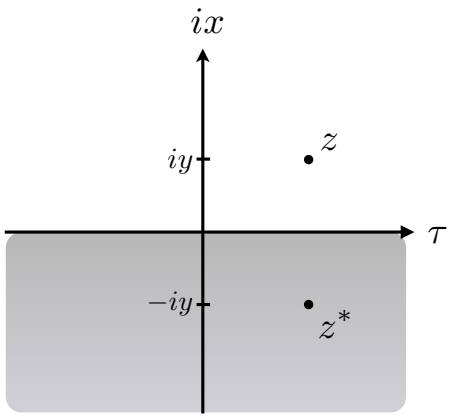

Figure 2.4: In the presence of a boundary, here the real axis $x = 0$, correlation functions on the upper half-plane are obtained by introducing mirror images on the other side of the boundary (the shaded lower half-plane).

One may now wonder what will happen as an operator approaches the boundary. The operator product expansion with its mirror image then gives

$$\phi(z)\phi(z^*) \sim \sum_i \frac{C_i^{(\phi)}}{(z-z^*)^{2x-x_b^{(i)}}} \phi_b^{(i)}(\tau) \tag{2.139}$$

where $x = \Delta$ is the scaling dimension of the holomorphic field $\phi(z)$ on the upper half-plane, and the sum is over primary *boundary operators* ϕ_b, with scaling dimensions x_b. They live on the boundary and have correlation functions $\langle \phi_b(\tau_1)\phi_b(\tau_2)\rangle = |\tau_1 - \tau_2|^{-2x_b}$. Boundary operators with $x_b < 1$ are relevant under the renormalization group, and will therefore be *boundary condition changing operators* since they will cause the system to flow away from the fixed point when inserted. One can introduce boundary states, in analogy with the states introduced above, by acting with such operators on the vacuum. In general, every conformally invariant boundary condition (CIBC) can be associated with a boundary state. If the space and imaginary time directions are interchanged, then one can formally write the partition function for a strip between two CIBCs A and B as $Z^{AB} = \langle A| \exp[-LH']|B\rangle$, where H' is a Hamiltonian that propagate the system across the distance L in the space direction between the two boundaries A and B. In the limit where $L \gg \beta$ one obtains the thermal entropy

$$S_{AB}^{Th} = \frac{\partial}{\partial T}\left[T \ln Z^{AB}\right] = \frac{\pi c L T}{3} + \ln g^{AB}, \tag{2.140}$$

where

$$g^{AB} = \langle A|0\rangle\langle 0|B\rangle \tag{2.141}$$

is the *boundary entropy* [75]. Here $|0\rangle$ is the ground state of the space-time-exchanged Hamiltonian H'. This part of the thermodynamic entropy therefore depends on the boundary conditions as opposed to the extensive term, and it encodes the entropy of the boundaries. Interestingly, it does not vanish at zero temperature. Therefore it is referred to as the ground-state degeneracy, but note that it does not need to be an integer. In quantum impurity problems a non-integer ground-state degeneracy encodes non-Fermi liquid properties of the system.

Irrelevant boundary operators however will appear as perturbations around the conformally invariant fixed point without changing the CIBC, and they play an important role in quantum impurity problems where they determine the thermodynamics of the system.

2.2.6 The free boson

Let us end this Section by giving a concrete example of a conformal field theory. In fact we have already encountered it before: the free boson. It has a Hamiltonian (2.63), rewritten as

$$H = \frac{v}{2}\int \mathrm{d}x\, \left[(\partial_t\varphi(x)/v)^2 + (\partial_x\varphi(x))^2 \right], \tag{2.142}$$

and an action which in complex coordinates and with the usual convention $v = 1$ is written as

$$S = \frac{1}{8\pi}\int \mathrm{d}z \int \mathrm{d}\bar{z}\; \partial_z\varphi(z,\bar{z})\, \partial_{\bar{z}}\varphi(z,\bar{z}). \tag{2.143}$$

The large-distance correlation function (2.70) in complex coordinates,

$$\langle \varphi(z,\bar{z})\varphi(0,0)\rangle \;=\; -\frac{1}{4\pi}\ln\left[z/a\right] - \frac{1}{4\pi}\ln\left[\bar{z}/a\right] \tag{2.144}$$

shows that the boson field $\varphi(z,\bar{z}) \equiv \varphi(z)+\bar{\varphi}(\bar{z})$ is not a primary. However its derivatives $\partial_z\varphi(z,\bar{z}) = \partial_z\varphi(z)$ and $\partial_{\bar{z}}\varphi(z,\bar{z}) = \partial_{\bar{z}}\bar{\varphi}(z)$ have correlation functions

$$\langle \partial_z\varphi(z)\partial_w\varphi(w)\rangle \;=\; -\frac{1}{4\pi}\frac{1}{(z-w)^2} \tag{2.145}$$

$$\langle \partial_{\bar{z}}\bar{\varphi}(\bar{z})\partial_{\bar{w}}\bar{\varphi}(\bar{w})\rangle \;=\; -\frac{1}{4\pi}\frac{1}{(\bar{z}-\bar{w})^2} \tag{2.146}$$

and operator product expansions with the stress-energy tensor, which is given by

$$T(z) = -2\pi : \partial_z\varphi(z)\partial_z\varphi(z) : \tag{2.147}$$

show that $\partial_z\varphi(z)$ and $\partial_{\bar{z}}\bar{\varphi}(z)$ are primary fields. The correlator $\langle T(z)T(w)\rangle = (1/2)(z-w)^{-4}$ for the stress-energy tensor shows that the free boson theory has central charge $c = 1$.

There is in fact an infinite number of primary fields that can be constructed from φ. These are the *vertex operators*,

$$\mathcal{V}_\alpha(z) \;=: e^{i\alpha\varphi(z)} : \qquad \bar{\mathcal{V}}_\alpha(\bar{z}) \;=: e^{i\alpha\bar{\varphi}(\bar{z})} : \tag{2.148}$$

familiar from the previous discussion of bosonization. The non-vanishing operator product expansions are

$$\mathcal{V}_\alpha(z)\mathcal{V}_{-\alpha}(w) \;=\; \frac{1}{(z-w)^{\alpha^2/2\pi}} + ... \tag{2.149}$$

and similarly for the antiholomorphic part, showing that their dimensions are given by

$$\Delta_\alpha = \frac{\alpha^2}{8\pi} \qquad \bar{\Delta}_\alpha = \frac{\alpha^2}{8\pi}. \tag{2.150}$$

3

The Kondo effect

The Kondo effect is one of the paradigms of strongly correlated phenomena [30]. It is historically associated with the surprising increase in electrical resistivity $\rho(T)$ as the temperature $T \to 0$ in normal metals containing *magnetic impurities* [76, 77]. When $T \to 0$ the usual scattering mechanisms in Fermi liquids give a resistivity $\rho(T) \sim \text{const.} + T^2$ according to Matthiessen's rule. The constant term comes from scattering off non-magnetic impurities and the term quadratic in temperature from electron-electron scattering [18]. In the presence of magnetic impurities, i.e. localized spins that can scatter the electrons, there is instead a resistivity minimum at a temperature typically on the order of 10 K, see the sketch in Fig. 3.1.

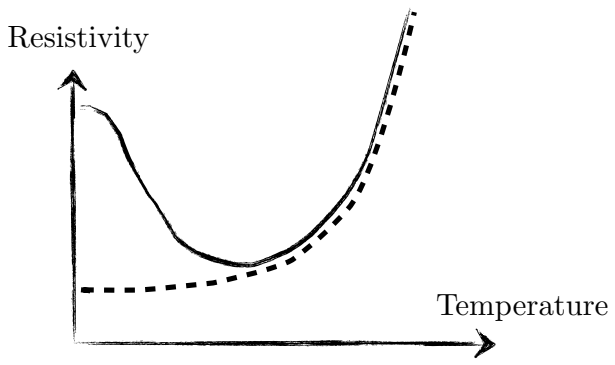

Figure 3.1: Sketch of the resistivity minimum in metals with magnetic impurities, compared to non-magnetic (dashed line).

3.1 The Kondo model

The resistance minimum was explained by Kondo [77], using a simple model now known as the "Kondo model". It describes a magnetic $s = 1/2$ impurity interacting with a single band of conduction electrons:

$$H_{Kondo} = \sum_{\vec{k},\alpha} \epsilon(\vec{k}) \psi^{\dagger}_{\vec{k}\alpha} \psi_{\vec{k}\alpha} + J\vec{S} \cdot \sum_{\vec{k},\vec{k}',\alpha,\beta} \psi^{\dagger}_{\vec{k}\alpha} \frac{\vec{\sigma}_{\alpha\beta}}{2} \psi_{\vec{k}'\beta} \,, \tag{3.1}$$

where $\alpha, \beta = \uparrow, \downarrow$ are spin indices, ψ is the electron annihilation operator, $\vec{\sigma}$ is the vector with the Pauli matrices as components and $\vec{S}$ is the impurity spin-1/2 magnetic moment localized at the origin.

When combined with the contribution from phonons, this simple model accurately predicts the existence of a resistance minimum. However, the calculations showed a breakdown of perturbation theory as the temperature was further reduced. Acquiring a solution below this breakdown temperature, the "Kondo temperature" T_K, became known as the "Kondo problem". In fact, it was the quest to solve this problem that spurred the development of scaling analysis by Anderson [78] and the renormalization group by Wilson [55]. The picture that emerged was that for antiferromagnetic coupling, the magnetic impurity gets screened at low temperatures by singlet formation with the conduction electrons. This occurs at a length scale $\xi_K \sim v_F/T_K$, the "Kondo length" (see Fig. 3.2). Hence when $T \to 0$ the impurity effectively becomes non-magnetic, only contributing a finite residual resistivity. As shown by Nozières [79], this low-temperature fixed-point corresponds to a Fermi liquid. An exact solution of the Kondo model, giving all the thermodynamic properties, was finally obtained independently by Andrei [80] and Wiegmann [81], using the Bethe Ansatz[1]. The simple Kondo model was also extended to incorporate more realistic situations, such as when the impurity interacts with several bands of conduction electrons. Hence Nozières and Blandin [83] introduced the multichannel Kondo model, which was shown by Andrei and Destri [84], and independently by Tsvelik and Wiegmann [85], in their Bethe Ansatz solutions to exhibit exotic non-Fermi-liquid behavior. A new approach to Kondo physics based on conformal field theory was developed by Affleck [86], and independently by Tsvelik [87], and further refinement by Affleck and Ludwig [88, 89] allowed the technique to give new insights to the non-Fermi-liquid phenomena.

The Kondo lattice model [90], believed to describe heavy-fermion systems displaying a rich variety of physical phenomena including quantum

[1] Reviewed in [82].

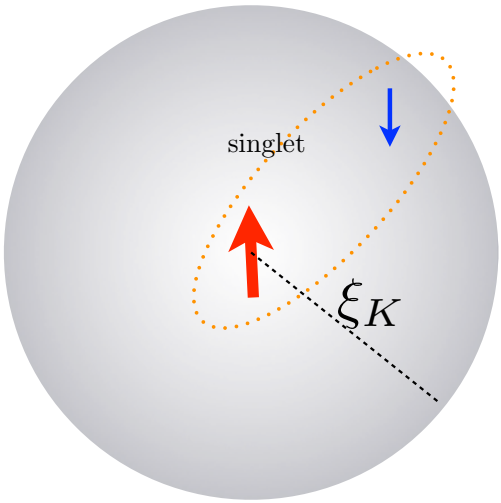

Figure 3.2: The Kondo screening cloud is formed when the conduction electrons try to screen the impurity spin by forming a singlet. The screening takes place on the scale of the "Kondo length" $\xi_K \sim v_F/T_K$, where T_K is given by Eq. (3.4).

phase transitions and non-Fermi-liquid behavior as well as unconventional superconductivity, still remains unsolved although much progress has been made. One of the principal physical mechanisms in the Kondo lattice, the competition between Kondo screening and indirect exchange between the impurities, is captured already in the two-impurity Kondo model.

Interest in the Kondo effect then experienced a revival when advancements in nanofabrication enabled its observation in artificially created quantum dot systems [91], where a tunable Kondo resonance provides new opportunities for device technology. Recently the Kondo effect has also attracted attention from the quantum information community, as the Kondo screening cloud has been recognized as a mechanism that may generate long-range entanglement between qubits [92, 93]. There also exists a mapping between the spin-anisotropic Kondo model and the spin-boson model, describing a qubit interacting with a dissipative environment [94].

An estimate of the Kondo temperature T_K can be obtained using the renormalization group perturbatively at weak coupling. By successively integrating out high-energy electrons, thus effectively reducing the band-

width D, one obtains the RG equation for the coupling constant J

$$\frac{\mathrm{d}J}{\mathrm{d}(\log D)} = -\nu J^2 + ... \tag{3.2}$$

where ν is the density of states at the Fermi level. This gives the solution

$$J_{\text{eff}} = \frac{J_0}{1 - \nu J_0 \log(D_0/D)} \tag{3.3}$$

for the effective coupling J_{eff} in terms of the bare values of the coupling J_0 and band-width D_0. Thus, for antiferromagnetic coupling ($J_0 > 0$) the effective coupling diverges as the cutoff is approaching $D \sim T_K$, the Kondo temperature

$$T_K \sim D_0 e^{-\frac{1}{\nu J_0}} . \tag{3.4}$$

This shows the appearance of a new length scale in the problem, the Kondo length $\xi_K \sim v_F/T_K$. It is within this length scale that the screening occurs, hence defining the extent of the "Kondo screening cloud". The crossover on this length scale has proven notoriously difficult to detect experimentally, and the nature of the Kondo screening cloud is hence perhaps the only remaining open question in what once was "the Kondo problem". For a more detailed account, see Refs. [95] and [96].

3.2 The boundary conformal field theory approach

Conformal field theory techniques have been very successful in the study of a large number of quantum impurity systems. The approach is based on the possibility to reduce the problem to one dimension with the impurity as a boundary. The low-energy physics can then be described by one-dimensional non-interacting fermions with the impurity spin having disappeared, its only effect being a (possibly non-trivial) conformally invariant boundary condition and a modified operator content of the resulting boundary conformal field theory. For a thorough review of the BCFT approach to the Kondo effect, the reader is referred to Ref. [68], or to the original articles by Affleck [86], and Affleck and Ludwig [88,89]. Let us only give a brief account here.

First, even when the impurity is interacting with bulk conduction electrons and the Kondo model (3.1) hence describes a three-dimensional system, it can always be mapped onto a one-dimensional model. Expanding the electron fields in partial waves

$$\psi(\vec{r}) = \frac{1}{\sqrt{2\pi}r}\psi_0(r) + ... \tag{3.5}$$

it follows that it is only the s-wave (i.e. zero angular momentum) component $\psi_0(r)$ that interacts with the impurity since the interaction in the Kondo Hamiltonian (3.1) is a delta function and the s-wave is the only non-vanishing component at the origin. Thus we are left with only the radial coordinate and the resulting one-dimensional model

$$H_{Kondo} = \sum_{k,\alpha} \epsilon(k)\psi^\dagger_{0\alpha}(k)\psi_{0\alpha}(k) + J\vec{S}\cdot\sum_{\vec{k},\vec{k}',\alpha,\beta}\psi^\dagger_{0\alpha}(k)\frac{\vec{\sigma}_{\alpha\beta}}{2}\psi_{0\beta}(k') \quad (3.6)$$

can then be treated with the bosonization techniques introduced in Chapter 2. First, consider a linearization around the Fermi level

$$\epsilon(k) \approx v_F(k - k_F) \quad (3.7)$$

and then decomposing the s-wave electron field in left and right movers, corresponding to in- and outgoing waves,

$$\psi_{L/R\,\alpha}(r) = \int_{k_F-\Lambda}^{k_F+\Lambda} \mathrm{d}k\; e^{\pm i(k-k_F)r}\psi_{0\alpha}(k)\,. \quad (3.8)$$

This puts the Kondo Hamiltonian on the form

$$\begin{aligned} H_{Kondo} &= \frac{v_F}{2\pi}\int_0^\infty \mathrm{d}r\big[\;\psi^\dagger_{L\alpha}(r)i\partial_r\psi_{L\alpha}(r) - \psi^\dagger_{R\alpha}(r)i\partial_r\psi_{R\alpha}(r)\;\big] \\ &\quad + J\vec{S}\cdot\psi^{\dagger\alpha}_L(0)\frac{\vec{\sigma}_{\alpha\beta}}{2}\psi_{L\beta}(0)\,. \end{aligned} \quad (3.9)$$

Note that the definition (3.8) of the left and right movers gives the boundary condition

$$\psi_L(0) = \psi_R(0)\,. \quad (3.10)$$

But as $J_{\text{eff}} \to \infty$ under renormalization, the impurity and a conduction electron get so strongly bound into a local singlet that no other conduction electron can be at the origin, then $\psi(0) = \psi_L(0) + \psi_R(0) = 0$ so that the boundary condition (3.10) is effectively changed to

$$\psi_L(0) = -\psi_R(0) \qquad \text{when } J_{\text{eff}} \to \infty\,. \quad (3.11)$$

This is at the core of Nozière's Fermi-liquid description, the strong-coupling regime corresponds to a phase shift of the otherwise unaffected electrons.

A purely chiral theory can be obtained by "folding", i.e. by extending to negative values of r by identifying

$$\psi_{R\alpha}(r) \equiv \psi_{L\alpha}(-r)\,, \quad (3.12)$$

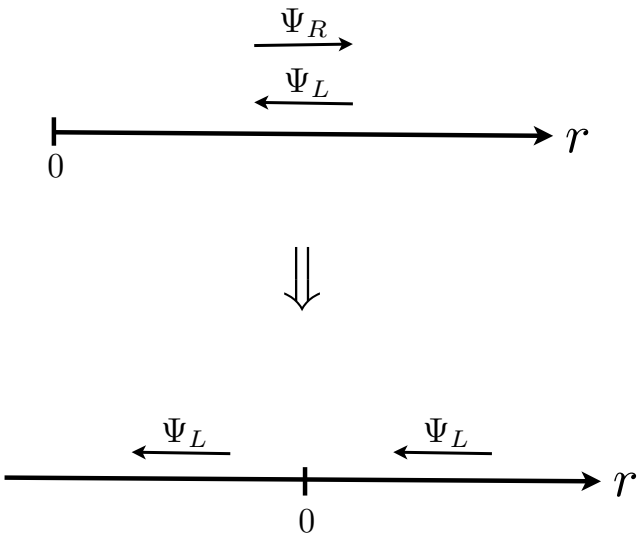

Figure 3.3: The "folding" process of the out- and in-going s-wave fields, represented as right- and left-moving fields $\Psi_R(r)$ and $\Psi_L(r)$ on the positive half-line. A chiral theory with only left-moving fields on the entire real line is obtained by the identification $\psi_R(r) \equiv \psi_L(-r)$.

see Fig. 3.3, so that

$$H_{Kondo} = \frac{v_F}{2\pi} \int_{-\infty}^{\infty} \mathrm{d}r \, \psi^\dagger_{L\alpha}(r) i\partial_r \psi_{L\alpha}(r) + J\vec{S} \cdot \psi^\dagger_{L\alpha}(0) \frac{\vec{\sigma}_{\alpha\beta}}{2} \psi_{L\beta}(0) \,. \quad (3.13)$$

Spin-charge separation is obtained by introducing the charge and spin currents

$$J_c = :\psi^\dagger_{L\alpha}\psi_{L\alpha}: , \quad (3.14)$$

$$\vec{J}_s = \psi^\dagger_{L\alpha} \frac{\vec{\sigma}_{\alpha\beta}}{2} \psi_{L\beta} \,, \quad (3.15)$$

where :: denotes normal ordering. Their commutation relations are

$$[J_c(r), J_c(r')] = 4\pi i \partial_r \delta(r - r') \,, \quad (3.16)$$

$$[J_c(r), J^a_s(r')] = 0 \,, \quad (3.17)$$

$$[J^a_s(r), J^b_s(r')] = 2\pi i \varepsilon^{abc} J^c_s(r) \delta(r - r') + \pi i \delta^{ab} \partial_r \delta(r - r') \,. \quad (3.18)$$

with ε^{abc} the Levi-Civita antisymmetric tensor. This puts the Hamiltonian on the spin-charge separated form

$$H_{Kondo} = \frac{\pi v_F}{2} J_c^2 + \frac{2\pi v_F}{3} \vec{J}_s^2 + J\vec{S} \cdot \vec{J}_s(0) \quad (3.19)$$

and the Kondo interaction only takes place in the spin sector. However, due to the boundary condition on the electrons, the two sectors are in fact not completely separated. To recover the correct free-fermion spectrum the states of the separate sectors must be combined according to particular "gluing conditions".

The charge current $J_c(r)$ has the same commutation relations as the derivative of the chiral free boson field, $\partial_z\phi(r)$,

$$[\partial_z\phi(r), \partial_z\phi(r')] = 2i\partial_r\delta(r-r') \tag{3.20}$$

so the identification

$$J_c = \partial_z\phi \tag{3.21}$$

can be made. Thus the charge sector is simply the chiral free boson conformal field theory, with Hamiltonian

$$H_c = \frac{1}{4}(\partial_z\phi)^2\,, \tag{3.22}$$

for the "charge boson" field $\phi = \phi_c$.

In the spin sector, the Fourier transformed spin current

$$\vec{J}_n = \frac{1}{2\pi}\int_{-L}^{L} \mathrm{d}r e^{i\pi nr/L}\vec{J}(r) \tag{3.23}$$

(where L is the system size) obeys the $SU(2)_1$ Kac-Moody algebra

$$[J_n^a, J_m^b] = i\epsilon^{abc}J_{n+m}^c + \frac{1}{2}\delta^{ab}\delta_{n,-m} \tag{3.24}$$

which is the $SU(2)$ level $k=1$ case of the general Kac-Moody algebra (affine Lie algebra)

$$[J_n^a, J_m^b] = if_c^{ab}J_{n+m}^c + \frac{k}{2}n\delta^{ab}\delta_{n,-m}\,. \tag{3.25}$$

Thus the quadratic part of the spin sector Hamiltonian can be put on the Sugawara form

$$H_s = \frac{\pi}{3L}\sum_{n=-\infty}^{\infty} :\vec{J}_{-n}\cdot\vec{J}_n:\,, \tag{3.26}$$

hence giving the $SU(2)_1$ Wess-Zumino-Witten (WZW) model. Bosonization can no longer be done only in terms of the currents. Non-Abelian bosonization, where the symmetry is explicitly preserved, expresses the

spin part of the electron field as a field g that takes its values in the symmetry group $SU(2)$, so that

$$\psi \propto g e^{i\sqrt{2\pi}\phi_c} \,. \tag{3.27}$$

When including the Kondo interaction

$$H_s = \frac{\pi}{3L} \sum_{n=-\infty}^{\infty} : \vec{J}_{-n} \cdot \vec{J}_n : + J \frac{\pi}{L} \sum_{n=-\infty}^{\infty} \vec{S} \cdot \vec{J}_n \,, \tag{3.28}$$

the above no longer holds. However, the approach is that the fixed points should correspond to removing the impurity and replacing it with a conformally invariant boundary condition (CIBC) on the free theories. The CIBC for the low-temperature fixed point of the Kondo model, where the electrons experience a $\pi/2$ phase shift at the origin, is equivalent to letting $\vec{J}_n \mapsto \vec{\mathcal{J}}_n$, with

$$\vec{\mathcal{J}}_n(r) = \vec{J}_n(r) + \delta(r)\vec{S} \tag{3.29}$$

giving

$$H_s = \frac{\pi}{3L} \sum_{n=-\infty}^{\infty} \vec{\mathcal{J}}_{-n} \cdot \vec{\mathcal{J}}_n \,, \tag{3.30}$$

and

$$[\mathcal{J}_n^a, \mathcal{J}_m^b] = i\epsilon^{abc}\mathcal{J}_{n+m}^c + \frac{1}{2} n \delta^{ab} \delta_{n,-m} \,. \tag{3.31}$$

Hence the theory is the same, showing that the strong-coupling fixed point is the same as the weak-coupling fixed point, i.e. as having no impurity. The effect of having the new spin operator (3.29) is instead that, as the impurity has spin s=1/2, the half-integer spin states will become integer-spin states, and vice versa, thus interchanging these two conformal towers. Equivalently, the spectrum at the strong-coupling fixed point is obtained by acting on all states with the spin j=1/2 field in the free theory. This way of obtaining new conformally invariant boundary conditions from the free theory is known as "fusion".

Thermodynamics

The BCFT formulation allows for a straight-forward calculation of thermodynamic properties at the fixed-points once the operator content has been found [89]. At a fixed point, the singular behavior of thermodynamic quantities is governed by the leading irrelevant operator in the operator content, not breaking the symmetries of the fixed-point Hamiltonian. The presence of the screened impurity will induce local perturbations at

the boundary, in the form of boundary operators, so that the effective Hamiltonian becomes

$$H = H_{FP} + \lambda\phi_b\,, \tag{3.32}$$

where H_{FP} is the fixed-point Hamiltonian and ϕ_b is an irrelevant boundary operator with scaling dimension $x_b > 1$ localized on the boundary. The partition function in the finite-temperature geometry on the upper half-plane $\mathbb{C}^+$ (with $z = \tau + ir$, $r \geq 0$), is then written as

$$Z = e^{-\beta F(\beta,\lambda)} = e^{-\beta F(\beta,0)} \Big\langle \exp\Big(\lambda \int_{-\beta/2}^{\beta/2} \mathrm{d}\tau\, \phi_b(\tau)\Big)\Big\rangle\,, \tag{3.33}$$

where F is the free energy. Then the impurity free energy contributed by the perturbation, $\delta F_{imp}(\beta,\lambda) = \delta F(\beta,\lambda) - F_{imp}(\beta,0)$ is given by

$$e^{-\beta\delta F_{imp}(\beta,\lambda)} = \Big\langle\, \exp\Big(\lambda \int_{-\beta/2}^{\beta/2} \mathrm{d}\tau\, \phi_b(\tau)\Big)\Big\rangle\,. \tag{3.34}$$

The conformally invariant boundary conditions imply $\langle\phi_b\rangle = 0$ so that

$$\delta F_{imp}(\beta,\lambda) = -\frac{\lambda^2}{2} \int_{-\beta/2}^{\beta/2} \mathrm{d}\tau_1 \int_{-\beta/2}^{\beta/2} \mathrm{d}\tau_2 \langle\phi_b(\tau_1)\phi_b(\tau_2)\rangle + \mathcal{O}(\lambda^3)\,. \tag{3.35}$$

From

$$\langle\phi_b(\tau_1)\phi_b(\tau_2)\rangle = \frac{1}{|\frac{\beta}{\pi}\sin(\frac{\pi}{\beta}(\tau_1-\tau_2))|^{2x_b}} \tag{3.36}$$

the leading singular behavior of $\delta F_{imp}(\beta,\lambda)$ can be calculated exactly using partial integration. The impurity specific heat C_{imp} is found from

$$C_{imp} = -T\frac{\partial^2 F_{imp}}{\partial T^2} \tag{3.37}$$

which, in terms of the inverse temperature β becomes [89, 97]

$$C_{imp} = \begin{cases} \lambda^2 A\beta^{2-2x_b} & \text{if } 1 < x_b < 3/2 \\ \lambda^2\pi^2\beta^{-1}\log(\beta/\tau_0) & \text{if } x_b = 3/2 \\ \lambda^2 B\beta^{-1} & \text{if } x_b > 3/2\,, \end{cases} \tag{3.38}$$

in the limit $\beta \to \infty$, where $A = 2(x_b-1)^2\pi^{2x_b-1}\Gamma(3/2-x_b)\Gamma(1/2)/\Gamma(2-x_b)$, $B = \pi^2 2x_b\tau_0^{3-2x_b}/3(2x_b-3)$ and τ_0 is the short-time cutoff.

The impurity specific heat C_{imp} is related to the thermodynamic impurity entropy S_{imp}^{Th} via the relation $C_{imp} = -\beta\,\partial S_{imp}^{Th}/\partial\beta$. Thus they describe the same power law, and one has the leading behavior

$$S_{imp}^{Th} = \log g + \begin{cases} \lambda^2 A\beta^{2-2x_b} & \text{if } 1 < x_b < 3/2 \\ \lambda^2\pi^2\beta^{-1}\log\beta & \text{if } x_b = 3/2 \\ \lambda^2 B\beta^{-1} & \text{if } x_b > 3/2\,, \end{cases} \tag{3.39}$$

as $\beta \to \infty$.

3.3 Non-Fermi liquid fixed points in Kondo systems

While the usual Kondo model in Eq. 3.1) has a low-temperature behavior described by Fermi-liquid theory [79], this will not necessary be the case when generalizing the model to include several electron bands, more impurities, and so on [31]. Below we give the two most prominent examples of such situations.

3.3.1 The multi-channel Kondo model

Let us consider the generalization of the Kondo model in Sec. 3.1 to the situation of a single $SU(2)$ spin-s impurity interacting with k degenerate bands of conduction electrons, the multi-channel Kondo model

$$H_{MC} = \sum_{\vec{k},\alpha,i} \epsilon(\vec{k}) \psi^\dagger_{\vec{k}\alpha i} \psi_{\vec{k}\alpha i} + J\vec{S} \cdot \sum_{\vec{k},\vec{k}',\alpha,\beta,i} \psi^\dagger_{\vec{k}\alpha i} \frac{\vec{\sigma}_{\alpha\beta}}{2} \psi_{\vec{k}'\beta i} \,, \tag{3.40}$$

where $i = 1, 2, ..., k$ is the additional channel index. For the *overscreened* multichannel Kondo model, i.e. when $k > 2s$, the system flows under renormalization for any non-zero Kondo coupling J towards a stable non-Fermi-liquid fixed point [68]. The model was first solved by Andrei and Destri [84], and by Tsvelik and Wiegmann [85], using the Bethe Ansatz. Later the BCFT solution was worked out by Affleck and Ludwig [88, 89]. At the fixed point there is a Kac-Moody symmetry $U(1) \times SU(2)_k \times SU(k)_2$, corresponding to the charge, spin and channel sectors, respectively. The Kondo interaction only involves the spin sector, and the non-Fermi-liquid fixed point is obtained from the free fermions by double fusion with the spin-s primary field in the level-k $SU(2)$ WZW model. The non-trivial boundary condition corresponds to a boundary entropy given by [75, 84]

$$\log g = \log \left[\frac{\sin(\pi(2s+1)/(2+k))}{\sin(\pi/(2+k))} \right] . \tag{3.41}$$

The leading irrelevant boundary operator is the singlet $\vec{\mathcal{J}}_{-1} \cdot \vec{\phi}$ (a Kac-Moody descendant, where $\vec{\phi}$ is the spin-1 primary field in the spin sector). This is a Virasoro primary with scaling dimension $x_b = 1 + 2(2 + k)$.

3.3.2 The two-impurity Kondo model

Adding a second spin-1/2 impurity to the Kondo model gives the two-impurity Kondo model (TIKM)

$$H_{TIKM} \;=\; H_0 \;+\; J\,[\;\vec{s}_c(\vec{r}_1)\cdot\vec{S}_1 + \vec{s}_c(\vec{r}_2)\cdot\vec{S}_2\;] + K\,\vec{S}_1\cdot\vec{S}_2\,, \tag{3.42}$$

where $H_0 = \sum_{\vec{k},\alpha}\epsilon(\vec{k})\psi^\dagger_{\vec{k}\alpha}\psi_{\vec{k}\alpha}$ is the kinetic energy and

$$\vec{s}_c(\vec{r}) = \sum_{\alpha,\beta}\psi^\dagger_\alpha(\vec{r})\frac{\vec{\sigma}_{\alpha\beta}}{2}\psi_\beta(\vec{r}) \tag{3.43}$$

where $\alpha,\beta = \uparrow,\downarrow$ are the spin indices [98]. K is the RKKY interaction strength between the two s=1/2 impurities $\vec{S}_i$ located at $\vec{r}_i$, with i=1,2. The RKKY interaction is an indirect exchange interaction to second order in perturbation theory, mediated by the conduction electrons [99–101]. The two important energy scales are K and the (single-impurity) Kondo temperature T_K. The limits $K \to \pm\infty$ correspond to Fermi-liquid fixed points, but for $K = K_c \sim T_K$ there is an unstable non-Fermi-liquid fixed point. The BCFT solution of the two-impurity Kondo model was found by Affleck, Ludwig and Jones [102]. Applying non-Abelian bosonization, they represented the fermionic theory as two level-1 Wess-Zumino-Witten (WZW) models (the two charge sectors; two since there are two impurities), a level-2 WZW model (the total spin sector) and an Ising model. The primary fields of the $SU(2)_1$ WZW models are the identity operator with spin j=0, and the j=1/2 field $(h_i)_A$ (where i=1,2 is the "channel" index and A is an "isospin" index). The $SU(2)_2$ WZW model has the primary fields **1** (the identity), g_α (with j=1/2) and $\vec{\phi}$ (with j=1). Their scaling dimensions are given by $x = j(j+1)/(2+k)$, where k is the level of the Kac-Moody algebra. The primary fields of the Ising model are the identity operator **1**, the order parameter σ with x=1/16 and the energy density ϵ with x=1/2. The fermion field then has the representation

$$\psi_{\alpha i} = (h_i)_1 g_\alpha \sigma\,. \tag{3.44}$$

The operator content at the non-Fermi-liquid fixed point is in this representation obtained from the free theory by double *fusion* with the σ operator in the Ising sector. This gives $\log g = \log\sqrt{2}$, showing a non-integer ground-state degeneracy. The irrelevant boundary operators that can appear as perturbations to the fixed-point Hamiltonian can then be found by symmetry considerations. The leading irrelevant operator at the unstable non-Fermi-iquid fixed point is $L_{-1}\epsilon$, the Virasoro first descendant of the ϵ field, with scaling dimension $x = 3/2$. However, being

a Virasoro first descendant, $L_{-1}\epsilon$ will not give any contribution to thermodynamic quantities *to any order* in perturbation theory. This follows from the evaluation of integrals of the type $\int_{-\infty}^{\infty} \mathrm{d}\tau \langle L_{-1}\epsilon\rangle = \int_{-\infty}^{\infty} \mathrm{d}\tau \partial_\tau \langle \epsilon\rangle$ which vanish due to the periodicity in the τ direction. The leading contributions to thermodynamic quantities therefore come from the stress-energy tensor, precisely as in the single-impurity case. The non-Fermi liquid behavior thus manifests itself mainly in the residual entropy $\log g$.

3.4 The Kondo effect in a Luttinger liquid

The one-dimensional formulations of the Kondo models considered above have all been concerned with non-interacting electrons coupled to the Kondo impurities, which follows from considering the model to originally describing a three-dimensional system. However, for a truly one-dimensional system the Fermi-liquid picture of non-interacting quasiparticles breaks down, and gets replaced by collective degrees of freedom described by the Tomonaga-Luttinger model as we saw in Chapter 2. Now, let these interacting fermions

$$\begin{aligned} H_{TL} &= \frac{1}{2\pi}\int \mathrm{d}x \Big\{ v_F \big[\, \psi^\dagger_{L,\alpha}(x) i\partial_x \psi_{L,\alpha}(x) - \psi^\dagger_{R,\alpha}(x) i\partial_x \psi_{R,\alpha}(x) \,\big] \\ &\quad + g' \sum_{\pm} \big[\frac{1}{2} \sum_{r,s=L,R} \psi^\dagger_{r,\alpha}(x)\psi_{r,\alpha}(x)\psi^\dagger_{s,\pm\alpha}(x+a)\psi_{s,\pm\alpha}(x+a) \\ &\quad + \psi^\dagger_{R,\alpha}(x)\psi_{L,\alpha}(x)\psi^\dagger_{L,\pm\alpha}(x)\psi_{R,\pm\alpha}(x)\big] \Big\}, \end{aligned} \tag{3.45}$$

be coupled to a spin-1/2 impurity by the Kondo interaction term

$$H_K = J \sum_{r,s=L,R} \psi^\dagger_{r,\alpha}(0) \frac{\vec{\sigma}_{\alpha,\beta}}{2} \psi_{s,\beta}(0) \cdot \vec{S}\,, \tag{3.46}$$

where in both Eqs. (3.45) and (3.46) there is an implicit summation over the spin indices $\alpha, \beta = \uparrow, \downarrow$. Note the point-splitting on the second line in Eq. (3.45), where a is the short-distance cutoff (typically the lattice parameter). For repulsive electron-electron interaction the parameter g' is positive. One can now proceed with standard bosonization and renormalization group analysis [103, 104].

At low temperature the Kondo coupling flows under renormalization towards infinity so that the impurity gets completely screened [105]. Thus, at the fixed point $\log g = 0$. In the boundary conformal field theory picture, there are two possible scenarios for this strong-coupling fixed point: either it describes a local Fermi liquid with an exactly marginal

boundary operator or an operator with $x_b > 3/2$ as leading boundary perturbation, or it describes a non-Fermi-liquid strong-coupling fixed point [97,106]. The non-Fermi-liquid fixed point scenario is the one realized [97,105], and the leading perturbation then comes from a boundary operator with $x_b = \frac{1}{2}(e^{2\theta}+1)$, where θ is given by $\tanh 2\theta = g'/(g'+v_F)$.

3.4.1 The Kondo effect in a helical Luttinger liquid

If one locks the spin of the electrons to their direction of propagation, such that right-movers only have spin-up and left-movers only have spin-down,

$$\begin{aligned} H_{HLL} &= \frac{1}{2\pi}\int \mathrm{d}x\Big\{ v_F\big[\ \psi^\dagger_{L\downarrow}(x) i\partial_x \psi_{L\downarrow}(x) - \psi^\dagger_{R\uparrow}(x) i\partial_x \psi_{R\uparrow}(x)\ \big] \\ &\quad + \frac{g'}{2}\sum_{s=R\uparrow,L\downarrow} \psi^\dagger_s(x)\psi_s(x+a)\psi^\dagger_s(x+a)\psi_s(x) \\ &\quad + g'\psi^\dagger_{R\uparrow}(x)\psi_{R\uparrow}(x)\psi^\dagger_{L\downarrow}(x)\psi_{L\downarrow}(x)\Big\}, \end{aligned} \tag{3.47}$$

one obtains the helical Luttinger liquid. This system will be discussed in Section 5.2.3 in connection to its realization as the edge state of a two-dimensional topological insulator. The Kondo effect in this model, with Hamiltonian $H = H_{HLL} + H_K$, where

$$H_K = J\sum_{\alpha,\beta=R\uparrow,L\downarrow} \psi^\dagger_\alpha(0)\frac{\vec{\sigma}_{\alpha,\beta}}{2}\psi_\beta(0)\cdot\vec{S}, \tag{3.48}$$

was studied early on [107,108] as a truncated version to gain some insight to the problem in the standard Luttinger liquid. It was found that the Kondo effect in this truncated model can be mapped exactly onto that in a Fermi liquid [107], hence resulting in a fully screened impurity at zero temperature with the usual Fermi-liquid scaling exponents. Previously being just a "toy model" model for the full Luttinger liquid, the discovery of the quantum spin Hall insulator with its helical edge states [109,110] has now provided a physical realization of the helical Luttinger liquid stimulating much interest in the physics of quantum impurities in this system [111–114].

4

Quantum entanglement

Entanglement lies at the very heart of quantum theory [115–118]. It has been recognized as the crucial resource needed for performing quantum computing and teleportation, and therefore constitute the foundation of quantum information science [119]. But it has also entered as an important concept in a wide range of other fields spanning from the studies of black holes [120] to biological systems [121]. In condensed matter physics, entanglement has been used as a theoretical tool to study zero-temperature quantum phase transitions and critical phenomena [122–134] as well as characterizing novel phases of matter [135–137] and developing numerical algorithms [138,139]. A particularly important result has been for one-dimensional critical systems, where conformal field theory yields a universal prediction for the scaling of the entanglement entropy [126,127]. Much effort has been put into relating entanglement entropy to experimentally measurable quantities [140–144], a task complicated by the very non-local feature that makes it such a powerful theoretical tool. For a thorough review on entanglement in many-particle systems, see Ref. [145].

4.1 Entanglement of quantum states

Two parts of a system are said to be entangled if the state of the system cannot be written as a direct product of the states of the two parts. That is, if the Hilbert space $\mathcal{H} = \mathcal{H}_A \otimes \mathcal{H}_B$ of the system is divided into a part called A and the rest which is called B, and the system is in a pure state $|\,\Psi\,\rangle$ in $\mathcal{H}$, then A and B are entangled if

$$|\,\Psi\,\rangle \neq |\,\psi\,\rangle_A \otimes |\,\phi\,\rangle_B \tag{4.1}$$

for any states $|\,\psi\,\rangle_A$ and $|\,\phi\,\rangle_B$ of the parts. When the whole system is in a mixed state, the parts are instead entangled if the density matrix $\hat{\rho}$ cannot be written as a linear combination of product states,

$$\hat{\rho} \neq \sum_i p_i \; \hat{\rho}_A^i \otimes \hat{\rho}_B^i \,, \tag{4.2}$$

where $\hat{\rho}_A^i$ and $\hat{\rho}_B^i$ are density matrices pertaining to part A and B, respectively, and p_i are probabilities[1].

4.2 Quantum correlations and entanglement

Let us give a simple, yet profound , example of an entangled state. Suppose we have two spin-1/2 particles that are in a singlet state

$$|\,\Psi\,\rangle = \frac{1}{\sqrt{2}} \Big(\; |\uparrow\rangle_A \otimes |\downarrow\rangle_B - |\downarrow\rangle_A \otimes |\uparrow\rangle_B \; \Big) \,. \tag{4.3}$$

It is easily seen that one cannot write this as a product state, Eq. (4.1). Let us now see what happens if we perform measurements on the particles. There is equal probability that A points either up or down, and there is also equal probability that B points either up or down. However, if the first measurement gives the outcome that spin A pointed up, then the state (4.3) has collapsed onto the product state $|\,\Psi\,\rangle = |\uparrow\rangle_A \otimes |\downarrow\rangle_B$ and a subsequent measurement on B will with complete certainty give the outcome that B points down. On the other hand, had the first measurement given that A pointed down, then the subsequent measurement would with complete certainty have shown that B pointed up. Thus, even though we have complete knowledge about the global state of the system, we cannot predict the outcome of a measurement. However, the measurements show perfect correlations, in that the result of a measurement on one particle completely decides the outcome of a subsequent measurement on the other. In the words of Schrödinger [117], entanglement means that "the best possible knowledge of a whole does not necessarily include the best possible knowledge of all its parts", something he "would not call *one* but rather *the* characteristic trait of quantum mechanics, the one that enforces its entire departure from classical lines of thought". Adding even more to this fascinating phenomenon, consider what happens if the two particles A and B are taken far apart from each other, while they remain in their common singlet state (4.3). Then a measurement on A will instantaneously affect a subsequent measurement on B, even if they are

[1]For a review on the theoretical aspects of entanglement, see Ref. [146]

light-years apart. This clearly violates the locality principle of classical physics, and the non-local correlations in quantum theory forms what has been known as the "EPR paradox" [115]. In fact, any local ("hidden variable") theory has been shown to impose serious constraints, known as "Bell inequalities", on possible measurement outcomes whereas they can be violated in quantum theory [147]. Later experimental evidence for the violation of Bell inequalities have provided some of the most striking confirmations of quantum mechanics [148–150]. However, it is important not to consider non-local correlations and entanglement to be equivalent. In fact, there are states that are entangled but do not generate non-local correlations [151]. Entanglement is a necessary, but not sufficient, condition for non-locality.

4.3 Entanglement entropy

For a bipartite many-body system in a pure state there is essentially one unique measure of the entanglement between the two parts, namely the von Neumann entropy of the reduced density matrix of (either) one of the parts. For a system in a pure state $|\,\Psi\,\rangle$ and with the Hilbert space partitioned into a direct product $\mathcal{H} = \mathcal{H}_A \otimes \mathcal{H}_B$, the entanglement between A and B is given by the von Neumann entropy

$$S_A = -\mathrm{Tr}\,\rho_A \log \rho_A\,, \tag{4.4}$$

with $S_A = S_B$. Here the reduced density matrix ρ_A of subsystem A is obtained by tracing out all degrees of freedom of subsystem B from the density matrix $\hat{\rho}$ of the entire system,

$$\hat{\rho}_A = \mathrm{Tr}_B\,\hat{\rho}. \tag{4.5}$$

We can get a clear picture of the meaning of the von Neumann entropy by performing the Schmidt decomposition of the pure state $|\,\Psi\,\rangle$,

$$|\,\Psi\,\rangle = \sum_i \alpha_i\; |\,\psi_i\,\rangle_A \otimes |\,\phi_i\,\rangle_B\;, \tag{4.6}$$

where α_i are non-negative real numbers satisfying $\sum_i \alpha_i^2 = 1$, and $\{|\,\psi_i\,\rangle_A\}$ and $|\,\phi_i\,\rangle_B$ are orthonormal bases for part A and B, respectively. When taking the partial trace in Eq. (4.5) to obtain the reduced density matrices $\hat{\rho}_A$ and $\hat{\rho}_B$, one gets

$$\hat{\rho}_A = \sum_i \alpha_i^2\; |\,\psi_i\,\rangle_A\;{}_A\langle\,\psi_i\,|, \qquad \hat{\rho}_B = \sum_i \alpha_i^2\; |\,\phi_i\,\rangle_B\;{}_B\langle\,\phi_i\,|. \tag{4.7}$$

Hence

$$S_\nu = -\mathrm{Tr}\hat{\rho}_\nu \log \hat{\rho}_\nu = -\sum_i \alpha_i^2 \log(\alpha_i^2)\,, \tag{4.8}$$

with $\nu{=}A, B$. Note that $S_A = S_B$. Thus the von Neumann entropy is just the Shannon entropy of the squares of the Schmidt coefficients, characterizing the spread of the pure state $|\,\Psi\,\rangle$ over different (separable) basis states and thus giving a quantitative measure of the non-separability of the pure state (4.6). Equivalently, the von Neumann entropy is the Shannon entropy of the eigenvalues of the reduced density matrix of either one of the parts, as seen from Eq. (4.7), therefore quantifying how mixed the subsystem has become by tracing out the rest. The "mixedness", or disorder, of the subsystem measures how much information about it that was shared with the rest of the system. The von Neumann entropy therefore gives the quantitative version of Schrödinger's [117] observation that in quantum mechanics complete information about the whole does not necessarily imply complete knowledge about its parts. More precisely, the entropy (disorder) of a subsystem can be larger than the entropy of the total system only when the state is entangled [152].

The von Neumann entropy (4.10) is a single number that measures the amount of entanglement in a bipartite system. However, there is often an interest in a more complete characterization of the entanglement. Such a characterization is most straight-forwardly based on the eigenvalues $\lambda_i = \alpha_i^2$ of the reduced density matrices, the distribution of which is referred to as the "entanglement spectrum" [137]. As a way to characterize the full entanglement spectrum one may extend the definition of the von Neumann entropy by introducing an additional parameter n, with n a positive real number, and define the Rényi entropies

$$S_A^{(n)} = \frac{1}{1-n} \log \mathrm{Tr}\, \hat{\rho}_A^n\,, \tag{4.9}$$

with $\lim_{n\to 1} S_A^{(n)} = S_A$. Thus the Rényi entropies encode the moments of the eigenvalue distribution, via

$$S_A^{(n)} = \frac{1}{1-n} \log \sum_i \lambda_i^n\,. \tag{4.10}$$

4.3.1 Entanglement entropy from conformal field theory

The entanglement entropy has been found to be a powerful tool for characterizing the scaling behavior of a one-dimensional quantum system near a critical point [127]. For an infinite system with an interval A

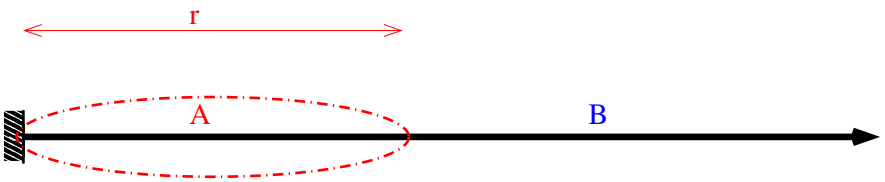

Figure 4.1: A one-dimensional system with a boundary, divided into a part A of size r next to the boundary, and the rest of the system in part B.

of length r the asymptotic behavior of the von Neumann entropy is given by [120, 124–126]

$$S_A \sim \frac{c}{3} \log \frac{r}{\epsilon} + c_1' \tag{4.11}$$

near the critical point. Here c is the central charge of the underlying conformal field theory. The constant ϵ is an arbitrary cutoff scale, with c_1' also being a non-universal number.

For a one-dimensional system with a boundary and at a finite inverse temperature β, a subsystem A of size r next to the boundary (see Fig. 4.1) will have a von Neumann entropy that scales as [126, 132]

$$S_A = \frac{c}{6} \log \left[\frac{\beta}{\epsilon \pi} \sinh \left(\frac{2\pi r}{\beta} \right) \right] + \log g + c' + \dots , \tag{4.12}$$

where $\log g$ is the universal boundary entropy [75], ϵ is the short-distance cutoff, and c' is a non-universal constant. Here "..." denotes the *corrections to scaling* of S_A. These are governed by the irrelevant operators (in the language of the renormalization group) in the boundary conformal field theory (BCFT), with both bulk and boundary contributions.

Let us briefly review how the scaling of entanglement entropy in Eq. (4.11) is calculated within the framework of conformal field theory, introduced in Chapter 2. For a more complete account the reader is referred to the extensive review by Cardy and Calabrese [127], or to their original article [126]. For simplicity, we first concentrate on the case without boundary, and then show how the result is extended to Eq. (4.12)

Writing the density matrix $\rho = e^{-\beta H}$ of the total system as a path integral with "open ends", i.e. with boundary conditions specified by which matrix element that is considered (see Fig. 4.2), gives

$$\rho = \frac{1}{Z} \int \mathrm{D}[\{\phi\}] \; e^{-\int_0^\beta L[\{\phi\}]} , \tag{4.13}$$

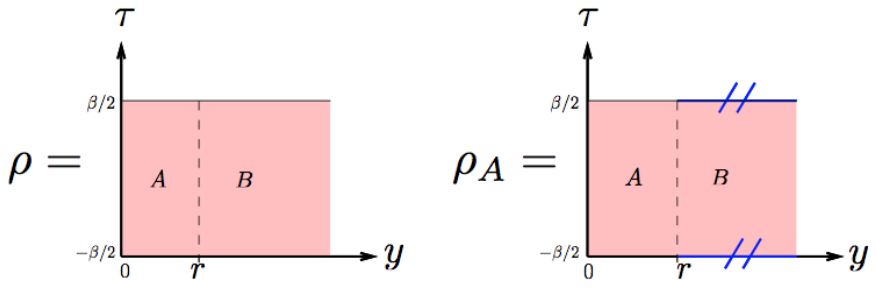

Figure 4.2: Left: The density matrix ρ of the system is a path integral in imaginary time τ, with "open ends" at $\tau = \beta/2$ and $\tau = -\beta/2$. The partition function $Z = \mathrm{Tr}\rho$ is obtained by "sewing together" the "open ends". Right: The reduced density matrix $\rho_A = \mathrm{Tr}_B\rho$ is obtained from ρ by only sewing together those parts of the ends that belong to subsystem B (shown in blue). See also Fig. 4.3.

where $\{\phi\}$ is a complete set of fields, L the Euclidean Lagrangian, and

$$Z = \mathrm{Tr}\ e^{-\beta H} \tag{4.14}$$

the partition function. Then the reduced density matrix $\rho_A = \mathrm{Tr_B}\rho$ is obtained by "sewing" together the open boundaries at $\tau = \beta/2$ and $\tau = -\beta/2$, but only along the part of the boundaries that are not in subsystem A (which here is a single interval of length r), see again Fig. 4.2.

When we then form $\mathrm{Tr}\,\rho_A^n$ it corresponds in the path integral picture to sewing together n copies of ρ_A in a cyclic fashion so that the previously open boundaries in subsystem A now connects copy number i with copy number $i+1$ (and copy number n is connected to number 1), see Fig. 4.3. This is equivalent to evaluating the partition function on an n-sheeted Riemann surface $\mathcal{R}_n$, and is therefore denoted as

$$\mathrm{Tr}\rho_A^n = \frac{Z_{\mathcal{R}_n}}{Z^n}\,. \tag{4.15}$$

Now, the important point is that instead of having a simple Lagrangian on a complicated surface, one can rewrite the problem as having a complicated Lagrangian on a simple surface. This will introduce a new type of fields which turns out to make the problem solvable. Hence we rewrite

$$Z_{\mathcal{R}_n} = \int \mathrm{D}[\{\phi\}]_{\mathcal{R}_n}\ \exp\Big[\ -\int_{\mathcal{R}_n} \mathrm{d}y\,\mathrm{d}\tau\ \mathcal{L}[\{\phi\}](y,\tau)\ \Big]\,, \tag{4.16}$$

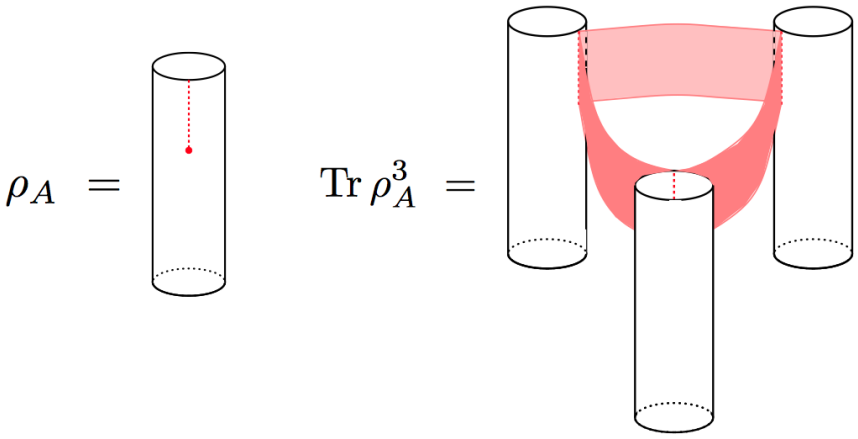

Figure 4.3: Left: The reduced density matrix ρ_A of subsystem A as a path integral on a cylinder with circumference β in the imaginary time direction. There is an open cut (shown as a red dashed line) corresponding to the "open ends" in Fig. 4.2, with boundary conditions corresponding to each matrix element $(\rho_A)_{ij}$. Right: The n-sheeted Riemann surface $\mathcal{R}_n$ representing $\mathrm{Tr}\,\rho_A^n$, here with $n = 3$, is formed by "sewing together" the open cuts in a cyclic fashion corresponding to the matrix multiplication $\sum_{ijk}(\rho_A)_{ij}(\rho_A)_{jk}(\rho_A)_{ki}$.

where $\mathcal{L}$ is the local Lagrangian density, as

$$Z_{\mathcal{R}_n} = \int_{\mathbb{C}_A} \mathrm{D}[\{\phi_1\}...\{\phi_n\}]\ \exp\Big[\ -\int_{\mathbb{C}} \mathrm{d}y\,\mathrm{d}\tau\ \big(\mathcal{L}[\{\phi_1\}](y,\tau) + ... + \mathcal{L}[\{\phi_n\}](y,\tau)\big)\ \Big]\,. \quad (4.17)$$

Here $\mathbb{C}$ is the ordinary complex plane $w = \tau + iy$, and with $\int_{\mathbb{C}_A}$ it is meant that the integration is to be done with the conditions

$$\phi_i(y,0^+) = \phi_{i+1}(y,0^-)\,, \qquad y \in A\,, \quad i = 1,...,n \quad (4.18)$$

and the periodicity $n+1 \equiv 1$. The Lagrangian density on $\mathbb{C}$ is therefore

$$\mathcal{L}^{(n)}[\{\phi_1\},...,\{\phi_n\}](y,\tau) = \mathcal{L}[\{\phi_1\}](y,\tau) + ... + \mathcal{L}[\{\phi_n\}](y,\tau)\,. \quad (4.19)$$

There is a global symmetry under cyclic permutations of the n copies. Thus what has been done is that the path integral is now evaluated on the ordinary complex plane but with n sets of fields, and when taking a field ϕ_i through the branch cut it is transformed into the field $\phi_{i\pm1}$. This is equivalent to having *twist fields* in the branch points, in such a way

that they induce a branch cut in between them. Denoting the twist fields as

$$\Phi_n \equiv \Phi_\sigma\,, \qquad \sigma : i \mapsto i+1 \mod n\,, \tag{4.20}$$

$$\Phi_{-n} \equiv \Phi_{\sigma^{-1}}\,, \qquad \sigma^{-1} : i \mapsto i-1 \mod n\,, \tag{4.21}$$

the normalized partition function can be written as a two-point function of the twist fields,

$$\frac{Z_{\mathcal{R}_n}}{Z^n} = \langle\, \Phi_n(0,0)\Phi_{-n}(r,0)\,\rangle_{\mathbb{C}}\,. \tag{4.22}$$

The two-point function $\langle\, \Phi_n(0,0)\Phi_{-n}(r,0)\,\rangle_{\mathbb{C}}$ is calculated by considering the conformal Ward identity. The conformal transformation that maps the n-sheeted Riemann surface $\mathcal{R}_n$ to the complex plane $\mathbb{C}$ is given by

$$w = \left(\frac{z}{z-ir}\right)^{1/n}\,. \tag{4.23}$$

The holomorphic part of the stress-energy tensor transforms as

$$T(z) = \left(\frac{\partial w}{\partial z}\right)^2 T(w) + \frac{c}{12}\{w,z\}\,, \tag{4.24}$$

where $\{w,z\} = (w'''w' - \frac{3}{2}w''^2)/w'^2$ is the Schwartzian derivative, as discussed in Section 2.2.3. Taking the expectation value of Eq. (4.24) gives

$$\langle\, T(z)\,\rangle_{\mathcal{R}_n} = \frac{c}{12}\{w,z\} = \frac{c}{24}(1-n^{-2})\frac{r^2}{z^2(z-ir)^2}\,, \tag{4.25}$$

since $\langle\, T(w)\,\rangle_{\mathbb{C}} = 0$ by translational and rotational invariance. But

$$\langle\, T(z)\,\rangle_{\mathcal{R}_n} = \frac{\langle\, \Phi_n(0,0)\Phi_{-n}(r,0)T(z)\,\rangle_{\mathbb{C}}}{\langle\, \Phi_n(0,0)\Phi_{-n}(r,0)\,\rangle_{\mathbb{C}}} \tag{4.26}$$

and for the stress-energy tensor $T^{(n)}$ of $\mathcal{L}^{(n)}$ this is multiplied with n,

$$\frac{\langle\, \Phi_n(0,0)\Phi_{-n}(r,0)T^{(n)}(z)\,\rangle_{\mathbb{C}}}{\langle\, \Phi_n(0,0)\Phi_{-n}(r,0)\,\rangle_{\mathbb{C}}} = \frac{c}{24n}(n^2-1)\frac{r^2}{z^2(z-ir)^2}\,. \tag{4.27}$$

Now, the conformal Ward identity reads

$$\begin{aligned}\langle\, \Phi_n(w_1)\Phi_{-n}(w_2)T^{(n)}(z)\,\rangle_{\mathbb{C}} = \Bigg(&\frac{1}{z-w_1}\frac{\partial}{\partial w_1} + \frac{h_{\Phi_n}}{(z-w_1)^2} \\ &+ \frac{1}{z-w_2}\frac{\partial}{\partial w_2} + \frac{h_{\Phi_{-n}}}{(z-w_2)^2}\Bigg) \times \langle\, \Phi_n(w_1)\Phi_{-n}(w_2)\,\rangle_{\mathbb{C}}\,,\end{aligned} \tag{4.28}$$

where in fact the scaling dimensions of the twist fields Φ_n and Φ_{-n} are equal, $h_{\Phi_n} = h_{\Phi_{-n}} \equiv d_n$, and $d_n = \bar{d}_n$. Comparing Eqs. (4.27) and (4.28) shows that the twist fields transform as primary fields,

$$\langle\, \Phi_n(0,0)\Phi_{-n}(r,0)\,\rangle_{\mathbb{C}} = r^{-4d_n}\,, \tag{4.29}$$

with

$$d_n = \frac{c}{24}\Big(n - \frac{1}{n}\Big)\,. \tag{4.30}$$

Hence

$$\mathrm{Tr}\rho_A^n = c_n\Big(\frac{r}{\epsilon}\Big)^{-c(n-1/n)/6}\,, \tag{4.31}$$

where ϵ is the short-distance cutoff, inserted for dimensional reasons, and c_n are constants. Note that $c_1 = 1$, since the trace of a density matrix is unity. Now Eq. (**??**) gives the scaling of the Rényi entropies,

$$S_A^{(n)} = \frac{c}{6}\Big(1 + \frac{1}{n}\Big)\log\frac{r}{\epsilon} + c_n'\,, \tag{4.32}$$

with $c_n' = (1-n)\log c_n$. The scaling of the von Neumann entropy follows from $S_A = \lim_{n\to 1} S_A^{(n)}$, giving

$$S_A = \frac{c}{3}\log\frac{r}{\epsilon} + c_1'\,, \tag{4.33}$$

The calculation is similar when the one-dimensional system at zero temperature has a boundary. For the system to still be conformally invariant, the boundary must be associated with a conformally invariant boundary condition (CIBC). The conformal transformation to be used is now

$$w = \left(\frac{z - ir}{z + ir}\right)^{1/n}\,, \tag{4.34}$$

which maps the n-sheeted Riemann surface $\mathcal{R}_n$, which now has a boundary, to the unit disc $|w| \le 1$ where $\langle\, T(w)\,\rangle = 0$ by rotational invariance. Now Eq. (4.24) gives

$$\langle\, T(z)\,\rangle_{\mathcal{R}_n} = \frac{c}{12}\{w, z\} = \frac{c}{24}(1 - n^{-2})\frac{(2r)^2}{(z - ir)^2(z + ir)^2}\,, \tag{4.35}$$

which implies that $\mathrm{Tr}\rho_A^n \sim \langle\, \Phi_n(ir)\,\rangle_{\mathbb{C}^+}$, where $\mathbb{C}^+$ is the upper complex half-plane $z = \tau + iy$, $y \ge 0$. Hence

$$\mathrm{Tr}\rho_A^n = \tilde{c}_n\Big(\frac{2r}{\epsilon}\Big)^{-c(n-1/n)/12}\,, \tag{4.36}$$

where $\tilde{c}_n$ is a constant. This leads to the scaling

$$S_A^{(n)} = \frac{c}{12}\Big(1+\frac{1}{n}\Big)\log\frac{2r}{\epsilon} + \tilde{c}_n'\,. \tag{4.37}$$

The finite-temperature expressions are easily obtained by conformal transformations. Using that $w = \frac{\beta}{\pi}\sin(\frac{\pi}{\beta}z)$ maps the complex plane onto a cylinder of circumference β, the finite-temperature two-point function of the twist operators is given by

$$\langle\,\Phi_n(ir)\,\rangle_{\mathbb{C}^+} \sim \Big|\frac{\beta}{\pi}\sinh(\frac{\pi}{\beta}2r)\Big|^{-2d_n} \tag{4.38}$$

so that Eq. (4.37) becomes

$$S_A^{(n)} = \frac{c}{12}\Big(1+\frac{1}{n}\Big)\log\Big[\frac{\beta}{\pi\epsilon}\sinh\big(\frac{\pi}{\beta}2r\big)\Big] + \tilde{c}_n' \tag{4.39}$$

at finite inverse temperature β. As $\beta\to\infty$ this of course reduces to Eq. (4.37). However, in the limit $\beta \ll r$ it follows from Eq. (4.39) that the von Neumann entropy $S_A = \lim_{n\to 1} S_A^{(n)}$ scales as

$$S_A = \frac{2\pi c}{6}r + \frac{c}{6}\log\Big[\frac{\beta}{2\pi\epsilon}\Big] + \tilde{c}' \tag{4.40}$$

up to terms $\mathcal{O}(e^{-4\pi r/\beta})$. This is very similar to the expression for the thermodynamic entropy S_A^{Th} for a system of size r in the same limit $\beta \ll r$,

$$S_A^{Th} = \frac{2\pi c}{6}r + \log g + \text{const.}, \tag{4.41}$$

also with corrections that decay exponentially in r/β. Here $\log g$ is the universal *boundary entropy* [75], which is the only term that depends on the boundary conditions. It is therefore possible to identify the part of the constant term in Eq. (4.39) that depends on the specific boundary condition as the thermodynamic boundary entropy, writing the von Neumann entropy on the final form

$$S_A = \frac{c}{6}\log\Big[\frac{\beta}{\pi\epsilon}\sinh\big(\frac{\pi}{\beta}2r\big)\Big] + \log g + s'\,, \tag{4.42}$$

where s' is a non-universal constant.

4.3.2 Entanglement in quantum impurity systems

Summarizing the results above, the scaling of the entanglement entropy of a block of size r next to the boundary of a semi-infinite one-dimensional system described by a BCFT is at zero temperature given by [126, 132]

$$S(r) = \frac{c}{6}\log\frac{2r}{\epsilon} + \log g + s' + \dots\,, \tag{4.43}$$

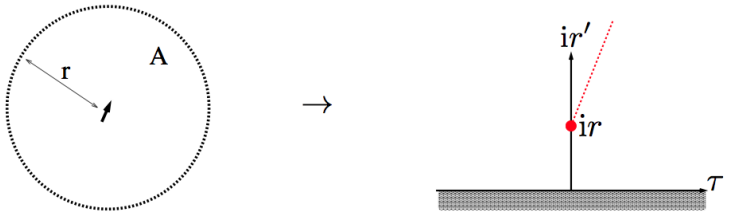

Figure 4.4: At a fixed point, the entanglement entropy of a region A of radius r around the impurity will in the BCFT picture correspond to a path integral on the upper complex half-plane $z = \tau + ir'$ with a branch point at $z = ir$ and a conformally invariant boundary condition.

where c is the central charge, $\log g$ is the boundary entropy [75] encoding the conformally invariant boundary condition (CIBC), ϵ is the short-distance cutoff, and s' is a non-universal constant. Here "..." denotes the corrections to scaling of $S(r)$, which are governed by the irrelevant operators in the BCFT, with both bulk and boundary contributions. Here we are interested in the boundary contributions, showing up due to defects or impurities [153–156].

The Kondo formation of a screening cloud when a quantum impurity interacts with surrounding itinerant electrons means that the impurity gets entangled with the electrons. It is therefore important for the understanding of the resulting correlated state [157–159], and for possible applications of the Kondo cloud in quantum information purposes [92, 93], to obtain the spatial distribution of the entanglement in these systems. For this purpose one may define the *impurity entanglement entropy*, which is given as $S_{imp} = S(\text{with impurity}) - S(\text{no impurity})$ and hence is the contribution to the entanglement entropy of a subsystem coming from the impurity [158].

As reviewed in Section 3.2, the low-energy physics of a quantum impurity system can be described as a BCFT with the effect of the impurity encoded in the specific CIBC and boundary operator content of the theory [86]. This make it possible to use the BCFT approach to obtain the large-distance asymptotics of the entanglement entropy of a region of radius r around the impurity. Note that when the models describe two- (three-) dimensional quantum impurity systems, the size r of the block at the boundary will correspond to the radius of a disc (sphere) centered at the impurity (or the midpoint between the impurities when they are two), see Fig. 4.4. Since the impurity only affects the boundary condition and operator content of the BCFT, we see from Eq. (4.43) that

the impurity contribution S_{imp} to the entanglement entropy $S(r)$ is

$$S_{imp} = \log g + \dots . \tag{4.44}$$

Here "..." is the boundary contribution to the scaling corrections of $S(r)$, which are governed by those irrelevant *boundary* operators in the operator content that do not break the symmetries of the theory. This means that corrections to scaling of the entanglement entropy from perturbing boundary operators in conformal field theory provide important information about entanglement in quantum impurity problems.

5

Topological states of matter

In this chapter we discuss different forms of topological states of matter. A topological phase is characterized by some topological invariant [160–162], i.e. a quantum number that is unaffected by smooth deformations of the system. Such topological phases appear in the integer quantum Hall effect [163], the fractional quantum Hall effect [37], one-dimensional antiferromagnets with "Haldane phases" [164–166] and topological insulators and superconductors [167], as well as two-dimensional frustrated magnets with spin-liquid states [168, 169]. These systems feature gapless edge states, which are topologically protected from local perturbations. The gapped bulk manifests an order which does not break any symmetry, instead there is a *topological order*. However, this term is usually reserved for those globally entangled topological states exhibiting "anyonic" quasiparticles in the bulk and topology-dependent degeneracies insensitive to local perturbations. Examples of such states appear in the fractional quantum Hall effect and some two-dimensional frustrated magnets. *Topological insulators* are also topological states of matter, but they do not have many of the characteristic properties of topological order. They can be understood from single-electron band theory for the bulk and there is a unique ground state. The topological protection of the edge states of topological insulators require time-reversal symmetry to be unbroken, hence they belong to the class of topological phases of matter said to possess "symmetry-protected topological order" [170]. This concept also encompass topological states in one-dimensional quantum systems [171], such as the Haldane phase [164, 165] in spin chains, and the AKLT model [166]. The AKLT chain has a gapped bulk ground states but a degeneracy that depends on boundary conditions, with gapless edge states for open boundaries. Another way of realizing this type

of gapless edge states is to have some pairing mechanism for spinless fermions, in which case there can be gapless edge states of non-local Majorana fermions [53,172]. It is important to remember that these one-dimensional topological phases, just as topological insulators, need some symmetry to be preserved and therefore are not as robust as phases with "intrinsic" topological order [170].

With this distinction between topological order and topological insulators, we discuss these two aspects of topology in condensed matter separately.

5.1 Topological order

Topological order is a concept introduced by Wen [173] to encompass those new phases, like in the fractional quantum Hall effect, falling outside of the standard Landau symmetry-breaking theory [20, 33]. Topologically ordered phases instead have a globally entangled structure characterized by some topological quantum numbers [38]. Such states, with anyonic quasiparticles and topologically protected degeneracies, have attracted much attention due to the potential applications for topological quantum computing [174].

5.1.1 Anyons and topological quantum computation

Nontrivial quasiparticle statistics is a phenomenon that only occurs in systems in two spatial dimensions, for very profound reasons [45]. It is only in two spatial dimensions that it can make a difference how one takes two particles around each other, in all higher dimensions the world-lines of this process can always be continuously deformed to the trivial operation that nothing happened. Thus exchanging particles can only give a plus or a minus sign to the wave function, meaning that there are only fermions or bosons. But in two dimensions there is no such restriction, see Fig. 5.1, hence there can exist particles called "anyons" that can have any statistics. The anyonic statistics might even be non-Abelian, meaning that the order in which the particles are exchanged matters! The existence of anyons that are neither fermions or bosons is one of the characteristics of a topological phase in two dimensions. Note that it is not the electrons that can be anyons, since these of course still are fermions, instead it is the many-particle excitations known as quasiparticles that can have this peculiar property.

Another characteristic feature of topological order is a ground state degeneracy that is topology-dependent. To be more precise, in a topologi-

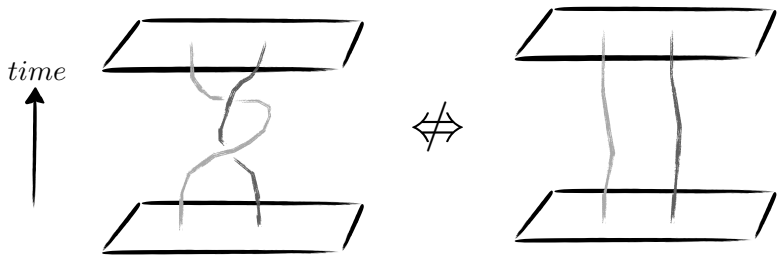

Figure 5.1: Exchanging identical particles can only give a plus or minus sign to the wavefunction in three or higher dimensions. In two dimensions this is no longer true. The left sketch shows one particle being taken around another particle, which is equivalent of exchanging them twice. Since the spatial dimensions are only two, there is no way that without crossing them one can continuously deform the world lines into the trivial process of doing nothing at all shown in the right sketch. Hence the statistical phase acquired can be arbitrary.

cal phase of matter the ground state degeneracy will depend on the topology of the manifold on which the system is defined. This means that if we place the system on a torus (i.e. impose periodic boundary conditions), then the ground-state degeneracy will be different compared to having the same system defined on the sphere or the infinite plane. There is actually an underlying connection between this statement about the ground-state degeneracy and the previously mentioned anyonic quasiparticle statistics, that follows from the observation that different ground states are connected by the process of creating quasiparticle-hole-pairs, doing something non-trivial with them, and finally annihilate them [175,176]. If the quasiparticle was an anyon then the final wave function has picked up a phase factor, hence there are non-commuting symmetry operators giving a degeneracy.

The third defining property of a topologically ordered phase is that it is gapped. This is a very useful property if we would like to use the non-Abelian anyons for topological quantum computation [174]. Due to the energy gap, at sufficiently low temperatures the only way to take the system between the degenerate ground states is to take quasiparticles around each other, "braiding" them. The degenerate ground states are then encoding the quantum information, i.e. forming the "qubits", and the braidings are the unitary operations that make up the quantum computation.

A number of lattice models have been constructed to study topological order and topological quantum phase transitions (see Ref. [39] for a

review). It was in the context of such a lattice model, the "toric code", that Kitaev [176] launched the idea of topological quantum computation. While topologically ordered fractional quantum Hall states seem intrinsically hard to manipulate for doing topological quantum computation, there have been proposals to realize lattice Hamiltonians giving topological order in specially engineered Josephson junction arrays [177] or cold atoms in optical lattices [178, 179].

Below we will give some simple examples of models that in a clear way illustrate the features of topological order, the "toric code" being the most prominent. It is also an extension of this model that provides one of the exactly solvable models used to study quantum phase transitions out of topologically ordered phases.

5.1.2 Kitaev's toric code model

Let us briefly describe the perhaps simplest model with topological order that has been constructed, the "toric code". For a full account the reader is referred to the original article by Kitaev [176]. The model is defined on the square lattice, with a spin-1/2 particle (or, equivalently, a qubit) on each bond of the lattice. Define the operators

$$A_s = \prod_{i \in s} \hat{\sigma}_i^x \,, \qquad B_p = \prod_{i \in p} \hat{\sigma}_i^z \,, \tag{5.1}$$

where $i \in s$ denotes the bonds around the vertex labelled by s, and $i \in p$ denotes the bonds around the plaquette labelled by p, see Fig. 5.2. Now,

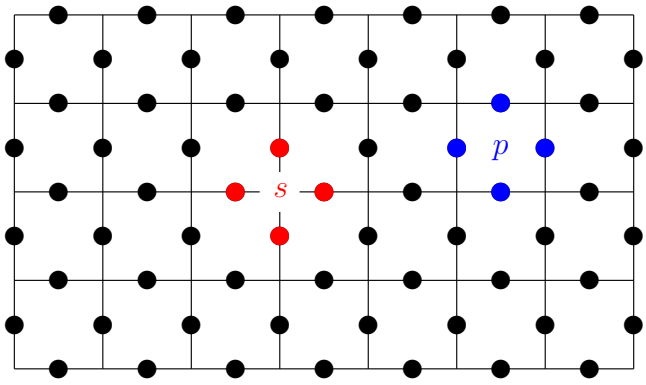

Figure 5.2: The spins in the toric code model reside on the bonds of the square lattice. The operator A_s in Eq. (5.1) involves the spins (in red) around the vertex s, whereas the operator B_p involves the spins (in blue) around the plaquette p.

the Hamiltonian of the model is given by

$$H = -\sum_s A_s - \sum_p B_p, \tag{5.2}$$

which is easily diagonalized since all the A_s and B_p operators commute with each other. Since the eigenvalues of A_s and B_p are ± 1, the ground state $|\, gs \,\rangle$ is given by

$$A_s \,|\, gs \,\rangle = |\, gs \,\rangle\,, \qquad B_p \,|\, gs \,\rangle = |\, gs \,\rangle\,, \qquad \forall\, s, p\ . \tag{5.3}$$

In fact, we can write the ground state as

$$|\, gs \,\rangle = \sum_{g \in G} g \,|\, 0 \,\rangle, \tag{5.4}$$

where $|\, 0 \,\rangle$ is the fully spin-polarized state ($\hat{\sigma}_i^z \,|\, 0 \,\rangle = |\, 0 \,\rangle$, $\forall\, i$), and G is the Abelian group of all possible combinations of different A_s operators. An element $g \in G$ thus looks like $g = A_{s_1} A_{s_2} A_{s_3} ....$ Another way of seeing this is to say that the ground state (5.4) is a coherent sum of all possible configurations of closed loops of flipped spins, something Wen [38] has called a "string net". From this picture we can intuitively understand why the ground state becomes degenerate when the system is put on a torus, or some other higher-genus surface. Then the winding numbers of the loops around the "punctures" of the surface cannot be changed by acting with the A_s operators, and therefore the ground state must be degenerate. For example, on a torus there can be a loop winding around the torus or along the torus, hence the ground-state degeneracy is four-fold. In general, the ground state degeneracy is 4^g-fold, where g is the genus, or number of punctures, of the surface.

To show this more explicitly and at the same time demonstrating the other defining characteristic of topological order, we now consider the excitations. This will also demonstrate the connection between the topological ground-state degeneracy and the anyonic nature of the excitations. First note that an elementary excitation is created by violating one (and only one) of the constraints in Eq. (5.3). But because of the constraints $\prod_s A_s = 1$ and $\prod_p B_p = 1$, these "elementary" excitations can only be created in pairs. In fact, such a double excitation can be written as a string operator acting on the ground state, where the end-points of the string corresponds to the elementary excitations. The string operators are defined as

$$S^z(t) = \prod_{i \in t} \hat{\sigma}_i^z\,, \tag{5.5}$$

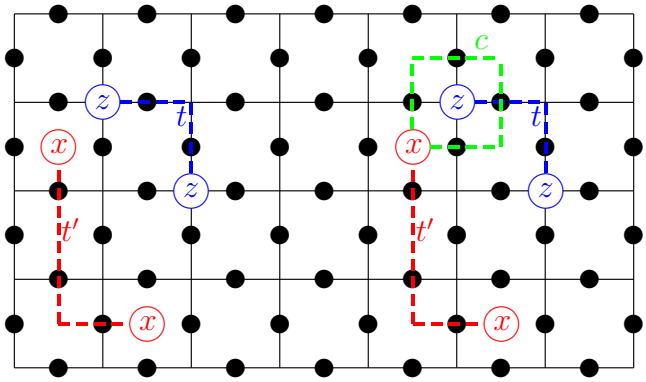

Figure 5.3: Left: A pair of x-type excitations connected by the string $S^x(t')$ given by Eq. (5.6), in red, and a pair of excitations of z-type connected by the string $S^z(t)$ given by Eq. (5.5), in blue. Right: Taking an x-type excitation around a z-type excitation along the path c (in green).

where t is a non-closed path between vertices, and

$$S^x(t') = \prod_{i \in t'} \hat{\sigma}_i^x \,, \tag{5.6}$$

where t' is a non-closed path between plaquettes, see Fig. 5.3. The two types of double excitations can then be written as $|\,\Psi^z(t)\,\rangle = S^z(t)|\,gs\,\rangle$ and $|\,\Psi^x(t')\,\rangle = S^x(t')|\,gs\,\rangle$, respectively. Now we will see that when moving one excitation around another excitation of a different type, the wave function acquires a minus sign. When moving an excitation of, say, x-type around an excitation of z-type, the x-string (5.6) will have to cross the z-string (5.5) of the other excitation at some point. Since $\hat{\sigma}_i^x$ and $\hat{\sigma}_i^z$ anticommute, the wave function has picked up a minus sign. This can be written as

$$|\,\Psi_{initial}\,\rangle = S^z(t)|\,\Psi^x(t')\,\rangle \,, \tag{5.7}$$

and

$$\begin{aligned} |\,\Psi_{final}\,\rangle &= S^x(c)S^z(t)|\,\Psi^x(t')\,\rangle \\ &= -S^z(t)S^x(c)|\,\Psi^x(t')\,\rangle = -|\,\Psi_{initial}\,\rangle \,, \end{aligned} \tag{5.8}$$

see Fig. 5.3. Thus the excitations are neither fermions nor bosons, and therefore anyons. Let us now consider the system put on a torus. We then see that the process of creating a pair of elementary excitations, taking one of them around the torus and finally annihilate them corresponds to creating a closed string that is winded around the torus. Hence we take the system from one ground state to another that is characterized

by a different winding number. Another way to see this is to consider the process of taking one x-string around the torus in one direction and a z-string around the torus in the other direction, and then taking them back along the same paths. Defining the string operators

$$Z \equiv \prod_{i \in c} \hat{\sigma}_i^z \,, \qquad X \equiv \prod_{i \in c'} \hat{\sigma}_i^x \,, \tag{5.9}$$

where c is a closed loop that winds around the torus in one direction and c' is a closed loop that winds around the torus in the other direction, we see that the process can be expressed as the operator $W = X^\dagger Z^\dagger X Z$. Now the process is actually equivalent to taking the excitation of x-type around that of z-type, as can be seen by continuously deforming the paths [175]. As shown above, this implies $W = -1$, and hence the anticommutation $XZ = -ZX$. With two operators that both commute with the Hamiltonian but not with each other, the ground state must be degenerate.

Since it costs a non-zero amount of energy to create the excitations, the system is gapped. Any process that takes the system from one of the degenerate ground states to another would correspond to moving an excitation all the way around the torus, hence such a process is exponentially suppressed as the system size is increased. The toric code model therefore displays the defining features of topological order.

5.1.3 Topological quantum phase transitions

As we have seen, there is no symmetry breaking associated with a topological order. Hence there is no local order parameter that identifies a quantum phase transition (QPT) out of a topologically ordered phase. Studies of such topological quantum phase transitions (TQPTs) have instead borrowed concepts from quantum information theory, such as *entanglement* [145] and *fidelity* [180]. They both measure properties of the ground state as the system undergoes the phase transition. The reason one might expect them to encode information about TQPTs is that they in some sense measure global properties of the ground state, and topological order is a property of the ground state wave function manifested in certain subleading terms in the entanglement entropy [135, 136].

The Castelnovo-Chamon model

A simple lattice model exhibiting a topological quantum phase transition based on the toric code has been constructed by Castelnovo and Chamon [181]. Its Hamiltonian describes localized spin-1/2 particles attached

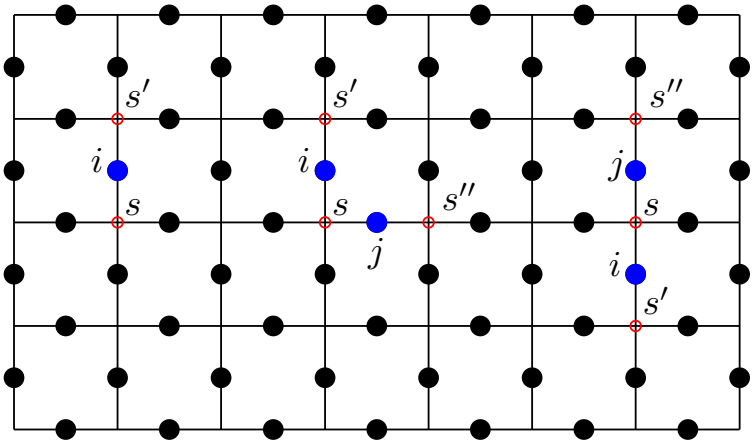

Figure 5.4: Mapping between the Castelnovo-Chamon model and the two-dimensional classical Ising model. The spins of the former reside on the lattice bonds (filled black circles), and the spins of the latter on the vertices. Left: $\sigma_i^z = \theta_s \theta_{s'}$, where i is the bond between the neighboring vertices $\langle s, s' \rangle$. Middle and right: For i and j nearest (next-nearest) neighbors, the mapping gives $\langle \hat{\sigma}_i^z \hat{\sigma}_j^z \rangle = \langle \theta_s \theta_{s'} \theta_{s''} \theta_s \rangle = \langle \theta_{s'} \theta_{s''} \rangle$, where $\langle s', s'' \rangle$ are next-nearest (third-nearest) neighbors.

to the bonds of a square lattice and is given by

$$H = -\lambda_0 \sum_p B_p - \lambda_1 \sum_s A_s + \lambda_1 \sum_s e^{-\beta \sum_{i \in s} \hat{\sigma}_i^z}, \tag{5.10}$$

where $A_s = \prod_{i \in s} \hat{\sigma}_i^x$ and $B_p = \prod_{i \in p} \hat{\sigma}_i^z$ are the star and plaquette operators of the Kitaev toric code model [176], Eq. (5.2). The star operator A_s acts on the spins around the vertex s, and the plaquette operator B_p acts on the spins on the boundary of the plaquette p. Note that here β is not an inverse temperature, but a free parameter in the Hamiltonian. The ground state is, by construction, known exactly. For $\lambda_{0,1} > 0$ the ground state in the topological sector containing the fully magnetized state $|0\rangle$ is given by [181]

$$|GS(\beta)\rangle = \sum_{g \in G} \frac{e^{\beta \sum_i \sigma_i^z(g)/2}}{\sqrt{Z(\beta)}} g|0\rangle, \tag{5.11}$$

with

$$Z(\beta) = \sum_{g \in G} e^{\beta \sum_i \sigma_i^z(g)}, \tag{5.12}$$

where G is the Abelian group generated by the star operators A_s, and $\sigma_i^z(g)$ is the z component of the spin at site i in the state $g|0\rangle$. When $\beta = 0$ the state in (5.11) reduces to the topologically ordered ground state of the toric code model (5.2). When $\beta \to \infty$ the ground state (5.11) becomes the magnetically ordered state $|0\rangle$. Hence β is the driving parameter in this model.

There is a one-to-two mapping between the configurations $\{g\} = G$ and the configurations $\{\theta\} \equiv \Theta$ of the classical 2D Ising model $H = -J\sum_{<s,s'>}\theta_s\theta_{s'}$ with $\theta_s = -1$ $(+1)$ when the corresponding star operator A_s is (is not) acting on the site s [181]. Thus $\sigma_i^z = \theta_s\theta_{s'}$, where i is the bond between the neighboring vertices $\langle s, s'\rangle$, see Fig. 5.4. This gives

$$\langle GS(\beta)|\hat{\sigma}_i^z|GS(\beta)\rangle = \frac{1}{Z(\beta)}\sum_{\theta\in\Theta}\theta_s\theta_{s'}e^{\beta\sum_{\langle s''s'''\rangle}\theta_{s''}\theta_{s'''}} = \frac{E_{\text{Ising}}(\beta)}{N}, \quad (5.13)$$

where β is identified as the reduced nearest neighbor coupling $J/T = \beta$ of the classical 2D Ising model [181]. We also have that

$$\langle GS(\beta)|\hat{\sigma}_i^x|GS(\beta)\rangle = 0\ , \quad (5.14)$$
$$\langle GS(\beta)|\hat{\sigma}_i^y|GS(\beta)\rangle = 0\ , \quad (5.15)$$

since $\langle 0|g\hat{\sigma}_i^x g'|0\rangle = 0$, $\forall g, g' \in G$, and similarly for $\hat{\sigma}_i^y$.

The mapping shows that there is a second-order TQPT at $\beta_c = (1/2)\ln(\sqrt{2}+1)$, which defines the second-order phase transition in the classical two-dimensional Ising model [50]. At this quantum critical point the topological entanglement entropy [135, 136] S_{topo} goes from $S_{\text{topo}} = 1$ for $\beta < \beta_c$ to $S_{\text{topo}} = 0$ for $\beta > \beta_c$ [181], showing that it acts as a discontinuous non-local order parameter for this TQPT.

The transverse Wen-plaquette model

We finally also mention the transverse Wen-plaquette model, which is the Wen-plaquette model [182] for spin-1/2 particles on the vertices of a square lattice with an added magnetic field [183]

$$H = g\sum_i \hat{F}_i + h\sum_i \hat{\sigma}_i^x, \quad (5.16)$$

where

$$\hat{F}_i = \hat{\sigma}_i^x\hat{\sigma}_{i+\hat{x}}^y\hat{\sigma}_{i+\hat{x}+\hat{y}}^x\hat{\sigma}_{i+\hat{y}}^y \quad (5.17)$$

and $g < 0$. The boundary conditions are periodic. At $h = 0$ the ground state is the topologically ordered ground state of the Wen-plaquette model [182] and in the limit $h \to \infty$ the ground state is magnetically

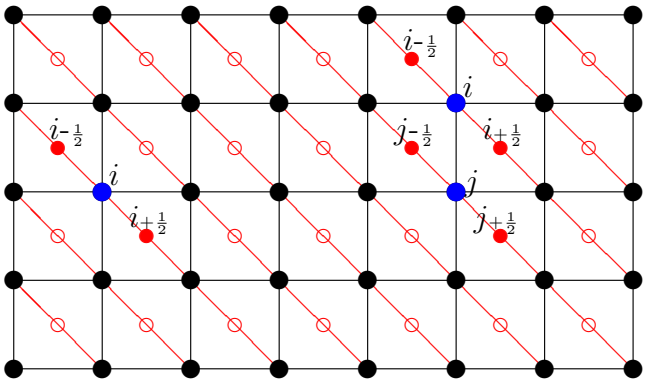

Figure 5.5: Mapping the transverse Wen-plaquette model (with spins shown as filled black circles on the vertices of the square lattice) onto 1D transverse Ising chains along the diagonals (shown in red, with spins at the centers of the plaquettes shown as red open circles). Left: $\hat{\sigma}_i^x \mapsto \hat{\tau}^x_{i-\frac{1}{2}}\hat{\tau}^x_{i+\frac{1}{2}}$. Right: For two nearest neighbor spins at sites i,j, we get $\langle\hat{\sigma}_i^x\hat{\sigma}_j^x\rangle = \langle\hat{\tau}^x_{i-\frac{1}{2}}\hat{\tau}^x_{i+\frac{1}{2}}\hat{\tau}^x_{j-\frac{1}{2}}\hat{\tau}^x_{j+\frac{1}{2}}\rangle = (\langle\hat{\tau}^x_{i-\frac{1}{2}}\hat{\tau}^x_{i+\frac{1}{2}}\rangle)^2$.

ordered. The model (5.16) cannot be solved exactly as it stands, but it can be mapped onto a system of one-dimensional quantum Ising chains in the following way [183]: Since $\hat{F}_i$ and $\hat{\sigma}_j^x$ have the same commutation relations as $\hat{\tau}^z_{i+\hat{x}/2+\hat{y}/2}$ and $\hat{\tau}^x_{j-\hat{x}/2+\hat{y}/2}\hat{\tau}^x_{j+\hat{x}/2-\hat{y}/2}$ (where the $\hat{\tau}$ operators act on spin-1/2 particles at the centers of the plaquettes), the Hamiltonian (5.16) can be mapped onto

$$H = -h\sum_a\sum_i\left(g_I\hat{\tau}^z_{a,i+\frac{1}{2}} + \hat{\tau}^x_{a,i-\frac{1}{2}}\hat{\tau}^x_{a,i+\frac{1}{2}}\right), \tag{5.18}$$

which we recognize as a number of decoupled quantum Ising chains (1.4). Here, the index a denotes the diagonal chains over the plaquette-centered sites, and i is the site index on each diagonal chain; cf. Fig 5.5. The coupling constant $g_I = g/h$. The mapping is thus written as

$$\hat{\sigma}_i^x\hat{\sigma}^y_{i+\hat{x}}\hat{\sigma}^x_{i+\hat{x}+\hat{y}}\hat{\sigma}^y_{i+\hat{y}} \mapsto \hat{\tau}^z_{i+\frac{1}{2}}, \qquad \hat{\sigma}_i^x \mapsto \hat{\tau}^x_{i-\frac{1}{2}}\hat{\tau}^x_{i+\frac{1}{2}}. \tag{5.19}$$

From the mapping (5.18) to quantum Ising chains it follows that the transverse Wen-plaquette model has a topological quantum phase transition at $g/h = 1$ [183], corresponding to the quantum critical point of the quantum Ising chain in Chapter 1.

5.2 Topological insulators

Topological insulators[1] constitute a new class of time-reversal invariant materials that are ordinary insulators in the bulk but with topologically protected gapless edge states. They can actually be understood from ordinary band theory [17], in contrast to systems with topological order. That is to say, the topological properties of topological insulators do not arise because of electron correlations but because of topological quantum numbers arising from the single-particle Bloch wave functions. These topological quantum numbers are very much like that appearing in the integer quantum Hall effect [160]. Two-dimensional topological insulators, also known as quantum spin Hall insulators, can in fact be seen as a time-reversal invariant version of the integer quantum Hall effect. Hence realizing such a system means that one has the same remarkably robust properties of integer quantum Hall systems without applying magnetic fields.

The studies of topological insulators originates from such ideas, with a model based on graphene proposed by Haldane [188] to obtain the integer quantum Hall effect with zero average magnetic field. This model was later generalized by Kane and Mele [189,190], showing that graphene with sufficiently strong spin-orbit interactions could turn into a quantum spin Hall insulator characterized by a $\mathbb{Z}_2$ topological invariant. In practice however, it turns out that the spin-orbit coupling in graphene is too weak for this novel phase to be realized. Following its theoretical prediction by Bernevig, Hughes and Zhang [191], the first experimental observation of the quantum spin Hall state was instead done with a HgTe quantum well by Molenkamp's group in Würzburg [109]. Simultaneous developments [192, 193] led to the prediction [194], and experimental observation [195], of three-dimensional topological insulators of bismuth compounds. This development has now lead to the realization of bulk materials with topologically protected transport up to room temperature [196], as well as the fabrication of topological insulator nanowires [197].

The topological protection of the edge states of topological insulators means that their metallic states at the boundary are immune to backscattering as long as time-reversal symmetry is unbroken. They therefore provide a possibility to realize dissipationless electronic transport, and the spin-filtered characteristics make these systems very interesting for spintronics applications [198]. Topological insulators in proximity of ordinary s-wave superconductors have also been predicted [199] to give rise to Majorana fermions, thereby providing a possibility of performing

[1] For extensive reviews, see Refs. [167, 184–187].

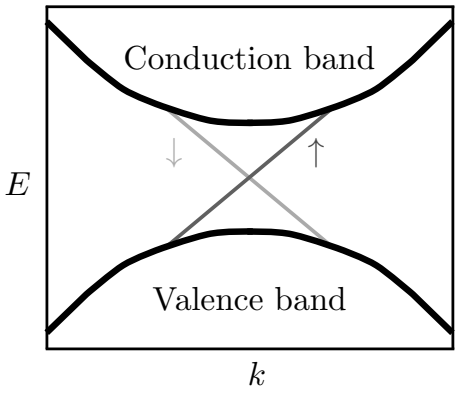

Figure 5.6: The characteristic dispersion of a topological insulator: for the bulk states there is an energy gap which splits the spectrum into a valence and a conduction band just as for an ordinary insulator. However inside the bulk gap there are gapless *edge* states, with spin coupled to momentum and protected by time-reversal invariance.

topological quantum computation in solid state systems. The experimental search for such Majorana fermions is currently a topic of intense activity [200].

5.2.1 Quantum spin Hall insulators

The quantum spin Hall (QSH) insulator is a two-dimensional time-reversal invariant topological insulator. It is formed in a two-dimensional electron gas confined in a quantum well, where strong atomic spin-orbit interaction has created an "inverted" band structure [191]. The gapless edge states appearing inside the bulk energy gap, as shown in Fig. 5.6, form a time-reversal connected pair. In the simplest model, right-movers have spin up and left-movers have spin down. However in real systems spin is no longer conserved, due to spin-orbit interactions, and the edge states should really be thought of as time-reversal connected pairs. In practice however, the spin-conserved model turns out to be adequate for most purposes and is the one commonly used. In any case, these gapless edge modes are topologically protected and provide dissipationless edge currents. In equilibrium, the electric currents at the edge cancel, instead there is a net spin current. Hence the name "quantum *spin* Hall effect" (although the spin Hall conductivity is only quantized in the case of conserved spin). Comparing to Fig. 5.8 it is clear that the quantum spin Hall insulator can be seen as two time-reversed copies of the integer quantum Hall effect. The topological protection from backscattering

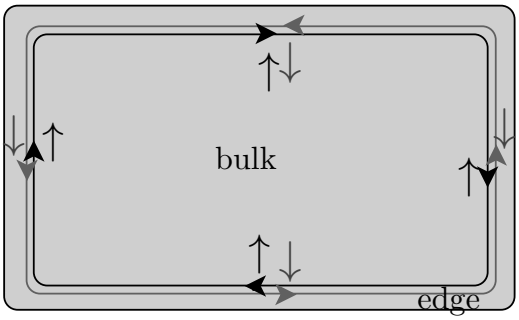

Figure 5.7: Sketch of the quantum spin Hall system, a two-dimensional time-reversal invariant topological insulator The two-dimensional electron gas, confined in a quantum well, is an insulator in the bulk. However at the edge there is a pair of time-reversal connected pair of gapless helical edge modes, where the spin is locked to the momentum. Hence the quantum spin Hall system can be seen as two time-reversed copies of the integer quantum Hall effect which is shown in Fig. 5.8.

mechanisms that might destroy the gapless edge states and cause localization come from the existence of a topological invariant, much like for the integer quantum Hall effect. The QSH insulator is however only protected against time-reversal invariant perturbations, thereby adding another distinction in comparison to systems with topological order as defined previously. Time-reversal invariance therefore provides an efficient way to understand the properties of the QSH state.

5.2.2 Topological band theory and Kramers pairs

Integer quantum Hall states

In order to get some feeling for the topological quantum numbers appearing for time-reversal invariant topological insulators, let us recall how it is constructed for the integer quantum Hall effect [160]. There, the quantized Hall conductivity [163]

$$\sigma_{xy} = ne^2/h, \tag{5.20}$$

where e^2/h is the conductance quantum, is given in terms of the integer n. The reason n is restricted to integer values comes from its quantization through the expression

$$n = \frac{1}{2\pi} \int \mathrm{d}\mathbf{k}\, \mathcal{F}, \tag{5.21}$$

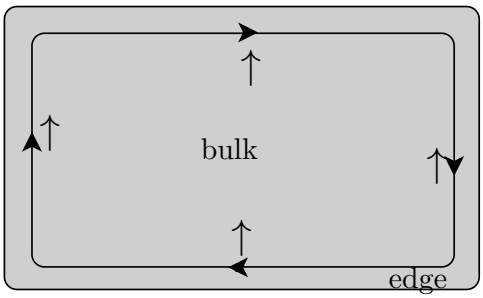

Figure 5.8: Sketch of an integer quantum Hall system. It has a bulk gap but gapless chiral edge modes, with spin polarized in the direction of the time-reversal symmetry breaking magnetic field.

where the integral of the Berry flux $\mathcal{F} \equiv i\nabla \times \sum_m \langle u_m | \nabla_k | u_m \rangle$ is over the magnetic Brillouin zone, and $|u_m(k)\rangle$ the Bloch wave function in the filled band m. The number n, known as the Chern number, cannot change if the Hamiltonian is varied smoothly. Hence n is a topological invariant.

An alternative way of understanding the topological nature of the quantization is the existence of gapless chiral edge states [201], and the connection between the bulk band structure and the edge states is known as the *bulk-boundary correspondence* [202].

Time-reversal invariance

Since the topological invariant n in Eq. (5.20) is odd under time reversal, it will vanish identically for a time-reversal invariant system. Instead, for the quantum spin Hall insulator there is a $\mathbb{Z}_2$ topological invariant [190] distinguishing it from the trivially insulating phase. In order to understand this $\mathbb{Z}_2$ classification we need to recall the consequences of time-reversal invariance on electronic systems.

The time-reversal operation $\mathcal{T}$ takes $t \to -t$, and therefore transforms position, momentum and spin according to $\mathbf{r} \to \mathbf{r}$, $\mathbf{p} \to -\mathbf{p}$ and $\mathbf{S} \to -\mathbf{S}$, respectively. Since these transformations change the sign of the canonical commutation relations, the quantum-mechanical $\mathcal{T}$ operator is antiunitary.[2] By letting $t \to -t$ in the Schrödinger equation for a spinless particle,

$$i\hbar \frac{\partial}{\partial t} |\psi(\mathbf{r}, t)\rangle = \hat{H} |\psi(\mathbf{r}, t)\rangle \quad \to \quad -i\hbar \frac{\partial}{\partial t} |\psi(\mathbf{r}, -t)\rangle = \hat{H} |\psi(\mathbf{r}, -t)\rangle, \tag{5.22}$$

and then taking the complex conjugation of this equation, it follows that

[2] See e.g. Ref. [203] for a textbook account.

the wave function transforms as

$$\psi(\mathbf{r}, t) \to \psi^*(\mathbf{r}, -t). \tag{5.23}$$

The time-reversal operator is therefore the complex conjugation operator K for spinless particles. For a single particle with spin-1/2, one can factorize $\mathcal{T} = \Theta K$ and then determine the operator Θ from

$$\Theta\,\mathbf{r}\,\Theta^{-1} = \mathbf{r}\ ,\quad \Theta\,\mathbf{k}\,\Theta^{-1} = \mathbf{k}\ ,\quad \Theta\,\sigma^{x/z}\,\Theta^{-1} = -\sigma^{x/z}\ ,\quad \Theta\,\sigma^{y}\,\Theta^{-1} = \sigma^{y}, \tag{5.24}$$

since the wave number $\mathbf{k} = -i\nabla$ and the Pauli matrix σ^y acquires minus signs under complex conjugation. It then follows that for a spin-1/2 particle the time-reversal operator is given by

$$\mathcal{T} = -i\,\sigma^y\,K, \tag{5.25}$$

from which it follows that $\mathcal{T}^2 = -1$. In general, for a system with n different spin-1/2 particles, $\mathcal{T}^2 = (-1)^n$.

We can now state the important *Kramers theorem* [204] stating that for a time-reversal invariant system with $\mathcal{T}^2 = -1$, each eigenvalue of the Hamiltonian is at least twofold degenerate and the degeneracy is necessarily of even order. This is known as Kramers degeneracy, and the degenerate eigenstates connected by $\mathcal{T}$ are called *Kramers pairs*.

It is now possible to understand the $\mathbb{Z}_2$ classification of $\mathcal{T}$ invariant band insulators as a consequence of Kramers theorem. For an odd number of edge fermions, $\mathcal{T}^2 = -1$, and it is not possible to make the gapless edge states gapped without closing the bulk band gap, see Fig. 5.9. However for an even number of gapless edge fermions it is possible to do this. The phase with $\mathcal{T}^2 = 1$ is therefore topologically equivalent to an ordinary band insulator, since the edge states can be smoothly deformed away. The $\mathbb{Z}_2$ topological quantum number can therefore be understood as encoding whether $\mathcal{T}^2 = \pm 1$. In particular, in order to go between the ordinary band insulator phase and the quantum spin Hall phase the system must pass through a quantum phase transition.[3]

5.2.3 The helical edge liquid

The gapless edge state of the quantum spin Hall insulator consists of a single spinful fermion, and therefore $\mathcal{T}^2 = -1$. As we have seen, this makes it protected from $\mathcal{T}$-invariant perturbations. Also, the spinful

[3] This type of analysis can be extended, using the generic symmetry classes of the Hamiltonian [205], to provide a classification of topological phases of matter also in higher dimensions [206, 207].

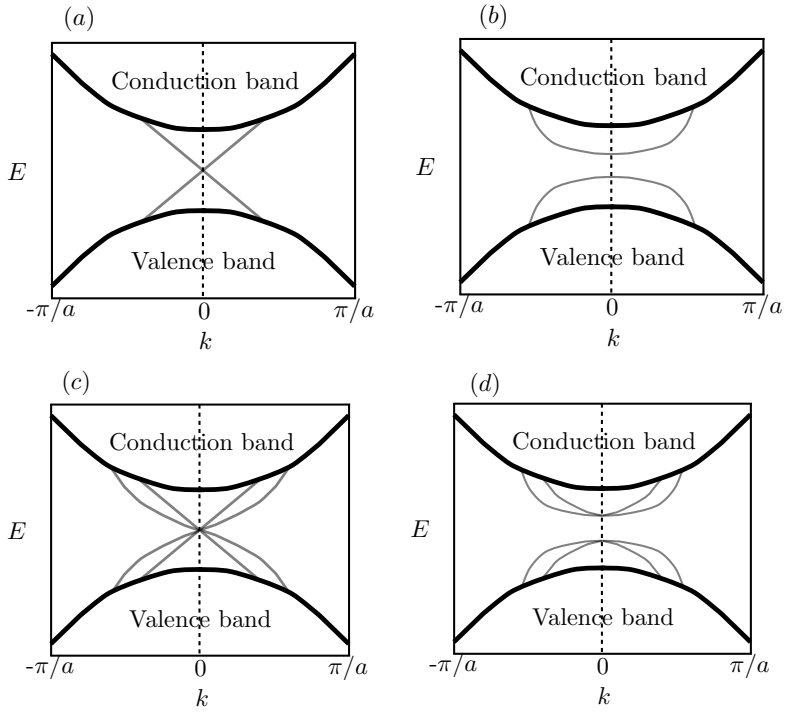

Figure 5.9: Sketch of different edge state dispersions, shown in grey. For a time-reversal invariant system $E(k) = E(-k)$, and from Kramers theorem it follows that when $\mathcal{T}^2 = -1$ there must be at least a twofold degeneracy. Hence there must be an even number of degenerate eigenstates at time-reversal invariant momenta such as $k = 0$. For an odd number of fermions it is therefore not possible to open up a gap without breaking Kramers theorem. In particular, smooth changes of the Hamiltonian can not change the disperion from (a) to (b) without closing the bulk gap. However with an even number of fermions this is possible. In particular, smooth changes of the Hamiltonian can take the dispersion from (c) to (d) without closing the bulk gap.

edge fermion is helical, with the spin-up component moving to the right and the spin-down component moving to the left. With this, the low-energy theory of the edge can now be analyzed with the techniques from Chapter 2. Linearizing the spectrum around the Fermi points, one now obtains the helical version of the Dirac Hamiltonian (2.14),

$$H_0 = -iv_F \int \mathrm{d}x \left[\psi^\dagger_{R\uparrow} \partial_x \psi_{R\uparrow} - \psi^\dagger_{L\downarrow} \partial_x \psi_{L\downarrow} \right]. \tag{5.26}$$

It is now possible to understand the topological protection of the edge states in a simple way. Under time-reversal, the components of the

fermion field transform as

$$\mathcal{T}\psi_{R\uparrow}\mathcal{T}^{-1} = \psi_{L\downarrow}, \qquad \mathcal{T}\psi_{L\downarrow}\mathcal{T}^{-1} = -\psi_{R\uparrow}. \tag{5.27}$$

Hence, in the QSH phase, weak disorder can not lead to localization since single-particle backscattering operators

$$\mathcal{O}_{bs}^{(1)} = \psi_{R\uparrow}^{\dagger}\psi_{L\downarrow} + \psi_{L\downarrow}^{\dagger}\psi_{R\uparrow} \quad \text{and} \quad \mathcal{O}_{bs}^{(2)} = i\psi_{R\uparrow}^{\dagger}\psi_{L\downarrow} - i\psi_{L\downarrow}^{\dagger}\psi_{R\uparrow} \tag{5.28}$$

are odd under time-reversal, i.e. $\mathcal{T}\mathcal{O}_{bs}^{(1,2)}\mathcal{T}^{-1} = -\mathcal{O}_{bs}^{(1,2)}$, and therefore can not be generated as long as the bulk gap remains.

So far the electron-electron interactions have been neglected. The topological effects have all been discussed from a non-interacting band structure picture, and one may wonder whether electron correlations would give rise to equally exotic new phases as when going from the integer to the fractional quantum Hall effect [37, 66, 208]. The study of correlation effects in topological insulators is a very active field[4]. However, once the system is in the QSH phase, correlation effects in the insulating bulk are not expected to affect the behavior of the system. However, electron-electron interactions on the gapless edge can have a dramatic influence and it is therefore important to understand the correlation effects on the edge. For the one-dimensional edge of the quantum spin Hall insulator, we can use the bosonization techniques in Chapter 2 to incorporate interactions. The electron-electron interactions allowed by time-reversal symmetry are Umklapp scattering

$$\begin{aligned} H_{um} &= g_{um}\int \mathrm{d}x\; e^{-i4k_F x}\psi_{R\uparrow}^{\dagger}(x)\psi_{R\uparrow}^{\dagger}(x+a) \\ &\quad \times\psi_{L\downarrow}(x)\psi_{L\downarrow}(x+a) + H.c. \end{aligned} \tag{5.29}$$

and dispersive and forward scattering

$$H_d = g_d\int \mathrm{d}x\; \psi_{R\uparrow}^{\dagger}(x)\psi_{R\uparrow}(x)\psi_{L\downarrow}^{\dagger}(x)\psi_{L\downarrow}(x), \tag{5.30}$$

$$H_f = \frac{g_f}{2}\sum_s \int \mathrm{d}x\; \psi_s^{\dagger}(x)\psi_s(x)\psi_s^{\dagger}(x+a)\psi_s(x+a), \tag{5.31}$$

which are the helical versions of Eqs. (2.20)-(2.22). Here a point splitting with the lattice constant a has been performed, and s is summed over $R\uparrow, L\downarrow$. Assuming a band away from half-filling, $k_F \neq \pi/2$, the Umklapp scattering can be ignored. From Chapter 2 we know that dispersive and

[4]For a recent review, see Ref. [209].

forward scattering do not cause a gap to open, instead the interacting electrons form the gapless *helical Luttinger liquid*

$$H_{HLL} = \frac{v}{2} \int \mathrm{d}x \left[(\partial_x \varphi)^2 + (\partial_x \vartheta)^2 \right], \tag{5.32}$$

where the bosonization formula (2.48) for spinless fermions was used

$$\psi_{R\uparrow,L\downarrow} = \frac{1}{\sqrt{2\pi a}} e^{-i\sqrt{\pi}(\vartheta \pm \varphi)} \tag{5.33}$$

since the helical electrons have the spin locked to the momentum. Hence one arrives at the important conclusion that the gapless edge state is robust against electron-electron interactions [110, 210].

However, impurities can cause local Umklapp interactions, also known as *correlated two-particle backscattering*, in the presence of electron-electron interactions. This interaction is time-reversal invariant and must therefore be considered. The correlated two-particle backscattering interaction at $x = 0$,

$$H_{2pb} \;=\; g_{um}\, e^{-i4k_F x} \psi^\dagger_{R\uparrow}(0) \psi^\dagger_{R\uparrow}(a) \psi_{L\downarrow}(0) \psi_{L\downarrow}(a) + H.c. \tag{5.34}$$

results after bosonization in the boundary sine-Gordon term

$$H_{2pb} \;=\; \frac{g_{bs}}{2(\pi a)^2} \cos[\sqrt{16\pi K}\varphi(0)] \tag{5.35}$$

which is well-studied in quantum tunneling problems [211]. With scaling dimension $4K$ it follows that for electron-electron interactions strong enough to make $K < 1/4$, the correlated two-particle backscattering becomes relevant and charge transport along the edge is blocked at zero temperature [110].

6

Bethe Ansatz and quantum integrability

In this chapter we will discuss the Bethe Ansatz, a powerful method to obtain exact solutions for some one-dimensional quantum models not reducible to free theories. These include the antiferromagnetic Heisenberg model [44], the Bose gas with delta-function interactions [212, 213], the Hubbard model [214] and massive Thirring model [215, 216] (equivalent to the sine-Gordon model), as well as the Kondo [80, 81] and Anderson [217] models. Bethe Ansatz solvable models have the special feature that their many-particle dynamics can be reduced to two-particle dynamics. This means that the many-particle scattering matrix can be factorized into two-particle scattering matrices, and the self-consistency relation for these is the famous Yang-Baxter equation [218,219]. It lies at the heart of the algebraic Bethe Ansatz, or quantum inverse scattering method, which allows correlation functions to be calulated [220]. However this is a very complicated problem that will not be treated here. Instead we will consider the coordinate Bethe Ansatz, which is the original Ansatz for the coordinate wave function first made by Bethe in 1931 [44] for the Hesenberg antiferromagnet, and which allows us to obtain the exact energy spectrum and indirect expressions for the corresponding eigenstates. Together with what is known as the thermodynamic Bethe Ansatz [221], this gives the full spectrum at any temperature and hence the thermodynamic properties of the system. Asymptotic correlation functions can be obtained from the finite-size spectrum using conformal field theory.

After introducing the coordinate Bethe Ansatz solutions of the one-dimensional Bose gas and Hubbard model, the concept of integrability and its consequences will be discussed. The reduction to two-particle

elastic scattering is intimately connected to the existence of a full set of local conservation laws for quantum integrable models. In the presence of such a large number of conserved quantities, the system is highly constrained and not expected to thermalize. The question what types of equilibrium ensembles such systems will realize is a subject of much present research [222], and has implications for many still unsettled issues regarding the foundations of quantum statistical mechanics.

6.1 The coordinate Bethe Ansatz

The Ansatz made by Bethe, and which now bears his name, consists of writing the wavefunction ψ of the system as a combination of plane waves [44]

$$\psi(x_1, ...x_N) = \sum_{\mathcal{P}} A_{\mathcal{P}}\, e^{i\sum_{k=1}^{N} p_0(\lambda_{\mathcal{P}k})x_k}, \tag{6.1}$$

where $x_1 < x_2 < ... < x_N$, and $\mathcal{P}$ are the permutations of the numbers $1, 2, ..., N$. The effect of plane-wave scattering is encoded in the two-particle reducible phase shift

$$A_{\mathcal{P}} \propto e^{i\frac{1}{2}\sum_{a<b}\theta(\lambda_{\mathcal{P}a}-\lambda_{\mathcal{P}b})}. \tag{6.2}$$

Here $p_0(\lambda_k)$ is the momentum and λ_k the "spectral parameters" or "rapidities" of the plane waves. Let us now see how this Ansatz works for a model which has this crucial property of two-particle reducible scattering.

6.1.1 Solution of the one-dimensional Bose gas

The one-dimensional Bose gas with delta-function interaction is also known as the Lieb-Liniger model, the quantum nonlinear Schrödinger model or, in the infinite-repulsion limit, the Tonks-Girardeau gas. Its spectrum was found by Lieb and Liniger in 1963 [212,213], and the thermodynamic properties by Yang and Yang [221]. The model is described by the Hamiltonian

$$\hat{H} = \int dx \left[\partial_x \Psi^\dagger(x)\partial_x\Psi(x) + c\Psi^\dagger(x)\Psi^\dagger(x)\Psi(x)\Psi(x)\right], \tag{6.3}$$

with repulsive coupling constant $c > 0$. The Bose fields Ψ have equal-time commutation relations

$$\left[\Psi(x), \Psi^\dagger(y)\right] = \delta(x-y) \tag{6.4}$$

$$[\Psi(x), \Psi(y)] = \left[\Psi^\dagger(x), \Psi^\dagger(y)\right] = 0. \tag{6.5}$$

Since we will only be interested in equal-time properties the time argument will generally be omitted. We are thus looking for eigenstates

$$|\psi\rangle = \frac{1}{\sqrt{N!}} \int \mathrm{d}^N x \, \psi(x_1, ..., x_N) \Psi^\dagger(x_1) ... \Psi^\dagger(x_N) |0\rangle, \tag{6.6}$$

to the Hamiltonian with N particles, with $\Psi(x)|0\rangle = 0$ defining the vacuum $|0\rangle$ and the wavefunction ψ obeying the Schrödinger equation $H\psi = E\psi$. Since the wavefunction is symmetric in the coordinates x_j, it is sufficient to consider the subspace where $x_1 \leq x_2 \leq ... \leq x_N$, and in this subspace one has

$$H = -\sum_{j=1}^{N} \frac{\partial^2}{\partial x_j^2} \tag{6.7}$$

$$H\psi = E\psi \tag{6.8}$$

$$\left(\frac{\partial}{\partial x_{j+1}} - \frac{\partial}{\partial x_j} \right) \psi \big|_{x_{j+1}=x_j} = c \, \psi \big|_{x_{j+1}=x_j}, \tag{6.9}$$

where the last line is the appropriate boundary condition with the delta-function potential.

Now make the Bethe Ansatz

$$\psi(x_1, ...x_N) = \sum_{\mathcal{P}} A_{\mathcal{P}} \, e^{i \sum_{k=1}^{N} \lambda_{\mathcal{P}k} x_k}, \tag{6.10}$$

within this subspace, hence choosing $p_0(\lambda) = \lambda$. This forms a complete and othogonal set of wavefunctions [223]. It can then be checked that for this Ansatz to satisfy Eqs. (6.7)-(6.9), it should be given by

$$\psi(x_1, ...x_N) \propto \prod_{1 \leq k < j \leq N} \left(\frac{\partial}{\partial x_j} - \frac{\partial}{\partial x_k} + c \right) \sum_{\mathcal{P}} (-1)^{[\mathcal{P}]} \, e^{i \sum_{n=1}^{N} \lambda_{\mathcal{P}n} x_n}, \tag{6.11}$$

where $[\mathcal{P}]$ denotes the parity of the permutation [224]. This leads to a normalized wavefunction

$$\begin{aligned} \psi(x_1, ...x_N) \;\; &= \;\; \left\{ N! \prod_{k<j} \left[(\lambda_j - \lambda_k)^2 + c^2 \right] \right\}^{-1/2} \\ &\times \;\; \sum_{\mathcal{P}} \prod_{k<j} \left[\lambda_{\mathcal{P}j} - \lambda_{\mathcal{P}k} - ic \right] (-1)^{[\mathcal{P}]} \, e^{i \sum_n \lambda_{\mathcal{P}n} x_n}, \end{aligned} \tag{6.12}$$

which, when lifting the restriction to the subspace $x_1 \leq x_2 \leq ... \leq x_N$,

can be written as

$$\begin{aligned}\psi(x_1,...x_N) &= \frac{(-i)^{N(N-1)/2}}{\sqrt{N!}}\left\{\prod_{j>k}\epsilon(x_j-x_k)\right\} \\ &\times \sum_{\mathcal{P}}\left\{(-1)^{[\mathcal{P}]}\exp\left[i\frac{1}{2}\sum_{j>k}\epsilon(x_j-x_k)\theta(\lambda_{\mathcal{P}j}-\lambda_{\mathcal{P}k})\right]\right. \\ &\left.\times\exp\left[i\sum_n \lambda_{\mathcal{P}n}x_n\right]\right\}, \end{aligned} \tag{6.13}$$

where the phase shift function θ is given by

$$\theta(\lambda-\mu) = i\ln\left(\frac{ic+\lambda-\mu}{ic-\lambda+\mu}\right). \tag{6.14}$$

Putting the N particles in a box of length L and imposing periodic boundary conditions will allow us to determine the possible values of the spectral parameters λ. Thus requiring that $\psi(x_1,...,x_j+L,...,x_N) = \psi(x_1,...,x_j,...,x_N)$, which means that the the phase $e^{i\lambda_j L}$ should equal the phase acquired from scattering with all other particles, leads to the Bethe equations

$$e^{i\lambda_j L} = -\prod_{k=1}^{N}\frac{\lambda_j-\lambda_k+ic}{\lambda_j-\lambda_k-ic}, \qquad j=1,...,N. \tag{6.15}$$

By taking the logarithm, these equations can equivalently be written as

$$L\lambda_j + \sum_{k=1}^{N}\theta(\lambda_j-\lambda_k) = 2\pi n_j, \qquad j=1,...,N, \tag{6.16}$$

with n_j integer when N is odd and half-integer when N is even. The Bethe equations determine the allowed values of the parameters λ. Note that they must all be different, otherwise the wavefunction (6.13) vanishes. In order to find the ground state we must now determine the allowed values of λ that minimize the energy of the system.

Acting with the Hamiltonian on the wavefunction (6.13), $\hat{H}\psi = E\psi$, gives the expression for the energy eigenvalues

$$E = \sum_{j=1}^{N}\lambda_j^2. \tag{6.17}$$

Since all n_j must be different, it is now clear that the energy E is minimized by choosing the following numbers n_j in Eq. (6.16),

$$n_j = -\left(\frac{N-1}{2}\right) + j - 1, \qquad j=1,...,N. \tag{6.18}$$

This will fill the states up to a certain value of $|\lambda|$. Thinking about those λ_j that are occupied as *particles*, and those that are not as *holes*, we see that the ground state is formed by filling all states up to the *Fermi level* with particles. Hence we have particles with a "Pauli principle" and a Fermi surface. We have therefore mapped the original repulsive bosonic problem to a fermionic problem. For infinite delta-function repulsion between the bosons, the mapping gives free fermions. For finite positive repulsion of the bosons the fermion system is interacting, and the single-fermion particles are not the stable excitations. One therefore refers to them as the "bare" particles with bare dispersion $E(\lambda) = \lambda^2$, with energy and momentum becoming "dressed" by the interactions.

Similarly, acting with the momentum operator

$$\hat{P} = -i \sum_{j=1}^{N} \frac{\partial}{\partial x_j} \tag{6.19}$$

on the wavefunction gives $\hat{P}\psi = P\psi$, with the momentum

$$P = \sum_{j=1}^{N} \lambda_j. \tag{6.20}$$

Thus, the particles with bare energy λ_j^2 also have a bare momentum λ_j, which can be summarized as saying that the bare particles have a quadratic dispersion relation.

Higher conservation laws

With the particle number operator $\hat{N} = \int \mathrm{d}x\, \Psi^\dagger(x)\Psi(x)$ having eigenvalue $N = \sum_{j=1}^{N} \lambda_j^0$, the momentum operator $-i\frac{1}{2}\int \mathrm{d}x\, \Psi^\dagger(x)\partial_x\Psi(x) +$ H.c. having eigenvalue $P = \sum_{j=1}^{N} \lambda_j^1$ and the Hamiltonian (6.3) having eigenvalue $E = \sum_{j=1}^{N} \lambda_j^2$, one may wonder whether this logic also holds for all the other conserved quantities that appear in this integrable model, i.e. for all those operators $\hat{Q}_k$ that commute with the Hamiltonian. The answer is yes, it has indeed been shown that the higher conservation laws for the Lieb-Liniger model all have the form [220, 225]

$$Q_k = \sum_{j=1}^{N} \lambda_j^k \tag{6.21}$$

for their eigenvalues. As an example, the third conserved quantity is given by the operator [225]

$$\hat{Q}_3 = \int dx \left[\Psi^\dagger(x)\partial_x^3\Psi(x) - (3c/2)\Psi^\dagger(x)\Psi^\dagger(x)\partial_x\Psi(x)^2\right]. \tag{6.22}$$

Dressed energy

Now taking the thermodynamic limit, i.e. letting $N \to \infty$ and $L \to \infty$ while keeping the density $N/L = D$ fixed, the continuum version of the Bethe equations (6.16), after differentiation, becomes the linear integral equation

$$\rho_t(\lambda) - \frac{1}{2\pi}\int_{-q}^{q} d\mu\, K(\lambda,\mu)\rho_t(\mu) = \frac{1}{2\pi} \tag{6.23}$$

at zero temperature, where $\rho_t(\lambda)$ is the particle density of states in momentum space and the kernel

$$K(\lambda,\mu) = \theta'(\lambda-\mu) = \frac{2c}{c^2+(\lambda-\mu)^2}, \tag{6.24}$$

with the integration at zero temperature constrained to within the Fermi sphere $q \le \lambda \le q$. Hence

$$\int_{-q}^{q} \mathrm{d}\lambda\, \rho_t(\lambda) = \frac{N}{L} = D. \tag{6.25}$$

Returning to the expression (6.17) for the energy, we now include also a chemical potential h and write it as

$$E = \sum_{j=1}^{N} \varepsilon_0(\lambda_j) \tag{6.26}$$

where $\varepsilon_0(\lambda_j) = \lambda_j^2 - h$ is the bare energy of the particle. As an integral this becomes

$$E = \int_{-q}^{q} \mathrm{d}\lambda\, \rho_t(\lambda)\varepsilon_0(\lambda) \tag{6.27}$$

which can be rewritten as

$$E = \int_{-q}^{q} \mathrm{d}\lambda\, \varepsilon(\lambda), \tag{6.28}$$

where the dressed energy $\varepsilon(\lambda)$ is given by the linear integral equation

$$\varepsilon(\lambda) - \frac{1}{2\pi}\int_{-q}^{q} d\mu\, K(\lambda,\mu)\varepsilon(\mu) = \varepsilon_0(\lambda). \tag{6.29}$$

The Fermi points $\lambda = \pm q$ are determined by the condition

$$\varepsilon(\pm q) = 0. \tag{6.30}$$

The dressed energy (6.29) is the observable energy of the excitations. Removing one particle with momentum $-q < \lambda_h < q$ from the ground state distribution and adding one with momentum $|\lambda_p| > q$ will change the energy by

$$\Delta E = \varepsilon(\lambda_p) - \varepsilon(\lambda_h). \tag{6.31}$$

Finite-size corrections and the dressed charge

Let us now investigate the finite-size corrections from low-energy excited states at zero temperature. Expanding the energy $E(q) = E_0 + \delta E$ as function of the deviation from the value of q that minimizes the energy Eq. (6.27), we obtain

$$\delta E = \frac{\partial E}{\partial q}\delta q + \frac{1}{2}\frac{\partial^2 E}{\partial q^2}(\delta q)^2, \tag{6.32}$$

using the parity symmetry in λ. Now, one can show that

$$\frac{\partial E}{\partial q} = L\rho(q)\varepsilon(q). \tag{6.33}$$

This gives Eq. (6.30), since the ground state minimizes E. Then

$$\delta E = \frac{L}{2}\frac{\partial}{\partial q}\left(\rho(q)\varepsilon(q)\right)(\delta q)^2 \tag{6.34}$$

which due to Eq. (6.30) equals

$$\delta E = \frac{L}{2}\rho(q)\varepsilon'(q)\left(\delta q\right)^2 = \frac{L}{2}v_F 2\pi\left[\rho(q)\right]^2\left(\delta q\right)^2 \tag{6.35}$$

where the Fermi velocity is defined by

$$v_F = \frac{1}{2\pi\rho_t(q)}\frac{\partial\varepsilon}{\partial\lambda}\bigg|_{\lambda=q}. \tag{6.36}$$

Now we want to express δq in terms of the quantum numbers describing the different kinds of particle excitations. Let ΔN denote the change in the number of particles N, let d denote the number of particles that jump over the Fermi sea from $\lambda = -q$ to $\lambda = q$, and $N^{\pm}$ the number of particle-hole excitations at the Fermi points $\lambda = \pm q$. Then the change in the Fermi surface can be expressed as

$$\delta q = \frac{\partial q}{\partial D}\delta D + \frac{\partial q}{\partial d}d \tag{6.37}$$

where $\delta D = \Delta N/2L$. The derivatives are found to be

$$\frac{\partial q}{\partial D} = \frac{1}{\rho(q)Z(q)} \tag{6.38}$$

and

$$\frac{\partial q}{\partial d} = \frac{Z(q)}{L\rho(q)}, \tag{6.39}$$

where the dressed charge Z is defined by

$$Z(\lambda) - \frac{1}{2\pi}\int_{-q}^{q} d\mu\, K(\lambda,\mu)Z(\mu) = 1. \tag{6.40}$$

Comparing Eqs. (6.40) and (6.23) we see that $Z(\lambda) = 2\pi\rho_t(\lambda)$ for the present model, while for other models there is no such simple relation. Inserting the above equations into Eq. (6.35) now gives

$$\delta E = \frac{\pi}{L} v_F \left[2N^+ + 2N^- + \left(\frac{\Delta N}{2Z(q)} + Z(q)d \right)^2 \right] \tag{6.41}$$

when also including the particle-hole excitations $N^{\pm}$.

The corrections to the momentum are much easier to calculate. Since

$$P = \sum_{j=1}^{N} \lambda_j = \sum_{j=1}^{N} \left[\frac{2\pi}{L} n_j - \sum_{k=1}^{N} \theta(\lambda_j - \lambda_k) \right] = \frac{2\pi}{L} \sum_{j=1}^{N} n_j \tag{6.42}$$

due to the antisymmetry of $\theta(\lambda)$, δP is simply given by

$$\delta P = 2k_F d + \frac{2\pi}{L} \left[N^+ - N^- + d\,\Delta N \right], \tag{6.43}$$

where k_F is the Fermi momentum $k_F = \pi N/L$.

The finite-size corrections give us the scaling dimensions in the conformal field theory describing the low-energy physics, and hence allow us to obtain the asymptotic behavior of correlation functions. As it turns out, the low-energy limit of the Lieb-Liniger model is given by the $c = 1$ free boson conformal field theory, which should come as no surprise due to the analogies with the Luttinger liquid in Chapter 2, cf. Refs. [226,227]

Yang-Yang thermodynamics

Let us also mention the extension to finite temperatures, known as Yang-Yang thermodynamics or thermodynamic Bethe Ansatz.

In the thermodynamic limit, the entropy is given by [221, 228]

$$S = L \int_{-\infty}^{\infty} \mathrm{d}\lambda \left[\rho_t(\lambda) \ln \rho_t(\lambda) - \rho_p(\lambda) \ln \rho_p(\lambda) - \rho_h(\lambda) \ln \rho_h(\lambda) \right], \tag{6.44}$$

where $L\rho_t(\lambda)\mathrm{d}\lambda$ is the number of states in the interval $[\lambda, \lambda + \mathrm{d}\lambda]$, and $L\rho_p(\lambda)\mathrm{d}\lambda$ and $L\rho_h(\lambda)\mathrm{d}\lambda$ are the numbers of particles and holes in this interval, with $\rho_p(\lambda) + \rho_h(\lambda) = \rho_t(\lambda)$. The entropy of Eq. (6.44) follows

as the logarithm of the number of ways to put $L\rho_p(\lambda)\mathrm{d}\lambda$ particles into $L\rho_t(\lambda)\mathrm{d}\lambda$ states. The partition function then follows as

$$Z = \int \mathcal{D}\left[\frac{\rho_t(\lambda)}{\rho_p(\lambda)}\right] e^{S-E/T}, \tag{6.45}$$

which, by varying the exponent under the constraint of fixed number of particles and applying the saddle-point approximation, gives the equation

$$\ln\frac{\rho_h(\lambda)}{\rho_p(\lambda)} = \frac{\varepsilon_0(\lambda)}{T} - \frac{1}{2\pi}\int_{-\infty}^{\infty} d\mu\, K(\lambda,\mu)\ln\left[1+\frac{\rho_p(\lambda)}{\rho_h(\lambda)}\right]. \tag{6.46}$$

Now write $\rho_h(\lambda)/\rho_p(\lambda)$ as

$$\frac{\rho_h(\lambda)}{\rho_p(\lambda)} = e^{\varepsilon(\lambda)/T}, \tag{6.47}$$

which turns Eq. (6.46) into

$$\varepsilon(\lambda) + \frac{T}{2\pi}\int_{-\infty}^{\infty} d\mu\, K(\lambda,\mu)\ln(1+e^{-\varepsilon(\mu)/T}) = \varepsilon_0(\lambda). \tag{6.48}$$

This is the Yang-Yang equation. At zero temperature it reproduces Eq. (6.29), and it gives the observable energy of the finite-temperature excitations. The function $\varepsilon(\lambda)$ in Eqs. (6.47)-(6.48) is therefore the dressed energy at finite temperatures.

From Eq. (6.47) we obtain the distribution function $\vartheta(\lambda) = \rho_p(\lambda) = \rho_t(\lambda)$ for the particles, which is the Fermi function

$$\vartheta(\lambda) = \frac{1}{1+e^{\varepsilon(\lambda)/T}}. \tag{6.49}$$

The integral equations for zero-temperature quantities are now straightforwardly generalized to finite temperatures by the substitution

$$\int_{-q}^{q}\mathrm{d}\lambda\,[...] \to \int_{-\infty}^{\infty}\mathrm{d}\lambda\,\vartheta(\lambda)\,[...]. \tag{6.50}$$

It is interesting to note that the validity of the Yang-Yang thermodynamics recently has been experimentally verified [229].

6.2 Integrability and the generalized Gibbs ensemble

Let us now discuss in a more general sense the concept of integrability and its effects on quantum statistical mechanics. Classically, exact integrability is defined through the presence of as many independent integrals of motion as there are degrees of freedom. Thus the equations of motion can be explicitly integrated, preventing the system from ergodically exploring phase-space and no thermalization will occur.

6.2.1 Quantum integrability

The notion of quantum integrability is much more subtle than the classical version. In fact, the precise definition is still a disputed issue [230–233]. The prevailing working definition nevertheless is that *quantum integrability means the presence of a full set of local conserved charges*, i.e. there are as many local independent commuting symmetry operators $\hat{Q}_i$,

$$[\hat{Q}_i\,,\,\hat{H}]=0, \qquad [\hat{Q}_i\,,\,\hat{Q}_j]=0, \qquad i,j=1,2,...,\dim(\mathcal{H}), \tag{6.51}$$

as the size $\dim(\mathcal{H})$ of the Hilbert space. The requirement of locality is important, as otherwise any quantum system would fall under the definition since one can always construct a full set out of the projection operators $\hat{Q}_a=|\Psi_a\rangle\langle\Psi_a|$ onto the eigenstates $|\Psi_a\rangle$ of the Hamiltonian.

An alternative definition of quantum integrability is that *all scattering is non-diffractive*, meaning that the set of outgoing momenta is the same as the set of incoming momenta. It connects to the presence of the conserved charges since they can be constructed from the conserved momenta, and to the solvability through the Bethe Ansatz. To see this connection more clearly, and also understand why Bethe Ansatz is applicable only for *one-dimensional* quantum systems, let us consider the following simple argument from Refs. [234, 235]:

Consider a one-dimensional system of particles scattering off each other. If the system has a full set of conserved charges, then these conserved charges can be used to form generators of momentum-dependent translations of the wave packets. Hence the world lines of different particles can be translated independently, separating many-particle collisions into several two-particle collisions, cf. Figs. 6.1 and 6.2. Therefore the many-particle S matrix (scattering matrix) is factorizable into

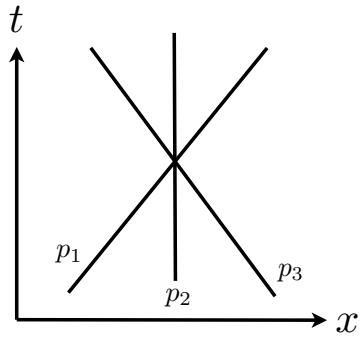

Figure 6.1: The world lines for a three-particle scattering event.

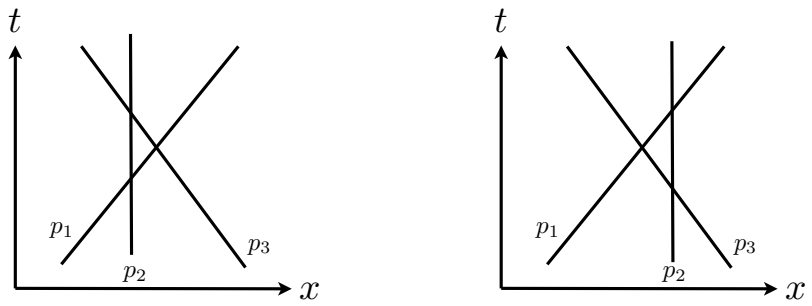

Figure 6.2: Two different three-particle scattering events that can be seen as a sequence of two-particle scattering events. Note that if translating only the particle with e.g. momentum p_2 is a symmetry operation, then both these events should have the same S matrix as the event in Fig. 6.1. Thus the S matrix is factorizable into two-particle scattering matrices S_2, obeying the Yang-Baxter equation (6.52).

two-particle S matrices S_2. Evidently this must however lead to self-consistency relations for the S_2 matrices, considering the different ways the same many-particle S matrix can be factorized. This leads to the celebrated Yang-Baxter equation [218, 219, 236],

$$S_2(p_2,p_3)S_2(p_3,p_1)S_2(p_1,p_2) = S_2(p_1,p_2)S_2(p_1,p_3)S_2(p_2,p_3), \qquad (6.52)$$

which in its different forms lies at the heart of Bethe Ansatz integrability[1] and the search for, and classification of, its solutions is a central theme o the research field [238]. We now also see why Bethe Ansatz is such a powerful method only for integrable *one-dimensional* quantum models: In higher dimensions one could simply avoid any scattering altogether by translating the world lines. Hence the S matrices are trivial, i.e. the model is reducible to a free (non-interacting) theory. Only in one dimension can there be non-trivial theories with a full set of conserved charges.

6.2.2 The generalized Gibbs ensemble

Just as the notion of quantum integrability is more subtle than its classical counterpart, so is the process of quantum thermalization [239–242]. For an isolated quantum system the linear equations of motion and the

[1]Note also the interesting connections between the Yang-Baxter equation and universal topological quantum computation [174, 237].

discrete spectrum prevents dynamical chaos, hence the mechanisms underlying the relaxation process to some equilibrium distribution are far less understood. In fact, the quantum version [239, 243] of the ergodic theorem is weaker than its classical counterpart that lays the foundation of classical statistical physics [244]. The quantum version results in the assumption known as "normal typicality", which loosely can be stated as: "for a 'typical' finite family of commuting macroscopic observables, every initial wave function ψ_0 from a micro-canonical energy shell so evolves that for most times t in the long run, the joint probability distribution of these observables obtained from $\psi(t)$ is close to their micro-canonical distribution" [243]. Given the micro-canonical distribution for the isolated system, stating that all microscopic states with the same energy are equally probable, one can write down the entropy from which the statistical ensemble of the system follows by maximizing this entropy under the relevant constraints. As is well-known, the density matrix describing a stationary state will be a function of all the conserved charges [244–246]. In particular, suppose $\{\hat{Q}_n\}$ is a set of local conserved charges, i.e. $[\hat{Q}_i\,,\,\hat{H}] = [\hat{Q}_i\,,\,\hat{Q}_j] = 0$, $\forall i, j$. Then following the prescription of maximizing the von Neumann entropy $S = -k_B \mathrm{Tr}\,\hat{\rho}\log\hat{\rho}$ under the constraints of the conservation laws imposed by Lagrange multipliers λ_i, gives

$$\delta[\mathrm{Tr}\,(\sum_i \lambda_i \hat{Q}_i - k_B \hat{\rho}\log\hat{\rho})] = \mathrm{Tr}\,([\sum_i \lambda_i \hat{Q}_i - k_B \log\hat{\rho}]\delta\hat{\rho}) = 0 \tag{6.53}$$

Hence $\sum_i \lambda_i \hat{Q}_i - k_B \log\hat{\rho} = 0$ and one arrives at the density matrix

$$\hat{\rho}_{GGE} = \frac{1}{Z_{GGE}}\; e^{-\sum_i \beta_i \hat{Q}_i}, \tag{6.54}$$

known as the *generalized Gibbs ensemble*. When the only constraints are conserved particle number $\hat{Q}_1 = \hat{N}$ and energy $\hat{Q}_2 = \hat{H}$ the prescription above gives the usual Gibbs ensemble

$$\hat{\rho}_{Gibbs} = \frac{1}{Z_{Gibbs}}\; e^{-\beta(\hat{H}-\mu\hat{N})}, \tag{6.55}$$

also known as the grand canonical ensemble with β defining the inverse temperature and μ the chemical potential. In the above the constraint of unity trace of the density matrix, $\mathrm{Tr}\,\hat{\rho} = 1$ results in the normalizing prefactor Z^{-1}, where $Z = \mathrm{Tr}\,\exp[-\sum_i \beta_i \hat{Q}_i]$ is the partition function.

For a generic non-integrable many-particle system, being it classical or quantum, the only conserved quantities are just particle number and

total energy (neglecting total momentum and angular momentum). In an isolated system, i.e. with neither particle nor energy exchange with the environment, "normal typicality" asserts the stationary density matrix to be that for the micro-canonical ensemble. When the system is in contact with an environment allowing energy transfer, it is no longer isolated (but still closed if there is no particle exchange). The canonical ensemble $\hat{\rho}_c = Z_c^{-1}\, e^{-\beta \hat{H}}$ then describes the mean values of observables $\hat{\mathcal{O}}$ as $\langle \hat{\mathcal{O}} \rangle = \mathrm{Tr}\, \hat{\rho}_c \hat{\mathcal{O}}$ around which they fluctuate. In the thermodynamic limit one expects these fluctuations to be negligible. The same holds for the grand canonical ensemble (6.55) for an open system where both particles and energy are exchanged with the environment.

Turning to an isolated integrable quantum many-particle systems, it is clear that the system is in a pure state at all times. However, it might still be possible to treat open subsystems with the prescription above, given that it is small enough for the rest of the system to be considered an effective bath. The whole set of local conservation laws should then presumably enter into the generalized Gibbs ensemble describing the subsystem. A protocol for testing such a scenario is a *quantum quench*, where the initial state of the system is not an eigenstate of the Hamiltonian [247–250]. Such non-equilibrium dynamics of quantum systems is now a very active area of both theoretical and experimental investigation.

With the recent advancements in the field of cold atoms and quantum optics [251], it is now possible to experimentally realize sufficiently isolated and well-controlled system so that unitary time-evolution can be observed for times long enough to examine fundamental questions about ergodicity and thermalization [252]. With the many integrable quantum models now being realized in the labs[2], it has become a subject of intense study to investigate exactly what sets of conserved quantities that do constrain relaxation and which of them that should enter into an effective generalized Gibbs ensemble (6.54) describing local observables in possible stationary states[3].

[2]See references in Ref. [253].

[3]For a review, see Ref. [222]. Discussions of recent developments can e.g. be found in Refs. [254] and [255].

7

Introduction to the papers

7.1 Paper I: Scaling of reduced fidelity in TQPTs

In Paper I we study the scaling of reduced fidelity in the topological quantum phase transitions appearing in the models introduced in Section 5.1.3. Before discussing the results, let us introduce the concepts of fidelity and reduced fidelity.

7.1.1 Fidelity and fidelity susceptibility

Fidelity is a measure from quantum information theory that quantifies the similarity between two quantum states. It can be used to capture a quantum phase transition (QPT) by considering the change in the ground state as the system is driven through the transition. Let us write the Hamiltonian as

$$H = H_0 + \lambda H_I \,, \tag{7.1}$$

where λ is a tunable parameter that takes the system through the QPT. For two states given by the density matrices $\rho(\lambda)$ and $\rho(\lambda')$, the fidelity $F(\rho(\lambda), \rho(\lambda'))$ is defined as [256]

$$F(\rho(\lambda), \rho(\lambda')) = \mathrm{Tr}\sqrt{\sqrt{\rho(\lambda)}\rho(\lambda')\sqrt{\rho(\lambda)}}. \tag{7.2}$$

When the two states are pure, i.e. $\rho(\lambda) = |\Psi(\lambda)\rangle\langle\Psi(\lambda)|$, we see that the fidelity is simply given by the state overlap, $F(\lambda, \lambda') = |\langle\Psi(\lambda')|\Psi(\lambda)\rangle|$. Since the ground state changes rapidly at a quantum phase transition, the fidelity $F(\lambda, \lambda + \delta\lambda)$ between two ground states that differ by a small change $\delta\lambda$ in the driving parameter should exhibit a sharp drop. This

has been confirmed in a number of case studies of different systems undergoing QPTs [180].

In order to remove the arbitrariness in the choice of $\delta\lambda$, one should instead consider the *fidelity susceptibility* χ_F, defined as [257]

$$\chi_F = \lim_{\delta\lambda\to 0} \frac{-2\ln F}{\delta\lambda^2}. \tag{7.3}$$

For pure states, $F(\lambda,\lambda') \approx 1 - \chi_F\delta\lambda^2/2$ when $\delta\lambda$ is small, hence the fidelity susceptibility describes the leading response of the fidelity to changes in the driving parameter. The fidelity susceptibility is therefore a good quantitative measure of how much the ground state changes as the systems goes through the QPT. In fact, the fidelity susceptibility shows scaling behavior near QPTs in a number of systems, enabling the extraction of critical exponents [180].

When the density matrices at λ and λ' commute, Eq. (7.2) becomes

$$F(\lambda,\lambda') = \mathrm{Tr}\sqrt{\rho(\lambda)\rho(\lambda')} = \sum_i \sqrt{\alpha_i\alpha_i'}, \tag{7.4}$$

where $\{\alpha_i\}$ and $\{\alpha_i'\}$ are the eigenvalues of $\rho(\lambda)$ and $\rho(\lambda')$, respectively. This gives the fidelity susceptibility in terms of the density matrix eigenvalues as [258]

$$\chi_F = \sum_i \frac{(\partial_\lambda\alpha_i)^2}{4\alpha_i}. \tag{7.5}$$

Reduced fidelity

The fidelity between the mixed states of a subsystem is called *reduced fidelity* [256, 259]. Recall that when the Hilbert space of the full system is partitioned into a direct product $\mathcal{H} = \mathcal{H}_A\otimes\mathcal{H}_B$, where A is the particular subsystem and B is the rest, the reduced density matrix ρ_A of subsystem A is obtained by tracing out all the degrees of freedoms pertaining to B in the full density matrix ρ of the entire system,

$$\rho_A = \mathrm{Tr}_B\,\rho\,. \tag{7.6}$$

Then the reduced fidelity is simply the fidelity (7.2) between the reduced density matrices ρ_A at different values of the driving parameter λ in the Hamiltonian (7.1). Reduced fidelity has provided an alternative in situations where the global fidelity is not a suitable quantity [180], e.g. one might envisage situations where the global ground state is unknown. Moreover, as the reduced fidelity is a local quantity it might have a stronger experimental relevance, being easier to connect to a local observable.

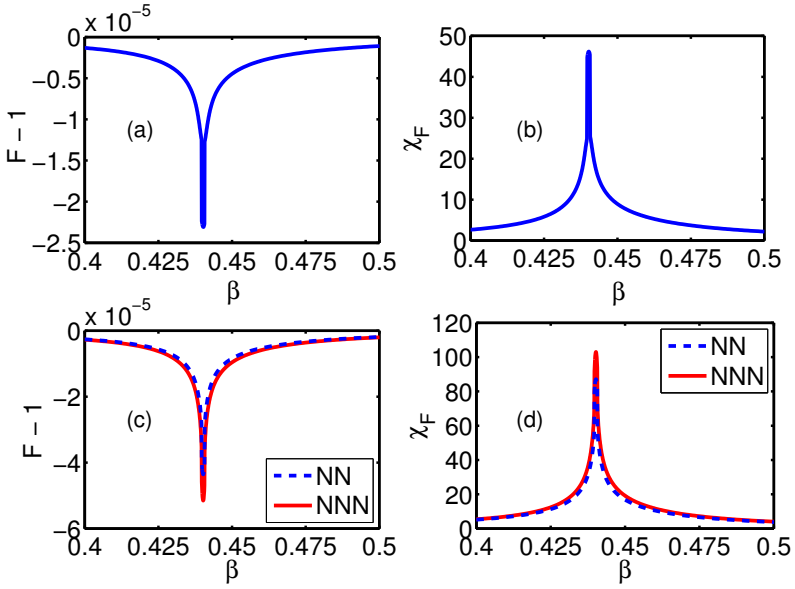

Figure 7.1: Single-site fidelity (a), single-site fidelity susceptibility (b), two-site fidelity (c) and two-site fidelity susceptibility (d) of the Castelnovo-Chamon model plotted using the analytical results in the thermodynamic limit with $\delta\beta = 0.001$. The reduced fidelity susceptibilities will diverge according to Eq. (7.7) when $\delta\beta \to 0$. In (c) and (d) we plot for both nearest (NN) and next-nearest (NNN) neighbors. From Paper I.

Now, with this local nature of the reduced fidelity one may think that it would be less sensitive to a topological quantum phase transition (TQPT), at which the system undergoes a global rearrangement of quantum correlations that cannot be captured by any local order parameter. However, we showed in Paper I that this intuition turns out to be wrong. Instead, our results for some exactly solvable 2d lattice models suggest that the reduced fidelity serves as an accurate marker of a topological quantum phase transition.

7.1.2 Results and discussion

In Paper I we have analytically studied the single-site and two-site reduced fidelities in the Castelnovo-Chamon (5.10) and transverse Wen-plaquette (5.16) models, as functions of the driving parameters β and h respectively.

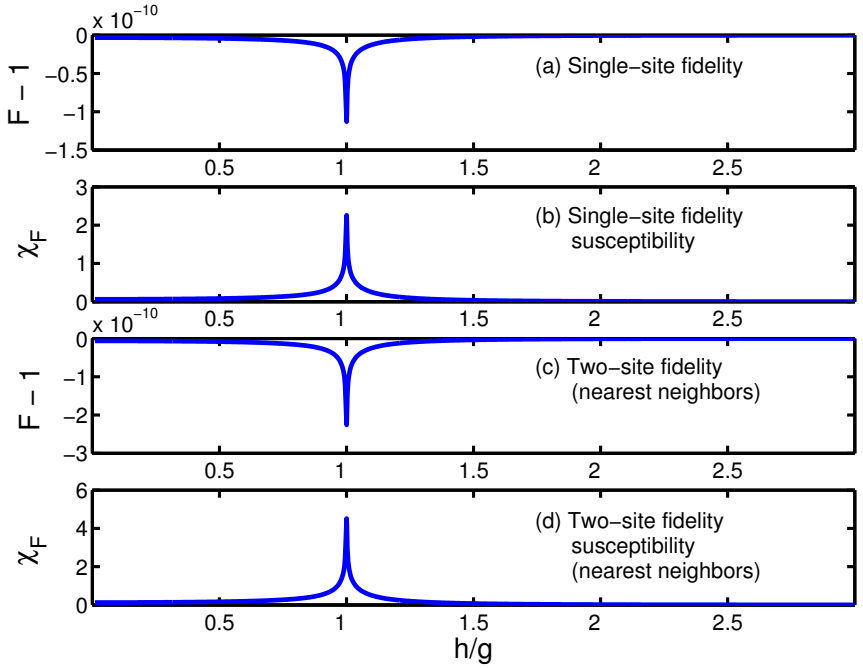

Figure 7.2: Single-site fidelity (a), single-site fidelity susceptibility (b), two-site fidelity (c) and (nearest neighbor) two-site fidelity susceptibility (d) of the transverse Wen-plaquette model in the thermodynamic limit plotted using the analytical results with a parameter difference $\delta(h/g) = 10^{-5}$. It is clear that the TQPT at $h/g = 1$ is marked by drops in the reduced fidelities. The reduced fidelity susceptibilities will diverge according to Eq. (7.9) when $\delta(h/g) \to 0$. From Paper I.

For the Castelnovo-Chamon model, it is found that the single-site reduced fidelity susceptibility χ_F diverges as

$$\chi_F \sim \ln^2 |\beta - \beta_c|, \tag{7.7}$$

at $\beta \to \beta_c$, cf. Fig. 7.1. This should be contrasted to the global ground-state fidelity susceptibility which diverges as [260]

$$\chi_F^{(gs)} \sim \ln |\beta - \beta_c|. \tag{7.8}$$

Hence we have shown that the divergence of the reduced fidelity susceptibility at criticality is even stronger than that of the global fidelity [260] in this model, which comes as a surprise since the reduced fidelity initially was conceived of as a measure with "reduced orthogonality" [180].

For the transverse Wen-plaquette model it is found that the single-site and two-site reduced fidelities both diverge as

$$\chi_F \sim \ln^2 |g/h - 1| \tag{7.9}$$

as $h \to g$, cf. Fig. 7.2.

Our analytical results for these important lattice models rely on exact mappings of the TQPTs onto ordinary symmetry-breaking phase transitions. Other lattice models exhibiting TQPTs have also been shown to be dual to models with classical order (see Refs. [261, 262]), suggesting that our line of approach may be applicable also in these cases, and that the property that a reduced fidelity can detect a TQPT may perhaps be rather generic. It is somewhat counterintuitive, considering that the reduced fidelity is a *local probe* of the topologically ordered phase and there exists no local order parameter that describes the transition. However, related results have previously been published. Specifically, in Refs. [181] and [263], it was found that the local magnetization in the Castelnovo-Chamon model and the Kitaev toric code model in a magnetic field, while being continuous and non-vanishing across the transition out of topological order, has a singularity in its first derivative. In fact, since the singularity in the reduced fidelity susceptibility depends on a non-analyticity in the local expectation values appearing in the reduced density matrices, the findings have the same origin. However, reduced fidelity as a measure does not rely on identifying any particular local expectation value with non-analytic behavior, and is especially well suited in situations where only the local reduced density matrix has been found. Furthermore, the fact that a local quantity such as the reduced fidelity can detect TQPTs is conceptually satisfying, as physical observables are local in nature.

7.2 Papers II-III: Impurity entanglement entropy from CFT

In Paper II we derive general expressions for the scaling corrections of the entanglement entropy when perturbing a boundary conformal field theory with (primary) irrelevant boundary operators. In Paper III these results are applied to the study of quantum impurity systems, in particular we discuss the relation to the Kondo screening cloud. By obtaining the finite-temperature corrections to the von Neumann entropy, we show that the zero-temperature corrections $\delta S_{imp}(r)$ to the entanglement entropy have the same power-law decay as the finite-temperature corrections $\delta S^{Th}_{imp}(\beta)$ to the thermodynamic entropy when $r \gg \beta$. This extends the well-known

connection between these two quantities in the scaling limit to include also the leading scaling corrections. In particular, it might provide a direct connection between the exponents governing measurable quantities like the specific heat to the exponent governing the decay of the Kondo screening cloud.

The results, which are derived in Appendix A, can be summarized on the following form:

$$S_A = -\mathrm{Tr}\,\rho_A \log \rho_A \;\begin{cases} \nearrow & r/\beta \to 0 \quad S_A = \dfrac{c}{6}\log\dfrac{2r}{\epsilon} + \log g + c' \; + \; \begin{cases} A_1 r^{2-2x_b} \\ A_2 r^{-1}\log r \\ A_3 r^{-1} \end{cases} \\ \searrow & r/\beta \to \infty \quad S_A = \underbrace{\dfrac{2\pi c}{6\beta} r + \log g}_{S_A^{Th}} + \dfrac{c}{6}\log\Big[\dfrac{\beta}{2\pi\epsilon}\Big] + c' + \underbrace{\begin{cases} B_1 \beta^{2-2x_b} \\ B_2 \beta^{-1}\log\beta \\ B_3 \beta^{-1} \end{cases}}_{\sim \delta S_A^{Th}} \end{cases}$$

The von Neumann entropy $S_A(r)$ for a region A of size r next to the boundary (i.e. the impurity) has the well-known scaling form of Eq. (4.12) as $r/\beta \to 0$. In paper II we show that the scaling corrections that arise due to an irrelevant boundary operator with scaling dimension x_b to leading order are given by

$$\delta S_A \sim \begin{cases} A_1\, r^{2-2x_b} & \text{when} \quad 1 < x_b < 3/2 \\ A_2\, r^{-1}\log r & \text{when} \quad x_b = 3/2 \\ A_3\, r^{-1} & \text{when} \quad x_b > 3/2\,, \end{cases} \tag{7.10}$$

and as $\delta S_A \sim (\ln r)^{-3}$ when perturbing with a marginally irrelevant boundary operator. Here A_1, A_2, A_3 are non-universal constants. In Paper III we show that the corresponding expression for the corrections to the von Neumann entropy when $r \gg \beta$ are given by

$$\delta S_A \sim \begin{cases} B_1\, \beta^{2-2x_b} & \text{when} \quad 1 < x_b < 3/2 \\ B_2\, \beta^{-1}\log\beta & \text{when} \quad x_b = 3/2 \\ B_3\, \beta^{-1} & \text{when} \quad x_b > 3/2\,, \end{cases} \tag{7.11}$$

to $\mathcal{O}(\beta^{-1})$ in β and $\mathcal{O}(e^{-2\pi r/\beta})$ in r/β. Comparing to Eq. (3.39) for the thermodynamic impurity entropy S_A^{Th} in a quantum impurity system in the same limit, we see that $\delta S_A \sim S_A^{Th}$ for a quantum impurity system in the double limit $r \gg \beta$ and $\beta \to \infty$. The thermodynamic impurity entropy in turn has the same power-law scaling as the impurity specific heat (3.38). This establishes a connection between entanglement and thermodynamics [126, 264] on the level of scaling corrections.

The decay (7.10) of the boundary contribution to the entanglement entropy $\delta S_B = \delta S_A$ of the other part B of the system, as its distance r

from to the boundary increases, tells how the screening cloud decays [157]. We therefore arrive at the conclusion that the asymptotic decay of the screening cloud with distance follows the same power-law as the impurity specific heat with inverse temperature.

7.3 Papers IV-V: Kondo effect in helical Luttinger liquids

In Paper IV we study the effect of Rashba spin-orbit coupling on the Kondo physics in a helical Luttinger liquid at the edge of a two-dimensional topological insulator, obtaining the Kondo temperature and the linear conductance. In Paper V these results are generalized to include also Dresselhaus spin-orbit interaction.

7.3.1 Background

The helical electrons, with spin locked to the direction of propagation, are schematically shown in Fig. 7.3. Previous studies, not including spin-orbit effects, of the Kondo effect in this system have resulted in the following picture for the effect from Kondo scattering on the conductance of the system [111]: At low temperatures $T \ll T_K$, the Kondo effect has set in and the impurity spin is essentially removed from the system. The conductance is then governed by two-particle correlated backscattering generated at the impurity site, with scaling dimension $4K$. Hence, for $K > 1/4$, i.e. weak electron-electron interactions, the unitary edge conductance $G = e^2/h$ is restored as $T \to 0$ with an unusual power law $\delta G \sim T^{2(4K-1)}$, distinctive of a helical edge liquid. For $K < 1/4$, i.e. strong interactions, the edge liquid freezes into an insulator at $T = 0$, whith a power-law $G \sim T^{2(1/4K-1)}$ from tunneling of fractionalized charge. At high temperatures and low frequencies $\omega \ll T$, there is

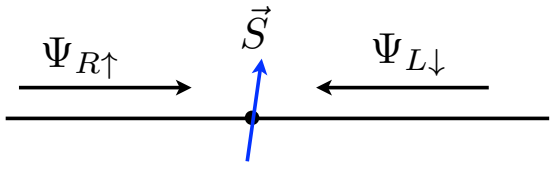

Figure 7.3: Illustration of the spin-1/2 Kondo impurity in a helical edge liquid. The right-moving electrons have spin-up and the left-moving electrons have spin-down. Kondo scattering simultaneously flip the spins of the impurity and electron.

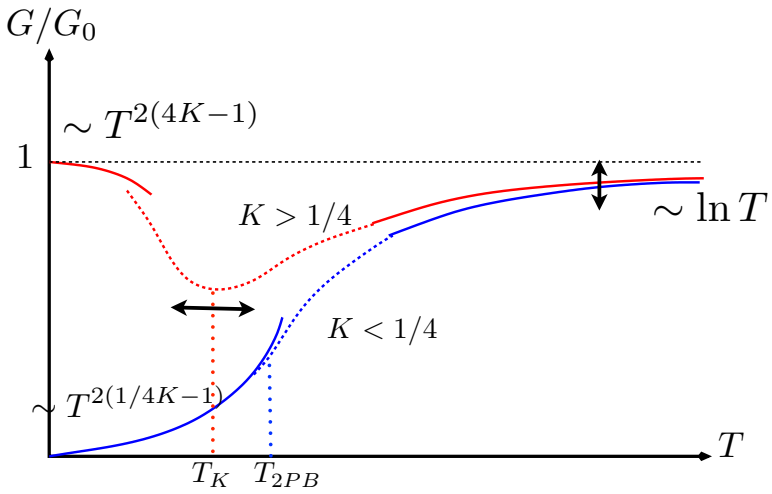

Figure 7.4: Summary of the picture for the temperature dependence of the conductance of a helical edge liquid with a Kondo impurity, as it appears in Ref. [111]. Note however that the logarithmic correction from Kondo scattering vanishes in the dc limit [112]. The effects from Rashba and Dresselhaus spin-orbit interaction will be to modify both the Kondo temperature and the high-temperature conductance correction, as indicated by the arrows.

a logarithmic temperature dependence of the conductance, obtained by RG improving the linear-response result $\delta G \sim T^{2(K-1)}$. This is summarized in Fig. 7.4. However, in the dc limit, $\omega \to 0$, it was found [112] that this perturbative analysis yields incorrect results. Instead a rate-equation approach for the Kondo scattering process results in the conclusion that the conductance correction vanishes in the dc limit. This can be understood from the following heuristic argument: in the zero-frequency limit the fact that the impurity spin is flipped at every scattering event means that for the helical liquid every second electron must come from the right and every second from the left, hence giving zero net effect.

7.3.2 Results and discussion

It is however important to also study the effects of spin-orbit interactions, which are expected to play an important role in the semiconductor heterostructures where quantum spin Hall experiments are usually carried out [265]. In addition, a Rashba interaction is controllable by external gate voltages, and therefore presents a means to electrically control transport properties which is important for technological applications in electronics and spintronics.

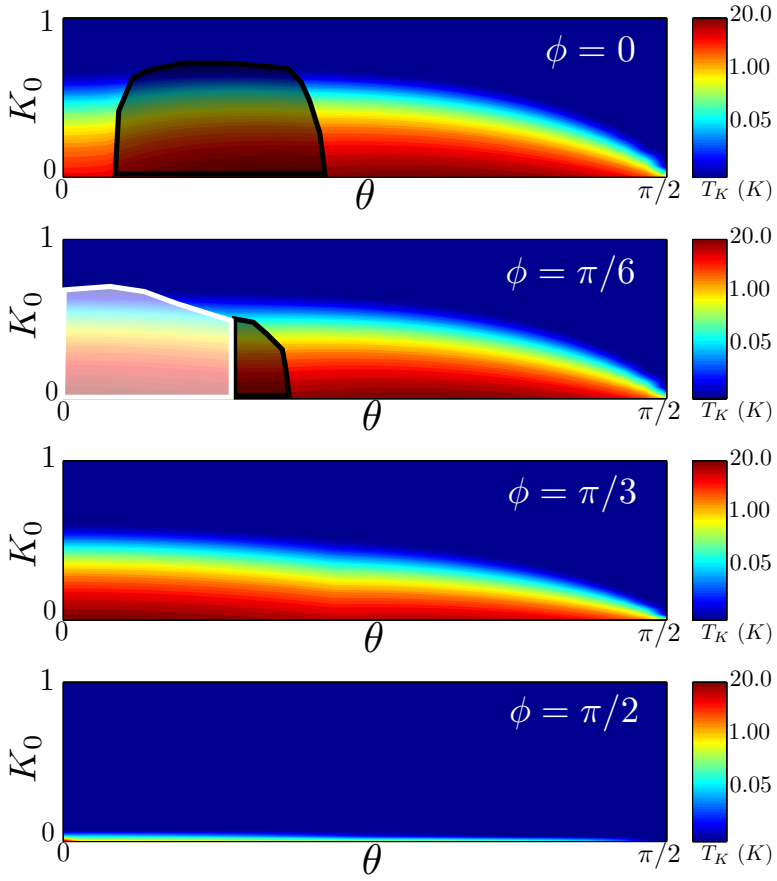

Figure 7.5: The Kondo temperature T_K in a helical Luttinger liquid with a magnetic impurity with Kondo couplings satisfying $J_x = J_y < J_z$. The Kondo temperature is plotted in a logarithmic scale as a function of the Rashba angle θ for four values of the Dresselhaus angle ϕ, the angles parameterizing the strengths of the spin-orbit interactions, and as a function of the ordinary Luttinger parameter K_0, parameterizing the strength of the electron-electron interaction. Note that the vanishing Kondo temperature at $\theta, \phi = \pi/2$ simply reflect the diverging spin-orbit coupling strength in these limits, and that the model is not expected to be valid in these limits. In the black (white) shaded area, J_{yz} (J_{xz}) dominates the perturbative RG flow, hence preventing the low-temperature formation of a Kondo singlet. From Paper V.

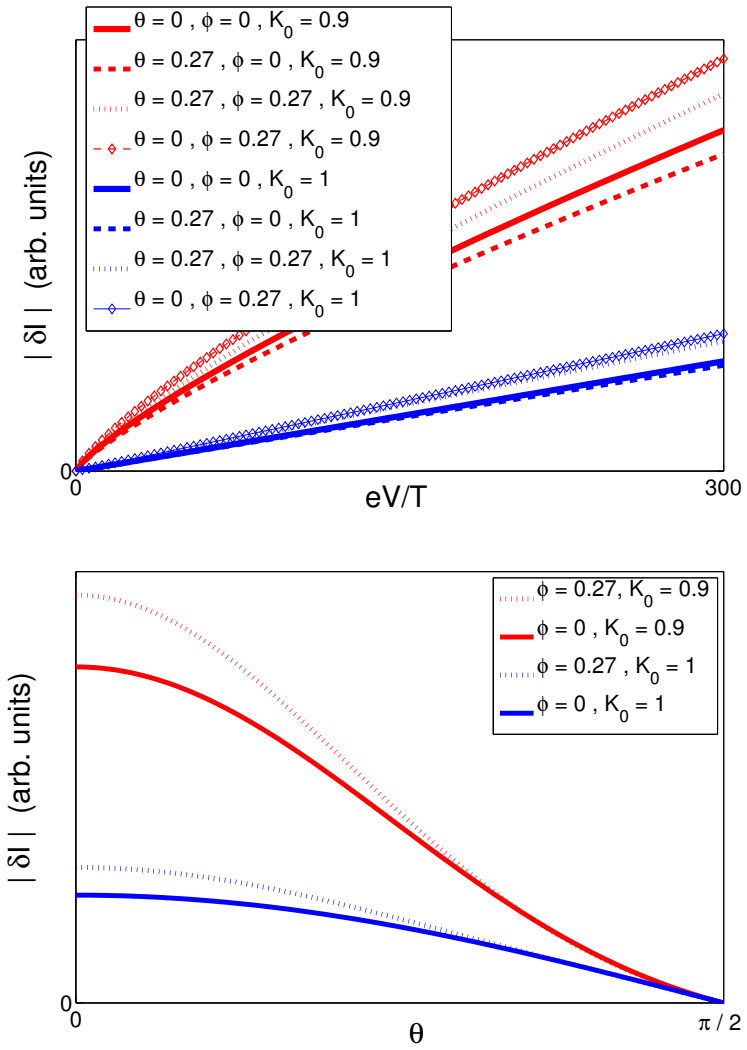

Figure 7.6: The backscattered current δI due to a Kondo impurity in a helical Luttinger liquid, for different values of the Rashba and Dresselhaus angles θ and ϕ (parameterizing the strengths of the spin-orbit interactions), and the Luttinger parameter K_0. Upper: Current-voltage characteristics for δI at fixed temperature T. Lower: δI at fixed voltage and temperature, plotted as a function of the Rashba angle θ. From Paper V.

The effect of a Rashba interaction on the helical electrons can be studied exactly by a spinor rotation [266]. In the new rotated basis, the theory with Dirac fermions with Rashba interaction becomes a theory with new Dirac fermions which do not have a Rashba interaction. The effect is therefore only to rotate the spin quantization axis. However, in the presence of a Kondo impurity with anisotropic exchange interaction the price to pay for this simplification is that the Kondo interaction in the new basis becomes more complicated. Now there will not only be the $S^x\sigma^x$, $S^y\sigma^y$ and $S^z\sigma^z$ interactions (where S refers to the impurity and σ to the electron spins), but in the rotated basis also $S^z\sigma^y$ etc. will appear. Similarly, the Dresselhaus interaction can be treated with a spinor rotation around another axis.

The Kondo temperature is now obtained by perturbative RG, where it is defined as the temperature at which the Kondo couplings start dominating the theory. The RG equations for the generalized Kondo couplings appearing due to the Rashba interaction were obtained in Paper IV[1], and in Paper V these equations were straight-forwardly generalized to the full set of flow equations generated by the simultaneous presence of Rashba and Dresselhaus interaction. The results for Kondo couplings satisfying $J_x = J_y > J_z$ show a Kondo temperature which for fixed strength of the electron-electron interaction decreases with increasing Rashba and/or Dresselhaus interaction strength. The results for $J_x = J_y < J_z$ show a similar behavior, but here there is a very interesting effect appearing. For some values of the Luttinger parameter K_0 and Rashba and Dresselhaus strengths, it is not one of the usual Kondo couplings $J_x, J_y.J_z$ that diverges the fastest. Instead, in the shaded regions in Fig. 7.5 the interactions that diverge fastest are non-collinear couplings. Hence the resulting state the system appears to be flowing towards is not a singlet, which means that the Kondo singlet formation is obstructed. Within the limits of the perturbative treatment, it therefore appears as if the Kondo effect is hampered by a conspiracy of electron-electron and spin-orbit interactions in some parameter regimes.

Away from these special parameter regimes, the Kondo effect will work as usual and we can treat the Kondo interaction perturbatively to obtain the current-voltage characteristics, shown in Fig. 7.6, as well as linear conductance for both electrical and thermal transport and noise characteristics. These results all show the appearance of multiple power-laws for the different kinds of Kondo scatterings that will take place in the rotated basis, and the dependence of the current correction on the electric field which controls the Rashba interaction.

[1]The details of the perturbative renormalization-group calculations in Paper IV for the Kondo temperature with a Rashba interaction can be found in Ref. [267].

7.4 Paper VI: Correlations in one-dimensional Bose gases

In Paper VI we study possible effects from higher conservation laws on correlations in the one-dimensional Bose gas. Assuming the state of the system is described by a generalized Gibbs ensemble (6.54), where the full set of conserved charges appears, we obtain the finite-size corrections in energy and momentum at zero temperature and use the conformal relations (2.134) and (2.135) to deduce the asymptotics of correlation functions. See Section 6.1.1 for an introduction to the original model.

At zero temperature the system is in the ground state of the generalized Hamiltonian

$$H = \sum_i b_i Q_i \tag{7.12}$$

appearing in the density matrix. Here Q_i are all the local conserved charges (6.21), entering with coefficients b_i. It then follows that the bare dispersion (6.26) of the single-particle excitations now becomes

$$\varepsilon_0(\lambda) = \sum_{n=0}^{\infty} b_n \lambda^n \tag{7.13}$$

i.e. some polynomial function, determined by some initial condition on the conserved charges. The dressed energy (6.29) will then also be generalized to some more general function of the bare momenta [268]. In particular, at zero temperature there may now be many different Fermi points with different Fermi velocities. In terms of the excitation quantum numbers described in Fig. 7.7, the finite-size corrections of ground-state energy E_0, and energy E and momentum P, are found to be on the form

$$E_0 - E_0(L\to\infty) = -\frac{\pi}{6L}\sum_j c_j |v_j| \tag{7.14}$$

$$E - E_0 = \frac{2\pi}{L}\sum_j |v_j| \left[\Delta_j^+ + \Delta_j^-\right] \tag{7.15}$$

$$P - P_0 = -\sum_j 2q_j\, d_j + \frac{2\pi}{L}\sum_j \left[\Delta_j^+ - \Delta_j^-\right] \tag{7.16}$$

in the parity symmetric case ($\varepsilon_0(\lambda) = \varepsilon_0(-\lambda)$), where we obtain

$$c_j = 1 \tag{7.17}$$

and

$$\Delta_j^{\pm} = N_j^{\pm} + \frac{1}{2}\left(\sum_k (Z^{-1})_{jk}\frac{\Delta N_k}{2} \pm \sum_k Z_{kj} d_k\right)^2. \tag{7.18}$$

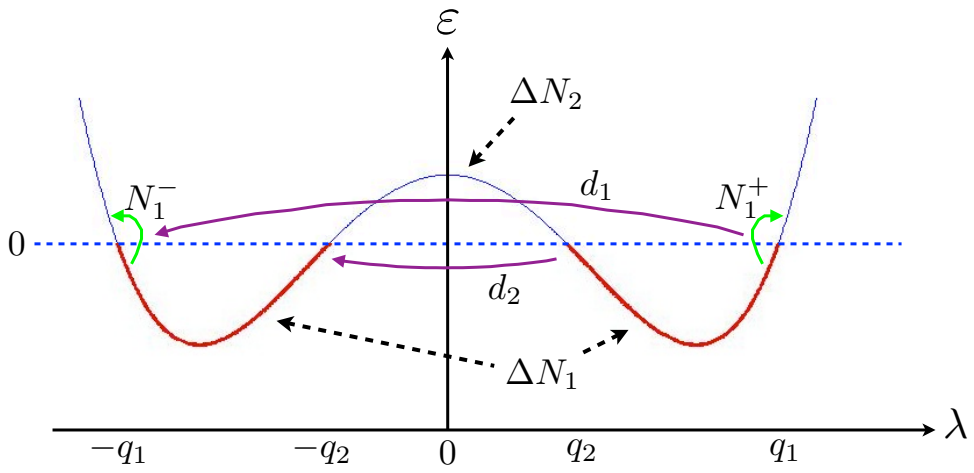

Figure 7.7: A generalized dispersion for the dressed particle energy of the one-dimensional Bose gas with conserved charges added to the Hamiltonian, in this example with parity symmetry and four Fermi points at $\lambda = -q_1, -q_2, q_2, q_1$. The different types of excitations are shown in the figure; ΔN_1 (ΔN_2) particles (holes) added to the Fermi sea $[-q_1, q_1]$ ($[-q_2.q_2]$), $N_i^{\pm}$ particle-hole excitations at Fermi point $\pm q_i$, and d_1 (d_2) particles (holes) backscattered over the Fermi seas.

Here Z_{ij} is the *dressed charge* matrix, which can be computed through linear integral equations.

The low-energy physics is therefore described by a sum of conformal field theories each with central charge $c_j = c = 1$, where the dimensions of the operators are given by Eq. (7.18) in terms of their quantum numbers, see Section 2.2.4. Hence correlation functions can be obtained, e.g. the boson field equal-time correlator

$$\langle \Psi(x)\Psi^\dagger(0)\rangle \sim x^{-\alpha}, \tag{7.19}$$

where α is the smallest of the numbers $\left(\sum_j (Z^{-1})_{jk}\right)^2/2$, and the density-density equal-time correlation function

$$\langle j(x)j(0)\rangle - \langle j(0)\rangle^2 \sim A_1 x^{-2} + A_2 \cos(2q_k d_k x) x^{-\theta}, \tag{7.20}$$

where θ the smallest of the numbers $2\left(\sum_j Z_{kj}\right)^2$.

The findings show that the generalized one-dimensional Bose gas gives rise to similar correlation effects as in multicomponent Bethe-Ansatz solvable models like spin chains with competing interactions and the one-dimensional Hubbard model. In particular, generalized dispersions with

many Fermi points may give rise to several different speeds of sound in the system when also considering the time-evolution governed by the generalized Hamiltonian.

8

Discussion

Let us now conclude this thesis by a brief summary and discussion. We have seen that the development in condensed matter physics during the past decades has brought about many intriguing new phenomena in quantum many-particle systems, in particular in connection to reduced dimensionality. These can often be treated with powerful non-perturbative field-theory methods. In the introductory chapters we discussed the following topics:

- The Luttinger liquid paradigm for interacting one-dimensional systems.
- The conformal-field theory approach to one-dimensional critical phenomena, in particular the Kondo effect and scaling of entanglement entropy.
- Topological order in two-dimensional systems.
- The exact Bethe Ansatz solution for the one-dimensional Bose gas.

We then wished to answer some open questions regarding these problems. The results of these studies were published in Papers I-VI. In summary, these studies concerned

1. **Reduced fidelity and topological quantum phase transitions**

   Question Even though there is no local order parameter for a topological quantum phase transition, is it still possible to capture it by a local fidelity measure?

Result By studying some exactly solvable 2d lattice models, we found that it actually is possible to use local fidelity measures to capture topological quantum phase transitions.

2. **Scaling corrections in impurity entanglement entropy**

   Question Is it possible to obtain exact asymptotic expressions for the scaling corrections of the entanglement entropy from the boundary of a critical one-dimensional systems, and what can this tell us about the elusive Kondo cloud?

   Result We obtained exact asymptotic expressions for the scaling corrections coming from perturbing boundary operators of a one-dimensional system using boundary conformal field theory. Such corrections give information about the shape of the Kondo screening cloud, and we found that the critical exponent for the spatial decay of the ground-state entanglement entropy is the same as the exponent for the impurity specific heat.

3. **Effects from spin-orbit interactions on the Kondo effect in helical Luttinger liquids**

   Question How do spin-orbit interactions influence the Kondo effect in the helical Luttinger liquid appearing on the edge of a two-dimensional topological insulator?

   Result We found that Rashba and Dresselhaus spin-orbit interactions indeed have an effect, although generally small, on the transport properties of a helical edge liquid with a Kondo impurity. However, in some special parameter regimes the effect appears to be quite dramatic since there the low-energy behavior may be different from that of a Kondo singlet. Tuning the system in and out of this region with the electric field could perhaps offer a promising mechanism to control edge transport.

4. **Correlations in generalized Gibbs ensemble of a one-dimensional Bose gas**

   Question What will be the effect on correlations in a one-dimensional Bose gas when including all conservation laws?

   Result Our Bethe Ansatz results for the generalized Lieb-Liniger model, describing the generalized Gibbs ensemble of an interacting one-dimensional Bose gas, show that it is possible to obtain similar types of correlation effects as for the one-dimensional

Hubbard model and spin chains with competing interactions. This includes the possibility of several different Fermi points. Hence with additional conservation law in the Hamiltonian there might be several different velocities appearing in the correlation functions.

Outlook

Let us end with a brief discussion of current trends and future directions associated with the topics of this thesis.

Strongly correlated quantum many-particle systems are intrinsically hard to understand, and continue to spur much development in theoretical physics. Indeed, high-temperature superconductivity still lacks an explanation [32,269,270], 27 years after its discovery [271], and the quest to solve the problem will certainly continue to drive much of the field.

General theories for correlated topological phases of matter with interacting electrons are still missing [209,272]. New types of such systems, like "topological Mott insulators" [273, 274], "fractional topological insulators" [275] and "topological Kondo insulators" [276] attract much attention, and the general relation to the entanglement structure [137, 277] is intriguing. Prospects of creating topological states in cold-atom systems stimulates much research [278].

The Kondo cloud [95] still evades detection. An interesting issue regarding entanglement in quantum impurity problems is the measure of "negativity". This measure allows for the entanglement between two disjoint parts of a system to be calculated. New CFT methods [279] could here give exact results for this measure of entanglement between an impurity and the surrounding electrons [280], allowing for more information about the distribution of entanglement than that given by the entropy. A full understanding of the entanglement generated by Kondo clouds holds promise for future applications in quantum information science [92, 93].

Quantum many-particle systems out of equilibrium continues to be an intense area of research, with questions regarding the foundations of quantum statistical mechanics still open [222]. Particularly interesting cases are the extensions of Bethe Ansatz [281], Luttinger liquid [282,283] and CFT [284] techniques to non-equilibrium situations. New approaches to study non-equilibrium quench dynamics in integrable systems based on the Bethe Ansatz are being developed [285, 286] and may shed new light on quantum equilibration phenomena and the generalized Gibbs ensemble.

Quantum impurities on edges of topological insulators present challenging issues, in particular in three dimensions [287, 288] where it also

has relevance for graphene [289]. For quantum spin Hall insulators the effect from spin-orbit coupling on a Kondo lattice on the edge [113] remains to be investigated. The relevance of Kondo physics to current attempts [290] to detect Majorana particles in semiconductor wires coupled to a superconductor [200] is still open. Such Majorana bound states in spin-orbit coupled quantum wires [291], which mimic the helical liquid, could also present an interesting system to study Kondo physics in. Detection of non-Abelian particles in standard solid-state systems would present a major advancement towards the dream of performing topological quantum computation [174], with the ultimate goal of revolutionizing information technology [292].

Emergent phenomena in strongly correlated quantum many-particle systems represents a rapidly evolving field of research. Potential technological applications, like room-temperature superconductivity and quantum computers, and fundamental theoretical challenges give such systems a prominent place in science. Due to the intrinsic complexity of the problem, unexpected new phenomena will most certainly continue to appear.

A

Scaling corrections in von Neumann entropy from irrelevant boundary operators

Let us here show how to obtain the finite-temperature scaling corrections to the critical Rényi entropies (4.9) of a semi-infinite one-dimensional system which are generated by irrelevant *boundary operators*, results that were presented in Paper III. We follow the same procedure as Cardy and Calabrese in Ref. [293], however when perturbing with a boundary operator the surface integral of the perturbing field in the action will be replaced by a line integral on the boundary. As we shall see, this will prevent the appearance of unusual n-dependent corrections. In fact, this is anticipated since n-dependent exponents only arise from the region at the branch point, which is located away from the boundary. Nevertheless, there still are results for the boundary case that do not follow from standard finite-size scaling. We will also extend the analysis to finite temperature. This will reveal an interesting connection to previous results for the thermodynamic boundary entropy and specific heat.

Thus, consider a BCFT on the upper half $y \geq 0$ of the complex plane $z = \tau + iy$. At finite inverse temperature $\beta = 1/(k_B T)$ the imaginary-time coordinate τ becomes periodic with $-\beta/2 \leq \tau \leq \beta/2$, and the complex plane is turned into a cylinder. The BCFT is therefore defined on a semi-infinite strip in the complex plane, and on the boundary at $y = 0$ the boundary coordinate is $-\beta/2 \leq \tau \leq \beta/2$, see Fig. A.1. The n-sheeted Riemann surface $\mathcal{R}_n$ is then obtained by sewing together n copies of this cylinder along $0 \leq y < r$ at $\tau = 0$. To evaluate the correlation functions on $\mathcal{R}_n$ for a chiral operator $\phi(z)$ with scaling dimension x_b, we need to

use the transformation property

$$\langle\phi(z_1)\cdots\phi(z_N)\rangle_{\mathcal{R}_n} = \prod_{j=1}^{N}\left|\frac{\partial z}{\partial w}\right|_{w=w_j}^{-x_b}\langle\phi(w_1)\cdots\phi(w_N)\rangle_{\mathbb{C}^+}\,, \tag{A.1}$$

where the map $z \mapsto w$ from $\mathcal{R}_n$ to the finite-temperature strip in the upper half-plane $\mathbb{C}^+$ is given by

$$w = -\frac{\beta}{\pi}\arcsin\left[i\frac{\pi}{\beta}\,\frac{\left(\frac{\sin\frac{\pi z}{\beta}-i\sinh\frac{\pi r}{\beta}}{\sin\frac{\pi z}{\beta}+i\sinh\frac{\pi r}{\beta}}\right)^{1/n}+1}{\left(\frac{\sin\frac{\pi z}{\beta}-i\sinh\frac{\pi r}{\beta}}{\sin\frac{\pi z}{\beta}+i\sinh\frac{\pi r}{\beta}}\right)^{1/n}-1}\right]\,, \tag{A.2}$$

see Fig. A.1. The inverse transformation is then given by

$$z = -\frac{\beta}{\pi}\arcsin\left[i\sinh\left(\frac{\pi r}{\beta}\right)\,\frac{\left(\frac{\frac{\beta}{\pi}\sin\frac{\pi w}{\beta}-i}{\frac{\beta}{\pi}\sin\frac{\pi w}{\beta}+i}\right)^{n}+1}{\left(\frac{\frac{\beta}{\pi}\sin\frac{\pi w}{\beta}-i}{\frac{\beta}{\pi}\sin\frac{\pi w}{\beta}+i}\right)^{n}-1}\right]\,. \tag{A.3}$$

This gives (using the Mathematica software)

$$\frac{\partial z}{\partial w} = -4n\frac{\beta}{\pi}\sinh\left(\frac{\pi r}{\beta}\right)\,\frac{\left(\frac{\frac{\beta}{\pi}\sin\frac{\pi w}{\beta}-i}{\frac{\beta}{\pi}\sin\frac{\pi w}{\beta}+i}\right)^{n}}{\left(1+\left(\frac{\beta}{\pi}\sin\frac{\pi w}{\beta}\right)^2\right)\left[\left(\frac{\frac{\beta}{\pi}\sin\frac{\pi w}{\beta}-i}{\frac{\beta}{\pi}\sin\frac{\pi w}{\beta}+i}\right)^{n}-1\right]^2}$$

$$\times\cos\left(\frac{\pi w}{\beta}\right)\left[1+\left(\sinh\left(\frac{\pi r}{\beta}\right)\frac{\left(\frac{\frac{\beta}{\pi}\sin\frac{\pi w}{\beta}-i}{\frac{\beta}{\pi}\sin\frac{\pi w}{\beta}+i}\right)^{n}+1}{\left(\frac{\frac{\beta}{\pi}\sin\frac{\pi w}{\beta}-i}{\frac{\beta}{\pi}\sin\frac{\pi w}{\beta}+i}\right)^{n}-1}\right)^2\right]^{-1/2} \tag{A.4}$$

Naturally, the mapping (A.2) takes the boundary of $\mathcal{R}_n$ to the boundary of $\mathbb{C}^+$. Since w is real on the boundary we see from (A.4) that $|\partial z/\partial w|^{-x_b}$ is analytic on the boundary, as the only singularity is at

$$\frac{\beta}{\pi}\sin\frac{\pi w}{\beta} = i\,, \tag{A.5}$$

i.e. when z is at the branch point $z = ir$. In particular, note that the point $|z| \to \infty$ gives a divergence in $|\partial z/\partial w|$ which only means that $|\partial z/\partial w|^{-x_b} \to 0$.

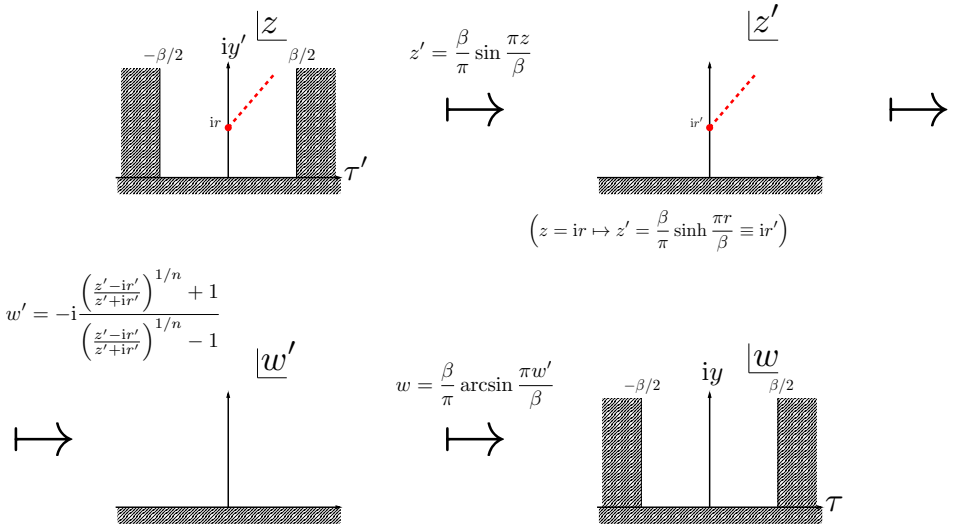

Figure A.1: The series of conformal transformations that map the Riemann surface $\mathcal{R}_n$, here represented as the upper complex half-plane with a branch cut (dashed line), to the ordinary upper complex half-plane $\mathbb{C}^+$ without the branch cut. The series of transformations $z \mapsto z' \mapsto w' \mapsto w$ make up the conformal transformation $z \mapsto w$ in Eq. (A.2).

Now we can use this to study the scaling corrections of $S_A^{(n)} \propto (F_{\mathcal{R}_n} - nF)$ when adding a boundary perturbation,

$$S = S_{CFT} + \lambda \int \mathrm{d}\tau\, \phi_b(\tau)\,, \tag{A.6}$$

where ϕ_b is an irrelevant operator with scaling dimension $x_b > 1$ on the boundary $y = 0$.

We will assume the boundary conditions to be such that $\langle \phi_b(\tau) \rangle = 0$. This is natural if we demand conformal boundary conditions. Then the first-order correction vanishes. An important exception is when the perturbing boundary operator is the stress-energy tensor, a case that was treated in Refs. [157, 158]. Since this operator has a non-vanishing expectation value on $\mathcal{R}_n$ it will give rise to a first-order correction to $S_A^{(n)}$, which was found to have the form $\sim \beta^{-1} \coth(r/\beta)$. We therefore consider the second-order corrections to $F_{\mathcal{R}_n}$ and F, denoted $\delta^2 F_{\mathcal{R}_n}$ and $\delta^2 F$ respectively. They are given by

$$\delta^2 F_{\mathcal{R}_n} = -\frac{\lambda^2}{2} \int \mathrm{d}\tau_1' \int \mathrm{d}\tau_2' \, \langle \phi_b(\tau_1') \phi_b(\tau_2') \rangle_{\mathcal{R}_n} \tag{A.7}$$

and

$$\delta^2 F = -\frac{\lambda^2}{2}\int \mathrm{d}\tau_1 \int \mathrm{d}\tau_2 \, \langle \phi_b(\tau_1)\phi_b(\tau_2)\rangle_{\mathbb{C}^+} \,, \tag{A.8}$$

respectively, where τ_1', τ_2' are boundary coordinates on $\mathcal{R}_n$ and $\tau_1 = w(\tau_1')$, $\tau_2 = w(\tau_2')$ are boundary coordinates on $\mathbb{C}^+$. From Eq. (A.1), we get

$$\begin{aligned}
\delta^2 F_{\mathcal{R}_n} &= -\frac{\lambda^2}{2}\int \mathrm{d}\tau_1' \int \mathrm{d}\tau_2' \left|\frac{\partial z}{\partial w}\right|_{z=\tau_1'}^{-x_b} \left|\frac{\partial z}{\partial w}\right|_{z=\tau_2'}^{-x_b} \langle \phi_b(w(\tau_1'))\phi_b(w(\tau_2'))\rangle_{\mathbb{C}^+} \\
&= -\frac{\lambda^2}{2}\int \mathrm{d}\tau_1 \int \mathrm{d}\tau_2 \left|\frac{\partial z}{\partial w}\right|_{w=\tau_1}^{1-x_b} \left|\frac{\partial z}{\partial w}\right|_{w=\tau_2}^{1-x_b} \langle \phi_b(\tau_1)\phi_b(\tau_2)\rangle_{\mathbb{C}^+} \\
&= -\frac{\lambda^2}{2}\int_{-\beta/2}^{\beta/2} \mathrm{d}\tau_1 \int_{-\beta/2}^{\beta/2} \mathrm{d}\tau_2 \, \frac{\left|\frac{\partial z}{\partial w}\right|_{w=\tau_1}^{1-x_b} \left|\frac{\partial z}{\partial w}\right|_{w=\tau_2}^{1-x_b}}{|\frac{\beta}{\pi}\sin(\frac{\pi}{\beta}(\tau_1-\tau_2)|^{2x_b}} \,.
\end{aligned} \tag{A.9}$$

In order to compare the two integrals in $\delta^2 F_{\mathcal{R}_n} - n\delta^2 F$ it is convenient to rewrite $n\delta^2 F$ on the same form as $\delta^2 F_{\mathcal{R}_n}$,

$$\begin{aligned}
n\delta^2 F &= -\frac{\lambda^2}{2} n \int_{-\beta/2}^{\beta/2} \mathrm{d}\tau_1 \int_{-\beta/2}^{\beta/2} \mathrm{d}\tau_2 \frac{1}{|\frac{\beta}{\pi}\sin(\frac{\pi}{\beta}(\tau_1-\tau_2))|^{2x_b}} \\
&= -\lambda^2 n \int_{-\beta/2}^{\beta/2} \mathrm{d}\tau_1 \int_0^{\beta} \mathrm{d}\tau \frac{1}{|\frac{\beta}{\pi}\sin(\frac{\pi}{\beta}\tau)|^{2x_b}} \,,
\end{aligned} \tag{A.10}$$

where we defined $\tau \equiv \tau_1 - \tau_2$. Now, with the change of variable $u = \tan(\pi\tau/\beta)$, which means that

$$\tau = \frac{\beta}{\pi}\arctan u \,, \tag{A.11}$$

$$\mathrm{d}\tau = \frac{\beta}{\pi}\frac{1}{1+u^2}\mathrm{d}u \,, \tag{A.12}$$

$$\sin\frac{\pi\tau}{\beta} = \frac{u}{\sqrt{1+u^2}} \,, \tag{A.13}$$

the integral becomes

$$n\delta^2 F = -\frac{\lambda^2}{2}\left(\frac{\beta}{\pi}\right)^{1-2x_b} n \int_{-\beta/2}^{\beta/2} \mathrm{d}\tau_1 \int_0^{\infty} \mathrm{d}u \frac{(1+u^2)^{x_b-1}}{u^{2x_b}} \,. \tag{A.14}$$

The integral diverges when $u \to 0$, and we must introduce a cutoff. In the original boundary coordinate this cutoff reads $|\tau_1 - \tau_2| > \tau_0$, which in the new variable becomes $u > \tan(\pi\tau_0/\beta)$. In the low-temperature limit, which is what we are interested in, this means that $u > \pi\tau_0/\beta$. Now, using that

$$n\int_{-\beta/2}^{\beta/2} \mathrm{d}\tau_1 = \int \mathrm{d}\tau_1' = \int_{-\beta/2}^{\beta/2} \mathrm{d}\tau_1 \left|\frac{\partial z}{\partial w}\right|_{w=\tau_1} \,, \tag{A.15}$$

together with the change of variable

$$u \mapsto u \left| \frac{\partial z}{\partial w} \right|_{w=\tau_1} , \tag{A.16}$$

we can rewrite Eq. (A.14) as

$$\begin{aligned} n\delta^2 F &= -\frac{\lambda^2}{2} \left(\frac{\beta}{\pi}\right)^{1-2x_b} \int_{-\beta/2}^{\beta/2} \mathrm{d}\tau_1 \left| \frac{\partial z}{\partial w} \right|^2_{w=\tau_1} \int_0^\infty \mathrm{d}u \frac{(1+(u\left|\frac{\partial z}{\partial w}\right|_{w=\tau_1})^2)^{x_b-1}}{(u\left|\frac{\partial z}{\partial w}\right|_{w=\tau_1})^{2x_b}} \\ &= -\frac{\lambda^2}{2} \left(\frac{\beta}{\pi}\right)^{1-2x_b} \int_{-\beta/2}^{\beta/2} \mathrm{d}\tau_1 \int_{-\beta/2}^{\beta/2} \mathrm{d}\tau_2 \frac{\left|\frac{\partial z}{\partial w}\right|^2_{w=\tau_1}}{|\left|\frac{\partial z}{\partial w}\right|_{w=\tau_1} \sin(\frac{\pi}{\beta}(\tau_1-\tau_2)|^{2x_b}} \\ &= -\frac{\lambda^2}{2} \int_{-\beta/2}^{\beta/2} \mathrm{d}\tau_1 \int_{-\beta/2}^{\beta/2} \mathrm{d}\tau_2 \, \frac{\left|\frac{\partial z}{\partial w}\right|^{2-2x_b}_{w=\tau_1}}{|\frac{\beta}{\pi}\sin(\frac{\pi}{\beta}(\tau_1-\tau_2)|^{2x_b}} , \end{aligned} \tag{A.17}$$

where the cutoff is given by

$$u = \tan(\frac{\pi}{\beta}|\tau_1-\tau_2|) \;>\; \frac{\tan(\frac{\pi}{\beta}\tau_0)}{\left|\frac{\partial z}{\partial w}\right|_{w=\tau_1}} . \tag{A.18}$$

As $\tau_0 \to 0$, we have

$$\tan(\frac{\pi}{\beta}|\tau_1-\tau_2|) \to \frac{\pi}{\beta}|\tau_1-\tau_2| \tag{A.19}$$

and the cutoff can be written as

$$|\tau_1-\tau_2| \left| \frac{\partial z}{\partial w} \right|_{w=\tau_1} \;>\; \tau_0 , \tag{A.20}$$

which is the same as

$$|\tau_1' - \tau_2'| \geq \tau_0 . \tag{A.21}$$

We are therefore now able to write $\delta^2 F_{\mathcal{R}_n} - n\delta^2 F$, i.e. Eqs. (A.7) and (A.8), as one single integral,

$$\delta^2 F_{\mathcal{R}_n} - n\delta^2 F \;=\; -\frac{\lambda^2}{2} \int_{-\beta/2}^{\beta/2} \mathrm{d}\tau_1 \int_{-\beta/2}^{\beta/2} \mathrm{d}\tau_2 \frac{\left|\frac{\partial z}{\partial w}\right|^{1-x_b}_{w=\tau_1} \left|\frac{\partial z}{\partial w}\right|^{1-x_b}_{w=\tau_2} - \left|\frac{\partial z}{\partial w}\right|^{2-2x_b}_{w=\tau_1}}{|\frac{\beta}{\pi}\sin(\frac{\pi}{\beta}(\tau_1-\tau_2)|^{2x_b}} . \tag{A.22}$$

with the cutoff given by Eq. (A.20). Using the symmetry of the integral under exchange of τ_1 and τ_2, we can put Eq. (A.22) on the symmetric

form

$$\begin{aligned}\delta^2 S_A^{(n)} &\sim \delta^2 F_{\mathcal{R}_n} - n\delta^2 F \\ &= \frac{\lambda^2}{4}\int_{-\beta/2}^{\beta/2}\mathrm{d}\tau_1\int_{-\beta/2}^{\beta/2}\mathrm{d}\tau_2 \frac{\Big(\big|\frac{\partial z}{\partial w}\big|_{w=\tau_1}^{1-x_b} - \big|\frac{\partial z}{\partial w}\big|_{w=\tau_2}^{1-x_b}\Big)^2}{|\frac{\beta}{\pi}\sin(\frac{\pi}{\beta}(\tau_1-\tau_2)|^{2x_b}}.\end{aligned} \tag{A.23}$$

It follows from Eq. (A.4) that $|\mathrm{d}z/\mathrm{d}w|^{1-x_b}$ is analytic everywhere except at $z = \mathrm{i}r$. In Ref. [293], where the integrals are surface integrals over $\mathbb{C}^+$, this singularity at the branch point was an important ingredient in the analysis. But when we now consider a perturbing operator on the boundary, the only divergence in the integrand in (A.23) comes when $\sin(\frac{\pi}{\beta}(\tau_1-\tau_2) = 0$, i.e. when $u = \tan(\pi\tau/\beta) = 0$. Since we re interested in the divergent behavior, we expand $\big|\frac{\partial z}{\partial w}\big|^{1-x_b} \equiv f(w)$ around $w = \tau_2$, which gives

$$\begin{aligned}\delta^2 S_A^{(n)} = \frac{\lambda^2}{4}\left(\frac{\beta}{\pi}\right)^{1-2x_b}\int_{-\beta/2}^{\beta/2}\mathrm{d}\tau_1\int_0^\infty \mathrm{d}u\frac{(1+u^2)^{x_b-1}}{u^{2x_b}}\Big[(f'(\tau_1)\frac{\beta}{\pi}\arctan u)^2 \\ + f'(\tau_1)f''(\tau_1)(\frac{\beta}{\pi}\arctan u)^3 + ...\Big],\end{aligned} \tag{A.24}$$

and expanding the integrand around the divergence at $u = 0$ we get

$$\begin{aligned}\delta^2 S_A^{(n)} &\sim \lambda^2\beta^{3-2x_b}\int_{-\beta/2}^{\beta/2}\mathrm{d}\tau_1\int_0^\infty \mathrm{d}u\Big[\big(a\,u^{2x_b} + b\,u^{2-2x_b} + ...\big) \\ &\qquad \times\big(c\,(f'(\tau_1))^2\,u^2 + (c\,f'(\tau_1)f''(\tau_1) + d\,(f'(\tau_1))^2\beta)\,u^3 + ...\big)\Big] \\ &\sim \lambda^2\beta^{3-2x_b}\int_{-\beta/2}^{\beta/2}\mathrm{d}\tau_1\int_0^\infty \mathrm{d}u\Big[\,a\,c\,(f'(\tau_1))^2\,u^{2-2x_b} + ...\Big],\end{aligned} \tag{A.25}$$

where $a, b, c, ...$ are used to denote constants. From this it follows that the leading divergence of $\delta^2 S_A^{(n)}$ goes as $\tau_0^{3-2x_b}$, i.e. the integral (A.23) converges when $x_b < 3/2$. Therefore the regularization $u > \pi\tau_0/(\beta\,\big|\frac{\partial z}{\partial w}\big|_{w=\tau_1})$ is only needed when $x_b \geq 3/2$, and then

$$\begin{aligned}\delta^2 S_A^{(n)} &\sim \lambda^2\beta^{3-2x_b}\int_{-\beta/2}^{\beta/2}\mathrm{d}\tau_1\int_0^\infty \mathrm{d}u\Big[a\,c\,(f'(\tau_1))^2\,u^{2-2x_b} + ...\Big] \\ &\sim \lambda^2\beta^{3-2x_b}\int_{-\beta/2}^{\beta/2}\mathrm{d}\tau_1\Big[(f'(\tau_1))^2\Big(\frac{\tau_0}{\beta\,\big|\frac{\partial z}{\partial w}\big|_{w=\tau_1}}\Big)^{3-2x_b} + ...\Big] \\ &\sim \lambda^2\tau_0^{3-2x_b}\int_{-\beta/2}^{\beta/2}\mathrm{d}\tau_1\frac{\Big(\frac{\partial}{\partial w}\,\big|\frac{\partial z}{\partial w}\big|^{1-x_b}\Big)^2}{\big|\frac{\partial z}{\partial w}\big|_{w=\tau_1}^{3-2x_b}}.\end{aligned} \tag{A.26}$$

when $x_b > 3/2$, with the divergence instead being logarithmic when $x_b = 3/2$.

From Eq. (A.4) we see that we can write $\mathrm{d}z/\mathrm{d}w$ as

$$\frac{\partial z}{\partial w} = \frac{\frac{\beta}{\pi}\sinh\left(\frac{\pi r}{\beta}\right)}{\sqrt{1+\left(h(\beta,w)\sinh\left(\frac{\pi r}{\beta}\right)\right)^2}}\, g(\beta,w)\,, \tag{A.27}$$

introducing the functions $g(\beta,w)$ and $h(\beta,w)$ which are β-independent in the low-temperature limit $\beta\to\infty$. From this we can analytically extract the scaling of $\delta^2 S_A^{(n)}$ in the limits $r/\beta\to 0$ and $r/\beta\to\infty$.

First, in the zero-temperature quantum mechanical limit $r/\beta\to 0$, we see from Eq. (A.27) that

$$\frac{\partial z}{\partial w} \quad\propto\quad r + \mathcal{O}((r/\beta)^3), \tag{A.28}$$

as $\beta\to\infty$. As we do not need to introduce the cutoff in Eq. (A.23) when $x_b < 3/2$, the only r-dependence comes from $\mathrm{d}z/\mathrm{d}w \propto r$. Note that since the action (A.6) is dimensionless, we can write $\lambda \sim \tau_0^{x_b-1}$. Thus when $x_b < 3/2$ it follows that $\delta^2 S_A^{(n)} \sim (r/\tau_0)^{2-2x_b}$ up to terms $\mathcal{O}((r/\beta)^3)$ and $\mathcal{O}(\beta^{-1})$. On the other hand, when $x_b > 3/2$ it follows from Eq. (A.26) that

$$\delta^2 S_A^{(n)} \sim \lambda^2 \tau_0^{3-2x_b} r^{2-2x_b} r^{2x_b-3} \sim (r/\tau_0)^{-1}. \tag{A.29}$$

Note that this is of the same form as the first-order correction from the stress-energy tensor. When $x_b = 3/2$, Eq. (A.26) implies that the integral diverges logarithmically, and then

$$\delta^2 S_A^{(n)} \sim \lambda^2 r^{2-2x_b}\log(\tau_0/r) \sim (\tau_0/r)\log(r/\tau_0). \tag{A.30}$$

Summarizing, in the limit when $r/\beta\to 0$ and $\beta\to\infty$ the leading corrections to the Rényi entropies are

$$\delta^2 S_A^{(n)} \sim \begin{cases} r^{2-2x_b} & \text{when } 1 < x_b < 3/2 \\ r^{-1}\log r & \text{when } x_b = 3/2 \\ r^{-1} & \text{when } x_b > 3/2\,, \end{cases} \tag{A.31}$$

up to terms $\mathcal{O}((r/\beta)^3)$ and $\mathcal{O}(\beta^{-1})$.

It is also possible to extract the behavior in the other limit, when $r/\beta\to\infty$, but still at low temperature. We then see from Eq. (A.27) that

$$\frac{\partial z}{\partial w} \quad\propto\quad \beta + \mathcal{O}(e^{-2\pi r/\beta}), \tag{A.32}$$

up to terms $\mathcal{O}(\beta^{-1})$. Once again, when $x_b < 3/2$ the only r-dependence in Eq. (A.23) comes from $\mathrm{d}z/\mathrm{d}w$ which now is proportional to β. Therefore we now get that $\delta^2 S_A^{(n)} \sim (\beta/\tau_0)^{2-2x_b}$ when $x_b < 3/2$. From Eq. (A.26) it now follows that $\delta^2 S_A^{(n)} \sim (\beta/\tau_0)^{-1}$ when $x_b > 3/2$, and $\delta^2 S_A^{(n)} \sim (\tau_0/\beta)\log(\beta/\tau_0)$. Note that we still consider the low-temperature limit $\beta \to \infty$, but with $r \gg \beta$.

In summary, considering the limit $r/\beta \to \infty$ and $\beta \to \infty$ the leading corrections to the Rényi entropies are

$$\delta^2 S_A^{(n)} \sim \begin{cases} \beta^{2-2x_b} & \text{when} 1 < x_b < 3/2 \\ \beta^{-1}\log\beta & \text{when } x_b = 3/2 \\ \beta^{-1} & \text{when } x_b > 3/2\,, \end{cases} \tag{A.33}$$

to $\mathcal{O}(\beta^{-1})$ in β and $\mathcal{O}(e^{-2\pi r/\beta})$ in r/β.

The von Neumann entropy S_A follows from the Rényi entropy $S_A^{(n)}$ simply by letting $n \to 1$.

Bibliography

[1] Aristotle, *Metaphysics*, Book H 1045a 8-10.

[2] S. Weinberg, *Dreams of a Final Theory: The Scientist's Search for the Ultimate Laws of Nature*. Pantheon Books, New York, 1992.

[3] P. W. Anderson, *More is different*, Science **177**, 393 (1972).

[4] R. B. Laughlin and D. Pines, *The theory of everything*, Proc. Natl. Acad. Sci. USA **97**, 28 (2000).

[5] W. Heisenberg, *Physikalische Prinzipien der Quantentheorie*. S. Hirzel Verlag, Leipzig, 1930.

[6] P. Dirac, *The Principles of Quantum Mechanics*. Clarendon Press, Oxford, 1930.

[7] J. von Neumann, *Mathematische Grundlagen der Quantenmechanik*. Springer-Verlag, Berlin, 1932.

[8] A. L. Fetter and J. D. Walecka, *Quantum Theory of Many-Particle Systems*. McGraw-Hill, New York, 1971.

[9] J. W. Negele and H. Orland, *Quantum Many-Particle Systems*. Westview Press, Boulder, 1998.

[10] P. Coleman, *Many body physics: Unfinished revolution*, Ann. Henri Poincaré **4**, 559 (2003).

[11] A. Altland and B. Simons, *Condensed Matter Field Theory*. Cambridge University Press, Cambridge, 2010.

[12] E. Fradkin, *Field Theories of Condensed Matter Physics*. Cambridge University Press, Cambridge, 2013.

[13] J. Cardy, *Scaling and Renormalization in Statistical Physics*. Cambridge University Press, Cambridge, 1996.

[14] S. Hartmann, *Effective field theories, reductionism and scientific explanation*, Stud. Hist. Phil. Sci. B **32**, 267 (2001).

[15] M. Born and R. Oppenheimer, *Zur Quantentheorie der Molekeln*, Ann. Phys. **389**, 457 (1927).

[16] E. Schrödinger, *Quantisierung als Eigenwertproblem*, Ann. Phys. **384**, 361 (1926).

[17] F. Bloch, *Über die Quantenmechanik der Elektronen in Kristallgittern*, Z. Phys. **52**, 555 (1929).

[18] N. W. Ashcroft and N. D. Mermin, *Solid State Physics*. Brooks/Cole, Belmont, 1976.

[19] L. Landau, *Theory of Fermi-liquids*, Zh. Eksp. Teor. Fiz. **30**, 1058 (1956). Eng. transl.: Sov. Phys. JETP **3** 920 (1957).

[20] L. Landau, *On the theory of phase transitions*, Zh. Eksp. Teor. Fiz. **7**, 19 (1937).

[21] P. W. Anderson, *Basic Notions of Condensed Matter Physics*. Benjamin/Cummings, Menlo Park, 1984.

[22] E. M. Lifshitz and P. Pitaevskii, *Statistical Physics, Part 2 (Course of Theoretical Physics, Volume 9)*. Butterworth-Heinemann, Oxford, 1980.

[23] R. Shankar, *Renormalization-group approach to interacting fermions*, Rev. Mod. Phys. **66**, 129 (1994).

[24] A. J. Schofield, *Non-Fermi liquids*, Contemp. Phys. **40**, 95 (1999).

[25] L. N. Cooper, *Bound electron pairs in a degenerate Fermi gas*, Phys. Rev. **104**, 1189 (1956).

[26] J. Bardeen, L. N. Cooper and J. R. Schrieffer, *Theory of superconductivity*, Phys. Rev. **108**, 1175 (1957).

[27] T. Giamarchi, *Quantum Physics in One Dimension*. Clarendon Press, Oxford, 2003.

[28] A. O. Gogolin, A. A. Nersesyan and A. M. Tsvelik, *Bosonization and Strongly Correlated Systems*. Cambridge University Press, Cambridge, 2004.

[29] S. Sachdev, *Quantum Phase Transitions*. Cambridge University Press, Cambridge, 1999.

[30] A. C. Hewson, *The Kondo Problem to Heavy Fermions*. Cambridge University Press, Cambridge, 1997.

[31] I. Affleck, *Non-Fermi liquid behavior in Kondo models*, J. Phys. Soc. Jpn. **74**, 59 (2005).

[32] P. W. Anderson, *The Theory of Superconductivity in the High-Tc Cuprate Superconductors*. Princeton University Press, Princeton, 1997.

[33] L. D. Landau and E. M. Lifshitz, *Statistical Physics, 3rd Edition, Part 1 (Course of Theoretical Physics, Volume 5)*. Pergamon, Oxford, 1980.

[34] Y. Nambu, *Quasi-particles and gauge invariance in the theory of superconductivity*, Phys. Rev. **117**, 648 (1960).

[35] J. Goldstone, *Field theories with "superconductor" solutions*, Il Nuovo Cim. **19**, 154 (1961).

[36] J. Goldstone, A. Salam and S. Weinberg, *Broken symmetries*, Phys. Rev. **127**, 965 (1962).

[37] D. C. Tsui, H. L. Stormer and A. C. Gossard, *Two-dimensional magnetotransport in the extreme quantum limit*, Phys. Rev. Lett. **48**, 1559–1562 (1982).

[38] X.-G. Wen, *Quantum Field Theory of Many-Body Systems*. Oxford University Press, Oxford, 2004.

[39] C. Castelnovo, S. Trebst and M. Troyer, *Topological Order and Quantum Criticality*, chapter of the book "Understanding Quantum Phase Transitions", edited by L. D. Carr (CRC Press / Taylor and Francis, 2010). [arXiv:0912.3272].

[40] S.-I. Tomonaga, *Remarks on Bloch's method of sound waves applied to many-fermion problems*, Prog. Theor. Phys. **5**, 544 (1950).

[41] J. M. Luttinger, *An exactly soluble model of a many-fermion system*, J. Math. Phys. **4**, 1154 (1963).

[42] F. D. M. Haldane, *'Luttinger liquid theory' of one-dimensional quantum fluids. I. Properties of the Luttinger model and their extension to the general 1D interacting spinless Fermi gas*, J. Phys. C **14**, 2585 (1981).

[43] P. Di Francesco, P. Mathieu and D. D. Sénéchal, *Conformal Field Theory*. Springer-Verlag, New York, 1997.

[44] H. Bethe, *Zur Theorie der Metalle. I. Eigenwerte und Eigenfunktionen der linearen Atomkette*, Z. Physik **71**, 205 (1931).

[45] J. Leinaas and J. Myrheim, *On the theory of identical particles*, Nuovo Cim. B **37**, 1–23 (1977).

[46] J. A. Hertz, *Quantum critical phenomena*, Phys. Rev. B **14**, 1165 (1976).

[47] E. Lieb, T. Schultz and D. Mattis, *Two soluble models of an antiferromagnetic chain*, Ann. Phys. (N.Y.) **16**, 407 (1961).

[48] S. Katsura, *Statistical mechanics of the anisotropic linear Heisenberg model*, Phys. Rev. **127**, 1508 (1962).

[49] P. Pfeuty, *The one-dimensional Ising model with a transverse field*, Annals of Physics **57**, 79 (1970).

[50] L. Onsager, *Crystal statistics. I. A two-dimensional model with an order-disorder transition*, Phys. Rev. **65**, 117 (1944).

[51] J. B. Zuber and C. Itzykson, *Quantum field theory and the two-dimensional Ising model*, Phys. Rev. D **15**, 2875 (1977).

[52] E. Majorana, *Teoria simmetrica dell'elettrone e del positrone*, Il Nuovo Cim. **14**, 171 (1937).

[53] A. Y. Kitaev, *Unpaired Majorana fermions in quantum wires*, Phys.-Usp. **44**, 131 (2001).

[54] L. P. Kadanoff, *Scaling laws for Ising models near T_C*, Physics **2**, 263 (1966).

[55] K. G. Wilson, *The renormalization group: Critical phenomena and the Kondo problem*, Rev. Mod. Phys. **47**, 773 (1975).

[56] D. Sénéchal, *An introduction to bosonization*, in *Theoretical Methods for Strongly Correlated Electrons*, D. Sénéchal, A.-M. Tremblay and C. Bourbonnais, eds., CRM Series in Mathematical Physics, p. 139. Springer, New York, 2004. [arXiv:cond-mat/9908262].

[57] M. Henkel, *Conformal Invariance and Critical Phenomena*. Springer-Verlag, Berlin, 1999.

[58] D. C. Mattis and E. H. Lieb, *Exact solution of a many-fermion system and its associated boson field*, J. Math. Phys. **6**, 304 (1965).

[59] A. Luther and I. Peschel, *Calculation of critical exponents in two dimensions from quantum field theory in one dimension*, Phys. Rev. B **12**, 3908 (1975).

[60] A. Belavin, A. Polyakov and A. Zamolodchikov, *Infinite conformal symmetry in two-dimensional quantum field theory*, Nucl. Phys. B **241**, 333 (1984).

[61] A. Luther, *Tomonaga fermions and the Dirac equation in three dimensions*, Phys. Rev. B **19**, 320 (1979).

[62] P. Kopietz, *Bosonization of Interacting Fermions in Arbitrary Dimensions*. Springer, New York, 1996.

[63] J. de Woul and E. Langmann, *Fermions in two dimensions, bosonization, and exactly solvable models*, Int. J. Mod. Phys. B **26**, 1244005 (2012).

[64] P. A. M. Dirac, *The quantum theory of the electron*, Proc. R. Soc. Lond. A **117**, 610 (1928).

[65] M. Malard, *Sine-Gordon model: Renormalization group solution and applications*, Braz. J. Phys. 1 (2013).

[66] G. Moore and N. Read, *Nonabelions in the fractional quantum Hall effect*, Nucl. Phys. B **360**, 362 (1991).

[67] E. Ardonne, P. Fendley and E. Fradkin, *Topological order and conformal quantum critical points*, Ann. Phys. **310**, 493 (2004).

[68] I. Affleck, *Conformal field theory approach to the Kondo effect*, Acta Phys. Pol. **26**, 1869 (1995).

[69] H. Saleur, *Lectures on Non Perturbative Field Theory and Quantum Impurity Problems*, arXiv:cond-mat/9812110, arXiv:cond-mat/0007309.

[70] J. L. Cardy, *Conformal invariance and universality in finite-size scaling*, J. Phys. A: Math. Gen. **17**, L385 (1984).

[71] H. W. J. Blöte, J. L. Cardy and M. P. Nightingale, *Conformal invariance, the central charge, and universal finite-size amplitudes at criticality*, Phys. Rev. Lett. **56**, 742 (1986).

[72] J. L. Cardy, *Conformal invariance and surface critical behavior*, Nucl. Phys. B **240**, 514 (1984).

[73] J. L. Cardy, *Boundary conditions, fusion rules and the Verlinde formula*, Nucl. Phys. B **324**, 581 (1989).

[74] J. L. Cardy, *Boundary conformal field theory*, in "Encyclopedia of Mathematical Physics". (Elsevier, Amsterdam, 2006). [arXiv:hep-th/0411189] .

[75] I. Affleck and A. W. W. Ludwig, *Universal noninteger "ground-state degeneracy" in critical quantum systems*, Phys. Rev. Lett. **67**, 161 (1991).

[76] W. J. de Haas, J. de Boer and G. J. van den Berg, *The electrical resistance of gold, copper and lead at low temperatures*, Physica **1**, 1115 (1934).

[77] J. Kondo, *Resistance minimum in dilute magnetic alloys*, Prog. Theor. Phys. **32**, 37 (1964).

[78] P. W. Anderson, *A poor man's derivation of scaling laws for the Kondo problem*, J. Phys. C **3**, 2436 (1970).

[79] P. Nozières, *A "Fermi-liquid" description of the Kondo problem at low temperatures*, J. Low Temp. Phys. **17**, 31 (1974).

[80] N. Andrei, *Diagonalization of the Kondo Hamiltonian*, Phys. Rev. Lett. **45**, 379 (1980).

[81] P. B. Wiegmann, *Exact solution of s-d exchange model at $T = 0$*, Sov. Phys. JETP Lett. **31**, 392 (1980).

[82] N. Andrei, K. Furuya and J. H. Lowenstein, *Solution of the Kondo problem*, Rev. Mod. Phys. **55**, 331 (1983).

[83] P. Nozières and A. Blandin, *Kondo effect in real metals*, J. Phys. **41**, 193 (1980).

[84] N. Andrei and C. Destri, *Solution of the multichannel Kondo problem*, Phys. Rev. Lett. **52**, 364 (1984). Erratum *ibid.* **59**, 155 (1987).

[85] A. M. Tsvelick and P. B. Wiegmann, *Solution of the n-channel kondo problem (scaling and integrability)*, Z. Phys. B **54**, 201 (1984).

[86] I. Affleck, *A current algebra approach to the Kondo effect*, Nucl. Phys. B **336**, 517 (1990).

[87] A. M. Tsvelick, *The transport properties of magnetic alloys with multi-channel Kondo impurities*, J. Phys.: Cond. Mat. **2**, 2833 (1990).

[88] I. Affleck and A. W. W. Ludwig, *The Kondo effect, conformal field theory and fusion rules*, Nucl. Phys. B **352**, 849 (1991).

[89] I. Affleck and A. W. W. Ludwig, *Critical theory of overscreened Kondo fixed points*, Nucl. Phys. B **360**, 641 (1991).

[90] S. Doniach, *The Kondo lattice and weak antiferromagnetism*, Physica B **91**, 231 (1977).

[91] D. Goldhaber-Gordon, H. Shtrikman, D. Mahalu, D. Abusch-Magder, U. Meirav and M. A. Kastner, *Kondo effect in a single-electron transistor*, Nature **391**, 156 (1998).

[92] P. Sodano, A. Bayat and S. Bose, *Kondo cloud mediated long-range entanglement after local quench in a spin chain*, Phys. Rev. B **81**, 100412 (2010).

[93] A. Bayat, S. Bose and P. Sodano, *Entanglement routers using macroscopic singlets*, Phys. Rev. Lett. **105**, 187204 (2010).

[94] A. J. Leggett, S. Chakravarty, A. T. Dorsey, M. P. A. Fisher, A. Garg and W. Zwerger, *Dynamics of the dissipative two-state system*, Rev. Mod. Phys. **59**, 1 (1987).

[95] I. Affleck, *The Kondo Screening Cloud*, chapter of the book "Strongly Correlated Fermions And Bosons In Low-Dimensional Disordered Systems", edited by I. V. Lerner, B. L. Althsuler, V. I. Falko and T. Giamarchi (Kluwer Academic Publishers, 2002).

[96] I. Affleck, *The Kondo screening cloud: what it is and how to observe it*, arXiv:0911.2209.

[97] P. Fröjdh and H. Johannesson, *Magnetic impurity in a Luttinger liquid: A conformal field theory approach*, Phys. Rev. B **53**, 3211 (1996).

[98] C. Jayaprakash, H. R. Krishna-murthy and J. W. Wilkins, *Two-impurity Kondo problem*, Phys. Rev. Lett. **47**, 737 (1981).

[99] M. A. Ruderman and C. Kittel, *Indirect exchange coupling of nuclear magnetic moments by conduction electrons*, Phys. Rev. **96**, 99 (1954).

[100] T. Kasuya, *A theory of metallic ferro- and antiferromagnetism on Zener's model*, Prog. Theor. Phys. **16**, 45 (1956).

[101] K. Yosida, *Magnetic properties of Cu-Mn alloys*, Phys. Rev. **106**, 893 (1957).

[102] I. Affleck, A. W. W. Ludwig and B. A. Jones, *Conformal-field-theory approach to the two-impurity Kondo problem: Comparison with numerical renormalization-group results*, Phys. Rev. B **52**, 9528 (1995).

[103] D.-H. Lee and J. Toner, *Kondo effect in a Luttinger liquid*, Phys. Rev. Lett. **69**, 3378 (1992).

[104] A. Furusaki, *Kondo Problems in Tomonaga-Luttinger Liquids*, J. Phys. Soc. Jpn. **74**, 73 (2005).

[105] A. Furusaki and N. Nagaosa, *Kondo effect in a Tomonaga-Luttinger liquid*, Phys. Rev. Lett. **72**, 892 (1994).

[106] P. Fröjdh and H. Johannesson, *Kondo effect in a Luttinger liquid: Exact results from conformal field theory*, Phys. Rev. Lett. **75**, 300 (1995).

[107] A. Schiller and K. Ingersent, *Exact results for the Kondo effect in a Luttinger liquid*, Phys. Rev. B **51**, 4676 (1995).

[108] P. Phillips and N. Sandler, *Enhanced local moment formation in a chiral Luttinger liquid*, Phys. Rev. B **53**, R468 (1996).

[109] M. König, S. Wiedmann, C. Brüne, A. Roth, H. Buhmann, L. W. Molenkamp, X.-L. Qi and S.-C. Zhang, *Quantum spin Hall insulator state in HgTe quantum wells*, Science **318**, 766 (2007).

[110] C. Wu, B. A. Bernevig and S.-C. Zhang, *Helical liquid and the edge of quantum spin Hall systems*, Phys. Rev. Lett. **96**, 106401 (2006).

[111] J. Maciejko, C. Liu, Y. Oreg, X.-L. Qi, C. Wu and S.-C. Zhang, *Kondo effect in the helical edge liquid of the quantum spin Hall state*, Phys. Rev. Lett. **102**, 256803 (2009).

[112] Y. Tanaka, A. Furusaki and K. A. Matveev, *Conductance of a helical edge liquid coupled to a magnetic impurity*, Phys. Rev. Lett. **106**, 236402 (2011).

[113] J. Maciejko, *Kondo lattice on the edge of a two-dimensional topological insulator*, Phys. Rev. B **85**, 245108 (2012).

[114] T. Posske, C.-X. Liu, J. C. Budich and B. Trauzettel, *Exact results for the Kondo screening cloud of two helical liquids*, Phys. Rev. Lett. **110**, 016602 (2013).

[115] A. Einstein, B. Podolsky and N. Rosen, *Can quantum-mechanical description of physical reality be considered complete?*, Phys. Rev. **47**, 777 (1935).

[116] E. Schrödinger, *Die gegenwärtige Situation in der Quantenmechanik*, Naturwiss. **23**, 807 (1935).

[117] E. Schrödinger, *Discussion of probability relations between separated systems*, Math. Proc. Cambr. Phil. Soc. **31**, 555 (1935).

[118] G. Jaeger, *Entanglement, Information, and the Interpretation of Quantum Mechanics*. Springer-Verlag, Berlin, 2009.

[119] M. Nielsen and I. Chuang, *Quantum Computation and Quantum Information*. Cambridge University Press, Cambridge, 2000.

[120] C. Holzhey, F. Larsen and F. Wilczek, *Geometric and renormalized entropy in conformal field theory*, Nucl. Phys. B **424**, 443 (1994).

[121] M. Sarovar, A. Ishizaki, G. R. Fleming and K. B. Whaley, *Quantum entanglement in photosynthetic light-harvesting complexes*, Nature Phys. **6**, 462 (2010).

[122] A. Osterloh, L. Amico, G. Falci and R. Fazio, *Scaling of entanglement close to a quantum phase transition*, Nature **416**, 608 (2002).

[123] T. J. Osborne and M. A. Nielsen, *Entanglement in a simple quantum phase transition*, Phys. Rev. A **66**, 032110 (2002).

[124] G. Vidal, J. I. Latorre, E. Rico and A. Kitaev, *Entanglement in quantum critical phenomena*, Phys. Rev. Lett. **90**, 227902 (2003).

[125] V. E. Korepin, *Universality of entropy scaling in one dimensional gapless models*, Phys. Rev. Lett. **92**, 096402 (2004).

[126] P. Calabrese and J. Cardy, *Entanglement entropy and quantum field theory*, J. Stat. Mech. P06002 (2004).

[127] P. Calabrese and J. Cardy, *Entanglement entropy and conformal field theory*, J. Phys. A: Math. Theor. **42**, 504005 (2009).

[128] L.-A. Wu, M. S. Sarandy and D. A. Lidar, *Quantum phase transitions and bipartite entanglement*, Phys. Rev. Lett. **93**, 250404 (2004).

[129] S.-J. Gu, S.-S. Deng, Y.-Q. Li and H.-Q. Lin, *Entanglement and quantum phase transition in the extended Hubbard model*, Phys. Rev. Lett. **93**, 086402 (2004).

[130] D. Larsson and H. Johannesson, *Entanglement scaling in the one-dimensional Hubbard model at criticality*, Phys. Rev. Lett. **95**, 196406 (2005).

[131] T.-C. Wei, D. Das, S. Mukhopadyay, S. Vishveshwara and P. M. Goldbart, *Global entanglement and quantum criticality in spin chains*, Phys. Rev. A **71**, 060305 (2005).

[132] H.-Q. Zhou, T. Barthel, J. O. Fjærestad and U. Schollwöck, *Entanglement and boundary critical phenomena*, Phys. Rev. A **74**, 050305(R) (2006).

[133] E. Fradkin and J. E. Moore, *Entanglement entropy of 2d conformal quantum critical points: Hearing the shape of a quantum drum*, Phys. Rev. Lett. **97**, 050404 (2006).

[134] K. Le Hur, P. Doucet-Beaupré and W. Hofstetter, *Entanglement and criticality in quantum impurity systems*, Phys. Rev. Lett. **99**, 126801 (2007).

[135] A. Kitaev and J. Preskill, *Topological entanglement entropy*, Phys. Rev. Lett. **96**, 110404 (2006).

[136] M. Levin and X.-G. Wen, *Detecting topological order in a ground state wave function*, Phys. Rev. Lett. **96**, 110405 (2006).

[137] H. Li and F. D. M. Haldane, *Entanglement spectrum as a generalization of entanglement entropy: Identification of topological order in non-Abelian fractional quantum Hall effect states*, Phys. Rev. Lett. **101**, 010504 (2008).

[138] F. Verstraete, J. I. Cirac and V. Murg, *Matrix product states, projected entangled pair states, and variational renormalization group methods for quantum spin systems*, Adv. Phys. **57**, 143 (2008).

[139] R. Augusiak, F. M. Cucchietti and M. Lewenstein, *Many-body physics from a quantum information perspective*, in *Modern Theories of Many-Particle Systems in Condensed Matter Physics*, D. C. Cabra, A. Honecker and P. Pujol, eds., vol. 843 of *Lecture Notes in Physics*, pp. 245–294. Springer Berlin Heidelberg, 2012. [arXiv:1003.3153].

[140] I. Klich and L. Levitov, *Quantum noise as an entanglement meter*, Phys. Rev. Lett. **102**, 012405 (2010).

[141] H. F. Song, S. Rachel and K. Le Hur, *General relation between entanglement and fluctuations in one dimension*, Phys. Rev. B **82**, 012405 (2010).

[142] M. Cramer, M. B. Plenio and H. Wunderlich, *Measuring entanglement in condensed matter systems*, Phys. Rev. Lett. **106**, 020401 (2011).

[143] J. Cardy, *Measuring entanglement using quantum quenches*, Phys. Rev. Lett. **106**, 150404 (2011).

[144] D. A. Abanin and E. Demler, *Measuring entanglement entropy of a generic many-body system with a quantum switch*, Phys. Rev. Lett. **109**, 020504 (2012).

[145] L. Amico, R. Fazio, A. Osterloh and V. Vedral, *Entanglement in many-body systems*, Rev. Mod. Phys. **80**, 517 (2008).

[146] R. Horodecki, P. Horodecki, M. Horodecki and K. Horodecki, *Quantum entanglement*, Rev. Mod. Phys. **81**, 865 (2009).

[147] J. S. Bell, *On the Einstein Podolsky Rosen paradox*, Physics **1**, 195 (1964).

[148] S. J. Freedman and J. F. Clauser, *Experimental test of local hidden-variable theories*, Phys. Rev. Lett. **28**, 938 (1972).

[149] A. Aspect, P. Grangier and G. Roger, *Experimental realization of Einstein-Podolsky-Rosen-Bohm Gedankenexperiment: A new violation of Bell's inequalities*, Phys. Rev. Lett. **49**, 91 (1982).

[150] G. Weihs, T. Jennewein, C. Simon, H. Weinfurter and A. Zeilinger, *Violation of Bell's inequality under strict Einstein locality conditions*, Phys. Rev. Lett. **81**, 5039 (1998).

[151] R. F. Werner, *Quantum states with Einstein-Podolsky-Rosen correlations admitting a hidden-variable model*, Phys. Rev. A **40**, 4277 (1989).

[152] R. Horodecki and P. Horodecki, *Quantum redundancies and local realism*, Phys. Lett. A **194**, 147 (1994).

[153] G. C. Levine, *Entanglement entropy in a boundary impurity model*, Phys. Rev. Lett. **93**, 266402 (2004).

[154] I. Peschel, *Entanglement entropy with interface defects*, J. Phys. A: Math. Gen. **38**, 4327 (2005).

[155] J. Zhao, I. Peschel and X. Wang, *Critical entanglement of XXZ Heisenberg chains with defects*, Phys. Rev. B **73**, 024417 (2006).

[156] J. Ren, S. Zhu and X. Hao, *Entanglement entropy in an antiferromagnetic Heisenberg spin chain with boundary impurities*, J. Phys. B **42**, 015504 (2009).

[157] E. S. Sørensen, M.-S. Chang, N. Laflorencie and I. Affleck, *Impurity entanglement entropy and the Kondo screening cloud*, J. Stat. Mech. L01001 (2007).

[158] E. S. Sørensen, M.-S. Chang, N. Laflorencie and I. Affleck, *Quantum impurity entanglement*, J. Stat. Mech. P08003 (2007).

[159] I. Affleck, N. Laflorencie and E. S. Sørensen, *Entanglement entropy in quantum impurity systems and systems with boundaries*, J. Phys. A: Math. Theor. **42**, 504009 (2009).

[160] D. J. Thouless, M. Kohmoto, M. P. Nightingale and M. den Nijs, *Quantized Hall conductance in a two-dimensional periodic potential*, Phys. Rev. Lett. **49**, 405 (1982).

[161] D. J. Thouless, *Topological Quantum Numbers in Nonrelativistic Physics*. World Scientific, Singapore, 1998.

[162] E. Witten, *Topological quantum field theory*, Comm. Math. Phys. **117**, 353 (1988).

[163] K. von Klitzing, G. Dorda and M. Pepper, *New method for high-accuracy determination of the fine-structure constant based on quantized Hall resistance*, Phys. Rev. Lett. **45**, 494 (1980).

[164] F. Haldane, *Continuum dynamics of the 1-D Heisenberg antiferromagnet: Identification with the O(3) nonlinear sigma model*, Phys. Lett. A **93**, 464 (1983).

[165] F. D. M. Haldane, *Nonlinear field theory of large-spin Heisenberg antiferromagnets: semiclassically quantized solitons of the one-dimensional easy-axis Néel state*, Phys. Rev. Lett. **50**, 1153 (1983).

[166] I. Affleck, T. Kennedy, E. H. Lieb and H. Tasaki, *Rigorous results on valence-bond ground states in antiferromagnets*, Phys. Rev. Lett. **59**, 799 (1987).

[167] X.-L. Qi and S.-C. Zhang, *Topological insulators and superconductors*, Rev. Mod. Phys. **83**, 1057 (2011).

[168] B. Normand, *Frontiers in frustrated magnetism*, Contemp. Phys. **50**, 533 (2009).

[169] H.-C. Jiang, Z. Wang and L. Balents, *Identifying topological order by entanglement entropy*, Nat. Phys. **8**, 902 (2012).

[170] Z.-C. Gu and X.-G. Wen, *Tensor-entanglement-filtering renormalization approach and symmetry-protected topological order*, Phys. Rev. B **80**, 155131 (2009).

[171] I. Affleck and F. D. M. Haldane, *Critical theory of quantum spin chains*, Phys. Rev. B **5291**, 36 (1987).

[172] P. Fendley, *Parafermionic edge zero modes in Z_n-invariant spin chains*, J. Stat. Mech. **2012**, P11020 (2012).

[173] X. G. Wen and Q. Niu, *Ground-state degeneracy of the fractional quantum hall states in the presence of a random potential and on high-genus Riemann surfaces*, Phys. Rev. B **41**, 9377 (1990).

[174] C. Nayak, S. H. Simon, A. Stern, M. Freedman and S. Das Sarma, *Non-abelian anyons and topological quantum computation*, Rev. Mod. Phys. **80**, 1083 (2008).

[175] T. Einarsson, *Fractional statistics on a torus*, Phys. Rev. Lett. **64**, 1995 (1990).

[176] A. Y. Kitaev, *Fault-tolerant quantum computation by anyons*, Ann. Phys. (N.Y.) **303**, 2 (2003).

[177] B. Douçot, L. B. Ioffe and J. Vidal, *Discrete non-Abelian gauge theories in Josephson-junction arrays and quantum computation*, Phys. Rev. B **69**, 214501 (2004).

[178] A. Micheli, G. K. Brennen and P. Zoller, *A toolbox for lattice-spin models with polar molecules*, Nature Phys. **2**, 341 (2006).

[179] M. Lewenstein, A. Sanpera, V. Ahufinger, B. Damski, A. Sen(De) and U. Sen, *Ultracold atomic gases in optical lattices: mimicking condensed matter physics and beyond*, Adv. Phys. **56**, 243 (2007).

[180] S.-J. Gu, *Fidelity approach to quantum phase transitions*, Int. J. Mod. Phys. B **24**, 4371 (2010).

[181] C. Castelnovo and C. Chamon, *Quantum topological phase transition at the microscopic level*, Phys. Rev. B **77**, 054433 (2008).

[182] X.-G. Wen, *Quantum orders in an exact soluble model*, Phys. Rev. Lett. **90**, 016803 (2003).

[183] J. Yu, S.-P. Kou and X.-G. Wen, *Topological quantum phase transition in the transverse wen-plaquette model*, EPL **84**, 17004 (2008).

[184] M. König, H. Buhmann, L. W. Molenkamp, T. Hughes, C.-X. Liu, X.-L. Qi and S.-C. Zhang, *The quantum spin Hall effect: Theory and experiment*, J. Phys. Soc. Jpn. **77**, 031007 (2008).

[185] M. Z. Hasan and C. L. Kane, *Colloquium: Topological insulators*, Rev. Mod. Phys. **82**, 3045 (2010).

[186] J. Maciejko, T. L. Hughes and S.-C. Zhang, *The quantum spin Hall effect*, Ann. Rev. Cond. Mat. Phys. **2**, 31 (2011).

[187] B. A. Bernevig and T. L. Hughes, *Topological Insulators and Topological Superconductors*. Princeton University Press, Princeton, 2013.

[188] F. D. M. Haldane, *Model for a quantum Hall effect without Landau levels: Condensed-matter realization of the "parity anomaly"*, Phys. Rev. Lett. **61**, 2015 (1988).

[189] C. L. Kane and E. J. Mele, *Quantum spin Hall effect in graphene*, Phys. Rev. Lett. **95**, 226801 (2005).

[190] C. L. Kane and E. J. Mele, *Z_2 topological order and the quantum spin Hall effect*, Phys. Rev. Lett. **95**, 146802 (2005).

[191] B. A. Bernevig, T. L. Hughes and S.-C. Zhang, *Quantum spin Hall effect and topological phase transition in HgTe quantum wells*, Science **314**, 1757 (2006).

[192] L. Fu, C. L. Kane and E. J. Mele, *Topological insulators in three dimensions*, Phys. Rev. Lett. **98**, 106803 (2007).

[193] J. E. Moore and L. Balents, *Topological invariants of time-reversal-invariant band structures*, Phys. Rev. B **75**, 121306 (2007).

[194] L. Fu and C. L. Kane, *Topological insulators with inversion symmetry*, Phys. Rev. B **76**, 045302 (2007).

[195] D. Hsieh, D. Qian, L. Wray, Y. Xia, Y. S. Hor, R. J. Cava and M. Z. Hasan, *A topological Dirac insulator in a quantum spin Hall phase*, Nature **452**, 970 (2008).

[196] D. Hsieh, Y. Xia, D. Qian, L. Wray, J. H. Dil, F. Meier, J. Osterwalder, L. Patthey, J. G. Checkelsky, N. P. Ong, A. V. Fedorov, H. Lin, A. Bansil, D. Grauer, Y. S. Hor, R. J. Cava and M. Z. Hasan, *A tunable topological insulator in the spin helical Dirac transport regime*, Nature **460**, 1101 (2009).

[197] D. Kong, J. C. Randel, H. Peng, J. J. Cha, S. Meister, K. Lai, Y. Chen, Z.-X. Shen, H. C. Manoharan and Y. Cui, *Topological insulator nanowires and nanoribbons*, Nano Letters **10**, 329 (2010).

[198] B. A. Bernevig and S.-C. Zhang, *Toward dissipationless spin transport in semiconductors*, IBM J. Res. Dev. **50**, 141 (2006).

[199] L. Fu and C. L. Kane, *Superconducting proximity effect and Majorana fermions at the surface of a topological insulator*, Phys. Rev. Lett. **100**, 096407 (2008).

[200] J. Alicea, *New directions in the pursuit of Majorana fermions in solid state systems*, Rep. Prog. Phys. **75**, 076501 (2012).

[201] B. I. Halperin, *Quantized Hall conductance, current-carrying edge states, and the existence of extended states in a two-dimensional disordered potential*, Phys. Rev. B **25**, 2185 (1982).

[202] Y. Hatsugai, *Chern number and edge states in the integer quantum Hall effect*, Phys. Rev. Lett. **71**, 3697 (1993).

[203] A. Messiah, *Quantum Mechanics*. Dover Publications, Mineola, 1999.

[204] H. A. Kramers, *Theorie générale de la rotation paramagnetique dans les cristaux*, Proc. Acad. Sci. Amsterdam **33**, 959 (1930).

[205] A. Altland and M. R. Zirnbauer, *Nonstandard symmetry classes in mesoscopic normal-superconducting hybrid structures*, Phys. Rev. B **55**, 1142 (1997).

[206] A. P. Schnyder, S. Ryu, A. Furusaki and A. W. W. Ludwig, *Classification of topological insulators and superconductors*, AIP Conf. Proc. **1134**, 10 (2009).

[207] A. Kitaev, *Periodic table for topological insulators and superconductors*, AIP Conf. Proc. **1134**, 22 (2009).

[208] R. B. Laughlin, *Anomalous quantum Hall effect: An incompressible quantum fluid with fractionally charged excitations*, Phys. Rev. Lett. **50**, 1395 (1983).

[209] M. Hohenadler and F. F. Assaad, *Correlation effects in two-dimensional topological insulators*, J. Phys.: Condens. Matter **25**, 143201 (2013).

[210] C. Xu and J. E. Moore, *Stability of the quantum spin Hall effect: Effects of interactions, disorder, and $\mathbb{Z}_2$ topology*, Phys. Rev. B **73**, 045322 (2006).

[211] C. L. Kane and M. P. A. Fisher, *Transmission through barriers and resonant tunneling in an interacting one-dimensional electron gas*, Phys. Rev. B **46**, 15233 (1992).

[212] E. H. Lieb and W. Liniger, *Exact analysis of an interacting Bose gas. I. The general solution and the ground state*, Phys. Rev. **130**, 1605–1616 (1963).

[213] E. H. Lieb, *Exact analysis of an interacting Bose gas. II. The excitation spectrum*, Phys. Rev. **130**, 1616 (1963).

[214] E. H. Lieb and F. Y. Wu, *Absence of Mott transition in an exact solution of the short-range, one-band model in one dimension*, Phys. Rev. Lett. **20**, 1445 (1968).

[215] H. Bergknoff and H. B. Thacker, *Structure and solution of the massive Thirring model*, Phys. Rev. D **19**, 3666 (1979).

[216] V. Korepin, *Direct calculation of the S matrix in the massive Thirring model*, Theor. Math. Phys. **41**, 953 (1979).

[217] P. Wiegmann, *Towards an exact solution of the Anderson model*, Phys. Lett. A **80**, 163 (1980).

[218] C. N. Yang, *Some exact results for the many-body problem in one dimension with repulsive delta-function interaction*, Phys. Rev. Lett. **19**, 1312 (1967).

[219] R. J. Baxter, *Partition function of the eight-vertex lattice model*, Ann. Phys. **70**, 193 (1972).

[220] V. E. Korepin, N. M. Bogoliubov and A. G. Izergin, *Quantum Inverse Scattering Method and Correlation Functions*. Cambridge University Press, Cambridge, 1993.

[221] C. N. Yang and C. P. Yang, *Thermodynamics of a one-dimensional system of Bosons with repulsive delta-function interaction*, J. Math. Phys. **10**, 1115 (1969).

[222] A. Polkovnikov, K. Sengupta, A. Silva and M. Vengalattore, *Nonequilibrium dynamics of closed interacting quantum systems*, Rev. Mod. Phys. **83**, 863 (2011).

[223] T. Dorlas, *Orthogonality and completeness of the Bethe Ansatz eigenstates of the nonlinear Schrödinger model*, Comm. Math. Phys. **154**, 347 (1993).

[224] M. Gaudin, *La Fonction d'Onde de Bethe*. Masson, Paris, 1983.

[225] B. Davies and V. E. Korepin, *Higher conservation laws for the quantum non-linear Schrödinger equation* Report No. CMA-R33-89, Centre for Mathematical Analysis, Australian National University, Canberra, 1989. [arXiv:1109.6604].

[226] F. Haldane, *Demonstration of the "Luttinger liquid" character of Bethe-ansatz-soluble models of 1-D quantum fluids*, Phys. Lett. A **81**, 153 (1981).

[227] F. D. M. Haldane, *Effective harmonic-fluid approach to low-energy properties of one-dimensional quantum fluids*, Phys. Rev. Lett. **47**, 1840 (1981).

[228] T. Dorlas, J. Lewis and J. Pulé, *The Yang-Yang thermodynamic formalism and large deviations*, Comm. Math. Phys. **124**, 365 (1989).

[229] A. H. van Amerongen, J. J. P. van Es, P. Wicke, K. V. Kheruntsyan and N. J. van Druten, *Yang-Yang thermodynamics on an atom chip*, Phys. Rev. Lett. **100**, 090402 (2008).

[230] S. Weigert, *The problem of quantum integrability*, Physica D **56**, 107 (1992).

[231] L. D. Faddeev, *What is complete integrability in quantum mechanics*, Proc. Symp. Henri Poincaré (Brussels, Oct. 2004) .

[232] J.-S. Caux and J. Mossel, *Remarks on the notion of quantum integrability*, J. Stat. Mech. **2011**, P02023 (2011).

[233] J. Larson, *Integrability vs quantum thermalization*, arXiv:1304.3585.

[234] S. Coleman and J. Mandula, *All possible symmetries of the S matrix*, Phys. Rev. **159**, 1251 (1967).

[235] R. Shankar and E. Witten, *S matrix of the supersymmetric nonlinear σ model*, Phys. Rev. D **17**, 2134 (1978).

[236] J. B. McGuire, *Study of exactly soluble one-dimensional N-body problems*, J. Math. Phys. **5**, 622 (1964).

[237] L. H. Kauffman and S. J. Lomonaco, *Braiding operators are universal quantum gates*, New J. Phys. **6**, 134 (2004).

[238] M. Jimbo, ed., *Yang-Baxter Equation in Integrable Systems.* World Scientific, Singapore, 1990.

[239] J. von Neumann, *Beweis des Ergodensatzes und des H-Theorems in der neuen Mechanik.*, Z. Phys. **57**, 30 (1929). Eng. transl.: Eur. Phys. J. H **35**, 201 (2010).

[240] J. M. Deutsch, *Quantum statistical mechanics in a closed system*, Phys. Rev. A **43**, 2046 (1991).

[241] M. Srednicki, *Chaos and quantum thermalization*, Phys. Rev. E **50**, 888 (1994).

[242] M. Rigol, V. Dunjko and M. Olshanii, *Thermalization and its mechanism for generic isolated quantum systems*, Nature **481**, 224 (2012).

[243] S. Goldstein, J. L. Lebowitz, R. Tumulka and N. Zanghì, *Long-time behavior of macroscopic quantum systems*, Eur. Phys. J. H **35**, 173 (2010).

[244] L. E. Reichl, *A Modern Course in Statistical Physics.* Wiley, New York, 1998.

[245] E. Schrödinger, *Statistical Thermodynamics.* Cambridge University Press, Cambridge, 1948.

[246] E. T. Jaynes, *Information theory and statistical mechanics*, Phys. Rev. **106**, 620 (1957).

[247] E. Barouch, B. M. McCoy and M. Dresden, *Statistical Mechanics of the XY Model. I*, Phys. Rev. A **2**, 1075 (1970).

[248] P. Calabrese and J. Cardy, *Quantum quenches in extended systems*, J. Stat. Mech. **2007**, P06008 (2007).

[249] P. Calabrese, F. H. L. Essler and M. Fagotti, *Quantum quench in the transverse field Ising chain: I. Time evolution of order parameter correlators*, J. Stat. Mech. **2012**, P07016 (2012).

[250] P. Calabrese, F. H. L. Essler and M. Fagotti, *Quantum quenches in the transverse field Ising chain: II. Stationary state properties*, J. Stat. Mech. **2012**, P07022 (2012).

[251] I. Bloch, J. Dalibard and W. Zwerger, *Many-body physics with ultracold gases*, Rev. Mod. Phys. **80**, 885 (2008).

[252] T. Kinoshita, T. Wenger and D. S. Weiss, *A quantum Newton's cradle*, Nature **440**, 900 (2006).

[253] M. Rigol, V. Dunjko, V. Yurovsky and M. Olshanii, *Relaxation in a completely integrable many-body quantum system: An ab initio study of the dynamics of the highly excited states of 1d lattice hard-core bosons*, Phys. Rev. Lett. **98**, 050405 (2007).

[254] M. Olshanii, *Geometry of quantum observables and thermodynamics of small systems*, arXiv:1208.0582.

[255] M. Fagotti, *Finite-size corrections versus relaxation after a sudden quench*, Phys. Rev. B **87**, 165106 (2013).

[256] A. Uhlmann, *The "transition probability" in the state space of a $*$-algebra*, Rep. Math. Phys. **9**, 273 (1976).

[257] W.-L. You, Y.-W. Li and S.-J. Gu, *Fidelity, dynamic structure factor, and susceptibility in critical phenomena*, Phys. Rev. E **76**, 022101 (2007).

[258] H.-N. Xiong, J. Ma, Y. Wang and X. Wang, *Reduced fidelity and quantum phase transitions in spin-1/2 frustrated Heisenberg chains*, J. Phys. A: Math. Theor. **42**, 065304 (2009).

[259] R. Jozsa, *Fidelity for mixed quantum states*, J. Mod. Opt. **41**, 2315 (1994).

[260] D. F. Abasto, A. Hamma and P. Zanardi, *Fidelity analysis of topological quantum phase transitions*, Phys. Rev. A **78**, 010301 (2008).

[261] X.-Y. Feng, G.-M. Zhang and T. Xiang, *Topological characterization of quantum phase transitions in a spin-*1/2 *model*, Phys. Rev. Lett. **98**, 087204 (2007).

[262] H.-Q. Zhou, R. Orús and G. Vidal, *Ground state fidelity from tensor network representations*, Phys. Rev. Lett. **100**, 080601 (2008).

[263] S. Trebst, P. Werner, M. Troyer, K. Shtengel and C. Nayak, *Breakdown of a topological phase: Quantum phase transition in a loop gas model with tension*, Phys. Rev. Lett. **98**, 070602 (2007).

[264] B. Swingle and T. Senthil, *Universal crossovers between entanglement entropy and thermal entropy*, Phys. Rev. B **87**, 045123 (2013).

[265] R. Winkler, *Spin-Orbit Interaction Effects in Two-Dimensional Electron and Hole Systems*. Springer-Verlag, Berlin, 2003.

[266] J. I. Väyrynen and T. Ojanen, *Electrical manipulation and measurement of spin properties of quantum spin hall edge states*, Phys. Rev. Lett. **106**, 076803 (2011).

[267] A. Ström, *Interaction and Disorder in Helical Conductors*, PhD thesis, University of Gothenburg, 2012.

[268] J. Mossel and J.-S. Caux, *Generalized TBA and generalized Gibbs*, J. Phys. A: Math. Theor. **45**, 255001 (2012).

[269] A. J. Leggett, *What DO we know about high Tc?*, Nat. Phys. **2**, 134 (2006).

[270] D. C. Johnston, *The puzzle of high temperature superconductivity in layered iron pnictides and chalcogenides*, Adv. Phys. **59**, 803 (2010).

[271] J. Bednorz and K. Müller, *Possible high-T_c superconductivity in the Ba-La-Cu-O system*, Z. Phys. B **64**, 189 (1986).

[272] S. A. Parameswaran, R. Roy and S. L. Sondhi, *Fractional quantum Hall physics in topological flat bands*, arXiv:1302.6606.

[273] S. Raghu, X.-L. Qi, C. Honerkamp and S.-C. Zhang, *Topological Mott insulators*, Phys. Rev. Lett. **100**, 156401 (2008).

[274] D. Pesin and L. Balents, *Mott physics and band topology in materials with strong spin-orbit interaction*, Nat. Phys. **6**, 376 (2010).

[275] M. Levin and A. Stern, *Fractional topological insulators*, Phys. Rev. Lett. **103**, 196803 (2009).

[276] M. Dzero, K. Sun, V. Galitski and P. Coleman, *Topological Kondo insulators*, Phys. Rev. Lett. **104**, 106408 (2010).

[277] L. Fidkowski, *Entanglement spectrum of topological insulators and superconductors*, Phys. Rev. Lett. **104**, 130502 (2010).

[278] N. Goldman, I. Satija, P. Nikolic, A. Bermudez, M. A. Martin-Delgado, M. Lewenstein and I. B. Spielman, *Realistic time-reversal invariant topological insulators with neutral atoms*, Phys. Rev. Lett. **105**, 255302 (2010).

[279] P. Calabrese, J. Cardy and E. Tonni, *Entanglement negativity in quantum field theory*, Phys. Rev. Lett. **109**, 130502 (2012).

[280] A. Bayat, P. Sodano and S. Bose, *Negativity as the entanglement measure to probe the Kondo regime in the spin-chain Kondo model*, Phys. Rev. B **81**, 064429 (2010).

[281] P. Mehta and N. Andrei, *Nonequilibrium transport in quantum impurity models: The Bethe Ansatz for open systems*, Phys. Rev. Lett. **96**, 216802 (2006).

[282] I. V. Protopopov, D. B. Gutman and A. D. Mirlin, *Many-particle correlations in a non-equilibrium Luttinger liquid*, J. Stat. Mech. **2011**, P11001 (2011).

[283] C. Karrasch, J. Rentrop, D. Schuricht and V. Meden, *Luttinger-liquid universality in the time evolution after an interaction quench*, Phys. Rev. Lett. **109**, 126406 (2012).

[284] D. Bernard and B. Doyon, *Non-equilibrium steady-states in conformal field theory*, arXiv:1302.3125.

[285] D. Iyer and N. Andrei, *Quench dynamics of the interacting Bose gas in one dimension*, Phys. Rev. Lett. **109**, 115304 (2012).

[286] D. Iyer, H. Guan and N. Andrei, *An exact formalism for quench dynamics*, arXiv:1304.0506.

[287] D. A. Abanin and D. A. Pesin, *Ordering of magnetic impurities and tunable electronic properties of topological insulators*, Phys. Rev. Lett. **106**, 136802 (2011).

[288] A. K. Mitchell, D. Schuricht, M. Vojta and L. Fritz, *Kondo effect on the surface of three-dimensional topological insulators: Signatures in scanning tunneling spectroscopy*, Phys. Rev. B **87**, 075430 (2013).

[289] L. Fritz and M. Vojta, *The physics of Kondo impurities in graphene*, Rep. Prog. Phys. **76**, 032501 (2013).

[290] V. Mourik, K. Zuo, S. M. Frolov, S. R. Plissard, E. P. A. M. Bakkers and L. P. Kouwenhoven, *Signatures of Majorana fermions in hybrid superconductor-semiconductor nanowire devices*, Science **336**, 1003 (2012).

[291] Y. Oreg, G. Refael and F. von Oppen, *Helical liquids and Majorana bound states in quantum wires*, Phys. Rev. Lett. **105**, 177002 (2010).

[292] J. Stajic, *The future of quantum information processing*, Science **339**, 1163 (2013).

[293] J. Cardy and P. Calabrese, *Unusual corrections to scaling in entanglement entropy*, J. Stat. Mech. P04023 (2010).

Paper I

Reduced fidelity in topological quantum phase transitions

Erik Eriksson and Henrik Johannesson
Phys. Rev. A **79**, 060301(R) (2009).

PHYSICAL REVIEW A **79**, 060301(R) (2009)

Reduced fidelity in topological quantum phase transitions

Erik Eriksson and Henrik Johannesson
Department of Physics, University of Gothenburg, SE 412 96 Gothenburg, Sweden
(Received 23 February 2009; published 3 June 2009)

We study the reduced fidelity between local states of lattice systems exhibiting topological order. By exploiting mappings to spin models with classical order, we are able to analytically extract the scaling behavior of the reduced fidelity at the corresponding quantum phase transitions out of the topologically ordered phases. Our results suggest that the reduced fidelity, albeit being a local measure, generically serves as an accurate marker of a topological quantum phase transition.

DOI: 10.1103/PhysRevA.79.060301 PACS number(s): 03.67.−a, 64.70.Tg, 03.65.Vf

I. INTRODUCTION

Electron correlations in condensed-matter systems sometimes produce topologically ordered phases where effects from local perturbations are exponentially suppressed [1]. The most prominent examples are the fifty or so observed fractional quantum Hall phases, with the topological order manifested in gapless edge states and excitations with fractional statistics. The fact that the ground-state degeneracy in phases with non-Abelian statistics cannot be lifted by local perturbations lies at the heart of current proposals for topological quantum computation [2].

The insensitivity to local perturbations invalidates the use of a local order parameter to identify a quantum phase transition out of a topologically ordered phase. Attempts to build a theory of topological quantum phase transitions (TQPTs)—replacing the Ginzburg-Landau symmetry-breaking paradigm—have instead borrowed concepts from quantum information theory, in particular those of *entanglement entropy* [3] and *fidelity* [4], none of which require the construction of an order parameter.

Fidelity measures the similarity between two quantum states and, for pure states, is defined as the modulus of their overlap. Since the ground state changes rapidly at a quantum phase transition, one expects that the fidelity between two ground states that differ by a small change in the driving parameter should exhibit a sharp drop. This expectation has been confirmed in a number of case studies [5], including several TQPTs [4,6,7].

Suppose that one replaces the two ground states in a fidelity analysis with two states that also differ slightly in the driving parameter, but which describe only a local region of the system of interest. The proper concept that encodes the similarity between such mixed states is that of the *reduced fidelity*, which is the maximum pure-state overlap between purifications of the mixed states [8]. It has proven useful in the analysis of a number of ordinary symmetry-breaking quantum phase transitions [9]. But since the reduced fidelity is a local property of the system, similar to that of a local order parameter, one may think that it would be less sensitive to a TQPT, which involves a global rearrangement of nonlocal quantum correlations [1]. However, this intuition turns out to be wrong. As we show in this Rapid Communication, several TQPTs are accurately signaled by a singularity in the second-order derivative of the reduced fidelity. Moreover, the singularity can be even stronger than for the (pure-state) global fidelity. The fact that a TQPT gets imprinted in a local quantity may at first seem surprising but, as we shall see, is parallel to and extends results from earlier studies [10,11].

II. FIDELITY AND FIDELITY SUSCEPTIBILITY

The fidelity $F(\beta,\beta')$ between two states described by the density matrices $\hat{\rho}(\beta)$ and $\hat{\rho}(\beta')$ is defined as [8]

$$F(\beta,\beta') = \mathrm{Tr}\sqrt{\sqrt{\hat{\rho}(\beta)}\hat{\rho}(\beta')\sqrt{\hat{\rho}(\beta)}}. \tag{1}$$

When a system is in a pure state, $\hat{\rho}(\beta)=|\Psi(\beta)\rangle\langle\Psi(\beta)|$, $F(\beta,\beta')$ becomes just the state overlap $|\langle\Psi(\beta')|\Psi(\beta)\rangle|$. When the states under consideration describe a subsystem, they will generally be mixed states, and we call the fidelity between such states *reduced fidelity*. In the limit where β and $\beta'=\beta+\delta\beta$ are very close, it is useful to define the *fidelity susceptibility* [12]

$$\chi_F = \lim_{\delta\beta\to 0} \frac{-2\ln F}{\delta\beta^2}, \tag{2}$$

consistent with the pure-state expansion $F\approx 1-\chi_F\delta\beta^2/2$.

III. CASTELNOVO-CHAMON MODEL

The first model we consider was introduced by Castelnovo and Chamon [10] and is a deformation of the Kitaev toric code model [13]. The Hamiltonian for N spin-1/2 particles on the bonds of a square lattice with periodic boundary conditions is

$$H = -\lambda_0\sum_p B_p - \lambda_1\sum_s A_s + \lambda_1\sum_s \exp\left(-\beta\sum_{i\in s}\hat{\sigma}_i^z\right), \tag{3}$$

where $A_s=\Pi_{i\in s}\hat{\sigma}_i^x$ and $B_p=\Pi_{i\in p}\hat{\sigma}_i^z$ are the star and plaquette operators of the original Kitaev toric code model. The star operator A_s acts on the spins around the vertex s and the plaquette operator B_p acts on the spins on the boundary of the plaquette p. For $\lambda_{0,1}>0$ the ground state in the topological sector containing the fully magnetized state $|0\rangle$ is given by [10]

$$|\mathrm{GS}(\beta)\rangle = \sum_{g\in G} \frac{\exp\left[\beta\sum_i \sigma_i^z(g)/2\right]}{\sqrt{Z(\beta)}} g|0\rangle \tag{4}$$

with $Z(\beta)=\Sigma_{g\in G}\exp[\beta\Sigma_i\sigma_i^z(g)]$, where G is the Abelian group generated by the star operators A_s and $\sigma_i^z(g)$ is the z

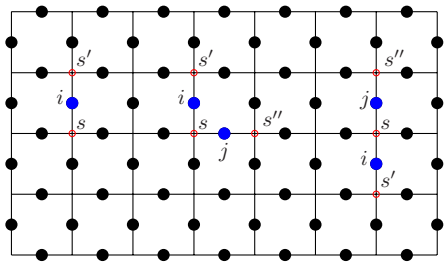

FIG. 1. (Color online) Mapping between the Castelnovo-Chamon model and the 2D Ising model. The spins of the former reside on the lattice bonds (filled black circles) and the spins of the latter on the vertices. Left: $\sigma_i^z=\theta_s\theta_{s'}$, where i is the bond between the neighboring vertices $\langle s,s'\rangle$. Middle and right: for i and j nearest (next-nearest) neighbors, the mapping gives $\langle\hat{\sigma}_i^z\hat{\sigma}_j^z\rangle=\langle\theta_s\theta_{s'}\theta_{s''}\theta_s\rangle=\langle\theta_{s'}\theta_{s''}\rangle$, where $\langle s',s''\rangle$ are next-nearest (third-nearest) neighbors.

component of the spin at site i in the state $g|0\rangle$. When $\beta=0$ the state in Eq. (4) reduces to the topologically ordered ground state of the toric code model [13]. When $\beta\to\infty$ the ground state (4) becomes the magnetically ordered state $|0\rangle$. At $\beta_c=(1/2)\ln(\sqrt{2}+1)$ there is a second-order TQPT where the topological entanglement entropy S_{topo} goes from $S_{topo}=1$ for $\beta<\beta_c$ to $S_{topo}=0$ for $\beta>\beta_c$ [10]. The global fidelity susceptibility χ_F close to β_c was obtained in Ref. [6] and found to diverge as

$$\chi_F\sim\ln|\beta_c/\beta-1|. \tag{5}$$

We here calculate the single-site reduced fidelity between the ground states of a single spin at two different parameter values β and β'. To construct the density matrix $\hat{\rho}_i$ for the spin at site i we use the expansion

$$\hat{\rho}_i=\frac{1}{2}\sum_{\mu=0}^{3}\langle\hat{\sigma}_i^\mu\rangle\hat{\sigma}_i^\mu \tag{6}$$

with $\hat{\sigma}_i^0\equiv\mathbb{1}_i$ and with the expectation values taken with respect to the ground state in Eq. (4). There is a one-to-two mapping between the configurations $\{g\}=G$ and the configurations $\{\theta\}\equiv\Theta$ of the classical two-dimensional (2D) Ising model $H=-J\Sigma_{\langle s,s'\rangle}\theta_s\theta_{s'}$ with $\theta_s=-1$ (+1) when the corresponding star operator A_s is (is not) acting on the site s [10]. Thus $\sigma_i^z=\theta_s\theta_{s'}$, where i is the bond between the neighboring vertices $\langle s,s'\rangle$ (see Fig. 1). This gives $\langle\mathrm{GS}(\beta)|\hat{\sigma}_i^z|\mathrm{GS}(\beta)\rangle=[1/Z(\beta)]\Sigma_{\theta\in\Theta}\theta_s\theta_{s'}\exp(\beta\Sigma_{\langle s'',s'''\rangle}\theta_{s''}\theta_{s'''})=E(\beta)/N$, where β is identified as the reduced nearest-neighbor coupling $J/T=\beta$ of the Ising model with energy $E(\beta)$. The two expectation values $\langle\mathrm{GS}(\beta)|\hat{\sigma}_i^x|\mathrm{GS}(\beta)\rangle$ and $\langle\mathrm{GS}(\beta)|\hat{\sigma}_i^y|\mathrm{GS}(\beta)\rangle$ are both zero since $\langle 0|g\hat{\sigma}_i^x g'|0\rangle=0$, $\forall g,g'\in G$, and similarly for $\hat{\sigma}_i^y$. It follows that $\hat{\rho}_i=(1/2)\mathrm{diag}[1+E(\beta)/N,1-E(\beta)/N]$ in the $\hat{\sigma}_i^z$ eigenbasis. Since the density matrices at different parameter values β and β' commute, the reduced fidelity (1) is

$$F(\beta,\beta')=\mathrm{Tr}\sqrt{\hat{\rho}_i(\beta)\hat{\rho}_i(\beta')}=\sum_i\sqrt{\lambda_i\lambda_i'}, \tag{7}$$

where $\{\lambda_i\}$ ($\{\lambda_i'\}$) are the eigenvalues of $\hat{\rho}_i(\beta)$ ($\hat{\rho}_i(\beta')$). The energy $E(\beta)$ of the 2D Ising model in the thermodynamic limit $N\to\infty$ is given by $E(\beta)/N=-\coth(2\beta)\{1+(2/\pi)[2\tanh^2(2\beta)-1]K(\kappa)\}/2$, where $K(\kappa)=\int_0^{\pi/2}d\theta(1-\kappa^2\sin^2\theta)^{-1/2}$ and $\kappa=2\sinh(2\beta)/\cosh^2(2\beta)$ [14]. This gives us the plot of the single-site fidelity shown in Fig. 2, where we see that the TQPT at $\beta_c=(1/2)\ln(\sqrt{2}+1)\approx 0.44$ is marked by a sudden drop in the fidelity.

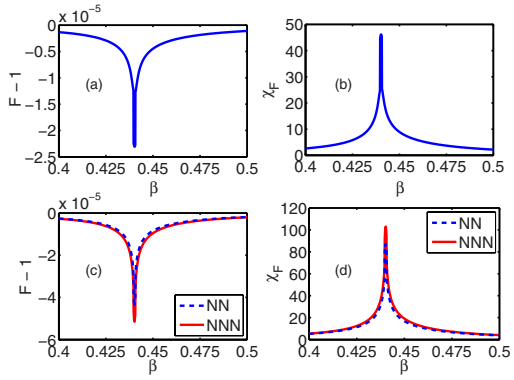

FIG. 2. (Color online) (a) Single-site fidelity, (b) single-site fidelity susceptibility, (c) two-site fidelity, and (d) two-site fidelity susceptibility of the Castelnovo-Chamon model calculated with a parameter difference $\delta\beta=0.001$ and with $N\to\infty$. The reduced fidelity susceptibilities will diverge according to Eq. (9) when $\delta\beta\to 0$. In (c) and (d) we plot for both nearest (NN) and next-nearest (NNN) neighbors.

The single-site fidelity susceptibility χ_F is

$$\chi_F=\sum_i\frac{(\partial_\beta\lambda_i)^2}{4\lambda_i} \tag{8}$$

for commuting density matrices [15]. Here $\partial_\beta\lambda_{1,2}=\pm(2N)^{-1}\partial_\beta E(\beta)=\pm(2N\beta^2)^{-1}C(\beta)$ with $C(\beta)$ as the specific heat of the 2D Ising model. Thus χ_F diverges as

$$\chi_F\sim\ln^2|\beta_c/\beta-1| \tag{9}$$

at β_c, which is faster than the global fidelity susceptibility in Eq. (5). In Fig. 2 we plot the single-site fidelity susceptibility using Eq. (2), but with finite $\delta\beta=0.001$.

The two-site fidelity can be obtained in a similar way. We expand the reduced density matrix $\hat{\rho}_{ij}$ as

$$\hat{\rho}_{ij}=\frac{1}{4}\sum_{\mu,\nu=0}^{3}\langle\hat{\sigma}_i^\mu\hat{\sigma}_j^\nu\rangle\hat{\sigma}_i^\mu\hat{\sigma}_j^\nu. \tag{10}$$

The only nonzero expectation values in Eq. (10) are $\langle\hat{\sigma}_i^0\hat{\sigma}_j^0\rangle=1$, $\langle\hat{\sigma}_i^z\hat{\sigma}_j^0\rangle=\langle\hat{\sigma}_i^z\rangle$, $\langle\hat{\sigma}_i^0\hat{\sigma}_j^z\rangle=\langle\hat{\sigma}_j^z\rangle$, and $\langle\hat{\sigma}_i^z\hat{\sigma}_j^z\rangle$. Translational invariance implies that $\langle\hat{\sigma}_j^z\rangle=\langle\hat{\sigma}_i^z\rangle$, so that

$$\hat{\rho}_{ij}=\frac{1}{4}(1+\langle\hat{\sigma}_i^z\rangle(\hat{\sigma}_i^z+\hat{\sigma}_j^z)+\langle\hat{\sigma}_i^z\hat{\sigma}_j^z\rangle\hat{\sigma}_i^z\hat{\sigma}_j^z). \tag{11}$$

The eigenvalues are seen to be $\lambda_{1,2}=(1/4)(1\pm 2\langle\hat{\sigma}_i^z\rangle+\langle\hat{\sigma}_i^z\hat{\sigma}_j^z\rangle)$ and $\lambda_{3,4}=(1/4)(1-\langle\hat{\sigma}_i^z\hat{\sigma}_j^z\rangle)$. Now the fidelity can be calculated using Eq. (7). Here we focus on the cases where i and j are nearest- and next-nearest neighbors. Then the mapping to the 2D Ising model gives $\langle\hat{\sigma}_i^z\rangle=\langle\theta_s\theta_{s'}\rangle$ and $\langle\hat{\sigma}_j^z\rangle=\langle\theta_{s''}\theta_{s'''}\rangle$, where i (j) is the bond between the neighboring vertices $\langle s,s'\rangle$ ($\langle s'',s'''\rangle$). When i and j are nearest (next-

nearest) neighbors, we get $\langle\hat{\sigma}_i^z\hat{\sigma}_j^z\rangle=\langle\theta_s\theta_{s'}\theta_{s''}\theta_s\rangle=\langle\theta_{s'}\theta_{s''}\rangle$, where $\langle s',s''\rangle$ are next-nearest (third-nearest) neighbors on the square lattice (cf. Fig. 1). As before, $\langle\hat{\sigma}_i^z\rangle=E(\beta)/N$. We obtain $\langle\theta_{s'}\theta_{s''}\rangle$ from the equivalence between the 2D Ising model and the quantum one-dimensional (1D) XY model,

$$H_{\mathrm{XY}}=-\sum_n(\alpha_+\hat{\sigma}_n^x\hat{\sigma}_{n+1}^x+\alpha_-\hat{\sigma}_n^y\hat{\sigma}_{n+1}^y+h\hat{\sigma}_n^z), \tag{12}$$

where $\alpha_\pm=(1\pm\gamma)/2$. This has been shown to give

$$\langle\theta_{0,0}\theta_{n,n}\rangle=\langle\hat{\sigma}_0^x\hat{\sigma}_n^x\rangle_{\mathrm{XY}}|_{\gamma=1,\ h=(\sinh 2\beta)^{-2}} \tag{13}$$

for Ising spins on the same diagonal and

$$\langle\theta_{n,m}\theta_{n,m'}\rangle=\cosh^2(\beta^*)\langle\hat{\sigma}_m^x\hat{\sigma}_{m'}^x\rangle_{\mathrm{XY}}|_{\gamma=\gamma_\beta,\ h=h_\beta}-\sinh^2(\beta^*)\langle\hat{\sigma}_m^y\hat{\sigma}_{m'}^y\rangle_{\mathrm{XY}}|_{\gamma=\gamma_\beta,\ h=h_\beta} \tag{14}$$

for Ising spins on the same row (or, by symmetry, column), where $\tanh\beta^*=e^{-2\beta}$, $\gamma_\beta=(\cosh 2\beta^*)^{-1}$ and $h_\beta=(1-\gamma^2)^{1/2}/\tanh 2\beta$ [16]. Known results for the 1D XY model give [17]

$$\langle\hat{\sigma}_m^x\hat{\sigma}_{m+r}^x\rangle_{\mathrm{XY}}=\begin{vmatrix}G_{-1}&G_{-2}&\cdots&G_{-r}\\G_0&G_{-1}&\cdots&G_{-r+1}\\\vdots&\vdots&\ddots&\vdots\\G_{r-2}&G_{r-3}&\cdots&G_{-1}\end{vmatrix}, \tag{15}$$

$$\langle\hat{\sigma}_m^y\hat{\sigma}_{m+r}^y\rangle_{\mathrm{XY}}=\begin{vmatrix}G_1&G_0&\cdots&G_{-r+2}\\G_2&G_1&\cdots&G_{-r+3}\\\vdots&\vdots&\ddots&\vdots\\G_r&G_{r-1}&\cdots&G_1\end{vmatrix}, \tag{16}$$

where

$$G_{r'}=(1/\pi)\int_0^\pi d\phi(h-\cos\phi)\cos(\phi r')/\Lambda_\phi(h)+(\gamma/\pi)\int_0^\pi d\phi\sin\phi\sin(\phi r')/\Lambda_\phi(h)$$

and $\Lambda_\phi(h)=[(\gamma\sin\phi)^2+(h-\cos\phi)^2]^{1/2}$. These relations allow us to plot the two-site fidelity and also the two-site fidelity susceptibility using Eq. (2) (see Fig. 2). Note that the two-site functions are only slightly different depending on whether the two sites are nearest neighbors or next-nearest neighbors. It follows from Eq. (8) that also the two-site χ_F has a stronger divergence at criticality than the global fidelity susceptibility. It is interesting to note the slight asymmetry of the reduced fidelities around the critical point, seen in Fig. 2, indicating a somewhat smaller response to changes in the driving parameter in the topological phase.

IV. TRANSVERSE WEN-PLAQUETTE MODEL

We now turn to the transverse Wen-plaquette model, obtained from the ordinary Wen-plaquette model [18] for spin-1/2 particles on the vertices of a square lattice by adding a magnetic field h [19],

$$H=g\sum_i\hat{F}_i+h\sum_i\hat{\sigma}_i^x, \tag{17}$$

where $\hat{F}_i=\hat{\sigma}_i^x\hat{\sigma}_{i+\hat{x}}^y\hat{\sigma}_{i+\hat{x}+\hat{y}}^x\hat{\sigma}_{i+\hat{y}}^y$ and $g<0$. The boundary conditions are periodic. At $h=0$ the ground state is the topologically ordered ground state of the Wen-plaquette model [18] and in the limit $h\to\infty$ the ground state is magnetically ordered. Since $\hat{F}_i,\hat{\sigma}_j^x$ have the same commutation relations as $\hat{\tau}_{i+\hat{x}/2+\hat{y}/2}^z,\hat{\tau}_{j-\hat{x}/2+\hat{y}/2}^x\hat{\tau}_{j+\hat{x}/2-\hat{y}/2}^x$ (where the Pauli matrices $\hat{\tau}$ act on spin-1/2 particles at the centers of the plaquettes), Hamiltonian (17) can be mapped onto independent quantum Ising chains,

$$H=-h\sum_a\sum_i(g_I\hat{\tau}_{a,i+1/2}^z+\hat{\tau}_{a,i-1/2}^x\hat{\tau}_{a,i+1/2}^x) \tag{18}$$

with $g_I=g/h$ and where $\hat{\tau}_{i+1/2}^z$ and $\hat{\tau}_{i-1/2}^x\hat{\tau}_{i+1/2}^x$ are the images of $\hat{\sigma}_i^x\hat{\sigma}_{i+\hat{x}}^y\hat{\sigma}_{i+\hat{x}+\hat{y}}^x\hat{\sigma}_{i+\hat{y}}^y$ and $\hat{\sigma}_i^x$, respectively [19]. The index a denotes the diagonal chains over the plaquette-centered sites and i is the site index on each diagonal chain. Known results for criticality in the quantum Ising chain imply that the transverse Wen-plaquette model has a TQPT at $g/h=1$ [19].

We now calculate the reduced fidelity. The mapping onto the quantum Ising chains immediately gives $\langle\hat{\sigma}_i^x\rangle=\langle\hat{\tau}_{i-1/2}^x\hat{\tau}_{i+1/2}^x\rangle$. In the $\hat{\sigma}_i^x$ basis, Hamiltonian (17) only flips spins in pairs; therefore, we get $\langle\hat{\sigma}_i^y\rangle=0$ and $\langle\hat{\sigma}_i^z\rangle=0$. The single-site reduced density matrix (6) is therefore given by $\hat{\rho}_i=(1/2)(1+\langle\hat{\tau}_{i-1/2}^x\hat{\tau}_{i+1/2}^x\rangle\hat{\sigma}_i^x)$, which is diagonal in the $\hat{\sigma}_i^x$ basis, with eigenvalues $\lambda_{1,2}=(1/2)(1\pm\langle\hat{\tau}_{i-1/2}^x\hat{\tau}_{i+1/2}^x\rangle)$. The single-site fidelity is thus given by Eq. (7), and $\langle\hat{\tau}_{i-1/2}^x\hat{\tau}_{i+1/2}^x\rangle$ is calculated using Eq. (15) with $\gamma=1$ and $h=g_I$. The result reveals that the TQPT is accompanied by a sudden drop in the single-site fidelity. Now, $\partial_{g_I}\lambda_{1,2}=\pm\frac{1}{2}\partial_{g_I}\langle\hat{\tau}_{i-1/2}^x\hat{\tau}_{i+1/2}^x\rangle$, which diverges logarithmically at the critical point $g_I=1$. Therefore Eq. (8) implies that at $h/g=1$, χ_F diverges as

$$\chi_F\sim\ln^2|g/h-1| \tag{19}$$

as in Eq. (9) for the Castelnovo-Chamon model.

We can also calculate the two-site fidelity for two nearest-neighbor spins at sites i and j. All nontrivial expectation values in expansion (10) of the reduced density matrix, except $\langle\hat{\sigma}_i^x\rangle$, $\langle\hat{\sigma}_j^x\rangle$, and $\langle\hat{\sigma}_i^x\hat{\sigma}_j^x\rangle$, will be zero since only these operators can be constructed from those in Hamiltonian (17). The mapping onto the quantum Ising chains gives $\langle\hat{\sigma}_i^x\hat{\sigma}_j^x\rangle=\langle\hat{\tau}_{i-1/2}^x\hat{\tau}_{i+1/2}^x\hat{\tau}_{j-1/2}^x\hat{\tau}_{j+1/2}^x\rangle=(\langle\hat{\tau}_{i-1/2}^x\hat{\tau}_{i+1/2}^x\rangle)^2$. Thus the two-site density matrix is given by $\hat{\rho}_{ij}=(1/4)[1+\langle\hat{\tau}_{i-1/2}^x\hat{\tau}_{i+1/2}^x\rangle\times(\hat{\sigma}_i^x+\hat{\sigma}_j^x)+(\langle\hat{\tau}_{i-1/2}^x\hat{\tau}_{i+1/2}^x\rangle)^2\hat{\sigma}_i^x\hat{\sigma}_j^x]$, which is diagonal in the $\hat{\sigma}_i^x\hat{\sigma}_j^x$ eigenbasis. The eigenvalues are $\lambda_{1,2}=(1/4)\times(1\pm\langle\hat{\tau}_{i-1/2}^x\hat{\tau}_{i+1/2}^x\rangle)^2$ and $\lambda_{3,4}=(1/4)[1-(\langle\hat{\tau}_{i-1/2}^x\hat{\tau}_{i+1/2}^x\rangle)^2]$. Taking the derivatives of the eigenvalues $\lambda_{1,2,3,4}$ and inserting them into Eq. (8) shows that also the two-site fidelity susceptibility diverges as $\chi_F\sim\ln^2|g/h-1|$ at $h/g=1$. Contrary to the case of the Castelnovo-Chamon model, χ_F for one and two spins now diverges slower than the global fidelity susceptibility, which shows the $\chi_F\sim|g/h-1|^{-1}$ divergence of the quantum Ising chain [20].

V. KITAEV TORIC CODE MODEL IN A MAGNETIC FIELD

Adding a magnetic field h to the Kitaev toric code model [13] gives the Hamiltonian [11]

$$H = -\lambda_0 \sum_p B_p - \lambda_1 \sum_s A_s - h \sum_i \hat{\sigma}_i^x, \tag{20}$$

where the operators B_p and A_s are the same as in Eq. (3). In the limit $\lambda_1 \gg \lambda_0, h$, the ground state $|\mathrm{GS}\rangle$ will obey $A_s|\mathrm{GS}\rangle = |\mathrm{GS}\rangle$, $\forall s$. Then there is a mapping to spin-1/2 operators $\hat{\tau}$ acting on spins at the centers of the plaquettes, according to $B_p \mapsto \hat{\tau}_p^x$, $\hat{\sigma}_i^x \mapsto \hat{\tau}_p^z \hat{\tau}_q^z$. Here i is the site shared by the two adjacent plaquettes $\langle p,q \rangle$. This maps Hamiltonian (20) onto [11]

$$H = -\lambda_0 \sum_p \hat{\tau}_p^x - h \sum_{\langle p,q \rangle} \hat{\tau}_p^z \hat{\tau}_q^z, \tag{21}$$

which is the 2D transverse field Ising model with magnetic field $\lambda_0/h = h'$. Now, the mapping tells us that $\langle \hat{\sigma}_i^x \rangle = \langle \hat{\tau}_p^z \hat{\tau}_q^z \rangle$ and the symmetries of Hamiltonian (20) imply $\langle \hat{\sigma}_i^y \rangle = 0$ and $\langle \hat{\sigma}_i^z \rangle = 0$. The single-site reduced density matrix is therefore given by $\hat{\rho}_i = (1/2)(1 + \langle \hat{\tau}_p^z \hat{\tau}_q^z \rangle \hat{\sigma}_i^x)$, which has the same form as in the transverse Wen-plaquette model. Since numerical results have shown a kink in $\langle \hat{\tau}_p^z \hat{\tau}_q^z \rangle$ at the phase transition at $h_c' \approx 3$ [11], it follows that the single-site fidelity will have a drop at this point. Further, the divergence of $\partial_{h'} \langle \hat{\tau}_p^z \hat{\tau}_q^z \rangle$ at the critical point implies a divergence of the single-site fidelity susceptibility at h_c'. Thus, the scenario that emerges is similar to those for the models above.

VI. DISCUSSION

To summarize, we have analyzed the reduced fidelity at several lattice system TQPTs and found that it serves as an accurate marker of the transitions. In the case of the Castelnovo-Chamon model [10], the divergence of the reduced fidelity susceptibility at criticality can explicitly be shown to be even stronger than that of the global fidelity [6]. Our analytical results rely on exact mappings of the TQPTs onto ordinary symmetry-breaking phase transitions. Other lattice models exhibiting TQPTs have also been shown to be dual to spin [21] or vertex [22] models with classical order, suggesting that our line of approach may be applicable also in these cases, and that the property that a reduced fidelity can detect a TQPT may in fact be generic. While counterintuitive, considering that the reduced fidelity is a *local probe* of the topologically ordered phase, related results have been reported in previous studies. Specifically, in Refs. [10,11], the authors found that the local magnetization in the Castelnovo-Chamon model and the Kitaev toric code model in a magnetic field, while being continuous and nonvanishing across the transition out of topological order, has a singularity in its first derivative. The fact that local quantities can spot a TQPT is conceptually satisfying as any physical observable is local in nature. Interesting open questions here are how the concept of reduced fidelity can be applied to TQPTs in more realistic systems, such as the fractional quantum Hall liquids, and how reduced fidelity susceptibility singularities depend on different topological and classical orders involved in the transitions.

ACKNOWLEDGMENTS

We acknowledge the Kavli Institute for Theoretical Physics at UCSB for hospitality during the completion of this work. This research was supported in part by the National Science Foundation under Grant No. PHY05-51164 and by the Swedish Research Council under Grant No. VR-2005-3942.

[1] X.-G. Wen, *Quantum Field Theory of Many-Body Systems* (Oxford University Press, Oxford, 2004).
[2] C. Nayak *et al.*, Rev. Mod. Phys. **80**, 1083 (2008).
[3] A. Hamma, R. Ionicioiu, and P. Zanardi, Phys. Rev. A **71**, 022315 (2005); A. Kitaev and J. Preskill, Phys. Rev. Lett. **96**, 110404 (2006); M. Levin and X.-G. Wen, *ibid.* **96**, 110405 (2006).
[4] A. Hamma *et al.*, Phys. Rev. B **77**, 155111 (2008).
[5] For a review, see S.-J. Gu, e-print arXiv:0811.3127.
[6] D. F. Abasto, A. Hamma, and P. Zanardi, Phys. Rev. A **78**, 010301(R) (2008).
[7] S. Yang *et al.*, Phys. Rev. A **78**, 012304 (2008); J.-H. Zhao and H.-Q. Zhou, e-print arXiv:0803.0814; S. Garnerone *et al.*, Phys. Rev. A **79**, 032302 (2009).
[8] A. Uhlmann, Rep. Math. Phys. **9**, 273 (1976); R. Jozsa, J. Mod. Opt. **41**, 2315 (1994).
[9] N. Paunkovic *et al.*, Phys. Rev. A **77**, 052302 (2008); J. Ma *et al.*, Phys. Rev. E **78**, 051126 (2008); H.-M. Kwok, C.-S. Ho, and S.-J. Gu, Phys. Rev. A **78**, 062302 (2008); J. Ma *et al.*, e-print arXiv:0808.1816.
[10] C. Castelnovo and C. Chamon, Phys. Rev. B **77**, 054433 (2008).
[11] S. Trebst *et al.*, Phys. Rev. Lett. **98**, 070602 (2007).
[12] W.-L. You, Y.-W. Li, and S.-J. Gu, Phys. Rev. E **76**, 022101 (2007).
[13] A. Y. Kitaev, Ann. Phys. (N.Y.) **303**, 2 (2003).
[14] L. Onsager, Phys. Rev. **65**, 117 (1944).
[15] H.-N. Xiong *et al.*, e-print arXiv:0808.1817.
[16] M. Suzuki, Phys. Lett. A **34**, 94 (1971); B. M. McCoy, in *Statistical Mechanics and Field Theory*, edited by V. V. Bazhanov and C. J. Burden (World Scientific, Singapore, 1995), pp. 26–128; e-print arXiv:hep-th/9403084.
[17] E. Barouch and B. M. McCoy, Phys. Rev. A **3**, 786 (1971).
[18] X.-G. Wen, Phys. Rev. Lett. **90**, 016803 (2003).
[19] J. Yu, S.-P. Kou, and X.-G. Wen, EPL **84**, 17004 (2008).
[20] S. Chen *et al.*, Phys. Rev. A **77**, 032111 (2008).
[21] X.-Y. Feng, G.-M. Zhang, and T. Xiang, Phys. Rev. Lett. **98**, 087204 (2007); H. D. Chen and J. Hu, Phys. Rev. B **76**, 193101 (2007).
[22] H.-Q. Zhou, R. Orus, and G. Vidal, Phys. Rev. Lett. **100**, 080601 (2008).

Paper II

Corrections to scaling in entanglement entropy from boundary perturbations

Erik Eriksson and Henrik Johannesson
J. Stat. Mech. (2011) P02008.

Journal of Statistical Mechanics: Theory and Experiment
An IOP and SISSA journal

Corrections to scaling in entanglement entropy from boundary perturbations

Erik Eriksson and Henrik Johannesson

Department of Physics, University of Gothenburg, SE 412 96 Gothenburg, Sweden
E-mail: erik.eriksson@physics.gu.se and henrik.johannesson@physics.gu.se

Received 2 November 2010
Accepted 9 January 2011
Published 1 February 2011

Online at stacks.iop.org/JSTAT/2011/P02008
doi:10.1088/1742-5468/2011/02/P02008

Abstract. We investigate the corrections to scaling of the Rényi entropies of a region of size ℓ at the end of a semi-infinite one-dimensional system described by a conformal field theory when the corrections come from irrelevant boundary operators. The corrections from irrelevant bulk operators with scaling dimension x have been studied by Cardy and Calabrese (2010), and they found not only the expected corrections of the form ℓ^{4-2x} but also unusual corrections that could not have been anticipated from standard finite-size scaling. However, for the case of perturbations from irrelevant boundary operators we find that the only corrections that can occur to leading order are of the form ℓ^{2-2x_b} for boundary operators with scaling dimension $x_\mathrm{b} < 3/2$, and ℓ^{-1} when $x_\mathrm{b} > 3/2$. When $x_\mathrm{b} = 3/2$ they are of the form $\ell^{-1}\log\ell$. A marginally irrelevant boundary perturbation will give leading corrections going as $(\log\ell)^{-3}$. No unusual corrections occur when perturbing with a boundary operator.

Keywords: conformal field theory (theory), Kondo effect (theory), spin chains, ladders and planes (theory), entanglement in extended quantum systems (theory)

ArXiv ePrint: 1011.0448

1742-5468/11/P02008+9$33.00

Contents

1. Introduction

The block entanglement of a quantum system has been found to be a powerful tool for characterizing the scaling behavior near a quantum critical point [1]. For a system in a pure state and with the Hilbert space partitioned into a direct product $\mathcal{H} = \mathcal{H}_{\rm A} \otimes \mathcal{H}_{\rm B}$ (with A and B the corresponding two parts of the system), the block entanglement is encoded by the von Neumann entropy $S_{\rm A} = -\operatorname{Tr} \rho_{\rm A} \log \rho_{\rm A}$ of the reduced density matrix $\rho_{\rm A}$, with $S_{\rm A} = S_{\rm B}$. The most interesting case is in one dimension. For an infinite system with an interval A of length ℓ the asymptotic behavior of the von Neumann entropy is given by [2]

$$S_{\rm A} \sim \frac{c}{3} \log \frac{\ell}{\epsilon} + c_1' \tag{1}$$

near the critical point. Here c is the central charge of the underlying conformal field theory. The constant ϵ is an arbitrary cutoff scale, with c_1' also being a non-universal number. As a way to characterize the full entanglement spectrum one may introduce an additional parameter n, with n a positive real number, and define the Rényi entropies

$$S_{\rm A}^{(n)} = \frac{1}{1-n} \log \operatorname{Tr} \rho_{\rm A}^n, \tag{2}$$

with $\lim_{n\to 1} S_{\rm A}^{(n)} = S_{\rm A}$. As expected from finite-size scaling theory, the critical scaling $S_{\rm A}^{(n)} \sim (c/6)(1 + n^{-1}) \log(\ell/\epsilon)$ of the Rényi entropies exhibits $\mathcal{O}(\ell^{4-2x})$ corrections [3]. Here $x > 2$ is the scaling dimension of the leading irrelevant operator (with 'irrelevant' being understood in the sense of the renormalization group). As shown in [3], there can also be unusual n-dependent corrections of $\mathcal{O}(\ell^{-2x/n})$ and $\mathcal{O}(\ell^{2-x-x/n})$, where, in the first case, x may in fact be less than 2, corresponding to a scaling correction produced by a relevant operator. These unusual corrections often come with an oscillating prefactor, which however vanishes when $n \to 1$ in all known cases [4, 5]. For a semi-infinite system, with a conformally invariant boundary condition (CIBC), operators in the bulk may produce additional unusual scaling corrections $\ell^{-x/n}$ to the Rényi entropies, on top of the ordinary $\mathcal{O}(\ell^{2-x})$ corrections with $x > 2$ predicted by finite-size scaling [3]. In contrast to

J. Stat. Mech. (2011) P02008

the case of an infinite system, the oscillating prefactor that multiplies the leading unusual $\ell^{-x/n}$-correction does not vanish in the limit $n \to 1$. This unexpected feature was first observed in numerical work in [6], and recently derived analytically for the case of the XX-chain with open boundary conditions [7].

In this paper we inquire about the scaling corrections to the critical Rényi entropies of a semi-infinite one-dimensional system which are generated by irrelevant boundary operators. Recall that boundary operators arise in the operator product expansion (OPE) of a chiral operator with its mirror image across the boundary. More precisely, given a boundary conformal field theory (BCFT) defined on the complex half-plane $\{z = \tau + \mathrm{i}y \mid y \geq 0\}$ with a CIBC at $y = 0$, the OPE of a chiral operator $\phi(\tau, y)$ with its mirror image $\phi(\tau, -y)$ reads [8, 9]

$$\phi(\tau, y)\phi(\tau, -y) \sim \sum_j \frac{C_{\phi,j}}{(2y)^{2x_\phi - x_j}} \phi_j(\tau), \qquad y \to 0. \tag{3}$$

Here x_ϕ is the scaling dimension of ϕ, and ϕ_j are boundary operators of dimension x_j. Nonzero values of the expansion coefficients $C_{\phi,j}$ select those boundary operators which are consistent with the particular CIBC imposed at $y = 0$. Knowing the boundary operator content associated with a system allows for a complete characterization of its boundary critical behavior, i.e. those terms in the critical scaling of observables contributed by the presence of the boundary. For a quantum theory, where τ is a Euclidean time, this allows for identifying the long-time (a.k.a. low-energy) asymptotic critical behavior of the system close to the boundary. BCFT has a manifold of applications, spanning from open-string theory (D branes) [11] to the study of quantum quenches [12]. A particularly important class of applications is that of a quantum impurity interacting with an electron liquid, where at low energies the impurity can be traded for a CIBC at the site of the impurity [10]. The increase of the block entanglement at quantum criticality due to the presence of the impurity is a universal number (boundary entropy) which characterizes the type of boundary critical behavior. However, for a finite block there will always be additive corrections to the boundary entropy coming from irrelevant bulk and boundary operators. These corrections are expected to reveal features about quantum impurity phenomena which are otherwise difficult to access, the extent and character of the enigmatic 'screening cloud' being a case in point [13].

2. Scaling corrections from bulk operators: a brief review

Consider a one-dimensional system with a boundary at $y = 0$ that is described by a BCFT. Let subsystem A be the region $0 \leq y \leq \ell$ and B the rest of the system, $y > \ell$. As shown by Calabrese and Cardy [1, 2], $\mathrm{Tr}\,\rho_{\mathrm{A}}^n$ (which enters the definition of the Rényi entropies in equation (2)) can be viewed as a path integral $Z_{\mathcal{R}_n}$ on an n-sheeted Riemann surface $\mathcal{R}_n$ with a boundary, and with proper normalization. Then

$$S_{\mathrm{A}}^{(n)} = \frac{1}{1-n} \log \frac{Z_{\mathcal{R}_n}}{Z^n} = -\frac{\beta}{1-n} (F_{\mathcal{R}_n} - nF), \tag{4}$$

where $F = -\beta^{-1} \log Z$ is the free energy, $F_{\mathcal{R}_n} = -\beta^{-1} \log Z_{\mathcal{R}_n}$ and β is the inverse temperature. For an unperturbed BCFT, $Z_{\mathcal{R}_n}/Z^n$ can be calculated as a one-point

J. Stat. Mech. (2011) P02008

function on the half-plane $\mathbb{C}^+$ of a twist field Φ_n inserted at the branch point $z = \mathrm{i}\ell$ [2]

$$\frac{Z_{\mathcal{R}_n}}{Z^n} = \langle \Phi_n(\mathrm{i}\ell)\rangle_{\mathbb{C}^+} = c_n \left(\frac{2\ell}{\epsilon}\right)^{-c(n-1/n)/12}, \tag{5}$$

where ϵ is the short-distance cutoff. This leads to

$$S_{\mathrm{A}}^{(n)} = \frac{c}{12}\left(1+\frac{1}{n}\right)\log\frac{2\ell}{\epsilon} + s^A + c_n', \tag{6}$$

where $s^A = \log g^A$ is the boundary entropy and c_n' are non-universal constants [2, 14]. The well-known result for the critical block entanglement on a semi-infinite line,

$$S_{\mathrm{A}} = \frac{c}{6}\log\frac{2\ell}{\epsilon} + s^A + c', \tag{7}$$

is obtained simply by letting $n \to 1^+$ in equation (6).

The corrections to this scaling behavior from irrelevant bulk operators were recently studied by Cardy and Calabrese [3]. Such a perturbation with a bulk operator $\Phi(z)$ having a scaling dimension $x > 2$ gives an action

$$S = S_{\mathrm{CFT}} + \lambda \int \mathrm{d}^2 z\, \Phi(z), \tag{8}$$

where λ is a coupling constant. The corrections to the free energies are given by the perturbation series

$$F_{\mathcal{R}_n} = F_{\mathcal{R}_n}^{\mathrm{CFT}} - \sum_{N=1}^{\infty} \frac{(-\lambda)^N}{N!} \int_{\mathcal{R}_n} \mathrm{d}^2 z_1 \cdots \int_{\mathcal{R}_n} \mathrm{d}^2 z_N \langle \Phi(z_1)\cdots\Phi(z_N)\rangle_{\mathcal{R}_n}, \tag{9}$$

over the Riemann surface $\mathcal{R}_n$, and

$$F = F^{\mathrm{CFT}} - \sum_{N=1}^{\infty} \frac{(-\lambda)^N}{N!} \int_{\mathbb{C}^+} \mathrm{d}^2 w_1 \cdots \int_{\mathbb{C}^+} \mathrm{d}^2 w_N \langle \Phi(w_1)\cdots\Phi(w_N)\rangle_{\mathbb{C}^+}, \tag{10}$$

over the ordinary complex half-plane $\mathbb{C}^+$. When the boundary conditions are such that $\langle\Phi(w)\rangle_{\mathbb{C}^+} \neq 0$ they found that the first-order correction to $F_{\mathcal{R}_n} - nF$ is of the form ℓ^{2-x}. However, for $n > x/(x-2)$ they also found the appearance of the unusual n-dependent correction $\ell^{-x/n}$, that comes from the singularity at the branch point. For an infinite system without a boundary, the corrections take the forms ℓ^{4-2x} and $\ell^{-2x/n}$.

3. Scaling corrections from irrelevant boundary operators

We now wish to study the case when the perturbations come from irrelevant operators on the boundary. In doing so, we can follow the same procedure as Cardy and Calabrese in [3]. However, when perturbing with a boundary operator the surface integral of the perturbing field in the action (8) will be replaced by a line integral on the boundary. As we shall see, this will prevent the appearance of unusual n-dependent corrections. In fact, this is anticipated since n-dependent exponents only arise from the region at the branch point, which is located away from the boundary. Nevertheless, there are still results for the boundary case that do not follow from standard finite-size scaling analysis.

J. Stat. Mech. (2011) P02008

Thus, consider a BCFT on the upper half $y \geq 0$ of the complex plane $z = \tau + \mathrm{i}y$, so that τ is the boundary coordinate at $y = 0$. The n-sheeted Riemann surface $\mathcal{R}_n$ is then obtained by sewing together n copies of this half-plane along $0 \leq y < \ell$ at $\tau = 0$. To evaluate the correlation functions on $\mathcal{R}_n$ for a chiral operator $\phi(z)$ with scaling dimension x_b, we need to use the transformation property

$$\langle \phi(z_1) \cdots \phi(z_N) \rangle_{\mathcal{R}_n} = \prod_{j=1}^{N} \left| \frac{\mathrm{d}z}{\mathrm{d}w} \right|_{w=w_j}^{-x_\mathrm{b}} \langle \phi(w_1) \cdots \phi(w_N) \rangle_{\mathbb{C}^+}, \tag{11}$$

where the map $z \mapsto w$ from $\mathcal{R}_n$ to the upper half-plane $\mathbb{C}^+$ is given by

$$w = -\mathrm{i} \frac{((z - \mathrm{i}\ell)/(z + \mathrm{i}\ell))^{1/n} + 1}{((z - \mathrm{i}\ell)/(z + \mathrm{i}\ell))^{1/n} - 1}. \tag{12}$$

This gives

$$\frac{\mathrm{d}z}{\mathrm{d}w} = -4n\ell \frac{((w - \mathrm{i})/(w + \mathrm{i}))^n}{(1 + w^2)[((w - \mathrm{i})/(w + \mathrm{i}))^n - 1]^2}. \tag{13}$$

Naturally, the mapping (12) takes the boundary of $\mathcal{R}_n$ to the boundary of $\mathbb{C}^+$. Since w is real on the boundary we see from (13) that $|\mathrm{d}z/\mathrm{d}w|^{-x_\mathrm{b}}$ is analytic on the boundary, as the only singularity is at $w = \mathrm{i}$, i.e. when z is at the branch point $z = \mathrm{i}\ell$. In particular, note that the point $|z| \to \infty$ gives a divergence in $|\mathrm{d}z/\mathrm{d}w|$ which only means that $|\mathrm{d}z/\mathrm{d}w|^{-x_\mathrm{b}} \to 0$.

Now we can use this to study the scaling corrections of $S_\mathrm{A}^{(n)} \propto (F_{\mathcal{R}_n} - nF)$ when adding a boundary perturbation,

$$S = S_\mathrm{CFT} + \lambda \int \mathrm{d}\tau \, \phi_\mathrm{b}(\tau), \tag{14}$$

where ϕ_b is an irrelevant operator with scaling dimension $x_\mathrm{b} > 1$ on the boundary $y = 0$.

We will assume the boundary conditions to be such that $\langle \phi_\mathrm{b}(\tau) \rangle = 0$. This is natural if we demand conformal boundary conditions. Then the first-order correction vanishes. An important exception is when the perturbing boundary operator is the stress-energy tensor, a case that was treated in [15]. Since this operator has a non-vanishing expectation value on $\mathcal{R}_n$ it will give rise to a first-order correction to $S_\mathrm{A}^{(n)}$, which was found to have the form ℓ^{-1}. We therefore consider the second-order corrections to $F_{\mathcal{R}_n}$ and F, denoted $\delta^2 F_{\mathcal{R}_n}$ and $\delta^2 F$ respectively. They are given by

$$\delta^2 F_{\mathcal{R}_n} = -\frac{\lambda^2}{2\beta} \int \mathrm{d}\tau_1' \int \mathrm{d}\tau_2' \langle \phi_\mathrm{b}(\tau_1') \phi_\mathrm{b}(\tau_2') \rangle_{\mathcal{R}_n} \tag{15}$$

and

$$\delta^2 F = -\frac{\lambda^2}{2\beta} \int \mathrm{d}\tau_1 \int \mathrm{d}\tau_2 \langle \phi_\mathrm{b}(\tau_1) \phi_\mathrm{b}(\tau_2) \rangle_{\mathbb{C}^+}, \tag{16}$$

doi:10.1088/1742-5468/2011/02/P02008

J. Stat. Mech. (2011) P02008

respectively, where τ_1', τ_2' are boundary coordinates on $\mathcal{R}_n$ and $\tau_1 = w(\tau_1')$, $\tau_2 = w(\tau_2')$ are boundary coordinates on $\mathbb{C}^+$. From equation (11), we get

$$\begin{aligned}\delta^2 F_{\mathcal{R}_n} &= -\frac{\lambda^2}{2\beta}\int \mathrm{d}\tau_1' \int \mathrm{d}\tau_2' \left|\frac{\mathrm{d}z}{\mathrm{d}w}\right|_{z=\tau_1'}^{-x_\mathrm{b}} \left|\frac{\mathrm{d}z}{\mathrm{d}w}\right|_{z=\tau_2'}^{-x_\mathrm{b}} \langle\phi_\mathrm{b}(w(\tau_1'))\phi_\mathrm{b}(w(\tau_2'))\rangle_{\mathbb{C}^+} \\ &= -\frac{\lambda^2}{2\beta}\int \mathrm{d}\tau_1 \int \mathrm{d}\tau_2 \left|\frac{\mathrm{d}z}{\mathrm{d}w}\right|_{w=\tau_1}^{1-x_\mathrm{b}} \left|\frac{\mathrm{d}z}{\mathrm{d}w}\right|_{w=\tau_2}^{1-x_\mathrm{b}} \langle\phi_\mathrm{b}(\tau_1)\phi_\mathrm{b}(\tau_2)\rangle_{\mathbb{C}^+}. \end{aligned} \tag{17}$$

We can now use the fact that $\delta^2 F_{\mathcal{R}_n} - n\delta^2 F$ only depends on the ratio ℓ/ϵ, where ϵ is the short-distance cutoff of the theory, to extract its ℓ-dependence. Since the action (14) is dimensionless, the coupling constant λ goes as $\lambda \sim \epsilon^{x_\mathrm{b}-1}$. Thus $\lambda^2 \sim \epsilon^{2x_\mathrm{b}-2}$, and since $\mathrm{d}z/\mathrm{d}w \propto \ell$ the integral in equation (17) includes an overall factor of $(\ell/\epsilon)^{2-2x_\mathrm{b}}$. However, there can also appear powers of ℓ/ϵ coming from the need to regularize divergences in the integrals.

In order to compare the two integrals in $\delta^2 F_{\mathcal{R}_n} - n\delta^2 F$ it is convenient to rewrite $n\delta^2 F$ in the same form as $\delta^2 F_{\mathcal{R}_n}$:

$$\begin{aligned} n\delta^2 F &= -\frac{\lambda^2}{2\beta} n \int \mathrm{d}\tau_1 \int \mathrm{d}\tau_2 \frac{1}{|\tau_1-\tau_2|^{2x_\mathrm{b}}} \\ &= -\frac{\lambda^2}{2\beta} n \int \mathrm{d}\tau_1 \int_\epsilon^\infty \mathrm{d}|\tau_1-\tau_2| \frac{1}{|\tau_1-\tau_2|^{2x_\mathrm{b}}} \\ &= \frac{\lambda^2}{2\beta} n \int \mathrm{d}\tau_1 \frac{\epsilon^{1-2x_\mathrm{b}}}{1-2x_\mathrm{b}}. \end{aligned}$$

Rewriting this as an integral over the boundary of $\mathcal{R}_n$, one gets

$$\begin{aligned} n\delta^2 F &= \frac{\lambda^2}{2\beta}\int \mathrm{d}\tau_1' \frac{\epsilon^{1-2x_\mathrm{b}}}{1-2x_\mathrm{b}} \\ &= \frac{\lambda^2}{2\beta}\int \mathrm{d}\tau_1 \left|\frac{\mathrm{d}z}{\mathrm{d}w}\right|_{w=\tau_1} \frac{\epsilon^{1-2x_\mathrm{b}}}{1-2x_\mathrm{b}} \end{aligned} \tag{18}$$

and then going back to writing this as a double integral over τ_1 and τ_2 gives

$$n\delta^2 F = -\frac{\lambda^2}{2\beta}\int \mathrm{d}\tau_1 \int_{|\tau_1-\tau_2|\geq\epsilon/|(\mathrm{d}z/\mathrm{d}w)_{w=\tau_1}|} \mathrm{d}\tau_2 \left|\frac{\mathrm{d}z}{\mathrm{d}w}\right|_{w=\tau_1}^{2-2x_\mathrm{b}} \frac{1}{|\tau_1-\tau_2|^{2x_\mathrm{b}}}. \tag{19}$$

As $\epsilon \to 0$, we have

$$|(\mathrm{d}z/\mathrm{d}w)_{w=\tau_1}||\tau_1-\tau_2| \geq \epsilon \Leftrightarrow |\tau_1'-\tau_2'| \geq \epsilon, \tag{20}$$

so that $\delta^2 F_{\mathcal{R}_n} - n\delta^2 F$ can be written as a single integral

$$\begin{aligned} \delta^2 F_{\mathcal{R}_n} - n\delta^2 F &= -\frac{\lambda^2}{2\beta}\int \mathrm{d}\tau_1 \int \mathrm{d}\tau_2 \frac{|\mathrm{d}z/\mathrm{d}w|_{w=\tau_1}^{1-x_\mathrm{b}} |\mathrm{d}z/\mathrm{d}w|_{w=\tau_2}^{1-x_\mathrm{b}} - |\mathrm{d}z/\mathrm{d}w|_{w=\tau_1}^{2-2x_\mathrm{b}}}{|\tau_1-\tau_2|^{2x_\mathrm{b}}} \\ &= \frac{\lambda^2}{4\beta}\int \mathrm{d}\tau_1 \int \mathrm{d}\tau_2 \frac{\left(|\mathrm{d}z/\mathrm{d}w|_{w=\tau_1}^{1-x_\mathrm{b}} - |\mathrm{d}z/\mathrm{d}w|_{w=\tau_2}^{1-x_\mathrm{b}}\right)^2}{|\tau_1-\tau_2|^{2x_\mathrm{b}}}, \end{aligned} \tag{21}$$

with the cutoff $|(\mathrm{d}z/\mathrm{d}w)_{w=\tau_1}||\tau_1-\tau_2| \geq \epsilon$. It follows from equation (13) that $|\mathrm{d}z/\mathrm{d}w|^{1-x_\mathrm{b}}$ is analytic everywhere except at $w = \pm\mathrm{i}$. In [3], where the integrals are over $\mathbb{C}^+$, this

J. Stat. Mech. (2011) P02008

singularity at the branch point was an important ingredient in the analysis. But when we now consider a perturbing operator on the boundary, the only divergence in the integrand in (21) comes when $\tau_1 = \tau_2$. Expanding $|\mathrm{d}z/\mathrm{d}w|^{1-x_\mathrm{b}} \equiv f(w)$ around $w = \tau_2$ gives

$$\begin{aligned}\delta^2 F_{\mathcal{R}_n} - n\delta^2 F &= \frac{\lambda^2}{4\beta}\int \mathrm{d}\tau_1 \int \mathrm{d}\tau_2 \frac{(f'(\tau_2)(\tau_1-\tau_2) + (1/2)f''(\tau_2)(\tau_1-\tau_2)^2 + \cdots)^2}{|\tau_1-\tau_2|^{2x_\mathrm{b}}} \\ &= \frac{\lambda^2}{4\beta}\int \mathrm{d}\tau_1 \int \mathrm{d}\tau_2 \,[\,(f'(\tau_2))^2|\tau_1-\tau_2|^{2-2x_\mathrm{b}} \\ &\quad + f'(\tau_2)f''(\tau_2)(\tau_1-\tau_2)|\tau_1-\tau_2|^{2-2x_\mathrm{b}} + \cdots]. \end{aligned} \tag{22}$$

From this it follows that the leading divergence of the double integral in (21) goes as $\epsilon^{3-2x_\mathrm{b}}$, i.e. it converges when $x_\mathrm{b} < 3/2$. Then no regularization is needed, and the only ℓ-dependence comes from $\mathrm{d}z/\mathrm{d}w \propto \ell$. Thus, when $x_\mathrm{b} < 3/2$

$$\delta^2 F_{\mathcal{R}_n} - n\delta^2 F \sim (\ell/\epsilon)^{2-2x_\mathrm{b}}, \tag{23}$$

and consequently the leading corrections $\delta^2 S_\mathrm{A}^{(n)}$ to the Rényi entropies are of the form

$$\delta^2 S_\mathrm{A}^{(n)} \sim \ell^{2-2x_\mathrm{b}}. \tag{24}$$

On the other hand, when $x_\mathrm{b} > 3/2$, the cutoff in the integral (21) must be kept, so that

$$\delta^2 F_{\mathcal{R}_n} - n\delta^2 F \sim (\ell/\epsilon)^{2-2x_\mathrm{b}}(\ell/\epsilon)^{2x_\mathrm{b}-3} = (\ell/\epsilon)^{-1}, \tag{25}$$

and then $\delta^2 S_\mathrm{A}^{(n)} \sim \ell^{-1}$ for all $x_\mathrm{b} > 3/2$. Note that this is of the same form as the first-order correction from the stress-energy tensor.

When $x_\mathrm{b} = 3/2$, it follows from equation (22) that the integral (21) diverges logarithmically, hence

$$\delta^2 S_\mathrm{A}^{(n)} \sim \ell^{-1}\log\ell. \tag{26}$$

4. Scaling corrections from marginal boundary operators

When perturbing with a marginal boundary operator one cannot simply put $x_\mathrm{b} = 1$ in equation (21) and conclude that the second-order corrections to scaling of the Rényi entropies vanish, since $|\mathrm{d}z/\mathrm{d}w|$ diverges when $|z| \to \infty$. However, it can be checked that there is no need to regularize the integral because of this. We therefore conclude that the second-order corrections will be ℓ-independent when $x_\mathrm{b} = 1$.

Instead of going to the higher-order integrals in the perturbation series of $F_{\mathcal{R}_n} - nF$ to find the leading ℓ-dependence of the corrections we will make use of the g-theorem [16], analogously to how Cardy and Calabrese [3] use the c-theorem in the marginal bulk case.

The boundary entropy s^A of equation (6) is governed by the 'gradient formula' of Friedan and Konechny [17] which in our case takes the simple form

$$\frac{\partial s^A}{\partial\lambda} = -\beta(\lambda), \tag{27}$$

where β is the renormalization group beta function given by [18]

$$-\beta(\lambda) = \ell\frac{\mathrm{d}\lambda}{\mathrm{d}\ell} = (1-x_\mathrm{b})\lambda - \pi b\lambda^2 + \mathcal{O}(\lambda^3). \tag{28}$$

J. Stat. Mech. (2011) P02008

In the marginally irrelevant case, i.e. with $x_\mathrm{b} = 1$ and $\lambda/b > 0$, this gives

$$\ell\frac{\mathrm{d}\lambda}{\mathrm{d}\ell} = -\pi b\lambda^2 + \mathcal{O}(\lambda^3), \tag{29}$$

with the asymptotic large-ℓ solution given by

$$\lambda(\ell) \sim \frac{1}{\pi b \log(\ell/\epsilon)}. \tag{30}$$

Now, as equation (27) becomes $\partial s^A/\partial\lambda = -\pi b\lambda^2 + \mathcal{O}(\lambda^3)$ when $x_\mathrm{b} = 1$, we have

$$s^A = \text{const.} - \frac{\pi b}{3}\lambda^3 + \mathcal{O}(\lambda^4) \sim \log g^A - \frac{1}{3\pi^2 b^2 \log^3(\ell/\epsilon)}. \tag{31}$$

Thus the leading correction to the Rényi entropies goes as $(\log\ell)^{-3}$.

5. Conclusions

The result that the leading second-order corrections to the Rényi entropies $S_\mathrm{A}^{(n)}$ are of the form ℓ^{2-2x_b} when perturbing with an irrelevant boundary operator with scaling dimension $x_\mathrm{b} < 3/2$ holds regardless of the value of n. This is the result anticipated from standard finite-size scaling, but for $x_\mathrm{b} \geq 3/2$ there is a deviation from this form. When $x_\mathrm{b} > 3/2$ the leading corrections will be of the same form as those from the stress-energy tensor, i.e. ℓ^{-1}. When $x_\mathrm{b} = 3/2$ there is also a multiplicative logarithmic contribution to the leading correction which then goes as $\ell^{-1}\log\ell$. A marginally irrelevant boundary perturbation gives a correction $\sim(\log\ell)^{-3}$. Thus there are no unusual n-dependent corrections to scaling of the Rényi entropies from boundary operators, as opposed to bulk perturbations where unusual corrections to scaling can occur. These unusual corrections originate from the part of the surface integral where the bulk operator approaches the branch point created by the Riemann surface construction [3]. However, when the perturbing field is *on* the boundary it never comes close to this singularity.

In [15] it was found that the first-order correction from the stress-energy tensor on the boundary is $\sim\ell^{-1}$. It should be noted that this operator is generically present, and gives a correction to the entanglement entropy of the same form as that from a boundary operator with scaling dimension $x_\mathrm{b} > 3/2$.

We also note that the leading corrections of the form ℓ^{2-2x_b} from a boundary perturbation are similar to what one can get when perturbing with a bulk operator in the presence of a boundary. In [3] it was found that this can give corrections of the form ℓ^{2-x}, where x is the bulk scaling dimension, but also unusual corrections which can dominate. This is therefore a very different situation compared to having the perturbing field on the boundary.

Acknowledgments

We wish to thank Pasquale Calabrese for helpful discussions. We also acknowledge NORDITA for hospitality during the completion of this work. This research was supported by the Swedish Research Council under Grant No. VR-2008-4358.

J. Stat. Mech. (2011) P02008

References

[1] For a review, see Calabrese P and Cardy J, *Entanglement entropy and conformal field theory*, 2009 *J. Phys. A: Math. Theor.* **42** 504005

[2] Calabrese P and Cardy J, *Entanglement entropy and quantum field theory*, 2004 *J. Stat. Mech.* P06002

[3] Cardy J and Calabrese P, *Unusual corrections to scaling in entanglement entropy*, 2010 *J. Stat. Mech.* P04023

[4] Calabrese P, Campostrini M, Essler F and Nienhuis B, *Parity effects in the scaling of block entanglement in gapless spin chains*, 2010 *Phys. Rev. Lett.* **104** 095701

[5] Calabrese P and Essler F, *Universal corrections to scaling for block entanglement in spin-1/2 XX chains*, 2010 *J. Stat. Mech.* P08029

[6] Laflorencie N, Sørensen E S, Chang M-S and Affleck I, *Boundary effects in the critical scaling of entanglement entropy in 1D systems*, 2006 *Phys. Rev. Lett.* **96** 100603

[7] Fagotti M and Calabrese P, *Universal parity effects in the entanglement entropy of XX chains with open boundary conditions*, 2011 *J. Stat. Mech.* P01017

[8] Cardy J and Lewellen D, *Bulk and boundary operators in conformal field theory*, 1991 *Phys. Lett.* B **259** 274

[9] Diehl H W and Dietrich S, *Field-theoretical approach to static critical phenomena in semi-infinite systems*, 1981 *Z. Phys.* B **42** 65
Diehl H W and Dietrich S, 1981 *Z. Phys.* B **43** 281 (erratum)

[10] For a review, see Affleck I, *Conformal field theory approach to the Kondo effect*, 1995 *Acta Phys. Pol.* B **26** 1869, arXiv:cond-mat/9512099

[11] For a review, see Angelantonj C and Sagnotti A, *Open strings*, 2002 *Phys. Rep.* **371** 1

[12] Calabrese P and Cardy J, *Time dependence of correlation functions following a quantum quench*, 2006 *Phys. Rev. Lett.* **96** 136801

[13] For a review, see Affleck I, Laflorencie N and Sørensen E S, *Entanglement entropy in quantum impurity systems and systems with boundaries*, 2009 *J. Phys. A: Math. Theor.* **42** 504009

[14] Zhou H-Q, Barthel T, Fjærestad J O and Schollwöck U, *Entanglement and boundary critical phenomena*, 2006 *Phys. Rev.* A **74** 050305(R)

[15] Sørensen E S, Chang M-S, Laflorencie N and Affleck I, *Impurity entanglement entropy and the Kondo screening cloud*, 2007 *J. Stat. Mech.* L01001

[16] Affleck I and Ludwig A W W, *Universal noninteger 'ground-state degeneracy' in critical quantum systems*, 1991 *Phys. Rev. Lett.* **67** 161

[17] Friedan D and Konechny A, *Boundary entropy of one-dimensional quantum systems at low temperature*, 2004 *Phys. Rev. Lett.* **93** 030402

[18] Cardy J, 1996 *Scaling and Renormalization in Statistical Physics* (*Cambridge Lecture Notes in Physics*) (Cambridge: Cambridge University Press)

J. Stat. Mech. (2011) P02008

Paper III

Impurity entanglement entropy in Kondo systems from conformal field theory

Erik Eriksson and Henrik Johannesson
Phys. Rev. B **8**4, 041107(R) (2011).

PHYSICAL REVIEW B **84**, 041107(R) (2011)

Impurity entanglement entropy in Kondo systems from conformal field theory

Erik Eriksson and Henrik Johannesson
Department of Physics, University of Gothenburg, SE 412 96 Gothenburg, Sweden
(Received 29 June 2011; published 28 July 2011)

The entanglement entropy in Kondo impurity systems is studied analytically using conformal field theory. From the impurity contribution to the scaling corrections of the entanglement entropy we extract information about the screening cloud profile for general non-Fermi-liquid fixed points. By also considering the finite-temperature corrections to scaling of the von Neumann entropy we point out a direct connection between the long-distance screening cloud profile and thermodynamic observables such as the specific heat.

DOI: 10.1103/PhysRevB.84.041107 PACS number(s): 64.70.Tg, 03.67.Mn, 75.30.Hx

Introduction. Entanglement—nonseparability of states—lies at the very heart of quantum theory. It has been recognized as the crucial resource needed for performing quantum computing and teleportation, but has also entered as an important concept in a wide range of fields spanning from black holes to biological systems.[1] Entanglement entropy, a measure of the entanglement between two parts of a quantum many-body system, has been used as a theoretical tool to study quantum phase transitions as well as characterizing topological phases of matter[2] and developing numerical algorithms.[3] A particularly important result has been for one-dimensional (1D) critical systems, where conformal field theory yields a universal prediction for the scaling of the entanglement entropy.[4,5] When such a system has a boundary, it provides a framework for the description of universal features of quantum impurity systems.[6] Important information can be obtained by studying the subleading corrections to the scaling of the entanglement entropy,[7] suggesting a new perspective on the long-standing problem of the evasive "Kondo screening cloud."[8]

Regarding the question of measuring entanglement entropy experimentally, it needs to be related to observable quantities. Recent attempts have focused on the connection between entanglement and fluctuations.[9,10] In particular, for critical one-dimensional systems with boundaries there is not only the same logarithmic scaling, but also the corrections to scaling of the entanglement entropy and those of the particle (or spin) fluctuations show interesting similarities.[10]

In this Rapid Communication, we employ boundary conformal field theory (BCFT) to give a unified picture of the entanglement entropy in quantum impurity problems. In particular, we unveil another type of connection between zero-temperature entanglement and fluctuations, this time finite-temperature thermodynamic fluctuations (in the form of the impurity specific heat), at the level of scaling corrections. As we shall argue below, this provides an experimental inroad to the study of Kondo screening clouds. The same framework allows us to extend the Fermi-liquid analysis of Sørensen *et al*.[8] of the long-distance behavior of the entanglement entropy generated by a Kondo impurity to the whole range of non-Fermi-liquid fixed points in the large family of Kondo systems.

For the Fermi-liquid case, there is an intuitive picture relating the impurity contribution to the entanglement entropy and the form of the Kondo screening cloud.[8] In a valence-bond basis, the screening cloud can be thought of as the distribution of singlet bonds between the impurity and conduction electrons; hence the valence bond entanglement entropy[11] provides the connection. Now, there is no such intuitive picture for the non-Fermi-liquid case of the more complex Kondo systems, but the analogy provides a rationale for regarding the impurity entanglement entropy as a good description of the screening cloud profile even when the (partial) screening is carried out by the highly nontrivial objects that make up the non-Fermi-liquid ground state. Importantly, our BCFT result which establishes an exact relation between the impurity contributions to the entanglement and the specific heat in terms of scaling corrections of the von Neumann entropy then shows that there is a direct connection between the long-distance behavior of the screening cloud and an experimental observable.

von Neumann entropy from BCFT. Entanglement entropy in a zero-temperature bipartite system is encoded in the von Neumann entropy. For a critical 1D semi-infinite bipartite system at inverse temperature β, the scaling of the von Neumann entropy $S(r) = -\mathrm{Tr}\hat{\rho}(r)\ln\hat{\rho}(r)$ of the reduced density matrix $\hat{\rho}(r)$ for an interval of length r at the boundary of the system is given by[4,12]

$$S(r) = \frac{c}{6}\ln\left[\frac{\beta}{\epsilon\pi}\sinh\left(\frac{2\pi r}{\beta}\right)\right] + \ln g + c' + \cdots . \quad (1)$$

Here c is the central charge, $\ln g$ is the boundary entropy,[13] ϵ is a short-distance cutoff, and c' is a nonuniversal constant. This relates the logarithmic scaling in r of the zero-temperature entanglement entropy to the scaling of the extensive thermodynamic entropy when $r/\beta \to \infty$. We will now see that there is a somewhat similar relation also for the *scaling corrections* of $S(r)$, denoted by "$\cdots$" in Eq. (1). These corrections are governed by the irrelevant operators (in the language of the renormalization group) in the BCFT that describes the critical properties of the system, and will have both bulk and boundary contributions. For quantum impurity systems, the fixed-point properties can be described by a BCFT where the impurity has been reduced to a specific boundary condition and boundary operator content.[14] Therefore, we see from Eq. (1) that the impurity contribution $S_{\mathrm{imp}}(r)$ to the von Neumann entropy $S(r)$ is

$$S_{\mathrm{imp}}(r) = \ln g + \cdots . \quad (2)$$

Now "$\cdots$" is the boundary contribution to the scaling corrections of $S(r)$, which is governed by the irrelevant *boundary* operators $\{\phi_b\}$ in the theory.

The von Neumann entropy is calculated as $S(r) = \lim_{n\to 1}(1-n)^{-1}\ln \mathrm{Tr}\hat{\rho}^n(r)$. When perturbing the BCFT with an irrelevant boundary operator, $H = H_{\mathrm{BCFT}} + \lambda\,\phi_b$, the leading correction to $S(r)$ is generically of second order in the scaling field λ and can be written as

$$\delta S \sim \frac{\lambda^2}{4}\int_{-\beta/2}^{\beta/2} d\tau_1 \int_{-\beta/2}^{\beta/2} d\tau_2 \frac{\left(\left|\frac{dz}{dw}\right|_{w=\tau_1}^{1-x_b} - \left|\frac{dz}{dw}\right|_{w=\tau_2}^{1-x_b}\right)^2}{\left|\frac{\beta}{\pi}\sin[\frac{\pi}{\beta}(\tau_1-\tau_2)]\right|^{2x_b}}. \quad (3)$$

Here $|dz/dw|$ comes from the mapping $z \mapsto w$ that takes the n-sheeted Riemann surface $\mathcal{R}_n$ in the finite-temperature geometry (representing $\mathrm{Tr}\hat{\rho}^n$) to the finite-temperature strip $\{w = \tau + iy \mid -\beta/2 \leqslant \tau \leqslant \beta/2, y \geqslant 0\}$ in the complex upper half plane $\mathbb{C}^+$. The cutoff in the integral is given by $|\tau_1 - \tau_2| \geqslant \epsilon/|dz/dw|_{w=\tau_1}$. Equation (3), where x_b is the scaling dimension of ϕ_b, follows from the analysis in Ref. 15, generalized to finite temperature.

In the limit $r/\beta \to 0$, we get $|dz/dw| \propto r + O((r/\beta)^3)$. This gives, as expected from the zero-temperature result in Ref. 15, that $S_{\mathrm{imp}} = \ln g + \delta S_{\mathrm{imp}}$, where δS_{imp} is found from Eq. (3) as

$$\delta S_{\mathrm{imp}} \sim \begin{cases} r^{2-2x_b} & \text{if } 1 < x_b < 3/2\,, \\ r^{-1}\ln r & \text{if } x_b = 3/2\,, \\ r^{-1} & \text{if } x_b > 3/2\,, \end{cases} \quad (4)$$

up to terms $O((r/\beta)^3)$. A marginally irrelevant perturbation generates a leading correction $\sim (\ln \ell)^{-3}$, while an exactly marginal perturbation describes new fixed points and hence changes S_{imp} by a constant. The corrections in Eq. (4) are all second order in λ; the only operator which gives a nonvanishing first-order correction is the stress-energy tensor which gives a correction[8] $\sim r^{-1}$.

It is also possible to extract the behavior in the limit $r/\beta \to \infty$ (still at low temperature, i.e., large β, but taking $r \gg \beta$). We then get that $|dz/dw| \propto \beta + O(\beta^{-1})$, up to terms $O(e^{-2\pi r/\beta})$. Changing the integration variable to $u = \tan(\pi|\tau_1 - \tau_2|/\beta)$ and expanding the integrand in Eq. (3) in a power series at the divergence at $u = 0$ gives

$$\delta S_{\mathrm{imp}} \sim \lambda^2\beta^{5-4x_b}\int_{-\beta/2}^{\beta/2} d\tau_1 \int_0^{\infty} du[f_1(\tau_1)u^{2-2x_b} + [f_2(\tau_1) + \beta f_3(\tau_1)]u^{3-2x_b} + \cdots], \quad (5)$$

where $f_i(\tau_1)$ are regular functions. When $x_b \geqslant 3/2$, we must use the short-time cutoff, which in the u variable becomes $u \geqslant \pi\epsilon/(\beta|dz/dw|_{w=\tau_1}) \sim \epsilon/\beta^2$. Then the leading β dependence goes as $\delta S_{\mathrm{imp}} \sim \beta^{5-4x_b}\beta^{4x_b-6} = \beta^{-1}$ when $x_b > 3/2$, and $\delta S_{\mathrm{imp}} \sim \beta^{5-4x_b}\ln\beta = \beta^{-1}\ln\beta$ when $x_b = 3/2$. When $1 < x_b < 3/2$, we see from Eq. (5) that the integral (3) converges. Hence the leading β dependence comes from the prefactor β^{2-2x_b} arising from $|dz/dw| \propto \beta$. Summarizing, in the limit $r/\beta \to \infty$ we get $S_{\mathrm{imp}} = \ln g + \delta S_{\mathrm{imp}}$, with

$$\delta S_{\mathrm{imp}} \sim \begin{cases} \beta^{2-2x_b} & \text{if } 1 < x_b < 3/2\,, \\ \beta^{-1}\ln\beta & \text{if } x_b = 3/2\,, \\ \beta^{-1} & \text{if } x_b > 3/2\,, \end{cases} \quad (6)$$

to $O(\beta^{-1})$ in β and $O(e^{-2\pi r/\beta})$ in r/β.

The results in Eq. (6) bear a close resemblance to the well-known expressions for the impurity specific heat C_{imp} at criticality.[16,17] In fact, as C_{imp} is related to the thermodynamic impurity entropy $S_{\mathrm{imp}}^{\mathrm{Th}}$ via the relation $C_{\mathrm{imp}} = -\beta\,\partial S_{\mathrm{imp}}^{\mathrm{Th}}/\partial\beta$, they describe the same power law, and one has the leading behavior

$$S_{\mathrm{imp}}^{\mathrm{Th}} = \ln g + \begin{cases} \lambda^2 A_1\beta^{2-2x_b} & \text{if } 1 < x_b < 3/2\,, \\ \lambda^2 A_2\beta^{-1}\ln\beta & \text{if } x_b = 3/2\,, \\ \lambda^2 A_3\beta^{-1} & \text{if } x_b > 3/2\,, \end{cases} \quad (7)$$

as $\beta \to \infty$, where A_1, A_2, and A_3 are constants. Thus the von Neumann and thermodynamic impurity entropies have the same form on their leading scaling corrections in the limit $r/\beta \to \infty$ at low temperature. However, the amplitudes of these scaling corrections are different, as the von Neumann entropy acquires an additional amplitude factor from the mapping from the Riemann surface, not present in the thermodynamic entropy.

Impurity entanglement entropy in Kondo systems. At zero temperature the von Neumann entropy measures the entanglement between the two parts of the bipartite system, and the impurity part $S_{\mathrm{imp}}(r)$ in Eq. (2) is then referred to as the impurity entanglement entropy.[8] We can therefore use the zero-temperature results in Eq. (4) to predict the impurity entanglement entropy in various Kondo impurity models. They all share the common feature that the only significant zero-temperature length scale is the Kondo length $\xi_K \sim v_F/T_K$, the characteristic length scale at which screening is supposed to occur (here v_F is the Fermi velocity and T_K the Kondo temperature). In particular, the distance dependence of S_{imp} can only come through r/ξ_K. Note that when the models describe two- (three-) dimensional systems the size r of the block at the boundary will correspond to the radius of a disk (sphere) centered at the impurity (or the midpoint between the impurities when they are two). Thus the impurity entanglement entropy measures the impurity-generated entanglement between the part of the system within radius r (including the impurity) and the rest of the system. It appears as a natural measure of the shape of this screening cloud since it captures the spatial distribution of the entanglement from the impurity. Compared to other ways of probing Kondo screening with entanglement,[18] the impurity entanglement entropy has the advantage of allowing analytical results based on BCFT.

The BCFT approach,[14] where the model is reduced to one spatial dimension with the impurity as a special boundary condition, is only valid in the limit $r \gg \xi_K$. Hence we expect the BCFT prediction for S_{imp} at zero temperature to describe the long-distance decay of the Kondo screening cloud. By our exact analysis above, the leading r dependence of S_{imp} in Eq. (4) has the same form as the leading β dependence of C_{imp}, so the long-distance zero-temperature profile of the screening cloud is encoded by the impurity specific heat. The relation to the impurity entanglement entropy is less direct for the impurity susceptibility, which is governed by the same irrelevant boundary operator but through coupling to the bulk spin operator.[16] We now illustrate our result for a large class of Kondo impurity systems.

The Kondo model. The original Kondo model describes a band of conduction electrons interacting with a single magnetic $s = 1/2$ impurity at the origin:

$$H_K = \sum_{\vec{k},\alpha=\uparrow,\downarrow} \epsilon(\vec{k}) \psi^{\dagger\alpha}_{\vec{k}} \psi_{\vec{k}\alpha} + J\,\vec{S} \cdot \sum_{\alpha,\beta=\uparrow,\downarrow} \psi^{\dagger\alpha}(\vec{0}) \frac{\vec{\sigma}^{\beta}_{\alpha}}{2} \psi_{\beta}(\vec{0}) \,. \quad (8)$$

At the low-temperature Kondo screening fixed point, $\ln g = 0$, and the leading irrelevant boundary operator is the stress-energy tensor T. As found in Ref. 8, adding the boundary perturbation $\delta H = -(\xi_K/2)\,T(0)$ to the fixed-point Hamiltonian $H_{\rm BCFT}$ gives $S_{\rm imp}(r) = \pi\xi_K/(12r)$ for $r \gg \xi_K$, in agreement with DMRG results and consistent with a valence-bond picture.

Breaking particle-hole symmetry introduces the exactly marginal charge current operator as a perturbation at the fixed point, only giving a constant shift of $S_{\rm imp}(r)$.

The two-impurity Kondo model. Adding a second spin-1/2 impurity to the Kondo model gives the two-impurity Kondo model (TIKM),

$$H_{\rm TIKM} = \sum_{\vec{k},\alpha=\uparrow,\downarrow} \epsilon(\vec{k}) \psi^{\dagger\alpha}_{\vec{k}} \psi_{\vec{k}\alpha} + J\,[\,\vec{s}_c(\vec{r}_1) \cdot \vec{S}_1 + \vec{s}_c(\vec{r}_2) \cdot \vec{S}_2\,] + K\,\vec{S}_1 \cdot \vec{S}_2 \,, \quad (9)$$

where $\vec{s}_c(\vec{r}) = (1/2) \sum_{\alpha,\beta} \psi^{\alpha\dagger}(\vec{r}) \vec{\sigma}^{\beta}_{\alpha} \psi_{\beta}(\vec{r})$. The BCFT solution of the model was found in Ref. 19. In short, the model features an unstable fixed point at $K = K_c \sim T_K$, where the system undergoes a quantum phase transition. At this fixed point $\ln g = \ln\sqrt{2}$, and the leading irrelevant boundary operator allowed by symmetry to appear as a perturbation is $L_{-1}\epsilon$, the Virasoro first descendant of the ϵ field, with scaling dimension $x_b = 3/2$. However, being a Virasoro first descendant, $L_{-1}\epsilon$ will not give any contribution to the entanglement entropy or any finite-temperature properties *to any order* in perturbation theory. This follows from the evaluation of integrals of the type $\int_{-\infty}^{\infty} d\tau \langle L_{-1}\epsilon \rangle_{\mathcal{R}_n} = \int_{-\infty}^{\infty} d\tau\, \partial_\tau \langle \epsilon \rangle_{\mathcal{R}_n}$ which vanish due to the periodicity of the boundary of the n-sheeted Riemann surface $\mathcal{R}_n$. The leading correction to the impurity entanglement entropy therefore comes from the stress-energy tensor T, precisely as in the single-impurity case. Thus, adding T as a boundary perturbation to the fixed-point Hamiltonian $H_{\rm BCFT}$,

$$H = H_{\rm BCFT} + a\sqrt{\xi_K} L_{-1}\epsilon(0) - b\,\xi_K T(0) \,, \quad (10)$$

with a and b dimensionless constants, gives the impurity entanglement entropy in the limit $r \gg \xi_K$ as

$$S_{\rm imp}(r) = \ln\sqrt{2} + \pi b\,\xi_K/(6r) \,. \quad (11)$$

Breaking the SU(2) spin-rotational symmetry or the parity symmetry introduces a boundary operator with scaling dimension[19] $x_b = 3/2$. Particle-hole symmetry breaking can be either relevant or exactly marginal. Simultaneously breaking the particle-hole and parity symmetries adds another $x_b = 3/2$ boundary operator.[20]

The multichannel Kondo model. The Hamiltonian is obtained by adding a channel index $i = 1,2,\ldots,k$ to the electrons in Eq. (8), so that the spin-s impurity interacts with k degenerate bands of conduction electrons. When $k > 2s$, the system is governed by an overscreened non-Fermi-liquid fixed point, corresponding to a boundary entropy[21] $\ln g = \ln\{\sin[\pi(2s+1)/(2+k)]/\sin[\pi/(2+k)]\}$. The leading irrelevant boundary operator has scaling dimension[16] $x_b = 1 + 2/(2+k)$, in agreement with the original Bethe ansatz solution.[21] Thus, when $k = 2$ the distance-dependent part of $S_{\rm imp}(r)$ falls off as $\sim (\xi_K/r)\ln(r/\xi_K)$. For arbitrary $k > 2$, where $1 < x_b < 3/2$, one gets

$$S_{\rm imp}(r) = \ln g + A\,(r/\xi_K)^{-4/(2+k)} , \quad (12)$$

for $r \gg \xi_K$, with A a constant. We see that the more channels that are added, the more long-range entanglement appears to be generated from the screening of the impurity by the composite soliton-like objects formed in the non-Fermi liquid.[21] The screening cloud falls off with an anomalous power law, a result rather similar to the one obtained by Barzykin and Affleck[22] when defining it as the form of the equal-time spin-spin correlator.

Channel asymmetry is a relevant perturbation,[23] whereas particle-hole symmetry breaking is exactly marginal.[16] The effect of spin-rotational symmetry breaking depends on s and k;[23] however for the special cases where the perturbation is irrelevant the only difference is a change in the constant A in Eq. (12).

Generalizing the multichannel Kondo model by extending the spin symmetry group from SU(2) to SU(N) gives the *multichannel SU(N) Kondo model*.[24] The leading irrelevant operator at the overscreened non-Fermi-liquid fixed point now has scaling dimension $x_b = 1 + N/(N+k)$. Hence $S_{\rm imp}(r) = \ln g + A\,(r/\xi_K)^{-2N/(N+k)}$ for $r \gg \xi_K$, with A a constant and $\ln g$ depending on the particular representation of SU(N).

The two-impurity, two-channel Kondo model features a continuous family of non-Fermi-liquid fixed points,[25] allowing for scaling-correction terms in $S_{\rm imp}(r)$ from boundary operators with scaling dimensions ranging all the way from $x_b = 1$ to infinity.

The final case we consider is a *Kondo impurity in a Luttinger liquid*. At zero temperature $\ln g = 0$,[26] but the leading perturbation typically has $1 < x_b < 3/2$ (Ref. 17) and Eq. (4) then predicts that $S_{\rm imp}(r) \sim r^{2-2x_b}$.

Discussion. We have provided a unified picture for the impurity entanglement entropy $S_{\rm imp}$ for the large class of Kondo models in terms of the scaling corrections arising from the boundary operators of the corresponding BCFT, valid for $r \gg \xi_K$. When $r/\beta \to \infty$ the scaling part of the von Neumann entropy approaches the thermodynamic entropy,[4] and it has been argued that this is expected on general grounds.[8] Our analysis shows that this reasoning can also be applied to the scaling corrections, but only in the following precise sense: The impurity von Neumann entropy and thermodynamic entropy have the same leading power-law dependence of β at low temperatures, however with different amplitudes. This connects the exponents for the temperature scaling of the impurity specific heat with those for the large-distance scaling of the zero-temperature impurity entanglement entropy, through the von Neumann entropy.

The result suggests that the long-distance profile of a zero-temperature Kondo screening cloud can be read off from the impurity specific heat at low temperature, an experimentally accessible observable. For the original single-impurity Kondo

model, $S_{\rm imp}(r)$ was indeed found[8] to follow the same power law as the impurity specific heat $C_{\rm imp}(\beta)$, showing that this also holds for the first-order correction from the stress-energy tensor. This is also what we see when considering the BCFT predictions for a number of more complex Kondo impurity models, thereby demonstrating the close connection between Kondo screening, entanglement, and thermodynamics in quantum impurity systems.

We wish to thank Natan Andrei and Fabien Alet for helpful communications. This research was supported by the Swedish Research Council under Grant No. VR-2008-4358.

[1]Reviewed in R. Horodecki, P. Horodecki, M. Horodecki, and K. Horodecki, Rev. Mod. Phys. **81**, 865 (2009).
[2]For a review, see L. Amico, R. Fazio, A. Osterloh, and V. Vedral, Rev. Mod. Phys. **80**, 517 (2008).
[3]For a review, see F. Verstraete, J. I. Cirac, and V. Murg, Adv. Phys. **57**, 143 (2008).
[4]P. Calabrese and J. Cardy, J. Stat. Mech. (2004) P06002.
[5]For a review, see P. Calabrese and J. Cardy, J. Phys. A: Math. Theor. **42**, 504005 (2009).
[6]For a review, see I. Affleck, N. Laflorencie, and E. S. Sørensen, J. Phys. A: Math. Theor. **42**, 504009 (2009).
[7]J. Cardy and P. Calabrese, J. Stat. Mech. (2010) P04023.
[8]E. S. Sørensen, M.-S. Chang, N. Laflorencie, and I. Affleck, J. Stat. Mech. (2007) L01001; (2007) P08003.
[9]I. Klich and L. Levitov, Phys. Rev. Lett. **102**, 100502 (2009).
[10]H. F. Song, S. Rachel, and K. Le Hur, Phys. Rev. B **82**, 012405 (2010).
[11]F. Alet, S. Capponi, N. Laflorencie, and M. Mambrini, Phys. Rev. Lett. **99**, 117204 (2007).
[12]H.-Q. Zhou, T. Barthel, J. O. Fjærestad, and U. Schollwöck, Phys. Rev. A **74**, 050305(R) (2006).
[13]I. Affleck and A. W. W. Ludwig, Phys. Rev. Lett. **67**, 161 (1991).
[14]Reviewed in I. Affleck, Acta Phys. Pol. B **26**, 1869 (1995).
[15]E. Eriksson and H. Johannesson, J. Stat. Mech. (2011) P02008.
[16]I. Affleck and A. W. W. Ludwig, Nucl. Phys. B **352**, 849 (1991); **360**, 641 (1991).
[17]P. Fröjdh and H. Johannesson, Phys. Rev. B **53**, 3211 (1996).
[18]A. Bayat, P. Sodano, and S. Bose, Phys. Rev. B **81**, 064429 (2010).
[19]I. Affleck, A. W. W. Ludwig, and B. A. Jones, Phys. Rev. B **52**, 9528 (1995).
[20]D. F. Mross and H. Johannesson, Phys. Rev. B **78**, 035449 (2008).
[21]N. Andrei and C. Destri, Phys. Rev. Lett. **52**, 364 (1984); **59**, 155 (1987).
[22]V. Barzykin and I. Affleck, Phys. Rev. B **57**, 432 (1998).
[23]I. Affleck, A. W. W. Ludwig, H.-B. Pang, and D. L. Cox, Phys. Rev. B **45**, 7918 (1992).
[24]O. Parcollet, A. Georges, G. Kotliar, and A. Sengupta, Phys. Rev. B **58**, 3794 (1998); P. Zinn-Justin and N. Andrei, Nucl. Phys. B **528**, 648 (1998).
[25]A. Georges and A. M. Sengupta, Phys. Rev. Lett. **74**, 2808 (1995); Nucl. Phys. B, Proc. Suppl. **58**, 105 (1997).
[26]A. Furusaki and N. Nagaosa, Phys. Rev. Lett. **72**, 892 (1994).

Paper IV

Electrical control of the Kondo effect in a helical edge liquid

Erik Eriksson, Anders Ström, Girish Sharma, and Henrik Johannesson
Phys. Rev. B **8**6, 161103(R) (2012).

PHYSICAL REVIEW B **86**, 161103(R) (2012)

Electrical control of the Kondo effect in a helical edge liquid

Erik Eriksson,[1] Anders Ström,[1] Girish Sharma,[2] and Henrik Johannesson[1]
[1]*Department of Physics, University of Gothenburg, SE-412 96 Gothenburg, Sweden*
[2]*Centre de Physique Théorique, Ecole Polytechnique, FR-91128 Palaiseau Cedex, France*
(Received 12 July 2012; published 5 October 2012)

Magnetic impurities affect the transport properties of the helical edge states of quantum spin Hall insulators by causing single-electron backscattering. We study such a system in the presence of a Rashba spin-orbit interaction induced by an external electric field, showing that this can be used to control the Kondo temperature, as well as the correction to the conductance due to the impurity. Surprisingly, for a strongly anisotropic electron-impurity spin exchange, Kondo screening may get obstructed by the presence of a noncollinear spin interaction mediated by the Rashba coupling. This challenges the expectation that the Kondo effect is stable against time-reversal invariant perturbations.

DOI: 10.1103/PhysRevB.86.161103 PACS number(s): 71.10.Pm, 72.10.Fk, 85.75.−d

Introduction. The discovery that HgTe quantum wells support a quantum spin Hall (QSH) state[1] has set off an avalanche of studies addressing the properties of this novel phase of matter.[2] A key issue has been to determine the conditions for stability of the current-carrying states at the edge of the sample as this is the feature that most directly impacts prospects for future applications in electronics and spintronics. In the simplest picture of a QSH system the edge states are *helical*, with counterpropagating electrons carrying opposite spins. By time-reversal invariance electron transport then becomes ballistic, provided that the electron-electron (*e-e*) interaction is sufficiently well screened so that higher-order scattering processes do not come into play.[3,4]

The picture gets an added twist when including effects from magnetic impurities, contributed by dopant ions or electrons trapped by potential inhomogeneities. Since an edge electron can backscatter from an impurity via spin exchange, time-reversal invariance no longer protects the helical states from mixing. In addition, correlated two-electron[5] and inelastic single-electron processes[6,7] must now also be accounted for. As a result, at high temperatures T electron scattering off the impurity leads to a $\ln(T)$ correction[8] of the conductance at low frequencies ω, which, however, vanishes[9] in the dc limit $\omega \to 0$. At low T, for weak *e-e* interactions, the quantized edge conductance $G_0 = e^2/h$ is restored as $T \to 0$ with power laws distinctive of a helical edge liquid. For strong interactions the edge liquid freezes into an insulator at $T = 0$, with thermally induced transport via tunneling of fractionalized charge excitations through the impurity.[8]

A more complete description of edge transport in a QSH system must include also the presence of a Rashba spin-orbit interaction. This interaction, which can be tuned by an external gate voltage, is a built-in feature of a quantum well.[10] In fact, HgTe quantum wells exhibit some of the largest known Rashba couplings of any semiconductor heterostructures.[11] As a consequence, spin is no longer conserved, contrary to what is assumed in the minimal model of a QSH system.[12] However, since the Rashba interaction preserves time-reversal invariance, Kramers' theorem guarantees that the edge states are still connected via a time-reversal transformation ("Kramers pair").[13] Provided that the Rashba interaction is spatially uniform and the *e-e* interaction is not too strong, this ensures the robustness of the helical edge liquid.[14]

What is the physics with both Kondo *and* Rashba interactions present? In this Rapid Communication we address this question with a renormalization group (RG) analysis as well as a linear-response and rate-equation approach. Specifically, we predict that the Kondo temperature T_K—which sets the scale below which the electrons screen the impurity—can be controlled by varying the strength of the Rashba interaction. Surprisingly, for a strongly anisotropic Kondo exchange, a noncollinear spin interaction mediated by the Rashba coupling becomes relevant (in the sense of RG) and competes with the Kondo screening. This challenges the expectation that the Kondo effect is stable against time-reversal invariant perturbations.[15] Moreover, we show that the impurity contribution to the dc conductance at temperatures $T > T_K$ can be switched on and off by adjusting the Rashba coupling. With the Rashba coupling being tunable by a gate voltage, this suggests an inroad to control charge transport at the edge of a QSH device.

Model. To model the edge electrons, we introduce the two-spinors $\Psi^T = (\psi_\uparrow, \psi_\downarrow)$, where $\psi_\uparrow$ ($\psi_\downarrow$) annihilates a right-moving (left-moving) electron with spin up (spin down) along the growth direction of the quantum well. Neglecting *e-e* interactions, the edge Hamiltonian can then be written as

$$\begin{aligned} H = v_F \int dx\ \Psi^\dagger(x)[-i\sigma^z\partial_x]\Psi(x) \\ + \alpha \int dx\ \Psi^\dagger(x)[-i\sigma^y\partial_x]\Psi(x) \\ + \Psi^\dagger(0)[J_x\sigma^x S^x + J_y\sigma^y S^y + J_z\sigma^z S^z]\Psi(0), \end{aligned} \quad (1)$$

with v_F the Fermi velocity parametrizing the linear kinetic energy. The second term encodes the Rashba interaction of strength α, with the third term being an antiferromagnetic Kondo interaction between electrons (with Pauli matrices $\sigma^i, i = x,y,z$) and a spin-1/2 magnetic impurity (with Pauli matrices $S^i, i = x,y,z$) at $x = 0$. The spin-orbit induced magnetic anisotropy for an impurity at a quantum well interface[16] implies that[17] $J_x = J_y \neq J_z$. Unless otherwise stated, we use $\hbar = k_B \equiv 1$.

The Rashba term in Eq. (1) can be absorbed into the kinetic term by a spinor rotation[18] $\Psi' = e^{-i\sigma^x\theta/2}\Psi$. By rotating also the impurity spin, $\boldsymbol{S}' = e^{-iS^x\theta/2}\boldsymbol{S}e^{iS^x\theta/2}$, one obtains

$H = H_0' + H_K'$, with

$$H_0' = v_\alpha \int dx\ \Psi'^{\dagger}(x)[-i\sigma^{z'}\partial_x]\Psi'(x), \tag{2}$$

$$H_K' = \Psi'^{\dagger}(0)[J_x\sigma^x S^x + J_y'\sigma^{y'}S^{y'} + J_z'\sigma^{z'}S^{z'} + J_E(\sigma^{y'}S^{z'} + \sigma^{z'}S^{y'})]\Psi'(0), \tag{3}$$

where $J_y' = J_y\cos^2\theta + J_z\sin^2\theta$, $J_z' = J_z\cos^2\theta + J_y\sin^2\theta$, and $J_E = (J_y - J_z)\cos\theta\sin\theta$. The Rashba rotation angle θ is determined through $\cos\theta = v_F/v_\alpha$, $\sin\theta = \alpha/v_\alpha$, and $v_\alpha = \sqrt{v_F^2 + \alpha^2}$. Note that the spin in the rotated basis is quantized along the z' direction which forms an angle θ with the z axis. Also note that the Kondo interaction in this basis not only becomes spin nonconserving, but also picks up a noncollinear term for $J_y \neq J_z$.

Including *e-e* interactions, and assuming a band filling incommensurate with the lattice,[2] time-reversal invariance constrains the possible scattering channels in the rotated basis to dispersive ($\sim g_d$) and forward ($\sim g_f$) scattering, in addition to correlated two-particle backscattering[3,4] ($\sim g_{\rm bs}$) and inelastic single-particle backscattering[6,7,19] ($\sim g_{\rm ie}$) at the impurity site. Adding the corresponding interaction terms to H_0' and H_K' in (2) and (3), and employing standard bosonization,[20] the full Hamiltonian for the edge liquid can now be expressed as a free boson model, $(v/2)\int dx[(\partial_x\varphi)^2 + (\partial_x\vartheta)^2]$, with three local terms added at $x = 0$:

$$H_K' = \frac{A}{\kappa}\cos(\sqrt{4\pi K}\varphi) + \frac{B}{\kappa}\sin(\sqrt{4\pi K}\varphi) + \frac{C}{\sqrt{K}}\partial_x\vartheta, \tag{4}$$

$$H_{\rm bs}' = \frac{g_{\rm bs}}{2(\pi\kappa)^2}\cos(\sqrt{16\pi K}\varphi), \tag{5}$$

$$H_{\rm ie}' = \frac{g_{\rm ie}}{2\pi^2\sqrt{K}} : \left(\partial_x^2\vartheta\right)\cos(\sqrt{4\pi K}\varphi) : . \tag{6}$$

Here φ is a nonchiral Bose field with ϑ its dual, $v\partial_x\vartheta = \partial_t\varphi$ with $v = [(v_\alpha + g_f/\pi)^2 - (g_d/\pi)^2]^{1/2}$, $K = [(\pi v_\alpha + g_f - g_d)/(\pi v_\alpha + g_f + g_d)]^{1/2}$, and $\kappa \approx v_F/D$ is the edge state penetration depth acting as short-distance cutoff with D the bandwidth, and $: \cdots :$ denotes normal ordering. In H_K' we have defined $A = J_x S^x/\pi$, $B = (J_y'S^{y'} + J_E S^{z'})/\pi$, and $C = (J_z'S^{z'} + J_E S^{y'})/\pi$. The presence of H_{ie}' requires breaking of the $U(1)$ spin symmetry, as brought about by the Rashba interaction.

Kondo temperature. The bosonized theory is tailor made for a perturbative RG analysis, allowing us to determine the temperature scale below which the edge electrons couple strongly to the impurity. We first note that the backscattering term in (5) is that of the well-known boundary-sine Gordon model. For $K < 2/3$ it dominates over the inelastic backscattering in (6), and turns relevant for $K < 1/4$ with a weak to strong-coupling crossover at a temperature[21] $T_{\rm bs} \approx D g_{\rm bs}^{1/(1-4K)}$. As a consequence, the enhancement of backscattering as $T \to 0$ results in a zero-temperature insulating state when $K < 1/4$.

Turning to the Rashba-rotated Kondo interaction H_K' in Eq. (4), we obtain for its one-loop RG equations

$$\begin{aligned} \partial_l\tilde{J}_x &= (1-K)\tilde{J}_x + \nu K(\tilde{J}_y'\tilde{J}_z' - \tilde{J}_{E1}\tilde{J}_{E2}),\\ \partial_l\tilde{J}_y' &= (1-K)\tilde{J}_y' + \nu K\tilde{J}_x\tilde{J}_z', \quad \partial_l\tilde{J}_z' = \nu K\tilde{J}_x\tilde{J}_y',\\ \partial_l\tilde{J}_{E1} &= (1-K)\tilde{J}_{E1} - \nu K\tilde{J}_x\tilde{J}_{E2}, \quad \partial_l\tilde{J}_{E2} = -\nu K\tilde{J}_x\tilde{J}_{E1}, \end{aligned} \tag{7}$$

with the "tilde" indicating that the couplings depend on the renormalization length l, and where $\nu \equiv 1/(\pi v)$. The two terms proportional to J_E in Eq. (4) flow individually under RG, with the corresponding renormalized coupling constants here denoted $\tilde{J}_{E1}$ and $\tilde{J}_{E2}$. In deriving Eqs. (7) we have used that higher-order contributions involving an intermediate process governed by $H_{\rm bs}'$ or $H_{\rm ie}'$ are suppressed, since these transfer spin or energy incompatible with H_K'. In a recent work,[22] Kondo scattering without Rashba interaction was studied, and different physics in the regime $\nu J_z \geqslant 2K$ was found, not accessible perturbatively in νJ_z. Since its realization in an HgTe quantum well requires anomalously weak screening of the *e-e* interaction we do not consider this regime here.

The role of the Rashba rotation in Eqs. (7) is both to determine the bare values $\tilde{J}_{y,z}'(l=0) \equiv J_{y,z}'$ and to introduce the noncollinear couplings $\tilde{J}_{E1,E2}$. To explore the outcome, we first examine the case of a strongly screened *e-e* interaction, $K \approx 1$. For this case, the first-order terms of Eq. (7) can be neglected and $\tilde{J}_{E1} = \tilde{J}_{E2} = \tilde{J}_E$, since their scaling equations will be identical. In this limit, $\tilde{J}_E$ quickly flows to zero. We take the Kondo temperature T_K to be the value of $T = D\exp(-l)$, where one of the couplings in Eq. (7) first grows past $1/(\nu K)$, making the renormalized H_K' in Eq. (4) dominate the free theory. For $K \approx 1$ we then see that

$$T_K \approx D\exp\left(-\frac{1}{\nu J_x}\frac{\operatorname{arcsinh}(\zeta)}{\zeta}\right), \tag{8}$$

where $\zeta = \sqrt{(J_z/J_x)^2 - 1}$ is an anisotropy parameter.[8] Here the θ dependence lies predominantly in ν. Note that Kondo temperatures modified by spin-orbit couplings, as in (8), or by spin-dependent hopping, have been proposed recently also for ordinary conduction electrons.[23–27]

In the opposite limit of a strong *e-e* interaction, the second-order terms of the scaling equations can be neglected, as long as $1 - K \gg \tilde{J}\nu K$, for all $\tilde{J} = \tilde{J}_x, \tilde{J}_y', \tilde{J}_{E1}$. The scaling equations in this limit reduce to $\partial_l\tilde{J} = (1-K)\tilde{J}$, with solutions $\tilde{J} = Je^{(1-K)l}$. With $l = \ln(D/T)$, one can now use the $\tilde{J} = 1/(\nu K)$ criterion to find the Kondo temperature

$$T_K \approx D(J_{\max}\nu K)^{1/(1-K)}, \tag{9}$$

where $J_{\max} = \max[J_x, J_y', J_E]$.

In Fig. 1 we exhibit T_K for both "easy-plane" and "easy-axis" Kondo interaction. To isolate the effect of the Rashba interaction from that of the *e-e* interaction we choose to plot T_K as a function of θ and K_0, with $K_0 \equiv K(\theta{=}0)$ the ordinary Luttinger parameter. For $|J_E| > |J_x|, |J_y'|$, the noncollinear term $\sim\sigma^{y'}S^{z'}$ in Eq. (3) dominates the RG flow for values of K in the shaded "dome" (the size of which is set by the ratio $J_z/J_{x,y}$). As this term disfavors a spin singlet, Kondo screening will be obstructed in the corresponding interval of Rashba couplings.[28] This runs contrary to the

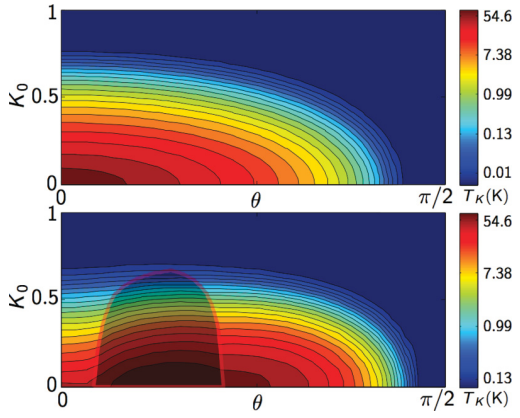

FIG. 1. (Color online) The Kondo temperature T_K as a function of the Rashba angle θ and the ordinary Luttinger parameter K_0. The T_K scale is logarithmic and red and blue colors indicate high and low T_K, respectively. Top: $J_x = J_y \geqslant J_z$ (here, $J_x/a_0 = J_z/a_0 = 10$ meV); bottom: $J_x = J_y < J_z$ (here, $J_x/a_0 = 5$ meV and $J_z/a_0 = 50$ meV). In the shaded area, $\tilde{J}_{E1}$ dominates the perturbative RG flow, hence obstructing singlet formation.

expectation that a spin-orbit interaction does not impair the Kondo effect.[15,29] However, this expectation is rooted in a noninteracting quasiparticle picture which breaks down in one dimension. Instead a Luttinger liquid is formed, with strongly correlated electron scattering.[20] As suggested by our RG analysis, when this scattering gets enhanced with lower values of K, it boosts the effect of the noncollinear spin interaction that works against the Kondo screening.

Conductance at low temperatures. Away from the "dome" in Fig. 1, the Rashba-rotated Kondo interaction easily sustains a Kondo temperature T_K below which the impurity gets screened. When $K > 1/4$ and two-particle backscattering is RG irrelevant, there is no correction δG to the conductance at zero temperature: As explained by Maciejko *et al.*,[8] the topological nature of the QSH state implies a "healing" of the edge after the impurity has been effectively removed by the Kondo screening. For finite $T \ll T_K$, the leading correction δG is generated by either $H'_{\rm bs}$ or $H'_{\rm ie}$, whatever operator has the lowest scaling dimension: For $1/4 < K < 2/3$ ($K > 2/3$) $H'_{\rm bs}(H'_{\rm ie})$ dominates, with[6–8] $\delta G_{\rm bs} \sim (T/T_K)^{8K-2}$ [$\delta G_{\rm ie} \sim (T/T_K)^{2K+2}$]. Thus, in the noninteracting limit $K \approx 1$, the presence of a Rashba interaction is revealed by a T^4 scaling of the conductance, rather than the expected T^6 scaling as in the minimal model with $U(1)$ spin symmetry.[8] The picture changes dramatically for $K < 1/4$. Now $H_{\rm bs}$ turns RG relevant, with $g_{\rm bs}$ entering a strong-coupling regime below the crossover temperature $T_{\rm bs}$, implying zero conductance at $T = 0$. At finite $T \ll T_{\rm bs}$, instanton processes restore its finite value, with[8] $G \sim (T/T_{\rm bs})^{2(1/4K-1)}$. To leading order this regime is blind to the Rashba interaction.

Conductance and currents at high temperatures. When $T > \max(T_K, T_{\rm bs})$, scattering from H'_K as well as from $H'_{\rm bs}$ and $H'_{\rm ie}$ remains weak, and transport properties can be obtained perturbatively. We here focus on the correction δG to the conductance due to H'_K, noting that the contributions from $H'_{\rm bs}$ and $H'_{\rm ie}$ decouple and are insensitive to the strength of the Rashba interaction.

The current operator $\hat{I}$ takes the form $\hat{I} = (e/2)\partial_t (\cos\theta \Psi'^{\dagger}\sigma^{z'}\Psi' - \sin\theta \Psi'^{\dagger}\sigma^{y'}\Psi')$ in the rotated basis. After the unitary transformation $U = e^{i\sqrt{\pi}\lambda\varphi(0)S^{z'}}$, which removes the J'_z term when $\lambda = J'_z/\pi v\sqrt{K}$, the bosonized part $\delta\hat{I}$ of the current operator due to H'_K is

$$\delta\hat{I} = \frac{ie}{2\pi\kappa}\Bigg[\sum_{j=\pm} A_j e^{i\sqrt{\pi}(2\sqrt{K}-j\lambda)\varphi} S^j + iA_0 e^{i\sqrt{4\pi K}\varphi} S^z - \frac{iJ_x}{\sqrt{\pi K}} \sin\theta : \partial_x \vartheta e^{-i\sqrt{\pi}\lambda\varphi} : S^+\Bigg] + \text{H.c.}, \qquad (10)$$

where $A_\pm = (1/2)(J_x \pm J_y)\cos\theta$, $A_0 = (J_E/2)\cos\theta$. Using the Kubo formula to calculate the conductance correction $\delta G(\omega)$ at a frequency ω in the limit $J^2 \ll \omega \ll T$, with $J^2 = J_x^2, J_y'^2, J_E^2$, we then find to $O(J^2)$

$$\delta G = -\frac{e^2}{\hbar}\sum_{j=-1}^{+1} F_j \cdot [A_j(T)]^2 - \frac{e^2}{\hbar}\mu J_x^2 \sin^2\theta, \qquad (11)$$

which, in this limit, is independent of ω. Here $A_j(T) = A_j \cdot (2\pi T/D)^{(\sqrt{K}-j\lambda/2)^2-1}$. The constant $F_j \equiv F(2\sqrt{K} - j\lambda)$ with $F(x) = [\Gamma(x^2/4)]^2/[4\pi(\hbar v)^2\Gamma(x^2/2)]$, while $\mu = (1 + \lambda^2/2)\sin(\pi\lambda^2/4)/(\pi\hbar v\sqrt{K})^2$. At zero Rashba coupling, $\theta = 0$, Eq. (11) reproduces the finding in Refs. 8 and 9. By replacing the bare couplings with renormalized ones, the result in Eq. (11) can be RG improved to numerically obtain δG to all orders in perturbation theory in a leading-log approximation. At $\theta = 0$ this gives $\delta G \sim \ln(T)$, in agreement with Ref. 8.

As stressed in Ref. 9, the use of the Kubo formula rests on a perturbation expansion (in our case assuming that $J^2 \ll \omega$) which breaks down as $\omega \to 0$. To study the scaling of δG in the dc limit we will instead fall back on a semiclassical rate equation approximation where we assign classical probabilities to the states. The details of this calculation are provided in the Supplemental Material,[30] and we here only give the main results. In the dc limit, i.e., $\omega \ll J^2 \ll T$, the conductance correction becomes

$$\delta G = -\frac{e^2\cos^2\theta}{2T}\left[\frac{4\gamma_0\gamma_0' + (\gamma_0 + \gamma_0')(\gamma_0^E + \tilde{\gamma}_0^E) + \tilde{\gamma}_0^E\gamma_0^E}{\gamma_0 + \gamma_0' + \tilde{\gamma}_0^E}\right],$$

with $\gamma_0 \sim (J_x + J_y')^2 T^{2(\sqrt{K}-\lambda/2)^2-1}, \gamma_0' \sim (J_x - J_y')^2 T^{2(\sqrt{K}+\lambda/2)^2-1}, \gamma_0^E \sim J_E^2 T^{2K-1}$, and $\tilde{\gamma}_0^E \sim J_E^2 T$, where, for brevity, we have omitted various K-dependent prefactors. Note that with $J_x = J_y$, the vanishing δG becomes nonzero when turning on the Rashba interaction by an electric field. This suggests a means to manipulate the edge current by varying the bias of an external gate.

To explore this possibility we have calculated the δI-V characteristics, exploiting that in the rotated basis H'_K can be treated as a tunneling Hamiltonian[31] and the part of δI corresponding to this tunneling current is then obtained as in Ref. 32. When $J^2 \ll \omega \ll T, eV$ we find

$$\delta I \approx -e\sum_{j=-1}^{+1} \text{Im}\{B(K_j + ieV'/2\pi T, K_j - ieV'/2\pi T) \times C_j(T/D)^{2K_j-1}\sin[\pi(K_j - ieV'/2\pi T)]/\cos(\pi K_j)\} \qquad (12)$$

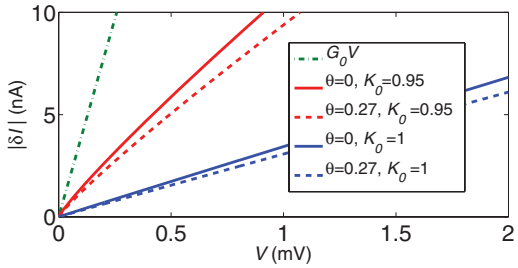

FIG. 2. (Color online) The RG-improved current correction (12) at $T = 30$ mK as a function of applied voltage, for different values of K_0 and θ. The dashed lines represent $\theta \approx 0.27$, corresponding to $\hbar\alpha = 10^{-10}$ eV m. Other parameters are defined in the text. The QSH edge current G_0V is plotted as a reference.

for $\delta I \equiv I - G_0V$, with $K_j \equiv (\sqrt{K} - j\lambda/2)^2$, B the beta function, and $V' \equiv V\cos\theta$. Here $C_{\pm1} = c_\pm(J_x \pm J_y')^2$ and $C_0 = c_0J_E^2$, with $c_{\pm,0}$ constants depending on K, λ, and θ. In Fig. 2 we plot this for parameter values given below.

Experimental realization. Given our result in Eq. (12), is the Rashba dependence of δI large enough to be seen in an experiment? As a case study, let us consider an Mn^{2+} ion implanted close to the edge of an HgTe quantum well.[33] Mn^{2+} has spin $S = 5/2$, but, due to the large and positive single-ion anisotropy $\propto(S^z)^2$ at the quantum well interface, the higher spin components freeze out in the sub-Kelvin range, leaving behind a spin-1/2 doublet.[16] Moreover, the single-ion anisotropy implies that the Kondo interaction with this effective spin-1/2 impurity is anisotropic, with $J_x = J_y = 3J_z = 3J_I$, where J_I is the isotropic bulk spin-exchange coupling.[17] Its value can be assessed from the *sp-d* exchange integrals for the bulk conduction electrons[34] in $Hg_{1-x}Mn_xTe$. Close to the Γ point of the Brillouin zone these integrals produce an antiferromagnetic exchange, $J_I > 0$. With the Mn^{2+} ion located within the penetration depth κ from the edge, a rough estimate yields an expected value of $J_I/a_0 \approx 10$ meV, with a_0 the lattice constant. Turning to the Rashba coupling α, gate controls have been demonstrated[35] in the laboratory with $\hbar\alpha$ for an HgTe quantum well device running from 5×10^{-11} to 1×10^{-10} eV m as the bias of a top gate is varied from 2 to -2 V. As for the value of the interaction parameter K_0 in an HgTe quantum well, estimates[8,14,36–38] range between 0.5 and 1, and depend on the geometry and composition of the heterostructure. Collecting the numbers, and putting[1,39] $a_0 \approx 0.5$ nm, $v_F \approx 5.0 \times 10^5$ m/s, and $D \approx 300$ meV, we can use Eq. (12) to numerically plot the δI-V characteristics for different values[40] of α and K_0, choosing $T = 30$ mK ($> T_K$) (see Fig. 2). As revealed by the graphs, the Rashba dependence of δI is appreciable, and should allow for an experimental test.[41]

Concluding remarks. We have studied the combined effect of a Kondo and a Rashba interaction at the edge of a quantum spin Hall system. The interplay between an anisotropic Kondo exchange and the Rashba interaction is found to result in a noncollinear electron-impurity spin interaction. A perturbative RG analysis indicates that this interaction may block the Kondo effect when the electron-electron interaction is weakly screened. We conjecture that this surprising result—challenging a time-honored expectation that the Kondo effect is blind to time-reversal invariant perturbations[15]—is due to the breakdown of single-particle physics in one dimension. It remains a challenge to unravel the microscopic scenario behind this intriguing phenomenon. In the second part of our work we derived expressions showing how charge transport at the edge is influenced by the simultaneous presence of a magnetic impurity and a Rashba interaction. A case study suggests that the predicted current-voltage characteristics should indeed be accessible in an experiment. Most interestingly, its manifest dependence on the gate-controllable Rashba coupling breaks a path for charge control in a helical electron system.

Acknowledgments. It is a pleasure to thank S. Eggert, D. Grundler, C.-Y. Hou, G. I. Japaridze, P. Laurell, T. Ojanen, and D. Schuricht for valuable discussions. This research was supported by the Swedish Research Council (Grant No. 621-2011-3942) and by STINT (Grant No. IG2011-2028).

[1] M. König *et al.*, Science **318**, 766 (2007).
[2] For a review, see X.-L. Qi and S.-C. Zhang, Rev. Mod. Phys. **83**, 1057 (2011).
[3] C. Wu, B. A. Bernevig, and S. C. Zhang, Phys. Rev. Lett. **96**, 106401 (2006).
[4] C. Xu and J. E. Moore, Phys. Rev. B **73**, 045322 (2006).
[5] D. Meidan and Y. Oreg, Phys. Rev. B **72**, 121312(R) (2005).
[6] T. L. Schmidt, S. Rachel, F. von Oppen, and L. I. Glazman, Phys. Rev. Lett. **108**, 156402 (2012).
[7] N. Lezmy *et al.*, Phys. Rev. B **85**, 235304 (2012).
[8] J. Maciejko, C. Liu, Y. Oreg, X. L. Qi, C. Wu, and S. C. Zhang, Phys. Rev. Lett. **102**, 256803 (2009).
[9] Y. Tanaka, A. Furusaki, and K. A. Matveev, Phys. Rev. Lett. **106**, 236402 (2011).
[10] R. Winkler, *Spin-Orbit Interaction Effects in Two-Dimensional Electron and Hole Systems* (Springer, Berlin, 2003).
[11] H. Buhmann, J. Appl. Phys. **109**, 102409 (2011).
[12] B. A. Bernevig *et al.*, Science **314**, 1757 (2006).
[13] C. L. Kane and E. J. Mele, Phys. Rev. Lett. **95**, 226801 (2005).
[14] A. Ström, H. Johannesson, and G. I. Japaridze, Phys. Rev. Lett. **104**, 256804 (2010).
[15] Y. Meir and N. S. Wingreen, Phys. Rev. B **50**, 4947 (1994).
[16] O. Újsághy and A. Zawadowski, Phys. Rev. B **57**, 11598 (1998).
[17] R. Zitko, R. Peters, and T. Pruschke, Phys. Rev. B **78**, 224404 (2008).
[18] J. I. Väyrynen and T. Ojanen, Phys. Rev. Lett. **106**, 076803 (2011).
[19] J. C. Budich, F. Dolcini, P. Recher, and B. Trauzettel, Phys. Rev. Lett. **108**, 086602 (2012).
[20] T. Giamarchi, *Quantum Physics in One Dimension* (Oxford University Press, Oxford, UK, 2003).
[21] C. L. Kane and M. P. A. Fisher, Phys. Rev. B **46**, 15233 (1992).
[22] J. Maciejko, Phys. Rev. B **85**, 245108 (2012).
[23] M. Pletyukhov and D. Schuricht, Phys. Rev. B **84**, 041309(R) (2011).

[24]X.-Y. Feng and F.-C. Zhang, J. Phys.: Condens. Matter **23**, 105602 (2011).
[25]R. Žitko and J. Bonča, Phys. Rev. B **84**, 193411 (2011).
[26]M. Zarea, S. E. Ulloa, and N. Sandler, Phys. Rev. Lett. **108**, 046601 (2012).
[27]L. Isaev, D. F. Agterberg, and I. Vekhter, Phys. Rev. B **85**, 081107 (2012).
[28]The position of the "dome" in Fig. 1 is determined by the condition that the magnitude $|\tilde{J}_{E1}|$ of the scale-dependent amplitude of the noncollinear term $\sim\sigma^{y'}S^{z'}$ outgrows $|\tilde{J}_x|$, $|\tilde{J}'_y|$, and $|\tilde{J}'_z|$ under RG. Note that when $\theta > \pi/4$, this does not happen since now $J'_y = J_y \cos^2\theta + J_z \sin^2\theta$ will be large for large J_z, making $|\tilde{J}'_y|$ dominate the RG flow.
[29]J. Malecki, J. Stat. Phys. **129**, 741 (2007).
[30]See Supplemental Material at http://link.aps.org/supplemental/10.1103/PhysRevB.86.161103 for a detailed account of the rate-equation calculations.
[31]G. Mahan, *Many-Particle Physics* (Kluwer Academic/Plenum, New York, 2000).
[32]X.-G. Wen, Phys. Rev. B **44**, 5708 (1991).
[33]S. Datta *et al*., Superlattices Microstruct. **1**, 327 (1985).
[34]J. K. Furdyna, J. Appl. Phys. **64**, R29 (1988).
[35]J. Hinz *et al*., Semicond. Sci. Technol. **21**, 501 (2006).
[36]C. Y. Hou, E. A. Kim, and C. Chamon, Phys. Rev. Lett. **102**, 076602 (2009).
[37]A. Ström and H. Johannesson, Phys. Rev. Lett. **102**, 096806 (2009).
[38]J. C. Y. Teo and C. L. Kane, Phys. Rev. B **79**, 235321 (2009).
[39]A. L. Efros and B. I. Shklovskii, *Electronic Properties of Doped Semiconductors* (Springer, Heidelberg, 1989).
[40]Since H'_K in Eq. (3) is RG relevant (marginally relevant) for $K < 1 (K = 1)$, the condition $\delta I \ll G_0 V$ for perturbation theory to be valid restrains K to values close to unity in the chosen voltage interval.
[41]Note that a test requires the concurrent tunability of a back gate, so as to keep the electron density fixed (Ref. 42).
[42]D. Grundler, Phys. Rev. Lett. **84**, 6074 (2000).

Supplemental material for "Electrical control of the Kondo effect in a helical edge liquid"

Erik Eriksson,[1] Anders Ström,[1] Girish Sharma,[2] and Henrik Johannesson[1]

[1]*Department of Physics, University of Gothenburg, SE 412 96 Gothenburg, Sweden*
[2]*Centre de Physique Théorique, Ecole Polytechnique, 91128 Palaiseau Cedex, France*

In this supplementary material we derive the conductance correction $\delta G(\omega)$ as a function of the frequency ω, using a semiclassical rate equation approximation in the spirit of Tanaka *et al.* [9]. However, our case is more involved since the Rashba interaction mixes left- and right-moving electrons, with the components of the Rashba-rotated spinor $\Psi' = \mathrm{e}^{-i\sigma^x\theta/2}\Psi$ being superpositions of left and right movers. Since the physical current is defined in terms of left (source) and right (drain), this prevents it from being expressed directly in terms of classical probabilities assigned to the states in the rotated basis. We will therefore only consider the diagonal part $(e/2)\,\partial_t\,(\cos\theta\,\Psi'^{\dagger}\sigma^{z'}\Psi')$ of the current operator $\hat{I} = (e/2)\,\partial_t\,(\cos\theta\,\Psi'^{\dagger}\sigma^{z'}\Psi' - \sin\theta\,\Psi'^{\dagger}\sigma^{y'}\Psi')$ in the rotated basis. As indicated by the linear response calculations leading to Eq. (11), one expects this to be sufficient to capture the scaling behavior since the set of scaling dimensions is unaffected this truncation. A voltage $V = V_0 e^{-\mathrm{i}\omega t}$ now adds a term $H_V = (eV/2)\int \mathrm{d}x\,(\psi^{\dagger}_{\uparrow}\psi_{\uparrow} - \psi^{\dagger}_{\downarrow}\psi_{\downarrow})$ to the Hamiltonian, which after the Rashba rotation no longer is diagonal. To make it possible to treat the bias semiclassically, we retain only its diagonal part $(eV/2)\cos\theta\int \mathrm{d}x\;\Psi'^{\dagger}\sigma^{z'}\Psi'$, as we did for $\hat{I}$. This truncation allows us to assign the bias $V' = V\cos\theta$ between spin-up ($\uparrow'$) and spin-down ($\downarrow'$) states in the rotated basis. The analysis can now be patterned upon that in Ref. 9, with the construction of a rate equation for the impurity spin,

$$\partial_t P^i_{\uparrow'} = (\gamma_+ + \gamma'_- + \tilde{\gamma}^E_0)P^i_{\downarrow'} - (\gamma_- + \gamma'_+ + \tilde{\gamma}^E_0)P^i_{\uparrow'}, \tag{S.1}$$

with $P^i_{\uparrow',\downarrow'}$ the probability of the impurity spin being in the $\uparrow'$ or $\downarrow'$ state, where $P^i_{\uparrow'} + P^i_{\downarrow'} = 1$. The solution is

$$P^i_{\uparrow'} = \frac{1}{2} + \frac{e}{2T}\,\frac{\gamma_0 - \gamma'_0}{2(\gamma_0 + \gamma'_0 + \tilde{\gamma}^E_0) - \mathrm{i}\omega}\,V_0 e^{-\mathrm{i}\omega t}\cos\theta. \tag{S.2}$$

The γ-parameters encode the various voltage-dependent spin-flip rates implied by H'_K in Eq. (3),

$$\sigma^{\mp}S^{\pm} \to \gamma_{\pm}, \quad \sigma^{\pm}S^{\pm} \to \gamma'_{\mp}, \quad \sigma^{\mp}S^{z'} \to \gamma^E_{\pm}, \quad \sigma^{z'}S^{\pm} \to \tilde{\gamma}^E_0.$$

Here $\gamma_{\pm} = \gamma_0\Lambda_{\pm}, \gamma'_{\pm} = \gamma'_0\Lambda_{\pm}, \gamma^E_{\pm} = \gamma^E_0\Lambda_{\pm}$, with $\Lambda_{\pm} \equiv (1 \pm (eV/2T)\cos\theta)$ for $eV \ll T$, where the rates γ_0, γ'_0, γ^E_0 and $\tilde{\gamma}^E_0$ are determined below.

The operator $\Psi'^{\dagger}\sigma^{+}\Psi'$ has a probability $\cos^4(\theta/2)$ of transforming a left-moving electron into a right-moving electron, and a probability $\sin^4(\theta/2)$ of transforming a right-mover into a left-mover, and vice versa for $\Psi'^{\dagger}\sigma^{-}\Psi'$. Since $\cos^4(\theta/2) - \sin^4(\theta/2) = \cos\theta$, the truncated current from left to right is given by

$$\delta I = -e\left(\gamma_+ P^i_{\downarrow'} - \gamma'_- P^i_{\downarrow'} + \gamma'_+ P^i_{\uparrow'} - \gamma_- P^i_{\uparrow'} + \gamma^E_+/2 - \gamma^E_-/2\right)\cos\theta. \tag{S.3}$$

Combining Eqs. (S.2) and (S.3) gives for the conductance, $\delta G(\omega) = \delta I/(V_0 e^{-\mathrm{i}\omega t})$,

$$\delta G(\omega) = -\frac{e^2}{2T}\cos^2\theta\Big[\frac{((\gamma_0 + \gamma'_0 + \gamma^E_0)\omega + \mathrm{i}8\gamma_0\gamma'_0 + \mathrm{i}2(\gamma_0 + \gamma'_0)(\gamma^E_0 + \tilde{\gamma}^E_0) + \mathrm{i}2\tilde{\gamma}_0\gamma^E_0}{\mathrm{i}2(\gamma_0 + \gamma'_0 + \tilde{\gamma}^E_0) + \omega}\Big]. \tag{S.4}$$

In the dc limit, i.e. $\omega \ll J^2 \ll T$, we then obtain

$$\delta G(\omega \to 0) = -\frac{e^2\cos^2\theta}{2T}\Big[\frac{4\gamma_0\gamma'_0 + (\gamma_0 + \gamma'_0)(\gamma^E_0 + \tilde{\gamma}^E_0) + \tilde{\gamma}^E_0\gamma^E_0}{\gamma_0 + \gamma'_0 + \tilde{\gamma}^E_0}\Big]. \tag{S.5}$$

The rates γ_0, γ'_0 and γ^E_0 are now determined by considering the regime $\gamma_0, \gamma'_0, \gamma^E_0, \tilde{\gamma}^E_0 \ll \omega \ll T$, where Eq. (S.4) gives

$$\delta G(\omega \gg \gamma) = -\frac{e^2}{2T}\left(\gamma_0 + \gamma'_0 + \gamma^E_0\right)\cos^2\theta. \tag{S.6}$$

This is to be compared with the linear-response result in Eq. (11), bearing in mind that Eq. (11) was obtained without any semiclassical approximations. The linear-response result $\delta\tilde{G}$ one would have obtained within such an

approximation consists of replacing $A_\pm = (1/2)(J_x \pm J_y)\cos\theta = (1/2)(J_x \pm J'_y)\cos\theta \pm (J_E/2)\sin\theta$ in Eq. (11) with only the $(1/2)(J_x \pm J'_y)\cos\theta$ part and removing the constant μ term, so that only the parts with $\cos\theta$ are kept, giving

$$\delta\tilde{G} \;=\; -\frac{e^2}{\hbar}\sum_{j=\pm}\left[\frac{J_x + jJ'_y}{2}\cos\theta\right]^2 F_j\cdot\left(\frac{2\pi T}{D}\right)^{2(\sqrt{K}-j\lambda/2)^2-2} \;-\; \frac{e^2}{\hbar}\left[\frac{J_E}{2}\cos\theta\right]^2 F_0\cdot\left(\frac{2\pi T}{D}\right)^{2K-2}. \tag{S.7}$$

Comparing Eqs. (S.6) and (S.7) immediately gives $\gamma_0 \sim (J_x + J'_y)^2 T^{2(\sqrt{K}-\lambda/2)^2-1}$, $\gamma'_0 \sim (J_x - J'_y)^2 T^{2(\sqrt{K}+\lambda/2)^2-1}$, and $\gamma_0^E \sim J_E^2 T^{2K-1}$.

Obtaining $\tilde{\gamma}_0^E$ requires some additional work, since the terms $\sigma^{z'}S^-$ and $\sigma^{z'}S^+$ in H'_K, Eq. (3), do not backscatter electrons. Hence the rate $\tilde{\gamma}_0^E$ does not enter the linear-response conductance result in Eq. (11). To make progress one may introduce an auxiliary field coupling to the impurity instead of the electrons. A suitable choice is to apply a magnetic field $h = h_0 e^{-\mathrm{i}\omega t}$ to the impurity spin and obtain the spin-flip rates when $h \to 0$ using linear response. The equilibrium probabilities for the impurity spin are then

$$P^i_{\uparrow',\downarrow'} = \frac{e^{\pm\mu h/2T}}{e^{\mu h/2T} + e^{-\mu h/2T}}, \tag{S.8}$$

and the spin-flip rates induced by H'_K now correspond to

$$\sigma^\mp S^\pm \to \gamma_\pm, \quad \sigma^\pm S^\pm \to \gamma'_\pm, \quad \sigma^\mp S^{z'} \to \gamma_0^E, \quad \sigma^{z'} S^\pm \to \tilde{\gamma}_\pm^E,$$

with $\gamma_\pm = \gamma_0\Lambda_\pm, \gamma'_\pm = \gamma'_0\Lambda_\pm, \tilde{\gamma}_\pm^E = \tilde{\gamma}_0^E\Lambda_\pm$, where we now have $\Lambda_\pm \equiv (1 \pm (\mu h/2T))$ in the limit $\mu h \ll T$. Since the ballistic conduction electrons are in equilibrium with the leads, the rate equation for the impurity spin can be written as

$$\partial_t P^i_{\uparrow'} = \frac{1}{2}\big[\,-\gamma_- + \gamma_+ + \gamma'_+ - \gamma'_- - \tilde{\gamma}_-^E + \tilde{\gamma}_+^E\,\big] = \frac{\mu h}{2T}\big(\gamma_0 + \gamma'_0 + \tilde{\gamma}_0^E\big). \tag{S.9}$$

This gives the "spin-flip susceptibility", $\chi \equiv \partial(\partial_t P^i_{\uparrow'})/\partial(\mu h)$,

$$\chi = \frac{1}{2T}\big(\gamma_0 + \gamma'_0 + \tilde{\gamma}_0^E\big). \tag{S.10}$$

The rate $\tilde{\gamma}_0^E$ can now be extracted from a linear response calculation similar to the previous one. The operator $\partial_t S^{z'}$, given by $\partial_t S^{z'} = (\mathrm{i}\hbar)^{-1}\left[S^{z'}, H'_K\right]$, becomes

$$\partial_t S^{z'} \;=\; \frac{\mathrm{i}}{\hbar}\frac{1}{2\pi\kappa}\sum_{j=\pm}\left(\frac{J_x + jJ'_y}{2}\right)e^{\mathrm{i}(2\sqrt{K}-j\lambda)\varphi(0)}S^j \;-\; \frac{1}{\hbar}\frac{J_E}{2}\frac{1}{\pi\sqrt{K}} : \partial_x\vartheta(0)e^{-\mathrm{i}\lambda\varphi(0)} : S^+ \;+\; h.c.. \tag{S.11}$$

Calculating the "spin-flip susceptibility" χ using the Kubo formula, $\chi(\omega) = (\hbar\omega)^{-1}\int_0^\infty \mathrm{d}t\, e^{\mathrm{i}\omega t}\langle\big[(\partial_t S^{z'})^\dagger(t), \partial_t S^{z'}(0)\big]\rangle$, in the regime $\gamma_0, \gamma'_0, \tilde{\gamma}_0^E, \tilde{\gamma}_0^E \ll \omega \ll T$, we get

$$\chi \;=\; \frac{1}{\hbar}\sum_{j=\pm}\left[\frac{J_x + jJ'_y}{2}\right]^2 F_j\cdot\left(\frac{2\pi T}{D}\right)^{2(\sqrt{K}-j\lambda/2)^2-2} + \frac{1}{\hbar}\left[\frac{J_E}{2}\right]^2\mu. \tag{S.12}$$

with $\mu = (1+\lambda^2/2)\sin(\pi\lambda^2/4)/(\pi\hbar v\sqrt{K})^2$ as in Eq. (11). Comparing Eqs. (S.10) and (S.12) we once again see that $\gamma_0 \sim (J_x + J'_y)^2 T^{2(\sqrt{K}-\lambda/2)^2-1}$ and $\gamma'_0 \sim (J_x - J'_y)^2 T^{2(\sqrt{K}+\lambda/2)^2-1}$, and now we can also conclude that $\tilde{\gamma}_0^E \sim J_E^2 T$.

Thus we have obtained all rates appearing in the the conductance $\delta G(\omega)$ in Eq. (S.4).

PHYSICAL REVIEW B **87**, 079902(E) (2013)

Erratum: Electrical control of the Kondo effect in a helical edge liquid [Phys. Rev. B 86, 161103(R) (2012)]

Erik Eriksson, Anders Ström, Girish Sharma, and Henrik Johannesson

(Received 30 January 2013; published 4 February 2013)

DOI: 10.1103/PhysRevB.87.079902 PACS number(s): 71.10.Pm, 72.10.Fk, 85.75.−d, 99.10.Cd

In our recent Rapid Communication, Fig. 2 was erroneously plotted due to an incorrect expression for the current operator. The correct figure is given below.

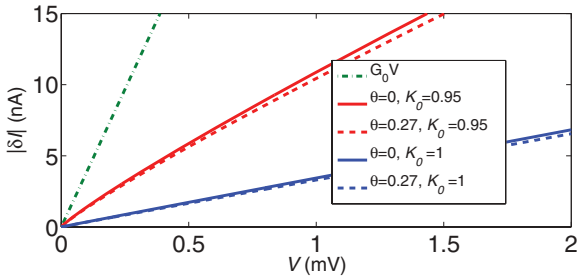

FIG. 2. (Color online) The RG-improved current correction (12) at $T = 30$ mK as a function of applied voltage, for different values of K_0 and θ. The dashed lines represent $\theta \approx 0.27$, corresponding to $\hbar\alpha = 10^{-10}$ eV m. Other parameters are defined in the text. The QSH edge current $G_0 V$ is plotted as a reference.

The corrected expression for the current operator $\hat{I}$, appearing on lines 1 and 2 from the top, second column, page 3, should read $\hat{I} = (e/2)\,\partial_t\,(\Psi'^{\dagger}\sigma^{z'}\Psi')$. As a consequence, Eqs. (10)–(12) are replaced by

$$\delta\hat{I} = \frac{ie}{2\pi\kappa}\left[\sum_{j=\pm} A_j e^{i\sqrt{\pi}(2\sqrt{K}-j\lambda)\varphi} S^j + iA_0\, e^{i\sqrt{4\pi K}\varphi} S^z\right] + \text{H.c.}, \tag{10}$$

where $A_\pm = (1/2)(J_x \pm J'_y)$ and $A_0 = J_E/2$,

$$\delta G = -\frac{e^2}{\hbar}\sum_{j=-1}^{+1} A_j^2 F(2\sqrt{K} - j\lambda)(2\pi T/D)^{2(\sqrt{K}-j\lambda/2)^2-2}, \tag{11}$$

and

$$\delta I \approx -e\sum_{j=-1}^{+1} \text{Im}\,\{B(K_j + ieV/2\pi T, K_j - ieV/2\pi T) C_j (T/D)^{2K_j-1} \sin[\pi(K_j - ieV/2\pi T)]/\cos(\pi K_j)\}, \tag{12}$$

respectively. Also, the multiplicative factor $\cos^2\theta$ in the expression for the conductance correction δG, line 31 from the top, second column, page 3, should be removed. The related equations (S2)–(S6) in the Supplemental Material should be changed accordingly, removing the factors of $\cos\theta$ and $\cos^2\theta$.

We also take the opportunity to point out that the sentences beginning "The presence of..." on line 33, page 2, and "Thus, in the noninteracting limit..." on line 21, page 3, should be removed. (For a discussion of the microscopic origin of the correlated two-particle and inelastic single-particle backscattering terms, see Refs. 1 and 2.)

None of the corrections change our conclusions in the published Rapid Communication.

We thank F. Crépin and P. Recher for drawing our attention to the erroneous expression for the current operator.

[1]F. Crépin, J. C. Budich, F. Dolcini, P. Recher, and B. Trauzettel, Phys. Rev. B **86**, 121106(R) (2012).

[2]T. L. Schmidt, S. Rachel, F. von Oppen, and L. I. Glazman, Phys. Rev. Lett. **108**, 156402 (2012).

Paper V

Spin-orbit interactions in a helical Luttinger liquid with a Kondo impurity

Erik Eriksson
Phys. Rev. B (in press).

Spin-orbit interactions in a helical Luttinger liquid with a Kondo impurity

Erik Eriksson
Department of Physics, University of Gothenburg, SE-412 96 Gothenburg, Sweden

The combined effect of Rashba and Dresselhaus spin-orbit interactions on the physics of a helical Luttinger liquid coupled to a Kondo impurity is studied. A Rashba coupling can potentially destroy the Kondo singlet formation in certain parameter regimes [Phys. Rev. B 86, 161103(R) (2012)]. This effect is here shown to vanish for sufficiently strong Dresselhaus interaction. The transport properties of the system are investigated by calculating electrical conductance, current and current fluctuations, and thermal conductance.

PACS numbers: 71.10.Pm, 72.10.Fk, 85.75.-d

I. INTRODUCTION

Topological insulators constitute a new phase of matter, with preserved time-reversal invariance and a bulk energy gap that is accompanied by topologically protected gapless states on the boundary.[1–5] These boundary states are helical, forming an odd number of Kramers' pairs where electron spin is coupled to the direction of propagation. On the edge of a two-dimensional (quantum spin Hall) topological insulator,[2,3] or in a topological insulator nanowire,[6–8] such helical states will in the presence of electron-electron interactions give rise to the new class of gapless one-dimensional correlated electron liquid known as the *helical Luttinger liquid*.[9,10]

This one-dimensional electron system is distinct from standard spinless, spinful and chiral Luttinger liquids,[11,12] and from the "spiral Luttinger liquids" formed by a spin-orbit coupled quantum wire[13] in a magnetic field,[14,15] due to its time-reversal invariance with a single Kramers' pair. This property makes the helical liquid stable against weak disorder since it forbids single-electron backscattering from spinless impurities,[1] and although electron-electron interaction may cause impurity-induced correlated two-electron backscattering, the gapless helical liquid is still left intact provided the screening is not very weak.[9,10] However, time-reversal invariance does not protect the helical liquid against the effects from magnetic impurities, occurring due to dopant ions or trapped bulk electrons caused by potential inhomogeneities, allowing electrons to backscatter via spin exchange.

Magnetic impurities in conventional Luttinger liquids are well-studied.[16] Single-electron backscattering from non-magnetic impurities is a relevant perturbation causing perfect reflection for repulsive electron-electron interaction.[17] The Kondo scattering off magnetic impurities leads to a low-energy behavior governed by a strong-coupling fixed point where the impurity is completely screened by the electrons, approached with the anomalous exponents of a non-Fermi liquid[18–20] and resulting in vanishing zero-temperature conductance. Instead considering a helical Luttinger liquid, studied early on as a truncated model for a standard Luttinger liquid, there is only backward Kondo scattering and the Kondo effect was shown to map exactly onto that in a Fermi liquid.[21] This yields the typical scaling behavior for the Kondo effect of ordinary conduction electrons.[22] Hence, for the helical Luttinger liquid with antiferromagnetic Kondo coupling there is a low-temperature strong-coupling fixed point, where the local magnetic moment (stabilized against charge fluctuations by the electron correlations[23]) is screened by the electrons effectively leaving behind a spinless impurity.[9,24,25] The edge of a two-dimensional topological insulator merely bypasses this Kondo singlet, thus restoring unitary conductance $G = G_0 = e^2/h$ at zero temperature.[24] Transport properties in the vicinity of this strong-coupling fixed point then follow power-laws governed by the correlated two-electron backscattering, whereas at high temperatures the Kondo scattering results in a logarithmic temperature correction in the linear conductance,[24] which however vanishes in the dc limit.[26]

In addition to the atomic spin-orbit coupling that lies behind the very existence of the quantum spin Hall state,[2] with the idealized helical edge states with right (left) movers with spin up (down), there will also be additional spin-orbit couplings which make spin no longer conserved.[27] As long as the bulk gap remains, preserved time-reversal invariance ensures the robustness of the helical liquid.[1,9] However, an important question is how the Kondo physics of magnetic impurities is affected by the additional spin-orbit interactions in the helical liquid. For a quantum well with structure inversion asymmetry (SIA), i.e. an asymmetry in the confining potential along the direction perpendicular to the well, there will be a *Rashba* spin-orbit interaction.[28–32] This interaction can be controlled by an external gate voltage, a scenario explored in Ref. 40. When the crystal structure lacks inversion symmetry, i.e. in the case of bulk inversion asymmetry (BIA), there will also be the *Dresselhaus* spin-orbit interaction.[29,30,33] Including this type of interaction hence adds a crucial piece to a fuller understanding of the effects of spin-orbit interactions in these systems. In fact, both HgTe and InAs have the inversion asymmetric zincblende crystal structure, thereby displaying the Dresselhaus interaction. HgTe/CdTe quantum wells, the first quantum spin Hall insulator experimentally observed,[3] is known for its large Rashba coupling[34] and one here

expects the Dresselhaus coupling to be much smaller in comparison.[35] For InAs/GaSb quantum wells, where helical edge states also have been demonstrated,[36,37] the Dresselhaus interaction is sizeable[38,39] and realistic predictions for spin-orbit effects must take it into account.

It is therefore the aim of this paper to revisit the problem of a Kondo impurity in a helical Luttinger liquid with spin-orbit interaction. The results announced in Ref. 40 are extended to include both Rashba and Dresselhaus interactions, showing that the obstruction of Kondo singlet formation in certain parameter regimes persists but will vanish for sufficiently strong Dresselhaus interaction. The linear conductance far above the Kondo temperature is obtained, also in the low-frequency limit where a rate-equation approach must be employed.[26] Furthermore, current-voltage and noise characteristics of the backscattered current are calculated, as well as the expression for the thermal conductance, showing how the electric-field adjustable Rashba interaction offers a mechanism to control transport properties.

II. MODEL

The low-energy dynamics of the helical electrons, neglecting interactions, is described by the one-dimensional Dirac Hamiltonian

$$H_0 = v_F \int \mathrm{d}x\ \Psi^\dagger(x)\left[-i\sigma^z\partial_x\right]\Psi(x) \tag{1}$$

where v_F is the Fermi velocity, and the two-component spinor $\Psi = \left(\psi_\uparrow, \psi_\downarrow\right)^T$. Here $\psi_\uparrow\,(\psi_\downarrow)$ annihilates an electron with spin up (down) in the z direction, the growth direction of the quantum well. Unless stated otherwise, the units are such that $\hbar = k_B = 1$ and the lattice constant $a = 1$.

Rashba and Dresselhaus spin-orbit interactions, of strength α and β respectively, to leading order add the terms[28,29,32,33]

$$H_R = \alpha \int \mathrm{d}x\ \Psi^\dagger(x)\left[-i\sigma^y\partial_x\right]\Psi(x) \tag{2}$$

$$H_D = \beta \int \mathrm{d}x\ \Psi^\dagger(x)\left[-i\sigma^x\partial_x\right]\Psi(x) \tag{3}$$

to the Hamiltonian. The Kondo interaction, describing the antiferromagnetic exchange coupling between the electrons and a spin-1/2 magnetic impurity located at $x = 0$, is given by

$$H_K = \Psi^\dagger(0)\left[J_x\sigma^x S^x + J_y\sigma^y S^y + J_z\sigma^z S^z\right]\Psi(0), \tag{4}$$

where σ^i (S^i), $i = x, y, z$, are the electron Pauli matrices (impurity spin operators). At a quantum well interface, spin-orbit induced magnetic anisotropy for an impurity would result in[41,42] $J_x = J_y \neq J_z$.

The effect of a Rashba interaction (2) on the helical states (1) was studied in Ref. 43, and that analysis can now be adapted to also include the Dresselhaus coupling (3). Since $H_0 + H_R + H_D$ is given by

$$\int \mathrm{d}x\ \Psi^\dagger(x)\left[-i\left(v_F\sigma^z + \alpha\sigma^y + \beta\sigma^x\right)\partial_x\right]\Psi(x), \tag{5}$$

it follows that a rotation $\Psi \to \Psi' = e^{i\sigma^y\phi/2}e^{-i\sigma^x\theta/2}\Psi$ diagonalizes $H_0 + H_R + H_D \to H_0'$, with

$$H_0' = v_{\alpha\beta}\int \mathrm{d}x\ \Psi'^\dagger(x)\left[-i\sigma^z\partial_x\right]\Psi'(x), \tag{6}$$

where $v_{\alpha\beta} = \sqrt{v_F^2 + \alpha^2 + \beta^2}$, and the rotation angles are determined by

$$\sin\theta = \alpha/\sqrt{v_F^2 + \alpha^2}, \tag{7}$$

$$\sin\phi = \beta/\sqrt{v_F^2 + \alpha^2 + \beta^2}. \tag{8}$$

Thus the spectrum of $H_0 + H_R + H_D$ is linear, and the components ψ_+' and ψ_-' of the spinor Ψ' are left- and right movers. It is therefore possible to treat the effects of the spin-orbit interactions (2)-(3) exactly by working in the rotated basis.

The Kondo interaction (4) is now analyzed in the rotated basis. In order to have the impurity and electron spins quantized along the same axis, rotate $\boldsymbol{S} \to \boldsymbol{S}' = e^{iS^y\phi/2}e^{-iS^x\theta/2}\boldsymbol{S}e^{iS^x\theta/2}e^{-iS^y\phi/2}$. Then the Kondo Hamiltonian becomes

$$\begin{aligned} H_K' = {} & \Psi'^\dagger(0)\ [\ J_x'\sigma^x S'^x + J_y'\sigma^y S'^y + J_z'\sigma^z S'^z \\ & + J_{xy}\sigma^x S'^y + J_{yx}\sigma^y S'^x + J_{xz}\sigma^x S'^z \\ & + J_{zx}\sigma^z S'^x + J_{yz}\sigma^y S'^z + J_{zy}\sigma^z S'^y\ ]\ \Psi'(0), \end{aligned} \tag{9}$$

where the coupling constants are given by

$$\begin{aligned} J_x' &= J_x\cos^2\phi + J_y\sin^2\theta\sin^2\phi + J_z\cos^2\theta\sin^2\phi, \\ J_y' &= J_y\cos^2\theta + J_z\sin^2\theta, \\ J_z' &= J_x\sin^2\phi + J_y\sin^2\theta\cos^2\phi + J_z\cos^2\theta\cos^2\phi, \\ J_{xy} &= J_{yx} = (J_z - J_y)\cos\theta\sin\theta\sin\phi, \\ J_{xz} &= J_{zx} = (J_x - J_y\sin^2\theta - J_z\cos^2\theta)\cos\phi\sin\phi, \\ J_{yz} &= J_{zy} = (J_y - J_z)\cos\theta\sin\theta\cos\phi. \end{aligned}$$

The next step is to include the electron-electron interactions allowed by time-reversal symmetry. Assuming a band away from half-filling, $k_F \neq \pi/2$, Umklapp scattering

$$\begin{aligned} H_{um}' = {} & g_{um}\int \mathrm{d}x\ e^{-i4k_F x}\psi_+'^\dagger(x)\psi_+'^\dagger(x+a) \\ & \times\psi_-'(x)\psi_-'(x+a) + H.c. \end{aligned} \tag{10}$$

can be ignored.[9] Here a point splitting with the lattice constant has been performed. Dispersive and forward scattering are given by

$$H_d' = g_d\int \mathrm{d}x\ \psi_+'^\dagger(x)\psi_+'(x)\psi_-'^\dagger(x)\psi_-'(x), \tag{11}$$

$$H_f' = \frac{g_f}{2}\sum_{s=\pm}\int \mathrm{d}x\ \psi_s'^\dagger(x)\psi_s'(x)\psi_s'^\dagger(x+a)\psi_s'(x+a), \tag{12}$$

and at the impurity site there will in addition be correlated two-particle backscattering[9,10,44]

$$H'_{2p} = g_{2p}\psi'^{\dagger}_{+}(0)\psi'^{\dagger}_{+}(a)\psi'_{-}(0)\psi'_{-}(a) + H.c. \tag{13}$$

and inelastic single-particle backscattering[45–47]

$$\begin{aligned} H'_{ie} &= g_{ie}\left(\psi'^{\dagger}_{+}(0)\psi'_{+}(0) - \psi'^{\dagger}_{-}(0)\psi'_{-}(0)\right) \\ &\quad \times\psi'^{\dagger}_{+}(a)\psi'_{-}(a) + H.c. \end{aligned} \tag{14}$$

Employing standard bosonization methods[11,12] the interacting Hamiltonian $H'_0 + H'_d + H'_f$ forms a helical Luttinger liquid

$$H'_{HLL} = \frac{v}{2}\int \mathrm{d}x\left[(\partial_x\varphi)^2 + (\partial_x\vartheta)^2\right], \tag{15}$$

where the electron operators $\psi_{\pm} = (2\pi\kappa)^{-1/2}e^{-i\sqrt{\pi}(\vartheta\pm\varphi)}$ are represented in terms of non-chiral Bose fields $\varphi(x)$ and $\vartheta(x)$, with $[\varphi(x), \partial_y\vartheta(y)] = i\pi\delta(x-y)$. Here $\kappa \approx v_F/D$ is the edge state penetration depth acting as short-distance cutoff with D the bandwidth. The velocity $v = [(v_{\alpha\beta}+g_f/\pi)^2-(g_d/\pi)^2]^{1/2}$, and the Luttinger parameter $K = [(\pi v_\alpha+g_f-g_d)/(\pi v_\alpha+g_f+g_d)]^{1/2}$. The correlated two-particle and inelastic single-particle backscattering terms in Eqs. (13)-(14) are now expressed as

$$H'_{2p} = \frac{g_{2p}}{2(\pi\kappa)^2}\cos[\sqrt{16\pi K}\varphi(0)] \tag{16}$$

$$H'_{ie} = \frac{g_{ie}}{2\pi^2\sqrt{K}} : \left[\partial_x^2\vartheta(0)\right]\cos[\sqrt{4\pi K}\varphi(0)] : \tag{17}$$

where : ... : denotes normal ordering. The Kondo interaction (9) is represented as

$$\begin{aligned} H'_K = \frac{A}{\pi\kappa}\cos[\sqrt{4\pi K}\varphi(0)] + \frac{B}{\pi\kappa}\sin[\sqrt{4\pi K}\varphi(0)] \\ + \frac{C}{\sqrt{\pi K}}\partial_x\vartheta(0) \end{aligned} \tag{18}$$

where the operators A, B and C are defined as

$$\begin{aligned} A &\equiv J'_x S'^x + J_{xy}S'^y + J_{xz}S'^z, \\ B &\equiv J_{yx}S'^x + J'_y S'^y + J_{yz}S'^z, \\ C &\equiv J_{zx}S'^x + J_{zy}S'^y + J'_z S'^z. \end{aligned} \tag{19}$$

III. KONDO TEMPERATURE

The low-temperature behavior of the model can now be determined through a perturbative renormalization-group analysis. First, from Eqs. (16) and (17) it is seen that the correlated two-particle and inelastic single-particle backscattering operators have scaling dimensions $4K$ and $K+2$, respectively. Hence, for Luttinger parameter $K < 2/3$, the two-particle backscattering is the dominating of the two. For $K < 1/4$ it turns relevant, with a crossover from weak to strong coupling at a temperature[24,48] $T_{2p} \approx D g_{2p}^{1/(1-4K)}$.

Let us now derive the renormalization-group equations for the Kondo couplings in Eq. (9). The local partition function at the impurity site corresponding to the Hamiltonian $H'_{HLL} + H'_K$ is written as a functional integral

$$\begin{aligned} \mathcal{Z} &= \int \mathcal{D}[\varphi]\; e^{-S[\varphi]} \\ &= \int \mathcal{D}[\varphi]\; \exp\left\{-\frac{1}{2\pi}\int \mathrm{d}\omega\; |\omega||\varphi(\omega)|^2 - S_K[\varphi(\tau)]\right\}, \end{aligned}$$

with the imaginary time action S_K for the Kondo terms given by

$$\begin{aligned} S_K[\varphi(\tau)] &= \int_0^\beta \mathrm{d}\tau\; \Big\{\frac{A}{\pi\kappa}\cos[\sqrt{4\pi K}\varphi(\tau)] \\ &\quad + \frac{B}{\pi\kappa}\sin[\sqrt{4\pi K}\varphi(\tau)] + \frac{iC\sqrt{K}}{\sqrt{\pi v}}\partial_\tau\varphi(\tau)\Big\} \end{aligned} \tag{20}$$

and the impurity operators A, B and C given by Eq. (19). The analysis will be perturbative in the Kondo couplings, with $S_0[\varphi] = S[\varphi] - S_K[\varphi]$ the unperturbed action. Although the J'_z coupling may be treated exactly in the case of zero spin-orbit couplings,[25] the additional coupling terms introduced in the Hamiltonian (9) by the spinor rotation precludes this line of attack. Since the exact analysis in J'_z yields different physics only for $J'_z/(\pi v) > 2(K+\sqrt{K})$, where the Kondo effect disappears,[25] for reasonable strength of the electron-electron interaction the perturbative treatment of J'_z is sufficient for the purposes here.

The procedure[49] is standard Wilsonian RG, where the field φ is divided into a slow and a fast part, $\varphi(\tau) = \varphi_s(\tau) + \varphi_f(\tau)$, with

$$\varphi_s(\tau) = \frac{1}{2\pi}\int_{-\Lambda/b}^{\Lambda/b}\mathrm{d}\omega\; e^{-i\omega\tau}\varphi(\omega), \tag{21}$$

$$\varphi_f(\tau) = \frac{1}{2\pi}\int_{\Lambda/b<|\omega|<\Lambda}\mathrm{d}\omega\; e^{-i\omega\tau}\varphi(\omega). \tag{22}$$

An effective action $S_s[\varphi_s]$ is then found for the slow field by integrating out the fast components,

$$e^{-S_s[\varphi_s]} = \int \mathcal{D}[\varphi_f]\; e^{-S[\varphi]}. \tag{23}$$

Rescaling the high-energy cutoff $\Lambda = v/\kappa$ with the parameter b, so that Λ/b is the new cutoff, gives the new rescaled effective action and allows extraction of the RG flow equations.

A linked cluster expansion to second order in the Kondo couplings,

$$\begin{aligned} S_s[\varphi_s] &= S_0[\varphi_s] + \langle S_K[\varphi]\rangle_f \\ &\quad -\frac{1}{2}\left(\langle S_K[\varphi]^2\rangle_f - \langle S_K[\varphi]\rangle_f^2\right), \end{aligned} \tag{24}$$

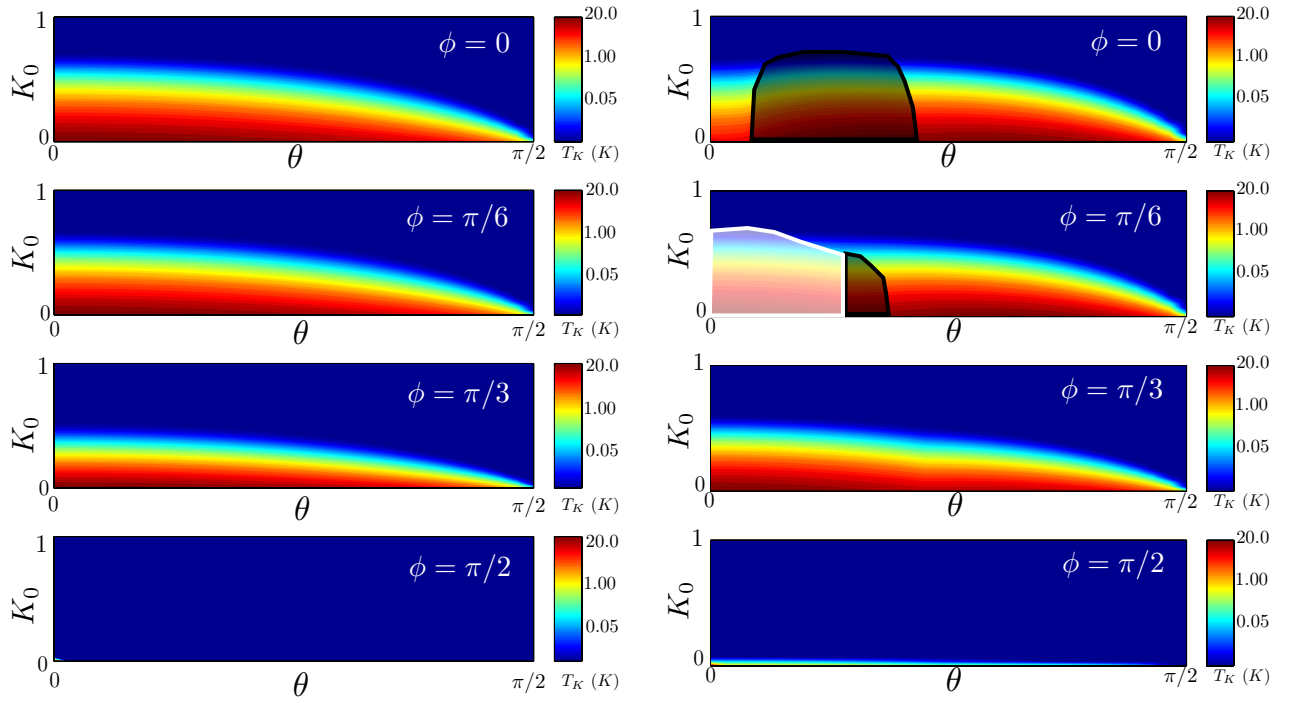

FIG. 1: The Kondo temperature T_K as a function of the Rashba angle θ and the ordinary Luttinger parameter K_0, for four different values of the Dresselhaus angle ϕ. Note that the temperature scale is logarithmic, and that the vanishing Kondo temperature at $\theta, \phi = \pi/2$ simply reflect the diverging spin-orbit coupling strength in these limits. Left column: $J_x = J_y \geq J_z$ (here with $J_x/a = J_z/a = 10$ meV). Right column: $J_x = J_y < J_z$ (here with $J_x/a = 5$ meV and $J_z/a = 50$ meV). In the black (white) shaded area, J_{yz} (J_{xz}) dominates the perturbative RG flow, hence preventing the low-temperature formation of a Kondo singlet.

gives the rescaled effective action[40,50]

$$\begin{aligned} S[\varphi] \;=\; & S_0[\varphi] + \\ & + \int \mathrm{d}\tau \, \Big\{ \, b^{1-K} \Big[\frac{A}{\pi\kappa} \cos[\sqrt{4\pi K}\varphi(\tau)] \\ & \qquad + \frac{B}{\pi\kappa} \sin[\sqrt{4\pi K}\varphi(\tau)] \Big] \\ & + \left(b^2 - b^{2-2K}\right) \frac{[A,B]}{2v^2\pi^{3/2}} \partial_\tau \varphi(\tau) \\ & - \left(b - b^{1-K}\right) \, i\frac{[B,C]}{\kappa v \pi^2} \cos[\sqrt{4\pi K}\varphi(\tau)] \\ & + \left(b - b^{1-K}\right) \, i\frac{[A,C]}{\kappa v \pi^2} \sin[\sqrt{4\pi K}\varphi(\tau)] \, \Big\}, \end{aligned} \tag{25}$$

where only the most relevant operators are kept. Among the less relevant operators that are neglected is the correlated two-particle backscattering operator $\cos[\sqrt{16\pi K}\varphi(\tau)]$. It is hence generated during the RG flow, which is expected in the presence of electron-electron interactions.[44,51] In order to determine the Kondo temperature of the strong-coupling crossover, only the Kondo scattering which is the most relevant process needs to be considered.

The commutators of the impurity operators (19) are

$$\begin{aligned} [A,B] \;=\; & 2i\Big[(J_{xy}J'_z - J_{xz}J_{zy})S^x \\ & + (J_{xz}J_{zx} - J'_xJ'_z)S^y \\ & + (J'_xJ_{zy} - J_{xy}J_{zx})S^z\Big], \end{aligned} \tag{26}$$

$$\begin{aligned} [B,C] \;=\; & 2i\Big[(J'_yJ'_z - J_{yz}J_{zy})S^x \\ & + (J_{yz}J_{zx} - J_{yx}J'_z)S^y \\ & + (J_{yx}J_{zy} - J'_yJ_{zx})S^z\Big], \end{aligned} \tag{27}$$

$$\begin{aligned} [A,C] \;=\; & 2i\Big[(J_{xy}J'_z - J_{xz}J_{zy})S^x \\ & + (J_{xz}J_{zx} - J'_xJ'_z)S^y \\ & + (J'_xJ_{zy} - J_{xy}J_{zx})S^z\Big]. \end{aligned} \tag{28}$$

Collecting the terms in Eq. (25), using Eqs. (26)-(28),

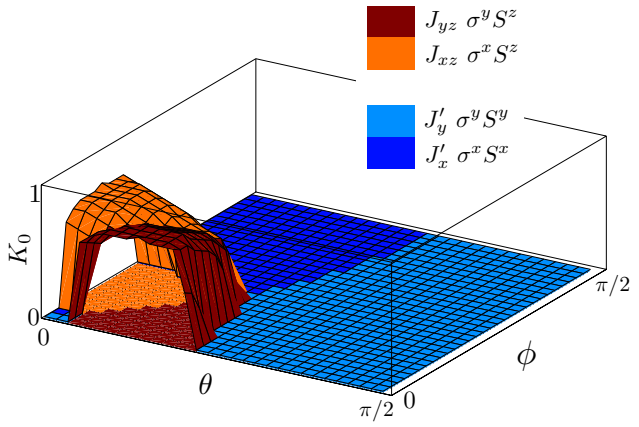

FIG. 2: The "phase diagram", showing which Kondo coupling constant that dominates the low-temperature behavior when $J_x = J_y < J_z$ [here with the same parameter values as for the right column in Fig. (1)]. Dark and light blue (J'_x and J'_y, respectively) means the formation of a singlet between the electrons and impurity below the Kondo temperature. Red and orange (J_{yz} and J_{xz}, respectively) denotes the "dome" within which the singlet formation is obstructed since instead the $J_{yz}\sigma^y S'^z$ or $J_{xz}\sigma^x S'^z$ interactions will dominate.

the RG equations for the Kondo couplings become

$$\begin{aligned}
\partial_\ell J'_x &= (1-K)J'_x + \nu K\left(J'_y J'_z - J_{yz}J_{zy}\right), \\
\partial_\ell J'_y &= (1-K)J'_y + \nu K\left(J'_x J'_z - J_{xz}J_{zx}\right), \\
\partial_\ell J'_z &= \nu K\left(J'_x J'_y - J_{xy}J_{yx}\right), \\
\partial_\ell J_{xy} &= (1-K)J_{xy} + \nu K\left(J_{yz}J_{zx} - J'_z J_{yx}\right), \\
\partial_\ell J_{yx} &= (1-K)J_{yx} + \nu K\left(J_{xz}J_{zy} - J'_z J_{xy}\right), \\
\partial_\ell J_{xz} &= (1-K)J_{xz} + \nu K\left(J_{yx}J_{zy} - J'_y J_{zx}\right), \\
\partial_\ell J_{zx} &= \nu K\left(J_{xy}J_{yz} - J'_y J_{xz}\right), \\
\partial_\ell J_{yz} &= (1-K)J_{yz} + \nu K\left(J_{xy}J_{zx} - J'_x J_{zy}\right), \\
\partial_\ell J_{zy} &= \nu K\left(J_{xz}J_{yx} - J'_x J_{yz}\right),
\end{aligned} \tag{29}$$

in terms of the "renormalization length" $\ell = \ln b$, and where $\nu = 1/(\pi v)$ is the density of states. Note that although the RG flows are different, the bare values of the coupling constants, given by Eq. (9) where $J_{xy}(\ell = 0) = J_{yx}(\ell = 0)$ etc., are not all independent.

The RG equations (29) are now solved numerically. As the temperature $T = D/b = D\,e^{-\ell}$ is reduced, the Kondo temperature T_K is reached when one of the Kondo couplings in Eq. (9) becomes of the same order of magnitude as the energy scale of the unperturbed Hamiltonian (6), i.e. $v_{\alpha\beta}$. Fig. 1 shows T_K as a function of the three independent parameters, the Rashba angle θ, the Dresselhaus angle ϕ, and the the ordinary Luttinger parameter $K_0 = K(\theta = 0, \phi = 0)$,

$$K_0 = \sqrt{\frac{\pi v_F}{\pi v_F + 2g}} \tag{30}$$

where $g = g_f = g_d$ refers to the original basis. The plots show a Kondo temperature that for given K_0 and Dresselhaus angle ϕ depends on the Rashba angle, which is controllable via an electric field. For "easy-plane" and isotropic Kondo coupling ($J_x, J_y > J_z$ and $J_x = J_y = J_z$, respectively, which lead to very similar plots) the system flows towards the Kondo fixed point with divergent J'_x or J'_y couplings resulting in a singlet between the impurity and electrons. However, for "easy-axis" Kondo coupling ($J_x, J_y < J_z$), there are parameter regions where instead the couplings $J_{yz}\sigma^y S'^z$ or $J_{xz}\sigma^x S'^z$ dominate the RG flow, preventing singlet formation. These regions are indicated in Fig. 1, but note that their precise sizes depend on the numerical values of J_x,J_y and J_z. In Fig. (2) they are shown for all values of ϕ, θ and K_0, indicating that the "dome" is not completely symmetric under rotation in the xy-plane.

IV. LINEAR CONDUCTANCE

A. Strong-coupling limit at zero temperature

The low-temperature limit of the conductance is governed by the RG flows of the Kondo (18), correlated two-particle (16) and inelastic single particle (17) backscattering terms in the Hamiltonian. The inelastic single-particle backscattering term H'_{ie} has scaling dimension $2 + K$, and is hence irrelevant in the sense of RG, contributing a term $\delta G_{ie} \sim T^{2+2K}$ to the conductance.[45,46] The correlated two-particle backscattering term H'_{2p} has scaling dimension $4K$ and is an irrelevant perturbation when $K > 1/4$, in which case it contributes a term $\delta G_{2p} \sim T^{8K-2}$ to the conductance.[24] For $K < 1/4$, the term H'_{2p} turns relevant, hence opening up a gap at the energy scale of T_{2p}, leading to zero conductance of the system at $T = 0$ which is approached as[24] $G \sim T^{2(1/4K-1)}$.

Since the Kondo backscattering is a relevant (marginally relevant) perturbation for $K < 1$ ($K = 1$), the transport properties of the system in the zero-temperature limit when $1/4 \leq K \leq 1$ depend on what type of Kondo fixed point is reached. Outside the domes of dominating $J_{yz}\sigma^y S'^z$ or $J_{xz}\sigma^x S'^z$ interactions, the impurity is locked into a Kondo singlet below the energy scale of the Kondo temperature T_K. For a helical edge liquid of a two-dimensional topological insulator, this means that the Kondo impurity effectively disappears from the problem, with no contribution to the zero-temperature conductance,[24] whereas a quantum wire would effectively be cut into two halves resulting in an insulating state. Inside the dome, where Kondo screening is obstructed resulting in a non-vanishing effective spin, the diverging scattering strength suggests the destruction of the gapless state below T_K.

B. Linear response at weak coupling

1. The ac conductance

For temperatures $T > T_K, T_{2p}$, the system is in a weak-coupling regime where the Kondo couplings J and the two-particle backscattering coupling g_{2p} remain small parameters. This allows a perturbative calculation of the linear conductance. Since the components ψ'_+ and ψ'_- of the spinor Ψ' in the rotated basis are left- and right movers, the current operator $\hat{I}$ is given by

$$\hat{I} = (e/2)\,\partial_t\,(\Psi'^{\dagger}\sigma^z\Psi'). \tag{31}$$

Hence the part $\delta\hat{I}$ of the current operator that is due to the Kondo scattering H'_K is given by $\delta\hat{I} = e/(i2\hbar)[\Psi'^{\dagger}\sigma^z\Psi', H'_K]$. It is here possible to conveniently consider the effects of the J'_z coupling constant in Eq. (9) to all orders in perturbation theory by performing the unitary transformation $U(H'_{HLL}+H'_K)U^{\dagger}$, with[52]

$$U = e^{i\lambda\varphi(0)S'^z}, \tag{32}$$

which cancels the J'_z term in H'_K against one that is generated in H'_{HLL} provided one chooses $\lambda = J'_z/\pi v\sqrt{K}$. This transforms the Kondo Hamiltonian H'_K to

$$\begin{aligned} H'_K \;=\; & \frac{1}{2\pi\kappa}\Bigg[\left(\frac{J'_x+J'_y}{2}\right)e^{i\sqrt{\pi}(2\sqrt{K}-\lambda)\varphi}S'^{+} \\ & +\left(\frac{J'_x-J'_y}{2}+i\frac{J_{xy}+J_{yx}}{2}\right)e^{i\sqrt{\pi}(2\sqrt{K}+\lambda)\varphi}S'^{-} \\ & +\left(\frac{iJ_{yz}+J_{xz}}{2}\right)e^{i\sqrt{4\pi K}\varphi}S'^{z}\Bigg] \\ & +\left(\frac{iJ_{zy}+J_{zx}}{2}\right)\frac{1}{\sqrt{\pi K}}:\partial_x\vartheta e^{-i\sqrt{\pi}\lambda\varphi}:S'^{+} \;+\text{H.c.} \end{aligned} \tag{33}$$

in terms of the spin raising and lowering operators $S'^{\pm} = S'^{x} \pm iS'^{y}$. The current correction operator $\delta\hat{I}$ then takes the form

$$\begin{aligned} \delta\hat{I} \;=\; & \frac{ie}{2\pi\kappa}\Bigg[\left(\frac{J'_x+J'_y}{2}\right)e^{i\sqrt{\pi}(2\sqrt{K}-\lambda)\varphi}S'^{+} \\ & +\left(\frac{J'_x-J'_y}{2}+i\frac{J_{xy}+J_{yx}}{2}\right)e^{i\sqrt{\pi}(2\sqrt{K}+\lambda)\varphi}S'^{-} \\ & +\left(\frac{iJ_{yz}+J_{xz}}{2}\right)e^{i\sqrt{4\pi K}\varphi}S'^{z}\Bigg] + \text{H.c.} \end{aligned} \tag{34}$$

Note that both H'_K and $\delta\hat{I}$ are local at $x = 0$, and for brevity only the time arguments of the fields are specified. The Kubo formula for the conductance, $G(\omega) = (1/\hbar\omega)\int_0^{\infty}\mathrm{d}t\,e^{i\omega t}\langle\big[I^{\dagger}(t), I(0)\big]\rangle$, now gives the linear conductance correction $\delta G = G - G_0$ due to the Kondo scattering. To second order in the Kondo couplings (except for J'_z which is treated exactly), the unperturbed retarded Green's functions[11]

$$\begin{aligned} \langle\big[e^{i2\sqrt{K_j}\varphi(t)}, e^{-i2\sqrt{K_j}\varphi(0)}\big]\rangle_0 \;&=\; \left(\frac{\pi\kappa}{\beta v}\right)^{2K_j} 2i\,\sin(\pi K_j) \\ &\quad\times\Big(\sinh\frac{\pi t}{\beta}\Big)^{-2K_j} \end{aligned} \tag{35}$$

contribute three terms in δG

$$\begin{aligned} \delta G(\omega) \;&=\; -\sum_{j=1}^{3}\frac{2e^2}{\hbar^3}\frac{|A_j|^2}{(2\pi\kappa)^2}\left(\frac{\pi T}{D}\right)^{2K_j} \\ &\quad\times\sin(\pi K_j)\frac{1}{i\omega}\int_0^{\infty}\mathrm{d}t\;\frac{e^{-\mathrm{i}\omega t}-1}{(\sinh\frac{\pi Tt}{\hbar})^{2K_j}}. \end{aligned} \tag{36}$$

where $A_1 = (J'_x+J'_y)/2$, $A_2 = (J'_x-J'_y)/2+i(J_{xy}+J_{yx})/2$, $A_3 = (iJ_{yz}+J_{xz})/2$, $K_{1,2} = K_{\mp} \equiv (\sqrt{K}\mp\lambda/2)^2$ and $K_3 = K$. As in Refs. 24 and 26, the standard integrals are calculated by changing integration variable to $x = \pi Tt/\hbar$ and then to $u = \tanh x$, giving in the limit $\omega \ll T$

$$\begin{aligned} & \frac{1}{i\omega}\int_0^{\infty}\mathrm{d}t\;\frac{e^{-\mathrm{i}\omega t}-1}{(\sinh\frac{\pi Tt}{\hbar})^{2K_j}} \\ & = \frac{\hbar}{\pi T}\frac{1}{\mathrm{i}\omega}\int_0^{\infty}\mathrm{d}x\;\frac{e^{-\mathrm{i}(\hbar\omega/\pi T)x}-1}{(\sinh x)^{2K_j}} \\ & \approx \left(\frac{\hbar}{\pi T}\right)^2\int_0^{\infty}\mathrm{d}x\;\frac{x}{(\sinh x)^{2K_j}} \\ & = \left(\frac{\hbar}{\pi T}\right)^2\int_0^{1}\mathrm{d}u\;u^{-2K_j}(1-u^2)^{K_j-1}\mathrm{arctanh}\,u, \end{aligned} \tag{37}$$

which is evaluated to give

$$\delta G(\omega) = -\frac{e^2}{2T}\sum_{j=1}^{3}|A_j|^2\frac{1}{(\pi\hbar)^2 v\kappa}\frac{[\Gamma(K_j)]^2}{\Gamma(2K_j)}\left(\frac{2\pi T}{D}\right)^{2K_j-1}. \tag{38}$$

Hence $\delta G(\omega)$ is ω-independent in the limit $J^2 \ll \omega \ll T$, where J denotes the set of Kondo couplings. Rewriting Eq. (38) gives the final expression for the conductance correction from the Kondo scattering when $J^2 \ll \omega \ll T$

$$\begin{aligned} \delta G = & -\frac{e^2}{\hbar}\frac{1}{4\pi(\hbar v)^2}\times \\ & \Bigg[\left(\frac{J'_x+J'_y}{2}\right)^2\frac{[\Gamma(K_-)]^2}{\Gamma(2K_-)}\left(\frac{2\pi T}{D}\right)^{2K_--2} \\ & +\left|\frac{J'_x-J'_y}{2}+i\frac{J_{xy}+J_{yx}}{2}\right|^2\frac{[\Gamma(K_+)]^2}{\Gamma(2K_+)}\left(\frac{2\pi T}{D}\right)^{2K_+-2} \\ & +\left|\frac{iJ_{yz}+J_{xz}}{2}\right|^2\frac{[\Gamma(K)]^2}{\Gamma(2K)}\left(\frac{2\pi T}{D}\right)^{2K-2}\Bigg]. \end{aligned} \tag{39}$$

2. The dc limit

It is important to keep in mind that Eq. (39) for the conductance correction was derived perturbatively in the

Kondo couplings J. Hence when $\omega \ll J^2$ the above type of analysis is no longer valid, as noted in Ref. 26 where instead a rate equation was set up for the impurity spin. In Ref. 40 this rate-equation approach was extended to incorporate the additional scattering types present when a Rashba interaction is added. Since a Dresselhaus interaction merely changes the different rates for the scattering events in these rate equations, the calculations in the supplemental material of Ref. 40 are easily modified to include also Dresselhaus interaction. For completeness, let us nevertheless carry them out explicitly also here.

Denoting the rates for the scattering events encoded in the Hamiltonian (9) with $\gamma_\pm$ for $\sigma^\mp S'^\pm$, $\gamma'_\mp$ for $\sigma^\pm S'^\pm$, $\gamma^z_\pm$ for $\sigma^\mp S'^z$ and $\tilde\gamma^z_0$ for $\sigma^z S'^\pm$, the rate equation for the impurity spin becomes

$$\partial_t P_+ = (\gamma_+ + \gamma'_- + \tilde\gamma^z_0)P_- - (\gamma_- + \gamma'_+ + \tilde\gamma^z_0)P_+, \quad (40)$$

with $P_\pm$ the probability of the impurity spin being in the $+$ or $-$ state, and the probabilities obeying $P_+ + P_- = 1$. When adding a voltage bias $V = V_0 e^{-i\omega t}$ between the left- and right-moving electrons, encoded by the term

$$H_V = \frac{eV}{2}\int \mathrm{d}x\ \Psi'^\dagger \sigma^z \Psi' \quad (41)$$

in the Hamiltonian, the voltage-dependent rates are given by $\gamma_\pm = \gamma_0\Lambda_\pm, \gamma'_\pm = \gamma'_0\Lambda_\pm, \gamma^z_\pm = \gamma^z_0\Lambda_\pm$, with $\Lambda_\pm \equiv 1 \pm eV/2T$ for $eV \ll T$. The current correction from the impurity scattering can now be written as

$$\begin{aligned}\delta I \ &= \ -e\big(\gamma_+P_- - \gamma'_-P_- + \gamma'_+P_+ - \gamma_-P_+ \\ &\quad +\gamma^z_+/2 - \gamma^z_-/2\big). \end{aligned} \quad (42)$$

Substituting the solution of Eq. (40) into Eq. (42), one finds the linear conductance correction $\delta G(\omega) = \delta I/(V_0 e^{-\mathrm{i}\omega t})$ to be

$$\begin{aligned}\delta G(\omega) \ &= \ -\frac{e^2}{2T}\big[(\gamma_0+\gamma'_0+\gamma^z_0)\omega + i8\gamma_0\gamma'_0 \\ &\quad +i2(\gamma_0+\gamma'_0)(\gamma^z_0+\tilde\gamma^z_0) + i2\tilde\gamma_0\gamma^z_0\big] \\ &\quad \times\big[i2(\gamma_0+\gamma'_0+\tilde\gamma^z_0)+\omega\big]^{-1}. \end{aligned} \quad (43)$$

In the dc limit, i.e. when $\omega \ll J^2 \ll T$, this becomes

$$\begin{aligned}&\delta G(\omega\to 0) = \\ &\quad -\frac{e^2}{2T}\Big[\frac{4\gamma_0\gamma'_0+(\gamma_0+\gamma'_0)(\gamma^z_0+\tilde\gamma^z_0)+\tilde\gamma^z_0\gamma^z_0}{\gamma_0+\gamma'_0+\tilde\gamma^z_0}\Big]. \end{aligned} \quad (44)$$

The remaining task is to determine the rates γ_0, γ'_0, γ^z_0 and $\tilde\gamma^z_0$. In the high-frequency regime one can compare Eq. (43), which gives $\delta G(\omega \gg \gamma) = -(e^2/2T)(\gamma_0 + \gamma'_0 + \gamma^z_0)$, with the linear-response result in Eq. (39). This gives

$$\begin{aligned}\gamma_0 \ &\sim \ (J'_x + J'_y)^2 (T/D)^{2(\sqrt{K}-\lambda/2)^2-1} \\ \gamma'_0 \ &\sim \ |J'_x - J'_y + i(J_{xy}+J_{yx})|^2 (T/D)^{2(\sqrt{K}+\lambda/2)^2-1} \\ \gamma^z_0 \ &\sim \ |iJ_{yz} + J_{xz}|^2 (T/D)^{2K-1} \end{aligned} \quad (45)$$

In order to obtain the rate $\tilde\gamma^z_0$ of impurity spin-flips not accompanied by electron backscattering, one needs to do an analogous linear-response analysis for a field that instead couples to the impurity.[40] Such a calculation yields

$$\tilde\gamma^z_0 \ \sim \ |iJ_{zy} + J_{zx}|^2\, T/D \quad (46)$$

coming from the last term in Eq. (33).

V. BACKSCATTERED CURRENT

A. I-V characteristics

A finite time-independent bias voltage $V = V_0$ is conveniently treated in a picture where the voltage term (41) in the Hamiltonian is replaced by a time dependence in the electron fields, $\psi'_\pm \to e^{-iH_V t/\hbar}\psi'_\pm$. In this picture

$$\begin{aligned}H'_K(t) \ &= \ \frac{1}{2\pi\kappa}\Big[A_1 e^{ieVt/\hbar} e^{i\sqrt{\pi}(2\sqrt{K}-\lambda)\varphi} S'^+ \\ &\quad +A_2\, e^{ieVt/\hbar} e^{i\sqrt{\pi}(2\sqrt{K}+\lambda)\varphi} S'^- \\ &\quad +A_3\, e^{ieVt/\hbar} e^{i\sqrt{4\pi K}\varphi} S'^z \\ &\quad +A_4 \frac{1}{\sqrt{\pi K}} :\partial_x\vartheta e^{-i\sqrt{\pi}\lambda\varphi}: S'^+ \Big] + \mathrm{H.c.} \end{aligned} \quad (47)$$

and

$$\begin{aligned}\delta\hat I(t) \ &= \ \frac{ie}{2\pi\kappa}\Big[A_1 e^{ieVt/\hbar} e^{i\sqrt{\pi}(2\sqrt{K}-\lambda)\varphi} S'^+ \\ &\quad +A_2\, e^{ieVt/\hbar} e^{i\sqrt{\pi}(2\sqrt{K}+\lambda)\varphi} S'^- \\ &\quad +A_3\, e^{ieVt/\hbar}\, e^{i\sqrt{4\pi K}\varphi} S'^z \Big] + \mathrm{H.c.} \end{aligned} \quad (48)$$

where $A_1 = (J'_x+J'_y)/2$, $A_2 = (J'_x - J'_y)/2 + i(J_{xy}+J_{yx})/2$ and $A_3 = (iJ_{yz} + J_{xz})/2$ as before, and $A_4 = (iJ_{zy} + J_{zx})/2$.

The non-equilibrium expectation value of the current operator is given by

$$\langle\delta\hat I(t)\rangle = \frac{1}{2}\sum_{\eta=\pm}\langle \hat T_K \left\{\delta\hat I(t^\eta)\, e^{-i\int_K \mathrm{d}t' H'_K(t')}\right\}\rangle, \quad (49)$$

where $\hat T_K$ is the time ordering operator on the Keldysh contour K, and $t^\pm$ is time t either on the upper $(+)$ or lower $(-)$ branch of K, see e.g. Ref. 53. To lowest order in the Kondo couplings, the most relevant terms are

$$\begin{aligned}\langle\delta\hat I(t)\rangle \ &= \ -\frac{e}{8\pi^2\kappa^2}\sum_{\eta=\pm}\int_K \mathrm{d}t' e^{ieV(t-t')/\hbar}\Big[\langle S'^+ S'^-\rangle \\ &\times\Big(\,|A_1|^2\langle\hat T_K\{e^{i\sqrt{4\pi K_-}\varphi(t^\eta)}e^{-i\sqrt{4\pi K_-}\varphi(t')} + H.c.\}\rangle \\ &+|A_2|^2\langle\hat T_K\{e^{i\sqrt{4\pi K_+}\varphi(t^\eta)}e^{-i\sqrt{4\pi K_+}\varphi(t')} + H.c.\}\rangle\,\Big) \\ &+|A_3|^2\langle\hat T_K\{e^{i\sqrt{4\pi K}\varphi(t^\eta)}e^{-i\sqrt{4\pi K}\varphi(t')} + H.c.\}\rangle\langle S'^z S'^z\rangle\Big]. \end{aligned} \quad (50)$$

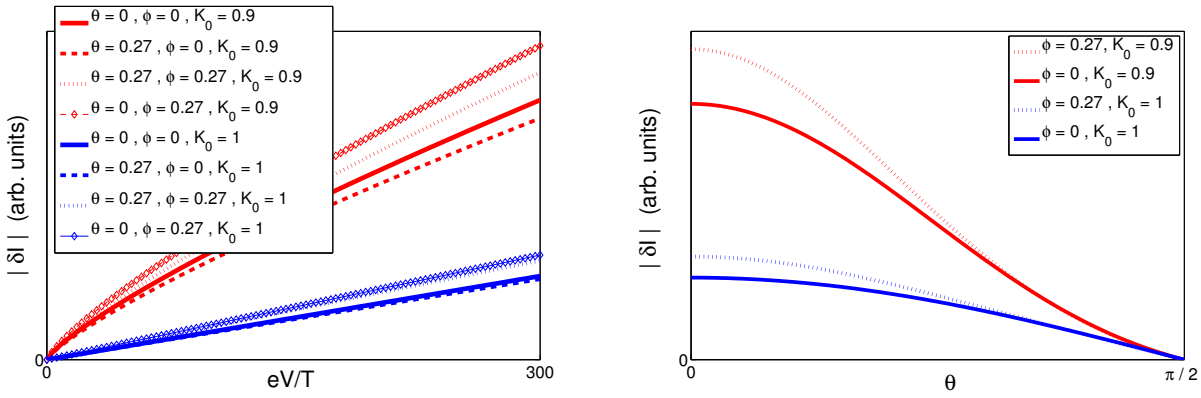

FIG. 3: The backscattered current δI due to the Kondo impurity, for different values of the Rashba and Dresselhaus angles θ and ϕ (parameterizing the strengths of the spin-orbit interactions), and the Luttinger parameter K_0. Left: Current-voltage characteristics for δI at fixed temperature T. Right: δI at fixed voltage and temperature, plotted as a function of the Rashba angle θ. The coupling constants have been RG improved at the fixed temperature. With typical parameter values as discussed in the text, voltages on the order of 1 mV at temperatures in the mK regime will give current corrections δI on the order of a nA.

The integrals on the Keldysh contour are found[53] to result in

$$\langle \delta\hat{I}(t)\rangle = -\frac{e}{2\pi^2 v\kappa}\sinh\left(\frac{eV}{2T}\right)\sum_{j=1}^{3}\left[|A_j|^2\left(\frac{2\pi T}{D}\right)^{2K_j-1} \times\frac{\left|\Gamma\left(K_j+ieV/2\pi T\right)\right|^2}{\Gamma(2K_j)}\right], \quad (51)$$

where Γ is the gamma function. This could equivalently be written in terms of the Euler beta function B as

$$\delta I = \frac{e}{2\pi^2 v\kappa}\sum_{j=1}^{3}\mathrm{Im}\Big\{|A_j|^2\left(\frac{2\pi T}{D}\right)^{2K_j-1} \times B(K_j+ieV/2\pi T, K_j-ieV/2\pi T) \times\frac{\sin[\pi(K_j-ieV/2\pi T)]}{\cos(\pi K_j)}\Big\} \quad (52)$$

which is on the form of the result presented in Ref. 40, derived using the tunneling formalism.[54,55] Note the difference in sign of the prefactors. Since the backscattering current $\delta I \equiv I - I_0$, where I_0 is the current in the absence of the impurity, it is negative. The current corrections due to correlated two-particle, and inelastic single-particle, backscattering can be found in Ref. 46.

In Fig. 3 the backscattered current δI, given by Eq. (51), is plotted for different strengths of the Rashba and Dresselhaus interactions and Luttinger parameters K_0. As an illustration, possible parameter values can be collected from Ref. 40 for the case of an Mn^{2+} ion implanted in the helical edge liquid of a HgTe quantum well.[56] For this material,[3] $v_F \approx 5.0\times10^5$ m/s, the lattice constant[57] $a \approx 0.5$ nm, and the bandwidth[3] $D \approx 300$ meV. Estimates for the value of the Luttinger parameter K_0 for the electron-electron interaction strength vary between[24,58–61] 0.5 and 1, depending on the geometry and composition of the specific semiconductor heterostructure. The Kondo coupling constants are taken to be $J_x = J_y = 3J_z = 3J_I$, where a rough estimate yields[40–42,62] J_I/a on the order of 10 meV. For HgTe quantum wells, values of the Rashba coupling $\hbar\alpha$ are typically in the range between[63] 5×10^{-11} eVm to 1×10^{-10} eVm, i.e. the value of the Rashba rotation angle is roughly in the interval $0.14 < \theta < 0.27$ for typical samples and voltages. For this particular heterostructure, the Dresselhaus interaction strength is typically negligible compared to the Rashba,[35] but note there are other materials with helical edge states where Dresselhaus is comparable in magnitude or even stronger than the Rashba interaction.[38,39] With these parameter values, a voltage bias in the mV regime at a temperature around 1 mK typically yields a current δI on the order of 1 nA, i.e. a correction of roughly one percent to $I_0 \equiv G_0 V$.

B. Current fluctuations

From the above results it is an easy task to extract the noise in the current correction δI. In terms of the symmetric combination of the noise correlators

$$S(t-t') = \langle\delta\hat{I}(t)\delta\hat{I}(t')\rangle + \langle\delta\hat{I}(t')\delta\hat{I}(t)\rangle - 2\langle\delta\hat{I}(t')\rangle\langle\delta\hat{I}(t)\rangle, \quad (53)$$

which in the Keldysh formalism takes the form

$$S(t-t') = \sum_{\eta=\pm}\langle\hat{T}_K\left\{\delta\hat{I}(t^\eta)\delta\hat{I}(t'^{-\eta})\,e^{-i\int_K \mathrm{d}t' H'_K(t')}\right\}\rangle - 2\langle\delta\hat{I}(t)\rangle, \quad (54)$$

the noise spectrum $S(\omega)$ follows as the Fourier transform $S(\omega) = \int_{-\infty}^{\infty}\mathrm{d}s\, e^{i\omega s}\, S(s)$; for a review see Ref. 53.

To lowest order in the Kondo couplings, Eq. (54) reduces to a current-current correlator, $S(t-t') = \sum_{\eta=\pm}\langle \hat{T}_K\{\delta\hat{I}(t^\eta)\delta\hat{I}(t'^{-\eta})\}\rangle - 2\langle\delta\hat{I}(t)\rangle$, which is evaluated precisely as Eq. (50). This yields the zero-frequency noise

$$S(\omega=0) = \frac{e^2}{\pi^2 v\kappa}\cosh\left(\frac{eV}{2T}\right)\sum_{j=1}^{3}\left[|A_j|^2\left(\frac{2\pi T}{D}\right)^{2K_j-1} \times\frac{\left|\Gamma\left(K_j+ieV/2\pi T\right)\right|^2}{\Gamma(2K_j)}\right], \quad (55)$$

i.e. $S(\omega=0) = 2e|\langle\delta\hat{I}(t)\rangle|\coth(eV/2T)$. Since $\coth(eV/2T)\approx 1$ for the temperature and voltages used in Fig. 3, this gives a Fano factor $S(\omega=0)/(2e|\langle\delta\hat{I}\rangle|)\approx 1$ for the current δI due to H'_K. The noise in the current corrections due to correlated two-particle, and inelastic single-particle, backscattering can be found in Ref. 46. In total, the combined backscattering current due to $H'_K + H'_{2p} + H'_{ie}$ has an enhanced Fano factor (between 1 and 2), due to the larger effective charge $e^* = 2e$ appearing in the two-particle backscattering noise.[64]

VI. THERMAL TRANSPORT

Let us also consider the thermal conductance of the system for temperatures $T > T_K$. In terms of left- and right-moving fields $\phi_{L,R} = (\vartheta \pm \varphi)/2$, such that $H'_{HLL} = (\hbar v/2)\int \mathrm{d}x[(\partial_x\phi_R)^2 + (\partial_x\phi_L)^2] = H'^R_{HLL} + H'^L_{HLL}$, the backscattered thermal current $\delta\hat{I}_Q$ is given by the operator[65]

$$\delta\hat{I}_Q = \int \mathrm{d}x\,\partial_t(H'^R_{HLL} - H'^L_{HLL})/2 = \frac{iv}{2}\int \mathrm{d}x\,[:\partial_x\varphi\,\partial_x\vartheta:(x)\,,\,H'_K(0)]\,, \quad (56)$$

which gives

$$\delta\hat{I}_Q = -\frac{\hbar v\sqrt{\pi K}}{e}\partial_x\varphi\,\delta\hat{I} + A_4\frac{\sqrt{\pi}v}{2\sqrt{K}}\left(:\partial_x^2\vartheta\, e^{-i\sqrt{\pi}\lambda\varphi}: S'^{+} + \mathrm{H.c.}\right), \quad (57)$$

where H'_K and $\delta\hat{I}$ are given by Eqs. (33) and (34), and $A_4 = (iJ_{zy} + J_{zx})/2$. The first term in Eq. (57) has its analog in Refs. 65 and 26, but the second term is new and is a result of the spin-orbit interaction. The correction $\delta\mathcal{K}$ to the (zero-frequency) linear thermal conductance due to the Kondo impurity is obtained from the Kubo formula, $\delta\mathcal{K} = \lim_{\omega\to 0}(1/\hbar\omega T)\int_0^\infty \mathrm{d}t\, e^{i\omega t}\langle\big[\delta\hat{I}_Q^\dagger(t),\delta\hat{I}_Q(0)\big]\rangle$, where the two terms in $\delta\hat{I}_Q$ add separately to $\delta\mathcal{K}$. Now, the contribution from the first term in Eq. (57) follows from Ref. 65. The contribution from the second term follows by noting the close resemblance between that operator, with scaling dimension $2+\lambda^2/4$, and the inelastic single-particle backscattering term in Eq. (17), with scaling dimension $2+K$. This makes it possible to perturbatively evaluate the contribution from the second term in Eq. (57) using known results from Ref. 46, valid at frequencies $\omega \gg J^2$. It follows from those results that this operator contributes a term $\sim(k_BT/D)^{\lambda^2/2+1}$ to $\delta\mathcal{K}$. In comparison, this contribution is subleading as $k_BT \ll D$, and the thermal conductance correction is hence given by the contribution from the first term in Eq. (57), which gives the usual formula,[26,65]

$$\delta\mathcal{K} \approx \frac{\hbar^3 K}{8e^2k_BT^2}\int \mathrm{d}\omega\,\frac{\omega^2\,\mathrm{Re}\,\delta G(\omega)}{\sinh^2(\hbar\omega/2k_BT)}, \quad (58)$$

for the zero-frequency thermal conductance correction. The same observation as in Ref. 26 therefore applies, namely that $\delta\mathcal{K}$ is determined by the electrical conductance correction $\delta G(\omega)$ within a frequency range $0\le\omega\lesssim 2k_BT/\hbar$, and that even when δG vanishes in the dc limit this is not necessarily true for $\delta\mathcal{K}$.

VII. DISCUSSION

The interplay between a magnetic impurity and spin-orbit interaction in a helical Luttinger liquid has been studied. Using a transformation[43] that effectively removes the spin-orbit interactions among the electrons, at the price of introducing additional coupling terms to the impurity, the results are non-perturbative in the spin-orbit couplings. The effect described in Ref. 40, that a Rashba spin-orbit interaction appears to prevent the Kondo singlet formation in certain parameter regimes, is found to persist also with a Dresselhaus spin-orbit interaction. The perturbative RG analysis therefore suggests that a time-reversal invariant perturbation can destroy the Kondo effect in one dimension, in stark contrast to the case for ordinary metals where the Kondo effect is robust,[66,67] and such perturbations only shift the Kondo temperature.[68–72]

In the other parameter regimes, the Kondo effect will set in. Since the Rashba interaction can be controlled by an external gate voltage, this offers a mechanism to electrically control the Kondo effect and therefore the transport properties of the edge at low temperatures.[40] At higher temperatures the Rashba dependence of the Kondo scattering permits a way to electrically control the small current corrections. For in-plane symmetric Kondo couplings $J_x = J_y \neq J_z$, and negligible Dresselhaus interaction, Eq. (44) reveals a vanishing dc linear conductance correction which can be made non-zero by tuning the gate voltage. With non-zero Dresselhaus interaction strength, the linear conductance correction however remains non-zero also in the dc limit even without Rashba interaction.

Unfortunately, there is no exactly solvable Toulouse limit as in the absence of spin-orbit interactions.[26] This rules out an exact analysis of the low-frequency behavior

at some special value for the interaction strengths, and has its root in the new operators generated by the spin-orbit interaction bringing several different scaling dimensions into the problem. The different exponents show up in the temperature dependence of conductances, and in the temperature and voltage dependence of the current correction due to the Kondo impurity.

The spin-orbit interactions hence introduce new types of scattering mechanisms compared to those for the original helical liquid with a Kondo impurity, adding yet another piece to the different types of correlations appearing in topological insulator materials,[73] including the effects on Kondo screening,[9,24–26] transport properties[24,26,65] and current noise correlations.[74,75] There is also the possibility of exotic multi-channel Kondo physics, like the two-channel effect appearing with a quantum dot between two helical edges[76,77] where the effects of a Rashba coupling were studied very recently.[78] Interesting extensions include the case of many impurities[79] forming a Kondo lattice[25] on a helical edge, where the effects of spin-orbit interactions remain unexplored.

ACKNOWLEDGMENTS

It is a pleasure to thank Henrik Johannesson and Anders Ström for very valuable discussions. This research was supported by the Swedish Research Council (Grant No. 621-2011-3942).

[1] C. L. Kane and E. J. Mele, Phys. Rev. Lett. **95**, 146802 (2005); **95**, 226801 (2005).
[2] B. A. Bernevig, T. L. Hughes and S.-C. Zhang, Science **314**, 1757 (2006).
[3] M. König, S. Wiedmann, C. Brüne, A. Roth, H. Buhmann, L. W. Molenkamp, X.-L. Qi and S.-C. Zhang, Science **318**, 766 (2007).
[4] M. Z. Hasan and C. L. Kane, Rev. Mod. Phys. **82**, 3045 (2010).
[5] X.-L. Qi and S.-C. Zhang, Rev. Mod. Phys. **83**, 1057 (2011).
[6] R. Egger, A. Zazunov and A. Levy Yeyati, Phys. Rev. Lett. **105**, 136403 (2010).
[7] H. Peng, K. Lai, D. Kong, S. Meister, Y. Chen, X.-L. Qi, S.-C. Zhang, Z.-X. Shen, and Y. Cui, Nat. Mater. **9**, 225 (2010).
[8] D. Kong, J. C. Randel, H. Peng, J. J. Cha, S. Meister, K. Lai, Y. Chen, Z.-X. Shen, H. C. Manoharan and Y. Cui, Nano Lett. **10**, 329 (2010).
[9] C. Wu, B. A. Bernevig and S.-C. Zhang, Phys. Rev. Lett. **96**, 106401 (2006).
[10] C. Xu and J. E. Moore, Phys. Rev. B **73**, 045322 (2006).
[11] T. Giamarchi, *Quantum Physics in One Dimension* (Oxford University Press, Oxford, 2003).
[12] A. O. Gogolin, A. A. Nersesyan and A. M. Tsvelik, *Bosonization and Strongly Correlated Systems* (Cambridge University Press, Cambridge, 1998).
[13] V. Gritsev, G. Japaridze, M. Pletyukhov and D. Baeriswyl, Phys. Rev. Lett. **94**, 137207 (2005).
[14] Reviewed in J. Alicea, Rep. Prog. Phys. **75**, 076501 (2012).
[15] B. Braunecker, C. Bena and P. Simon, Phys. Rev. B **85**, 035136 (2012).
[16] Reviewed in A. Furusaki, J. Phys. Soc. Jpn. **74**, 73 (2005).
[17] C. L. Kane and M. P. A. Fisher, Phys. Rev. Lett. **68**, 1220 (1992).
[18] D.-H. Lee and J. Toner, Phys. Rev. Lett. **69**, 3378 (1992).
[19] A. Furusaki and N. Nagaosa, Phys. Rev. Lett. **72**, 892 (1994).
[20] P. Fröjdh and H. Johannesson, Phys. Rev. Lett. **75**, 300 (1995).
[21] A. Schiller and K. Ingersent, Phys. Rev. B **51**, 4676 (1995).
[22] A. C. Hewson, *The Kondo Problem to Heavy Fermions* (Cambridge University Press, Cambridge, 1993).
[23] P. Phillips and N. Sandler, Phys. Rev. B **53**, R468 (1996).
[24] J. Maciejko, C. Liu, Y. Oreg, X.-L. Qi, C. Wu and S.-C. Zhang, Phys. Rev. Lett. **102** 256803 (2009).
[25] J. Maciejko, Phys. Rev. B **85**, 245108 (2012).
[26] Y. Tanaka, A. Furusaki and K. A. Matveev, Phys. Rev. Lett. **106** 236402 (2011).
[27] C. Brüne, A. Roth, H. Buhmann, E. M. Hankiewicz, L. W. Molenkamp, J. Maciejko, X.-L. Qi and S.-C. Zhang, Nature Phys. **8**, 485 (2012).
[28] Yu. Bychkov and E. I. Rashba, JETP Lett. **39**, 78 (1984).
[29] R. Winkler, *Spin-Orbit Interaction Effects in Two-Dimensional Electron and Hole Systems* (Springer, Berlin, 2003).
[30] H.-A. Engel, E. I. Rashba, and B. I. Halperin, in *Handbook of Magnetism and Advanced Magnetic Materials*, eds. H. Kronmüller and S. Parkin (John Wiley & Sons, Chichester, 2007) [arXiv:cond-mat/0603306].
[31] D. Grundler, Phys. Rev. Lett. **84**, 6074 (2000).
[32] D. G. Roth, R. W. Reinthaler, C.-X. Liu, L. W. Molenkamp, S.-C. Zhang and E. M. Hankiewicz, New J. Phys. **12**, 065012 (2010).
[33] G. Dresselhaus, Phys. Rev. **100**, 580 (1955).
[34] H. Buhmann, J. Appl. Phys. **109**, 102409 (2011).
[35] Reviewed in R. H. Silsbee, J. Phys.: Condens. Matter **16**, R179 (2004).
[36] C. Liu, T. L. Hughes, X.-L. Qi, K. Wang and S.-C. Zhang, Phys. Rev. Lett. **100**, 236601 (2008).
[37] I. Knez, R.-R. Du and G. Sullivan, Phys. Rev. Lett. **107**, 136603 (2011).
[38] P. Carrier and S.-H. Wei, Phys. Rev. B **70**, 035212 (2004).
[39] T. Matsuda and K. Yoh, Physica E **42**, 979 (2010).
[40] E. Eriksson, A. Ström, G. Sharma and H. Johannesson, Phys. Rev. B, **86** 161103(R) (2012); **87**, 079902(E) (2013).
[41] O. Újsághy and A. Zawadowski, Phys. Rev. B **57**, 11598 (1998).
[42] R. Žitko, R. Peters and Th. Pruschke, Phys. Rev. B **78**, 224404 (2008).
[43] J. I. Väyrynen and T. Ojanen, Phys. Rev. Lett. **106**, 076803 (2011).
[44] F. Crépin, J. C. Budich, F. Dolcini, P. Recher and B. Trauzettel, Phys. Rev. B **86**, 121106(R) (2012).
[45] T. L. Schmidt, S. Rachel, F. von Oppen and L. I. Glazman, Phys. Rev. Lett. **108** 156402 (2012).
[46] N. Lezmy, Y. Oreg and M. Berkooz, Phys. Rev. B **85** 235304 (2012).
[47] J. C. Budich, F. Dolcini, P. Recher and B. Trauzettel, Phys. Rev. Lett. **108**, 086602 (2012).
[48] C. L. Kane and M. P. A. Fisher, Phys. Rev. B **46**, 15233 (1992).
[49] R. Shankar, Rev. Mod. Phys. **66**, 129 (1994).
[50] A. Ström, Ph.D. thesis, University of Gothenburg, 2012.
[51] T. Giamarchi and H. J. Schulz, Phys. Rev. B **37**, 325 (1988)
[52] V. J. Emery and S. Kivelson, Phys. Rev. B **46**, 10812 (1992)
[53] T. Martin in *Nanophysics: Coherence and Transport*, eds. H. Bouchiat *et al.* (Elsevier, Amsterdam, 2005) [arXiv:cond-mat/0501208].
[54] G. Mahan, *Many-Particle Physics* (Kluwer Academic / Plenum Publishers, New York, 2000).
[55] X.-G. Wen, Phys. Rev. B **44** 5708 (1991).
[56] S. Datta, J. K. Furdyna and R. L. Gunshor, Superlattice Microst. **1**, 327 (1985).
[57] A. L. Efros and B. I. Shklovskii, *Electronic Properties of Doped Semiconductors* (Springer, Heidelberg, 1989).
[58] C.-Y. Hou, E.-A. Kim and C. Chamon, Phys. Rev. Lett. **102**, 076602 (2009).
[59] A. Ström and H. Johannesson, Phys. Rev. Lett. **102**, 096806 (2009).
[60] J. C. Y. Teo and C. L. Kane, Phys. Rev B **79**, 235321 (2009).
[61] A. Ström, H. Johannesson and G. I. Japaridze, Phys. Rev. Lett. **104**, 256804 (2010).
[62] J. K. Furdyna, J. Appl. Phys. **64**, R29 (1988).
[63] J. Hinz, H. Buhmann, M. Schäfer, V. Hock, C. R. Becker and L. W. Molenkamp, Semicond. Sci. Technol. **21**, 501 (2006).
[64] E. Sela, Y. Oreg, F. von Oppen and J. Koch, Phys. Rev. Lett. **97**, 086601 (2006).
[65] C. L. Kane and M. P. A. Fisher, Phys. Rev. Lett. **76**, 3192

(1996).
[66] Y. Meir and N. S. Wingreen, Phys. Rev. B **50**, 4947 (1994).
[67] J. Malecki, J. Stat. Phys. **129**, 741 (2007).
[68] M. Pletyukhov and D. Schuricht, Phys. Rev. B **84**, 041309(R) (2011).
[69] X.-Y. Feng and F.-C. Zhang, J. Phys. Condens. Matter **23**, 105602 (2011).
[70] R. Žitko and J. Bonča, Phys. Rev. B **84**, 193411 (2011).
[71] M. Zarea, S. E. Ulloa and N. Sandler, Phys. Rev. Lett. **108**, 046601 (2012).
[72] L. Isaev, D. F. Agterberg and I. Vekhter, Phys. Rev. B **85**, 081107 (2012).
[73] For a review, see M. Hohenadler and F. F. Assaad, J. Phys.: Condens. Matter **25**, 143201 (2013).
[74] J.-R. Souquet and P. Simon, Phys. Rev. B **86**, 161410(R) (2012).
[75] Y.-W. Lee, Y.-L. Lee and C.-H. Chung, Phys. Rev. B **86**, 235121 (2012).
[76] K. T. Law, C. Y. Seng, P. A. Lee and T. K. Ng, Phys. Rev. B **81**, 041305(R) (2010).
[77] T. Posske, C.-X. Liu, J. C. Budich and B. Trauzettel, Phys. Rev. Lett. **110**, 016602 (2013).
[78] Y.-L. Lee and Y.-W. Lee, arXiv:1303.1896.
[79] A. M. Lunde and G. Platero, Phys. Rev. B **86**, 035112 (2012).

Paper VI

Finite-size effects from higher conservation laws for the one-dimensional Bose gas

Erik Eriksson and Vladimir Korepin
J. Phys. A: Math. Theor. **46**, 235002 (2013).

J. Phys. A: Math. Theor. **46** (2013) 235002 (9pp) doi:10.1088/1751-8113/46/23/235002

Finite-size effects from higher conservation laws for the one-dimensional Bose gas

Erik Eriksson[1] **and Vladimir Korepin**[2]

[1] Department of Physics, University of Gothenburg, SE-412 96 Gothenburg, Sweden
[2] CN Yang Institute for Theoretical Physics, State University of New York at Stony Brook, NY 11794-3840, USA

E-mail: erik.eriksson@physics.gu.se and korepin@insti.physics.sunysb.edu

Received 21 February 2013, in final form 22 April 2013
Published 21 May 2013
Online at stacks.iop.org/JPhysA/46/235002

Abstract
We consider a generalized Lieb–Liniger model, describing a one-dimensional Bose gas with all its conservation laws appearing in the density matrix. This will be the case for the generalized Gibbs ensemble, or when the conserved charges are added to the Hamiltonian. The finite-size corrections are calculated for the energy spectrum. Large-distance asymptotics of correlation functions are then determined using methods from conformal field theory.

PACS numbers: 02.30.Ik, 05.30.Jp

1. Introduction

There has recently been much interest in so-called generalized Gibbs ensembles (GGEs), where the density matrix of a system is given by

$$\hat{\rho}_{\mathrm{GGE}} = Z_{\mathrm{GGE}}^{-1}\, \mathrm{e}^{-\sum_n \beta_n \hat{Q}_n}, \tag{1}$$

generalizing the usual Gibbs ensemble for generic (non-integrable) systems where only the Hamiltonian and a particle number operator appear in the exponent. Instead, for an integrable system, $\{\hat{Q}_n\}$ is the complete set of local conserved charges, with $\{\beta_n\}$ the generalized inverse temperatures (Lagrange multipliers) and $Z_{\mathrm{GGE}} = \mathrm{Tr}\, \mathrm{e}^{-\sum_n \beta_n \hat{Q}_n}$ the generalized partition function [1]. For such quantum ensembles, the expectation values of observables are obtained as

$$\langle \hat{O} \rangle_{\mathrm{GGE}} = \mathrm{Tr}\, \hat{\rho}_{\mathrm{GGE}} \hat{O}, \tag{2}$$

whereas the time evolution is governed by the usual Schrödinger Hamiltonian.

Recent experimental advances with quantum non-equilibrium dynamics of cold atoms [2], where the GGE was proposed [3] to describe local large-time behavior, have spurred a great interest in the possible equilibrium ensembles for integrable systems (see e.g. [4–6] and references therein, and in particular [7–10] for treatments of the one-dimensional Bose gas).

But effects from higher conservation laws in integrable systems were also studied longer ago in the context of competing interactions in spin chains [11, 12].

It is therefore a timely question to now ask in general what sort of effects one can anticipate when incorporating higher conservation laws into the density matrix for an integrable model. In this paper, we study finite-size effects and obtain conformal dimensions for the one-dimensional Bose gas (Lieb–Liniger model), when governed by a density matrix of the form (1). In particular, using the exact Bethe Ansatz solution we calculate the finite-size corrections for the energy and momentum. Comparing this to the expressions given by conformal field theory, we are able to obtain the large-distance asymptotics of correlation functions.

2. Lieb–Liniger model

The Lieb–Liniger model describes a one-dimensional Bose gas with point-like interaction through the Hamiltonian

$$\hat{H} = \int \mathrm{d}x[\partial_x \Psi^\dagger(x)\partial_x \Psi(x) + c\Psi^\dagger(x)\Psi^\dagger(x)\Psi(x)\Psi(x)], \tag{3}$$

with the coupling constant $c > 0$ and Bose fields Ψ with equal-time commutation relations $[\Psi(x), \Psi^\dagger(y)] = \delta(x-y)$ and $[\Psi(x), \Psi(y)] = [\Psi^\dagger(x), \Psi^\dagger(y)] = 0$. The model is solved through the Bethe Ansatz [13–15], yielding eigenstates $|\{\lambda_j\}\rangle$ given in terms of rapidities λ_j satisfying the Bethe equations

$$\mathrm{e}^{\mathrm{i}\lambda_j L} = -\prod_{k=1}^{N} \frac{\lambda_j - \lambda_k + \mathrm{i}c}{\lambda_j - \lambda_k - \mathrm{i}c}, \quad j = 1, \ldots, N, \tag{4}$$

for a system of N particles in a box of length L with periodic boundary conditions. The Bethe equations (4) can equivalently be written as

$$L\lambda_j + \sum_{k=1}^{N} \theta(\lambda_j - \lambda_k) = 2\pi n_j, \quad j = 1, \ldots, N, \tag{5}$$

with n_j integer when N odd and half-integer when N even and $\theta(\lambda) = \mathrm{i}\ln[(\mathrm{i}c + \lambda)/(\mathrm{i}c - \lambda)]$. For the non-zero wavefunction, $n_j \neq n_k$ when $j \neq k$.

The conserved charges $\hat{Q}_n$ have eigenvalues Q_n given by

$$Q_n = \sum_{j=1}^{N} \lambda_j^n, \tag{6}$$

the three lowest being particle number $N = Q_0$, momentum $P = Q_1$ and energy $E = Q_2$. Explicit expressions for some of the higher conserved charges $\hat{Q}_n$ can be found in [16]. Now, let us consider a generalized Hamiltonian $\hat{H}_G$ where all the conserved charges $\hat{Q}_n$ have been added to the Lieb–Liniger Hamiltonian (3),

$$\hat{H}_G = \hat{H} + \sum_{n \neq 2} b_n \hat{Q}_n, \tag{7}$$

with coefficients b_n. Extremizing the entropy gives a density matrix of the form (1),

$$\hat{\rho}_G = Z_G^{-1}\, \mathrm{e}^{-\beta \hat{H}_G}, \tag{8}$$

with $\beta = 1/T$ the inverse temperature and Z_G the generalized partition function. Hence, we can analyze both the situations of a system described by a generalized Gibbs ensemble (1) as well as a system where the Schrödinger Hamiltonian itself is given by $\hat{H}_G$ in equation (7).

The eigenvalues $E(\{\lambda_j\})$ of the generalized Hamiltonian $\hat{H}_G$ are given by

$$E(\{\lambda_j\}) = \sum_{j=1}^{N} \varepsilon_0(\lambda_j), \tag{9}$$

where the bare one-particle energy $\varepsilon_0(\lambda)$ is given by the polynomial function

$$\varepsilon_0(\lambda) = \sum_{n=0}^{\infty} b_n \lambda^n, \tag{10}$$

with $b_2 = 1$ and $b_0 = -h$ the chemical potential. It was shown in [17] that the generalized Yang–Yang thermodynamic Bethe Ansatz equation becomes

$$\varepsilon(\lambda) + \frac{1}{2\pi\beta} \int_{-\infty}^{\infty} \mathrm{d}\mu\, K(\lambda, \mu) \ln(1 + \mathrm{e}^{-\beta\varepsilon(\mu)}) = \varepsilon_0(\lambda), \tag{11}$$

and that a solution exists provided that $\varepsilon_0(\lambda)$ is bounded from below and $\lim_{\lambda\to\pm\infty} \varepsilon_0(\lambda) = +\infty$. The kernel $K(\lambda, \mu)$ is given by

$$K(\lambda, \mu) = \theta'(\lambda - \mu) = 2c/(c^2 + (\lambda - \mu)^2), \tag{12}$$

and the equilibrium particle distribution function $\rho(\lambda)$ by

$$\rho(\lambda) = \vartheta(\lambda) \left(\frac{1}{2\pi} + \frac{1}{2\pi} \int_{-\infty}^{\infty} \mathrm{d}\mu\, K(\lambda, \mu)\rho(\mu) \right), \tag{13}$$

with the Fermi weight

$$\vartheta(\lambda) = \frac{1}{1 + \mathrm{e}^{\beta\varepsilon(\lambda)}}. \tag{14}$$

This can also be written as $\rho(\lambda) = \vartheta(\lambda)\rho_t(\lambda)$, where

$$\rho_t(\lambda) - \frac{1}{2\pi} \int_{-\infty}^{\infty} \mathrm{d}\mu\, \vartheta(\mu) K(\lambda, \mu)\rho_t(\mu) = \frac{1}{2\pi} \tag{15}$$

is the density of states. Similarly, the so-called dressed charge $Z(\lambda)$ is defined by

$$Z(\lambda) - \frac{1}{2\pi} \int_{-\infty}^{\infty} \mathrm{d}\mu\, \vartheta(\mu) K(\lambda, \mu) Z(\mu) = 1, \tag{16}$$

reflecting that for the Lieb–Liniger model $Z(\lambda) = 2\pi\rho_t(\lambda)$.

3. Finite-size corrections at zero temperature

3.1. Energy

Let us now investigate the finite-size corrections to the generalized energy (9), focusing on the zero-temperature limit. Then the set of numbers n_j in equation (5) that minimizes the generalized energy (9) is such that all λ_j with $\varepsilon(\lambda_j) < 0$ are occupied and the rest empty of particles. In the thermodynamic limit, this gives Fermi points $q_i^{\pm}$ wherever $\varepsilon(q_i^{\pm}) = 0$, with a filled Fermi sea i for $q_i^- \leqslant \lambda \leqslant q_i^+$. The ground-state energy in the thermodynamic limit can then be written as

$$E_0 = L \int_{-\infty}^{\infty} \mathrm{d}\lambda\, \rho(\lambda)\varepsilon_0(\lambda) = L \sum_i \int_{q_i^-}^{q_i^+} \mathrm{d}\lambda\, \rho_t(\lambda)\varepsilon_0(\lambda), \tag{17}$$

with finite-size corrections coming from the replacement of the sum in equation (9) with an integral. These are obtained using the Euler–Maclaurin formula in complete analogy with the usual case [18, 19], yielding for the leading corrections

$$E_0 = L \sum_i \int_{q_i^-}^{q_i^+} \mathrm{d}\lambda\, \rho_t(\lambda)\varepsilon_0(\lambda) - \frac{\pi}{12L} \sum_{i,\nu} |v_i^{\nu}|, \tag{18}$$

where i is the Fermi sea index and $\nu = \pm$ the right/left index. Here, $v_i^{\pm}$ is the Fermi velocity at the Fermi point $q_i^{\pm}$, given by

$$v_i^{\pm} = \frac{1}{2\pi\,\rho_t(q_i^{\pm})}\frac{\partial\varepsilon}{\partial\lambda}\bigg|_{\lambda=q_i^{\pm}}. \tag{19}$$

Now we investigate the finite-size corrections of low-energy excited states, using the techniques found in [20–25]. First, we expand the energy $E(\{q_i^{\pm}\}) = E_0 + \delta E$ to second order around the ground-state energy E_0 in equation (18),

$$\delta E = \sum_{i,\nu}\left(\frac{\partial E}{\partial q_i^{\nu}}\right)\delta q_i^{\nu} + \frac{1}{2}\sum_{i,j,\nu,\nu'}\left(\frac{\partial^2 E}{\partial q_i^{\nu}\partial q_j^{\nu'}}\right)\delta q_i^{\nu}\delta q_j^{\nu'} \tag{20}$$

with $\delta q_i^{\pm}$ the change in Fermi momentum $q_i^{\pm}$ with respect to the ground state. Now,

$$\frac{\partial E}{\partial q_i^{\pm}} = \pm L\rho_t(q_i^{\pm})\varepsilon_0(q_i^{\pm}) + L\sum_j\int_{q_j^-}^{q_j^+}\mathrm{d}\lambda\,\frac{\partial\rho_t(\lambda)}{\partial q_i^{\pm}}\varepsilon_0(\lambda) = \pm L\rho_t(q_i^{\pm})\varepsilon(q_i^{\pm}), \tag{21}$$

where ε is the dressed energy (11). Since the ground state minimizes E, one has

$$\varepsilon(q_i^{\pm}) = 0. \tag{22}$$

Then, equation (20) becomes

$$\delta E = \frac{L}{2}\sum_{i,j,\nu,\nu'}\nu\delta q_i^{\nu}\delta q_j^{\nu'}\frac{\partial}{\partial q_j^{\nu'}}\left[\rho_t\left(q_i^{\nu}\right)\varepsilon\left(q_i^{\nu}\right)\right], \tag{23}$$

which is given by

$$\delta E = \frac{L}{2}\sum_{i,\nu}\nu\rho_t\left(q_i^{\nu}\right)\varepsilon'\left(q_i^{\nu}\right)\left(\delta q_i^{\nu}\right)^2 = \pi L\sum_{i,\nu}|v_i^{\nu}|\left[\rho_t\left(q_i^{\nu}\right)\delta q_i^{\nu}\right]^2. \tag{24}$$

Now, we will express $\delta q_i^{\pm}$ in terms of the quantum numbers ΔN_i and ΔD_i, defined as the changes in

$$N_i = L\int_{q_i^-}^{q_i^+}\mathrm{d}\mu\,\rho_t(\mu), \tag{25}$$

$$D_i = L\left(\int_{-\infty}^{q_i^-} - \int_{q_i^+}^{\infty}\right)\mathrm{d}\mu\,\rho_t(\mu), \tag{26}$$

compared to the ground state. Then,

$$\delta q_i^{\pm} = \sum_j\frac{\partial q_i^{\pm}}{\partial N_j}\Delta N_j + \sum_j\frac{\partial q_i^{\pm}}{\partial D_j}\Delta D_j. \tag{27}$$

The Jacobian is found from

$$\frac{\partial N_j}{\partial q_i^{\pm}} = \pm L\rho_t\left(q_i^{\pm}\right)\left[\delta_{ij} \pm \int_{q_j^-}^{q_j^+}\mathrm{d}\mu\,g\left(\mu|q_i^{\pm}\right)\right], \tag{28}$$

$$\frac{\partial D_j}{\partial q_i^{\pm}} = L\rho_t\left(q_i^{\pm}\right)\left[\delta_{ij} + \left(\int_{-\infty}^{q_j^-} - \int_{q_j^+}^{\infty}\right)\mathrm{d}\mu\,g\left(\mu|q_i^{\pm}\right)\right], \tag{29}$$

where the function $g(\lambda|q_i^{\pm})$ is defined through

$$g(\lambda|q_i^{\pm}) - \frac{1}{2\pi}\sum_k\int_{q_k^-}^{q_k^+}\mathrm{d}\mu\,K(\lambda,\mu)g(\mu|q_i^{\pm}) = \pm\frac{1}{2\pi}K\left(\lambda, q_i^{\pm}\right). \tag{30}$$

Equation (30) is equivalent to $g(\lambda|q_i^{\pm}) = [\partial\rho_t(\lambda)/\partial q_i^{\pm}]/\rho_t(q_i^{\pm})$. For the general case, we need to consider the vectors

$$\vec{n} = \begin{pmatrix} N_1 \\ \vdots \\ D_1 \\ \vdots \end{pmatrix}, \qquad \vec{p} = \begin{pmatrix} q_1^- \\ q_1^+ \\ q_2^- \\ \vdots \end{pmatrix} \tag{31}$$

so that we can write

$$\Delta n_i = L\sum_j M_{ij}\rho_t(p_j)\delta p_j, \quad M_{ij} = \frac{1}{L\rho_t(p_j)}\frac{\partial n_i}{\partial p_j}, \tag{32}$$

with $\partial n_i/\partial p_j$ given by equations (28)–(29), and hence obtain $\rho_t(q_i^{\pm})\delta q_i^{\pm}$ from

$$\rho_t(p_i)\delta p_i = \frac{1}{L}\sum_j (M^{-1})_{ij}\Delta n_j. \tag{33}$$

Inserting this into equation (24), and including the numbers N_i^- and N_i^+ of particle–hole excitations at q_i^- and q_i^+, respectively, gives the general expression

$$\delta E = \frac{\pi}{L}\sum_{i,v}|v_i^v|\left[2N_i^v + \left(\sum_j (M^{-1})_{q_i^v j}\Delta n_j\right)^2\right]. \tag{34}$$

This expression is simplified when the model has parity symmetry, e.g. around $\lambda = 0$ so that only even powers of λ appear in equation (10) and hence $\varepsilon_0(\lambda) = \varepsilon_0(-\lambda)$. If this is the case, we can consider the new pairs of Fermi points $q_j^{\pm} = \pm q_j$ ($q_1 > q_2 > \cdots > 0$), with a sea j of either particles or holes between them and Fermi velocities $|v_i^{\pm}| = v_i$. Now, define

$$N_j = L\int_{-q_j}^{q_j} \mathrm{d}\mu\, \rho_t(\mu), \tag{35}$$

$$D_j = L\left(\int_{-\infty}^{-q_j} - \int_{q_j}^{\infty}\right)\mathrm{d}\mu\, \rho_t(\mu), \tag{36}$$

i.e. ΔN_j being the number of particles/holes added to Fermi sea j of particles/holes, and $d_j = \Delta D_j/2$ the number jumping from q_j to $-q_j$. Let us now write

$$\frac{\partial N_i}{\partial q_j^{\pm}} = \pm L\rho_t(q_j)\,2\left[\delta_{ij} - (-1)^j\int_{-q_i}^{q_i}\mathrm{d}\mu\, g(\mu|q_j)\right] \equiv \pm L\rho_t(q_j)2Z_{ij}, \tag{37}$$

$$\frac{\partial D_i}{\partial q_j^{\pm}} = L\rho_t(q_j)\,2\left[\delta_{ij} - (-1)^j\left(\int_{-\infty}^{-q_i} - \int_{q_i}^{\infty}\right)\mathrm{d}\mu\, g(\mu|q_j)\right] \equiv L\rho_t(q_j)2Y_{ij}, \tag{38}$$

with $g(\lambda|q_i^{\pm})$ given by equation (30). By expressing the matrix elements of Z as $Z_{ij} = \delta_{ij} + \int_{-q_i}^{q_i}\mathrm{d}\mu\, g_{ij}(\mu)$, with $g_{ij}(\mu) \equiv (-1)^{j+1}g(\mu|q_j)$, one finds $Z_{ij} = \xi_{ij}(q_i)$, where $\xi(\lambda)$ is the dressed charge matrix defined through

$$\xi_{ij}(\lambda) - \frac{1}{2\pi}\sum_k\int_{-\infty}^{\infty}\mathrm{d}\mu\, K_{ik}(\lambda,\mu)\xi_{kj}(\mu) = \delta_{ij}, \tag{39}$$

so that here, the kernel matrix element is $K_{ij}(\lambda,\mu) = K(\lambda,\mu)$ when $-q_j \leqslant \mu \leqslant q_j$, otherwise zero. Now, from

$$Z_{ij} - \delta_{ij} = \int_{-\infty}^{-q_i}\mathrm{d}\lambda\,\frac{\partial\xi_{ij}(\lambda)}{\partial q_i}\bigg|_{\lambda=q_i} = -\sum_k\int_{-\infty}^{-q_i}\mathrm{d}\lambda\,[g_{ki}(\lambda) - g_{ki}(-\lambda)]\,Z_{kj}, \tag{40}$$

it follows that

$$Y_{ij} = \delta_{ij} + \left(\int_{-\infty}^{-q_i} - \int_{q_i}^{\infty}\right) \mathrm{d}\mu\, g_{ij}(\mu) = \delta_{ij} - \sum_k [Z_{ki} - \delta_{ki}]\,(Z^{-1})_{jk} = (Z^{-1})_{ji}. \tag{41}$$

Hence, $Y = (Z^T)^{-1}$. Putting this into equations (27) and (24) finally gives

$$\delta E = \frac{2\pi}{L} \sum_j v_j \big[\Delta_j^+ + \Delta_j^-\big], \tag{42}$$

where

$$\Delta_j^{\pm} = N_j^{\pm} + \frac{1}{2}\left(\sum_k (Z^{-1})_{jk} \frac{\Delta N_k}{2} \pm \sum_k Z_{kj} d_k\right)^2. \tag{43}$$

Obviously, when the bare single-particle dispersion in equation (10) is given by $\varepsilon_0(\lambda) = \lambda^2$, there is just a single Fermi sea, between $\lambda = -q$ and $\lambda = q$, and equations (42) and (43) reduce to those for the usual Lieb–Liniger model,

$$\delta E = \frac{2\pi}{L} v[\Delta^+ + \Delta^-], \qquad \Delta^{\pm} = N^{\pm} + \frac{1}{2}\left(\frac{\Delta N}{2Z(q)} \pm Z(q) d\right)^2. \tag{44}$$

3.2. Momentum

Since the momentum $P = \sum_i \lambda_i = \frac{2\pi}{L} \sum_i n_i$, as is easily seen from equation (5), it is trivially obtained as

$$P = P_0 + \sum_i \left[\, \tilde{P}_i\, \Delta N_i - k_i\, d_i + \frac{2\pi}{L} \left\{N_i^+ - N_i^- + d_i\, \Delta N_i\right\} \right], \tag{45}$$

for the excited states, where P_0 is the ground-state momentum. In the thermodynamic limit, $\tilde{P}_i = (q_i^+ + q_i^-)/2$ and $k_i = q_i^+ - q_i^-$. In the case of parity symmetry, $\tilde{P}_j = 0$ and $k_j = 2q_j$.

4. Conformal dimensions and correlation functions

It is now clear that the finite-size corrections in equations (18), (42) and (45) can be written in the form

$$E_0 - E_0(L \to \infty) = -\frac{\pi}{6L} \sum_j c_j |v_j| + \text{h.o.c.} \tag{46}$$

$$E - E_0 = \frac{2\pi}{L} \sum_j |v_j| \big[\Delta_j^+ + \Delta_j^-\big] + \text{h.o.c.} \tag{47}$$

$$P - P_0 = \sum_j [\tilde{P}_j\, \Delta N_j - k_j\, d_j] + \frac{2\pi}{L} \sum_j \big[\Delta_j^+ - \Delta_j^-\big] + \text{h.o.c.} \tag{48}$$

where h.o.c. denotes higher-order corrections. This tells us that the low-energy physics is given by a sum of conformal field theories [26, 27], where $\Delta_j^{\pm}$ are the scaling dimensions of the scaling operators of the theories and $c_j = 1$ the central charges. We will now use this to obtain the large-distance asymptotics of the equal-time correlation functions [21]. The field correlation function

$$\langle \Psi(x) \Psi^{\dagger}(0) \rangle = \mathrm{Tr}\, \hat{\rho}_G \Psi(x) \Psi^{\dagger}(0), \tag{49}$$

for which the total number of added *particles* is $\Delta N = \sum_j (\Delta N_{2j-1} - \Delta N_{2j}) = 1$, should then have the asymptotic form

$$\langle \Psi(x)\Psi^\dagger(0)\rangle \sim \sum_{\mathcal{Q}_\Psi} A(\mathcal{Q}_\Psi)\, \mathrm{e}^{\mathrm{i}\sum_j d_j k_j x}\, x^{-2\sum_j (\Delta_j^+ + \Delta_j^-)}, \tag{50}$$

where $\mathcal{Q}_\Psi = \{\{\Delta N_j\}, \{d_j\}, \{N_j^\pm\} \mid \Delta N = 1\}$ is the set of quantum numbers for the excitations, and $A(\mathcal{Q}_\Psi)$ the amplitudes. The leading term is given by

$$\langle \Psi(x)\Psi^\dagger(0)\rangle \sim x^{-\alpha}, \tag{51}$$

with α the smallest sum of scaling dimensions $2\sum_j (\Delta_j^+ + \Delta_j^-)$ given the constraint $\Delta N = 1$, i.e. α is the smallest of the numbers $(\sum_j (Z^{-1})_{jk})^2/2$. Similarly, density–density correlators are obtained with $\Delta N = 0$,

$$\langle j(x)j(0)\rangle - \langle j(0)\rangle^2 \sim \sum_{\mathcal{Q}_d} A(\mathcal{Q}_d)\, \mathrm{e}^{\mathrm{i}\sum_j d_j k_j x}\, x^{-2\sum_j (\Delta_j^+ + \Delta_j^-)}, \tag{52}$$

where $j(x) = \Psi^\dagger(x)\Psi(x)$ and $\mathcal{Q}_d = \{\{\Delta N_j\}, \{d_j\}, \{N_j^\pm\} \mid \Delta N = 0\}$. The leading terms are

$$\langle j(x)j(0)\rangle - \langle j(0)\rangle^2 \sim A_1 x^{-2} + A_2 \cos(d_k k_k x) x^{-\theta}, \tag{53}$$

where the first term comes from the processes with $d_k = 0$ and one single number $N_k^\pm$ equal to one, and the second term is from the two processes with the $d_k = \pm 1$ giving smallest θ, i.e. with θ the smallest of the numbers $2(\sum_j Z_{kj})^2$.

Importantly, the finite-temperature correlation functions for mixed states are obtained by the standard conformal mapping $z(w) = \mathrm{e}^{2\pi T w/v_i}$ in the complex plane $z = x - \mathrm{i}v_i t$, so that in the formulas above

$$x^{-2\Delta_j^\pm} \;\to\; \left\{(\pi T/v_j)/\sinh[\pi T x/v_j]\right\}^{2\Delta_j^\pm}. \tag{54}$$

5. Discussion

We have obtained the finite-size corrections for the energy and momentum of a one-dimensional Bose gas with delta-function interaction (Lieb–Liniger model) when additional conservation laws are present in the density matrix, or the conserved charges are added to the Hamiltonian. The results show that the low-energy physics is described by a sum of conformal field theories each with central charge $c = 1$, where each may have its own specific speed of sound. The picture is most clear when the bare dispersion is parity symmetric. In this case, we derived the asymptotic behavior of the correlation functions using standard arguments.

The finite-temperature mapping (54) provides a possible connection to present studies of quantum non-equilibrium dynamics. In the standard setup, an isolated system in a pure state is time evolved by, but not an eigenstate of, the usual Schrödinger Hamiltonian. The density matrix of a subsystem will however be in a mixed state, presumably approaching the form (1) with a finite effective temperature. It remains to be seen whether the new types of correlation effects in the generalized model studied here may appear in such systems.

It is interesting to note that the generalized one-dimensional Bose gas with a dispersion relation with many Fermi points for the bare particles gives similar types of finite-size effects as in well-studied examples of multicomponent (a.k.a. nested) Bethe Ansatz solvable models [29], such as integrable quantum spin chains [11, 12, 28, 30–34] and the one-dimensional Hubbard model [24, 35], even though the one-dimensional Bose gas only contains a single species of particles.

Acknowledgments

We wish to thank Holger Frahm for helpful discussions. EE acknowledges financial support from the Swedish Research Council (grant no. 621-2011-3942) and from STINT (grant no. IG2011-2028), and VK from NSF (grant no. DMS-1205422).

References

[1] Jaynes E T 1957 Information theory and statistical mechanics *Phys. Rev.* **106** 620
[2] Kinoshita T, Wenger T and Weiss T D 2006 A quantum Newton's cradle *Nature* **440** 900
[3] Rigol M, Dunjko V, Yurovsky V and Olshanii M 2007 Relaxation in a completely integrable many-body quantum system: an *ab initio* study of the dynamics of the highly excited states of 1D lattice hard-core bosons *Phys. Rev. Lett.* **98** 050405
[4] Polkovnikov A, Sengupta K, Silva A and Vengalattore M 2011 Nonequilibrium dynamics of closed interacting quantum systems *Rev. Mod. Phys.* **83** 863
[5] Calabrese P, Essler F H L and Fagotti M 2012 Quantum quenches in the transverse field Ising chain: II. Stationary state properties *J. Stat. Mech.* P07022
[6] Caux J-S and Essler F H L 2013 Time evolution of local observables after quenching to an integrable model arXiv:1301.3806
[7] Caux J-S and Konik R M 2012 Constructing the generalized Gibbs ensemble after a quantum quench *Phys. Rev. Lett.* **109** 175301
[8] Kormos M, Shashi A, Chou Y-Z and Imambekov A 2012 Interaction quenches in the Lieb–Liniger model arXiv:1204.3889
[9] Mossel J and Caux J-C 2012 Exact time evolution of space- and time-dependent correlation functions after an interaction quench in the one-dimensional Bose gas *New J. Phys.* **14** 075006
[10] Brandino G, Caux J-C and Konik R 2013 Relaxation dynamics of conserved quantities in a weakly non-integrable one-dimensional Bose gas arXiv:1301.0308
[11] Tsvelik A M 1990 Incommensurate phases of quantum one-dimensional magnetics *Phys. Rev.* B **42** 779
[12] Frahm H 1992 Integrable spin-1/2 XXZ Heisenberg chain with competing interactions *J. Phys. A: Math. Gen.* **25** 1417
[13] Lieb E H and Liniger W 1963 Exact analysis of an interacting Bose gas: I. The general solution and the ground state *Phys. Rev.* **130** 1605
[14] Lieb E H 1963 Exact analysis of an interacting Bose gas: II. The excitation spectrum *Phys. Rev.* **130** 1616
[15] Korepin V E, Bogoliubov N M and Izergin A G 1993 *Quantum Inverse Scattering Method and Correlation Functions* (Cambridge: Cambridge University Press)
[16] Davies B and Korepin V E 1989 Higher conservation laws for the quantum non-linear Schrödinger equation *Report No.* CMA-R33-89*, Centre for Mathematical Analysis Australian National University, Canberra* (arXiv:1109.6604)
[17] Mossel J and Caux J-S 2012 Generalized TBA and generalized Gibbs *J. Phys. A: Math. Theor.* **45** 255001
[18] Woynarovich F and Eckle H-P 1987 Finite-size corrections and numerical calculations for long spin-1/2 Heisenberg chains in the critical region *J. Phys. A: Math. Gen.* **20** L97
[19] Berkovich A and Murthy G 1988 Finite-size corrections in the non-linear Schrödinger model *J. Phys. A: Math. Gen.* **21** L395
[20] Korepin V E 1979 Direct calculation of the *S* matrix in the massive Thirring model *Theor. Math. Phys.* **41** 953
[21] Bogoliubov N M, Izergin A G and Reshetikhin N Y 1987 Finite-size effects and infrared asymptotics of the correlation functions in two dimensions *J. Phys. A: Math. Gen.* **20** 5361
[22] Woynarovich F, Eckle H-P and Truong T T 1989 Non-analytic finite-size corrections in the one-dimensional Bose gas and Heisenberg chain *J. Phys. A: Math. Gen.* **22** 4027
[23] Woynarovich F 1989 Finite-size effects in a non-half-filled Hubbard chain *J. Phys. A: Math. Gen.* **22** 4243
[24] Essler F H L, Frahm H, Göhmann F, Klümper A and Korepin V E 2005 *The One-Dimensional Hubbard Model* (Cambridge: Cambridge University Press)
[25] Zvyagin A A 2005 *Finite Size Effects in Correlated Electron Models: Exact Results* (London: Imperial College Press)
[26] Cardy J L 1984 Conformal invariance and universality in finite-size scaling *J. Phys. A: Math. Gen.* **17** L385
[27] Blöte H W, Cardy J L and Nightingale M P 1986 Conformal invariance, the central charge, and universal finite-size amplitudes at criticality *Phys. Rev. Lett.* **56** 742

[28] Pokrovskii S V and Tsvelik A M 1987 Conformal dimension spectrum for lattice integrable models of magnets *Zh. Eksp. Teor. Fiz.* **93** 2232
Pokrovskii S V and Tsvelik A M 1987 Conformal dimension spectrum for lattice integrable models of magnets *Sov. Phys.—JETP* **66** 1275 (Engl. transl.)
[29] Izergin A G, Korepin V E and Reshetikhin N Y 1989 Conformal dimensions in Bethe ansatz solvable models *J. Phys. A: Math. Gen.* **22** 2615
[30] Frahm H and Yu N-C 1990 Finite-size effects in the integrable XXZ Heisenberg model with arbitrary spin *J. Phys. A: Math. Gen.* **23** 2115
[31] Frahm H and Rödenbeck C 1997 Properties of the chiral spin liquid state in generalized spin ladders *J. Phys. A: Math. Gen.* **30** 4467
[32] Zvyagin A A 2000 Commensurate-incommensurate phase transitions for multichain quantum spin models: exact results *Low Temp. Phys.* **26** 134
[33] Zvyagin A A, Klümper A and Zittartz J 2001 Integrable correlated electron model with next-nearest-neighbour interactions *Eur. Phys. J.* B **19** 25
[34] Zvyagin A A and Klümper A 2003 Quantum phase transitions and thermodynamics of quantum antiferromagnets with next-nearest-neighbor couplings *Phys. Rev.* B **68** 144426
[35] Frahm H and Korepin V E 1990 Critical exponents for the one-dimensional Hubbard model *Phys. Rev.* B **42** 10553